UNIVERSITAT DE BARCELONA

Role of the Hippo pathway in planarians

Nidia de Sousa

ROLE OF THE HIPPO PATHWAY IN PLANARIANS

NÍDIA DE SOUSA

TESIS DOCTORAL 2017

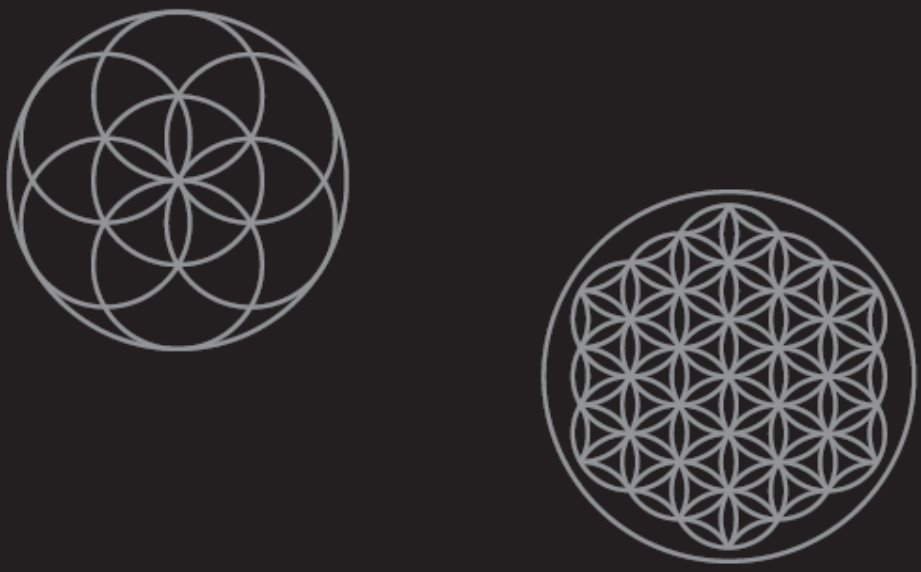

UNIVERSITAT DE BARCELONA

FACULTAD DE BIOLOGÍA

DEPARTAMENTO DE GENÉTICA, MICROBIOLOGÍA Y ESTADÍSTICA

PROGRAMA DE DOCTORADO EN GENÉTICA

Nídia de Sousa

Role of the Hippo pathway in planarians

Tesis Doctoral

2017

UNIVERSITAT DE BARCELONA

FACULTAD DE BIOLOGÍA

DEPARTAMENTO DE GENÉTICA, MICROBIOLOGÍA Y ESTADÍSTICA

PROGRAMA DE DOCTORADO EN GENÉTICA

Tesis Doctoral presentada por

Nídia de Sousa

bajo el título

Role of the Hippo pathway in planarians

Para optar al título de Doctora por la Universidad de Barcelona

Tesis Doctoral realizada en el Departamento de Genética, Microbiología y Estadística bajo la dirección de la Doctora Teresa Adell y del Doctor Emili Saló.

La Directora,	El Director,	La Autora,
Dra. Teresa Adell	Dr. Emili Saló	Nídia de Sousa

Barcelona
Abril 2017

Cover explanation (En)

In the early stages of embryonic development, one single cell is the origin of everything, the beginning of a new life on Earth, a blank page where anything can happen. In an incredible way, Mother Nature is able to take this single cell and transform it into a new organism, composed by perfectly coordinated complex systems. The beginning of the embryonic development of a new being is one of the most fascinating events happening in nature.

Explicación de la portada (Es)

Durante los primeros estadios del desarrollo embrionario, una única célula es el origen de todo, el comienzo de una nueva vida en la Tierra, una página en blanco donde todo puede pasar. De una manera increíble, la Madre Naturaleza es capaz de coger esta única célula y transformarla en un nuevo organismo, compuesto por complejos sistemas perfectamente coordinados. El inicio del desarrollo embrionario de un nuevo ser es una de las cosas más fascinantes que ocurren en la naturaleza.

Explicação da capa (Pt)

Nos primeiros estadíos embrionários, uma única célula é a origem de tudo, o começo de uma nova vida na Terra, uma página em branco onde tudo pode acontecer. De uma maneira incrível, a Mãe Natureza é capaz de pegar nesta única célula e transformar-la num novo organismo, repleto de complexos sistemas mas perfeitamente coordenado. O início do desenvolvimento embrionário de um novo ser é das coisas mais fascinantes que ocorrem na natureza.

O carácter e os valores de cada um vão-se afinando ao longo da vida. Não sei em que momento é suposto começarmos a formar a nossa personalidade nem como nos é transmitido o valor e a coragem que nos moldam, mas sou consciente que os meus pais o fizeram de uma maneira incrível. Não sei se um dia serei capaz de fazer tão bom trabalho como eles, mas tentarei transmitir aos meus filhos, seus netos, que na vida tudo é possível, se sabes de onde vens e onde queres chegar, sem nunca esquecer o como.

Esta tese, como tudo na minha vida, está dedicada aos meus pais que fizeram de mim quem sou hoje. Sem eles nada seria possível.

Acknowledgments

A maratona chegou ao fim e, neste momento, sou um mix de emoções. Estou contente porque consegui chegar à meta, mas por outro lado, deixarei para trás todos aqueles que me ajudaram a cortar a meta. Assim que não poderia deixar de agradecer a todos os que me deram o seu empurrãozinho para chegar aqui.

A Teresa, por todo. Por ayudarme a crecer, no solo como científica pero también como persona. Por ser un ejemplo a seguir, una mujer valiente y determinada. Gracias por todo lo que me has enseñado. Jamás te olvidaré.

A Emili, por haberme dado la oportunidad, de haber abierto las puertas de su laboratorio si ni siquiera conocerme. Gracias por todo el conocimiento que me has transmitido.

A Nieves y Aina, lo mejor que llevo de Barcelona. Ay mis chunguis… sin vosotras todo habría sido más difícil. Gracias por todo el apoyo, por nuestras cenitas y por haber escuchado mis líos durante estos años. Gracias por los buenos recuerdos que llevaré siempre conmigo. Os quiero!

A Eudald, mi compi de todos los momentos, desde siempre y para siempre. Mi primer amigo en Barna! Gracias por todos los buenos momentos que hemos compartido. Has sido un gran apoyo!

A Sari, por ser un ejemplo de persona. Gracias por toda la ayuda, por las palabras ciertas en los momentos ciertos. Gracias por todo el cariño y por siempre acreditar en mí. Te echo de menos!!!

A Bea y Ari, por haberme incorporado en el grupo desde el momento uno y por ayudarme con mi castellano de Portugal. Gracias por vuestra kukez y por vuestras palabras cuando las necesitaba escuchar.

A Maria A., Susi y Sisco por la ayuda cuando me sentía más perdida que nunca y por la palabras siempre sábias.

A José, Miquel, Kike y Carlos por el buen rollito en el Lab, por el compañerismo, por las discusiones científicas e por toda la ayuda.

A Heura y Elvira por el trabajo que han hecho y por las ganas de aprender.

A Natália y Maria G. por las ganas de aprender y por la ilusión con que miráis el Mundo. Sabiendo que hay gente como vosotras haciendo ciencia, no pierdo la esperanza en las nuevas generaciones.

A toda la gente de Moscas, Paula, Elena, Sandra, Haritz y Qi por el apoyo y la ayuda durante todo este tiempo y por los buenos momentos compartidos.

E con esto digo "Yo he venido aquí a trabajar, no hacer amiguitos", imagínate tu si vengo para hacer amigos!!

À Joana Basto pelo design da capa da tese. Adorei, obrigada.

Ao Pedro e Luís por sempre estarem presentes e disponíveis para os nossos cafezinhos quando vou a Portugal. Por me ouvirem falar de coisas estranhas e se calhar, às vezes aborrecidas sem nunca se queixarem. Obrigada.

À Maria e à Cindy porque mesmo estando longe, estarmos sempre perto. Por saber que as tenho sempre à distância de uma chamada. Pelo apoio incondicional mesmo não entendendo muito bem o que andei a fazer durante estes anos. Obrigada minhas babes!

Ao grupinho. Gigi, Gata, Belinha, Jojo, Lala e Ivinho por serem a minha família adoptiva desde há quase 10 anos. Por todos os bons momentos passados na Universidade, todas as noites sem dormir a estudar ou a fazer outras coisas... Pelos nossos reencontros, que quase nunca são perfeitos porque falta sempre alguém, mas mesmo assim fazemos o esforço. Vocês estarão sempre cá dentro, estejam donde estejam.

Ao Octávio, o pai dos meus futuros fillhos. Por dar-me o ombro para chorar, o colo para me acalmar e a mão, não só para me levantar, mas para me empurrar para a frente porque sabia que conseguia mais. Pelas aventuras vividas nestes últimos anos, pela paciência, amor e carinho. Por tudo. Obrigada.

Ao meu irmão e cunhada, pelo apoio e por estar sempre aí para me ouvir. Pela valentia de trazer-me um sobrinho a este mundo de loucos. Obrigada.

Aos meus papas, que viram como os seus dois filhos saíam de casa no mesmo ano, e sei que não foi fácil. Por nunca me terem cortado as asas e me terem deixado voar. Obrigada.

Abstract (En)

A successful cell renewal, which occurs throughout the life of an organism, relies on multiple events, including proliferation and differentiation of progenitor cell populations, and death of unnecessary cells. Out of the multiple molecular mechanisms involved in the control of cellular renewal, the Hippo signaling pathway currently appears as a hub. Although it was first identified as a key regulator of organ size through the control of cell death and proliferation, growing evidence suggests that it also plays pivotal roles in coordinating stem cell maintenance, cell differentiation, cell-fate decisions and cell survival.

To further understand the role of the Hippo pathway in driving adult cellular renewal and, specifically, in promoting cellular stemness, we studied its function in planarians. Due to the presence of a population of pluripotent adult stem cells (neoblasts), planarians have the ability to constantly grow and degrow depending on food availability, and to regenerate any missing body part within a few days. This active and continuous regulation of the stem cell and post-mitotic cell compartments makes planarians an ideal '*in vivo*' context to gain an integrated view of the different events underlying homeostatic cell renewal and tissue regeneration.

Here, we address whether downregulation of Hippo signaling exerts its stemness-promoting function by increasing the proliferation of resident stem cells or promoting cell dedifferentiation. We show that inhibition of *Smed-hippo* (to simplify, *hippo*) in planarians reduces apoptotic activity and increases mitotic rates. However, this imbalance between cell death and mitotic activity does not lead to an increase in planarian body size or cell number, since *hippo (RNAi)* does not increase the number of cycling cells but blocks mitotic exit. *hippo (RNAi)* animals develop overgrowths and extensive regions composed of undifferentiated cells, accompanied by a general decrease in the number of differentiated cells throughout their body. A detailed study of the epidermal lineage reveals that *hippo* is required to determine the hierarchical transitions required for proper epidermal differentiation, from epidermal-restricted

stem cells to differentiated epidermal cells. We also demonstrate that *hippo* is required to maintain the differentiated state in planarian cells, since *hippo* inhibition promotes dedifferentiation of post-mitotic cells. Overall, these results indicate that the overgrowths and undifferentiated regions observed after *hippo* inhibition in planarians are not caused by the unbalance between cell death and proliferation but to the inability of cells to reach and maintain the appropriate fate.

Furthermore, during this study we demonstrate that the Hippo-Yki signaling cascade is conserved in planarians and plays a role in cell differentiation during planarian regeneration. We further show the conservation of the up-stream regulators of the Hippo pathway in planarians since the inhibition of Hippo up-stream regulators, as *lgl-2*, phenocopies the *hippo (RNAi)* phenotype. Transcriptomic analysis of *hippo (RNAi)* animals allowed the identification of several putative Hippo pathway targets in planarians, which silencing reproduces the formation of overgrowths.

Overall, we propose an essential role for Hippo signaling in restricting cell plasticity and thus in preventing tumoral transformation.

Resumen (Es)

La renovación celular, que tiene lugar durante toda la vida en los organismos adultos, depende de múltiples eventos, incluyendo el control de la proliferación, la diferenciación de las células progenitoras y la muerte de células innecesarias. La vía de señalización de Hippo ejerce un papel central en el control de todos estos procesos. A pesar de haber sido primeramente identificada como una vía reguladora clave en el control del tamaño de los órganos a través de la regulación de la proliferación y la muerte, evidencias recientes sugieren que esta vía puede estar también involucrada en el mantenimiento de las células madre, en la diferenciación celular, en el mantenimiento del estado diferenciado y en la supervivencia de las células.

Para profundizar en el conocimiento del papel de la vía de Hippo durante la renovación celular en tejidos adultos, específicamente en su función reguladora del estado pluripotente de las células, abordamos su estudio en planarias. Debido a la presencia de una población de células pluripotentes adultas, los neoblastos, las planarias poseen la capacidad de crecer y decrecer dependiendo de la disponibilidad de alimento, así como de regenerar cualquier parte de su cuerpo en apenas algunos días. Esta activa y continua regulación de las células madre y de los compartimentos postmitóticos convierte a las planarias en un contexto "in vivo" ideal para obtener una visión integrada de los diferentes mecanismos que controlan la renovación celular durante la homeostasis y la regeneración de los tejidos.

En esta tesis hemos abordado la cuestión de si el silenciamiento de la vía de señalización de Hippo afecta a la promoción del estado indiferenciado, concretamente a través del control de la proliferación de células madre o bien promoviendo la desdiferenciación celular. Los resultados obtenidos demuestran que la inhibición de *Smed-hippo* (para simplificar, *hippo*) en planarias reduce la actividad apoptótica y aumenta los índices mitóticos. Sin embargo, este desequilibrio entre muerte celular y actividad mitótica no conduce al aumento del tamaño de las planarias ni al aumento del número de células. Uno de los motivos es que la inhibición

de *hippo* no aumenta el número de células que ciclan si no que bloquea la salida de mitosis. Sin embargo, aunque no hay un incremento en el número de células, el silenciamiento de *hippo* produce la aparición de sobrecrecimientos, precedidos por la aparición de amplias regiones compuestas por células no diferenciadas, y la reducción del número de células diferenciadas en todo el animal. El estudio detallado del linaje epidérmico, demuestra que *hippo* es necesario para determinar las transiciones jerárquicas requeridas para una correcta diferenciación de las células epidérmicas. Además, demostramos que *hippo* es necesario para mantener el estado diferenciado de las células, ya que su inhibición promueve la desdiferenciación de células postmitóticas. En conjunto, estos resultados indican que los sobrecrecimientos y regiones indiferenciadas observadas después de la inhibición de *hippo* no son causados por el desequilibrio entre la muerte celular y la proliferación sino por la incapacidad de las células adquirir y mantener su estado diferenciado.

Además, durante este estudio hemos demostrado que la cascada de señalización Hippo-Yki está conservada en planarias y desempeña un papel fundamental durante la regeneración. También hemos visto que los mecanismos reguladores "up-stream" de la vía Hippo parecen estar conservados en planarias, ya que la inhibición de algunos elementos, como *lgl2*, fenocopia el fenotipo de los animales *hippo (RNAi)*. A su vez, el análisis transcriptómico de los animales *hippo (RNAi)* ha permitido identificar genes diana de la vía Hippo en planarias. El silenciamiento de algunos de estos genes candidatos también promueve la aparición de sobrecrecimientos. Para finalizar, nuestros estudios nos permiten proponer que el papel principal de Hippo en las planarias es restringir la plasticidad celular y así prevenir la transformación tumoral.

Table of contents

Figures list

Introduction

1. Cell renewal

2. Hippo signaling pathway as a pivotal regulator of cell fate

3. Planarians as a model organism to study growth control

Results

Chapter 1: Hippo pathway core elements during planarian homeostasis

Chapter 2: Functional characterization of hippo during planarias homeostasis

Chapter 3: Functional characterization of the Hippo pathway during planarian regeneration

Chapter 4: Up-stream regulators and inhibitors of the Hippo pathway

Chapter 5: Hippo targets in planarians

Tables list

Results

Chapter 2: Functional characterization of hippo during planarian homeostasis

Chapter 5: Hippo targets in planarians

Abbreviations list

	Abbreviation	Full name
A	AD	Asymetric Division
	AJ	Adherent junctions
	AMOT	Angiomotin
	App	Approximated
	Aspm	Abnormal-spindle-like microcephaly-associated protein
B	BEC	Biliary epithelial cell
C	CA	Carbonic anhydrase
	Ccdc96	Coiled-coil domain containing protein 96
	Cenpe	Isoform 2 of centromere-associated protein E
	cNeoblasts	Clonogenic neoblasts
	CNS	Central nervous system
	CSCs	Cancer stem cells
	CTGF	Conective tissue growth factor
D	diap1	*Drosophila* inhibitor of apoptosis
	Dlg	Discs large
	DNA	Deoxyribonucleic acid
	Ds	Dachous
	dsRNA	double-strand RNA
	Dst3	Isoform of distonin 3
E	EdU	5-Ethynyl-2´-deoxyuridine
	EGF	Epidermal growth factor
	EGFR	Epidermal growth factor receptor
	EMC	Extra-cellular matrix
	EMT	Epithelial-mesenchymal transition
	ESCs	Embryonic stem cells
	Ex	Expanded
F	FACS	Fluorescence-activated cell sorting
	FBM	FERM-binding motif
	FISH	Flourescence in situ hybridization
	Ft	Fat
G	GO	Gene ontology
	GPCRs	G-protein couple receptors
	GPER	G-protein coupled estrogen receptor

	GTP	Guanosine Triphosphate
H	H3P	Histone-3 phosphorylated
	Hnf4-α	Hepatocyte nuclear factors 4 alpha
	Hth	Homothorax
	Hyprot	Hypothetical protein
I	iPSCs	Induced pluripotent stem cells
	ISCs	Intestinal stem cells
	ISH	in situ hybridization
J	JNK	c-Jun N-terminal kinase
L	Lats 1/2	Large Tumor Suppressor Kinase 1/2
	Lgl	Lethal giant larvea
M	MAPK	Mitogen-Activated Protein Kinase
	Med 17	Mediator RNA polymerase II transcription subunit 17
	Mer	Merlin
	mESCs	Mouse embryonic stem cells
	Mob1	Mps One Binder Kinase Activator 1
	mRNA	messenger RNA
	Msi2b	Musashi homolog 2b
	Mst1/2	Macrophage stimulating protein 1/2
	Muc	Mucin
	MyoD	Myogenic Differentiation
N	NCP	Neighborhood coherence principle
	NF2	Neurofibromatosis type 2
	NSCs	Neural stem cells
P	pc	Pigmented cells
	PCR	Polymerase chain reaction
	PDK1	Phosphoinositide-dependent kinase 1
	phc	Photoreceptor cells
	PI3K	Phosphoinositide 3-kinase
	PK1	Panthothenate kinase 1
	PTPN14	Protein tyrosine phosphatase 14
Q	qPCR	Quantitative PCR
R	RASSF	Ras Association Domain Family Member
	Rho	Rhodopsin
	RNA	Ribonucleic acid
	RNAi	interference RNA

	RNAseq	RNA sequencing
	ROS	Reactive oxygen species
S	S. mediterranea	Schmidtea mediterranea
	SC	Symmetric commitment
	Scrib	Scribble
	SCS	Single cell sequencing
	SD	Symmetric division
	Sd	Scalloped
	Spon	Spondin
	Sycp1	Synaptonemal complex protein 1
T	TAZ	Tafazzin
	TEAD	Transcriptional Enhancer Factor
	TGF-β	Transforming growth factor beta
	TH	Tyrosine Hydroxylase
	TJ	Tight junctions
	TPH	Tryptophan Hydroxylase
	Tsh	Teashirt
	TUNEL	Terminal deoxynucleotidyl transferase dUTP nick end labeling
V	Vim	Vimentin
	VNC	Ventral nerve cords
W	WT	Wild-type
X	Xrra1	X-ray radiation resistance-associated protein
Y	YAP	Yes-associated protein
	Yki	Yorkie
Z	ZO-2	Zona occludens-2
Symbols	γ	Gamma
	ζ	Zeta
	ν	Nu
	σ	Sigma

Introduction

1.Cell renewal

1. Cell renewal

Cell renewal is the basis of tissue and organ homeostasis during adulthood. Its disruption leads to common human diseases, such as cancer. Proper cell renewal requires the coordination of essential and complex cellular processes, including stem cell self-renewal, stem cell differentiation and commitment to specific lineages, and the death of old or unnecessary cells.

1.1 Cell renewal and regeneration

Cell or tissue renewal and regeneration are the two main developmental requirements of adult organisms. Both processes have as starting point a population of stem cells, normally located in a specific environment called the "niche"[1], which provides them the required signals to maintain the stemness properties, or to differentiate to the required different cell types (Figure I1.1). Stem cell proliferation and differentiation must be coordinated with the death of the cells that need to be replaced. In addition, processes such as cell migration, epigenetics, and cellular communication, are also necessary for proper cell renewal[2,3].

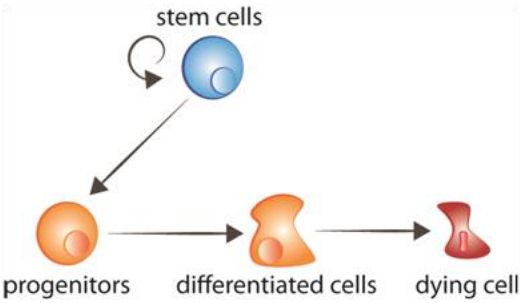

Figure I1.1: Cell turnover.
Stem cells proliferate, giving rise to progenitors that thereafter receive the signals to differentiate. Aged cells receive signals to die.

Fast renewing tissues can be recognized by a higher mitotic activity. Conversely, slow renewing tissues contain less mitosis, and may not be easily recognized from non-renewing areas which may also present some mitosis[2]. The fate decisions of stem cells

during proliferation directly influence tissue renewal and homeostasis. Therefore, understanding the regulatory mechanisms that sustain a balanced cell division and differentiation is critical. Extracellular signals (e.g., tissue microenvironment, intracellular ROS, and cytokines) as well as intracellular factors (e.g., epigenetic machineries, transcription factors and DNA damage response) are responsible for the regulation of stem cell division. Stem cells show three possible options of division: (1) asymmetric division, in which one stem cell and one committed daughter cell are originated ; (2) symmetric commitment, which yields two committed daughter cells; and (3) symmetric division, which yields two daughter cells that maintain stem cell properties[4] (Figure I1.2). Although it could be predicted that asymmetric division is the only mechanism that enables the maintenance of a stable population of stem cells, the current data from lineage-tracing experiments demonstrates that in most tissues, the balance between stem cell proliferation and the generation of differentiated offspring is achieved at the level of the whole stem cell population. The loss of stem cells due to differentiation or cell damage, induces symmetric division to fill this gap[5].

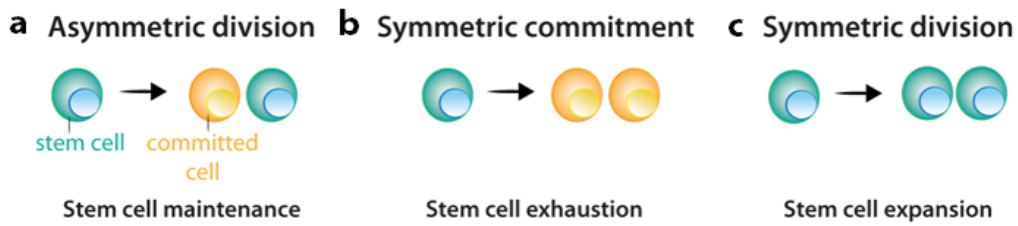

Figure I1.2: Division pattern of stem cells.
(a) During asymmetric division, stem cells give rise to one stem cell, which maintains the stem cell population, and one cell that becomes committed to differentiation. **(b)** During symmetric commitment, stem cell division gives rise to two daughter cells that became committed to differentiation. **(c)** During symmetric division, stem cell division gives rise to two stem cells. As explained in the text, current experimental data indicates that the three modes of division can occur while maintaining the stem cell population.

After stem cell division, the cells that follow the differentiation process pass through different stages that are defined by a combination of transcription factors that control the activity of the appropriate repertoire of genes, and allow their commitment and terminal differentiation. For each cell lineage the end product of the sequence of decisions is a specific differentiated cell type[6] (Figure I1.3a). Under most circumstances, cellular identity - the product of normal differentiation - is stable within tissues, and its maintenance is crucial for normal tissue function. Such stability is achieved through epigenetic regulation - e.g. histone demethylation and acetylation - that results in heritable patterns of tissue-specific gene expression[3,7]. However, loss of cell identity can occur. Indeed, cells from *Drosophila* imaginal disc are able to transdetermine and acquire a new adult fate following transplantation[8]. In this situation, extracellular cues seem to reprogram some precursor or differentiated cells to acquire characteristics of either a more stem state or a new differentiated state. There are two mechanisms by which a cell can change its identity: dedifferentiation, and transdifferentiation. Dedifferentiation refers to the process by which a differentiated or committed cell acquires characteristics of a less mature cell[9] (Figure I1.3b). The most dramatic example of dedifferentiation is the *in vitro* conversion of terminally differentiated cells into pluripotent cells (induced pluripotent stem cells, iPSCs), by the overexpression of a limited number of transcription factors[10]. Transdifferentiation, by contrast, occurs when a differentiated cell changes it transcriptional program and converts into another differentiated cell type. The process can occur directly, without the intermediated stage, or through an intermediated step of dedifferentiation towards a less mature stage before the conversion into the new differentiated cell[9] (Figure I1.3c-d). The direct conversion of fibroblasts into myoblasts by the ectopic expression of MyoD is an example of the second process[11].

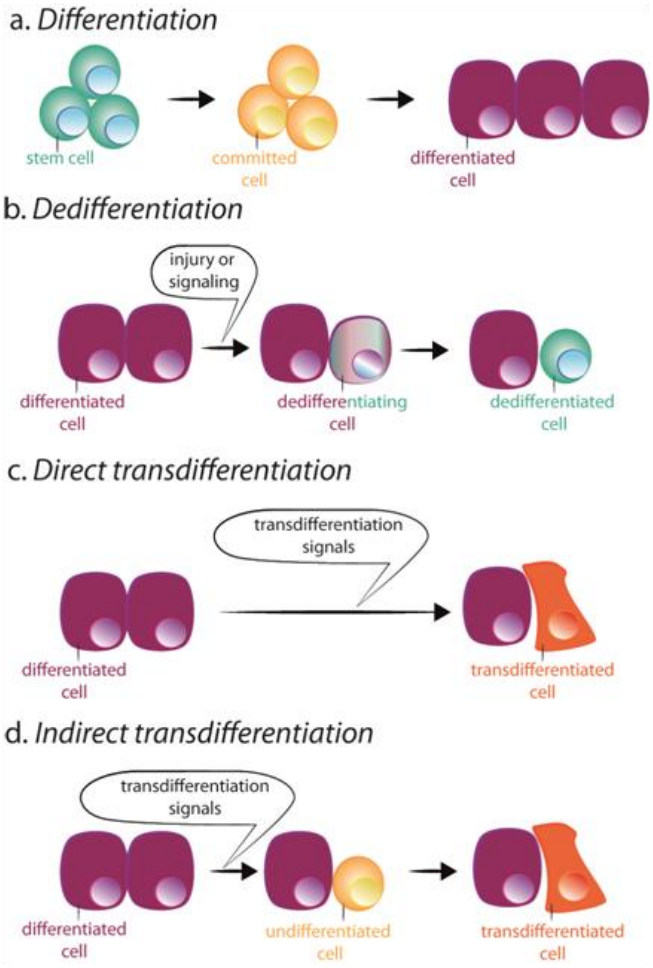

Figure I1.3: Schemes of differentiation, dedifferentiation and transdifferentiation.
(a) During normal differentiation, stem cells give rise to committed cells which in turn differentiate in different cell types. **(b)** Dedifferentiation consists of the acquisition of stem cell properties by a differentiated cell. **(c-d)** Transdifferentiation can occur in a direct or indirect way. **(c)** During direct transdifferentiation, a differentiated cell acquires the transcriptional program of another cell type, usually closely related, as for example exocrine to endocrine pancreatic cells, becoming a different differentiated cell. **(d)** During indirect transdifferentiation, a differentiated cell dedifferentiates before adopting the new transcriptional program of the other cell type.

Dedifferentiation and transdifferentiation also occur in a natural way in response to an injury, or tissue loss[127]. Dedifferentiation, for example, occurs naturally during limb regeneration in the urodele amphibians. After limb amputation, cells adjacent to the wound dedifferentiate, forming a blastema that consists of undifferentiated cells that proliferate and eventually, redifferentiate into the same cell type to create all the components of the lost limb[12]. Natural transdifferentiation occurs indirectly: first, the cell dedifferentiates; and then the natural developmental program is activated, allowing the cell to differentiate into the new lineage[12]. Tsonis and collaborators described a natural mechanism of transdifferentiation in a newt. They found that when lens are removed, pigmented epithelial cells from the dorsal iris transdifferentiate, and regenerate the missing tissue. To achieve this, pigmented epithelia cells must first dedifferentiate and proliferate to create new lens cells, and then differentiate into the mature cells of the lens[13]. In both situations – dedifferentiation and redifferentiation into the same cell type or transdifferentiate to a new cell type – a complex network of signaling pathways may control the transcriptional program acquired by each cell in the perfect time-point.

Thus, the spatiotemporal control of gene expression is continuously required during animal homeostasis, and during a regenerative process. However, during regeneration, cells must re-adjust to the new situation, which requires more profound decisions at a cellular level, often including processes of dedifferentiation and transdifferentiation that during homeostasis are scarce. Moreover, during homeostasis, and especially during regeneration, not only cell fate, but a precise control of tissue or organ size is crucial. The underlying mechanism of organ size determination remained largely unknown until the past decade, when the Hippo pathway was identified as a key regulator of organ size in *Drosophila* and mammals[14–16]. Since then, the extensive research on the role of the Hippo pathway has revealed that the Hippo pathway is an intercellular communication system that regulates the growth of a tissue in response to cell-cell contact signals [17].

1.2 Cell-cell communication

"A state (phenotype) observed at a site (cell) tends to impose itself upon contiguous sites, eventually leading to a local coherence." In 1990, Phipps and collaborators proposed a model in which cells interact between them to produce and maintain a spatial organization named neighborhood coherence principle (NCP). There are several types of physical interactions between cells and extra-cellular matrix (ECM). Adherens junctions (AJ), desmosomes, and tight junctions (TJ), physically connect cells to provide a regulation within a microenvironment. Another type of junction, the gap junction, link single cells within a population. This connection allows the share of cytoplasmic ions, small regulatory molecules, and macromolecular substrates, and to promote that a collection of single cells act as a group. When gap junction channels are disrupted, single cells can escape the normal regulatory signals passing within a group of cells[18]. Following the NCP, a cell would be influenced by its neighbors when deciding whether or not to enter a division cycle. Indeed, when apoptosis is induced in a cell, the environmental signals arrive to the stem cell niche in order to increase mitosis and reestablish the homeostatic condition. The disruption of the NCP underlies tumoral transformation. For instance, if the apoptotic signals are continuously induced, two scenarios are possible: (1) the entire population eventually dies, or (2) the mitotic population increases in cell number, causing eventual resistance to the apoptotic inducer and possible progression toward a cancerous phenotype[18–20]. On the other hand, loss of mature cell-cell junction communications prevents the progeny from differentiating. This failure of the differentiating process through defective mature communication, and the further locking of cells in the proliferative mode, is also the basis of tumorogenesis and a common effect of various carcinogenic agents[19]. One example of the importance of cell communication in the tissue organization is the Notch signaling. Notch is a transmembrane receptor that mediates local cell-cell communication, and coordinates a signaling cascade. Depending on the spatiotemporal context, Notch can inhibit, delay, or induce

differentiation, and can promote apoptosis, cell division, or a static state[21]. Tissue architecture, as well as the type of signal transmitted, also influences the environment by allowing the tissue to meet homeostatic set points and providing tissue stability. So, different tissues and organisms use distinct modes of communication that reflect their unique tissue structures and functions[20].

Apart from cell-cell communication by direct cell contact, cells can also communicate through secreted molecules that enable the communication between distant cells. Those secreted molecules include proteins, small peptides, amino acids, nucleotides, etc. Most of these signal molecules are secreted from the signaling cell into the extracellular space by exocytosis. Others are released through the plasma membrane, and are exposed to the extracellular space while remaining tightly bound to the signaling cell's surface. This signal can be paracrine (acting on neighboring cells), autocrine (acting on the cell that secretes the signaling molecule), endocrine (acting on cells that are remote from the secreting cell), or electrical (between two neurons or between a neuron and a target cell)[22].

Cell-cell communication serves as an anchor in the stem cell regulation and tissue spatiotemporal organization, in order to maintain the balance between the different cell populations. Within a tissue, there are multiple relationships between cells, in which stem cells can be regulated by differentiated cells and progenitors, but also by themselves in the stem cell niche.

2.Hippo signaling pathway as a pivotal regulator of cell fate

2. Hippo signaling pathway as a pivotal regulator of cell fate

Organ growth and tissue homeostasis rely on the coordinated proliferation and differentiation of progenitor cell populations, as well as, on the appropriate death of unnecessary cells. Coordination of these events is challenging in adult organisms during their everyday homeostasis, and in regenerative processes. Initially described as an essential mechanism to limit organ size through the control of cell death and proliferation in response to cell environment; nowadays, the Hippo signaling is a cell-cell communication system considered a key regulator of cell death and progenitor cell replication, survival, and differentiation[14,15,23–29].

On this chapter, I will summarize the core elements of the Hippo pathway in *Drosophila* and vertebrates outline the mechanisms that regulate it, and describe the different outputs that are modulated by this pathway.

2.1 Hippo pathway core

The Hippo pathway core consists of a kinase cascade, that controls the phosphorylation and nuclear localization of the effector, which modulates the transcription of several genes.

2.1.1 Hippo pathway in Drosophila

Initially discovered in *Drosophila*, the Hippo signaling pathway was defined as a conserved regulator of organ size. The core of this pathway is composed by *hippo,* that encodes a Ste20 family protein kinase, which interacts with Salvador (Sav), a protein composed by two WW domains and a coiled-coil domain, to phosphorylate and activate Warts[16,30]. Previously to Warts phosphorylation, Mats (Mob as tumor suppressor), a Warts partner, is also phosphorylated by Hippo, acquiring a high affinity to Warts. The elevated affinity between these two proteins increases the catalytic activity of Warts to phosphorylate, and inhibit Yorkie (Yki), the pathway effector[24,31] (Figure I2.1a). Yki functions as a transcriptional co-activator; however it lacks its own

DNA binding domain. Scalloped (Sd) was the first DNA-binding partner of Yki described in *Drosophila* (Figure I2.1b). Although this interaction was found in *Drosophila* wing discs and promotes Yki nuclear localization, Sd is not required in all imaginal tissues. This evidence indicates that Yki-Sd interaction acts in a tissue-specific fashion, and that Yki must have other partners[32]. Indeed, it was shown that Yki can also interact with Homothorax (Hth) and Teashirt (Tsh), two DNA-binding transcription factors expressed in the uncommitted progenitor cells of the *Drosophila* eye imaginal disc[33]. Interestingly, the transcriptional response of Yki depends on the DNA-binding partner, in the way that in each tissue Yki can interact with different DNA-binding partners. For example, when Yki interacts with Sd, there is an increase in the transcriptional activation of *diap1* (*Drosophila* inhibitor of apoptosis) and *CTGF* (Connective Tissue Growth Factor). In contrast, when Yki is associated with Hth or Tsh, they up-regulate the microRNA *bantam*, promoting cell proliferation and survival with no effects in the *diap1* expression[32,33]. The identification of both Sd and Hth/Tsh as DNA-binding partners of Yki, reveals a high complexity in the Hippo signaling response. Indeed, in addition to the control in cell proliferation and cell survival, the Hippo signaling has also been related to cell determination in *Drosophila*. Chen and collaborators show that the Hippo pathway controls polar cell specification through repressing Notch activity. In this scenario, Yki is repressing polar cell fate through Notch signaling during *Drosophila* oogenesis[34].

When the Hippo pathway is active, Yki function is inhibited. The process of Yki inhibition is a complex coordination of events that starts with Yki phosphorylation by Warts on S168. This phosphorylation promotes the binding to 14-3-3 proteins, sequestering Yki in the cytoplasm to be degraded, possibly by masking the Sd binding site[32,35]. Another mechanism of Yki inhibition is through CRM1-mediated nuclear export that translocates Yki to cytoplasm after its phosphorylation, decreasing its activity[35] (Figure I2.1a). Although phosphorylation at Yki S168 is a major regulatory mechanism of Yki nuclear localization and activity, it is not the only mechanism. Yki

can also be phosphorylated at two additional sites, S111 and S250, and mutations in these two sites enhances Yki nuclear localization and activity, with no interaction with 14-3-3 proteins demonstrated[35,36]. The wide range of Yki DNA-binding partners, as well as the targets that are regulated by this pathway depending on the spatiotemporal environment, demonstrates the complexity of the Hippo pathway.

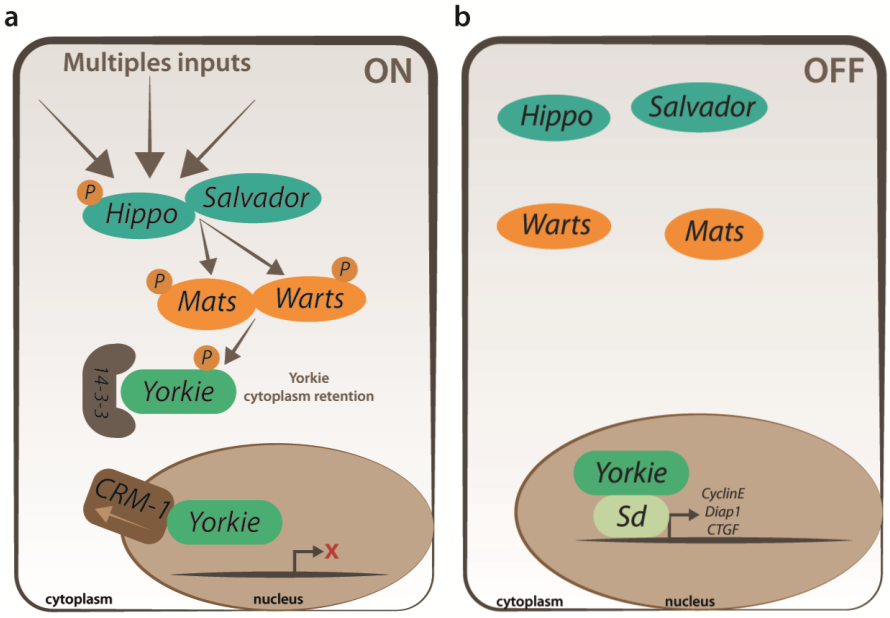

Figure I2.1: Hippo pathway in *Drosophila*.

(a) The phosphorylation of Hippo by different inputs, leads to an increasing affinity to Salvador. Together they phosphorylate Mats and Warts, which form a complex that phosphorylates Yorkie. Yorkie phosphorylation leads to an increase in its affinity to 14-3-3 proteins. This interaction sequesters Yorkie in the cytoplasm, avoiding the transcription of target genes. In addition, nuclear Yorkie can be exported by CMR-1, in order to decrease its activity. **(b)** When the Hippo pathway is silenced, the pathway core is inactive, allowing the entrance of Yorkie in the nucleus where in association with its DNA-binding partner Scalloped (Sd) to promote the transcription of the target genes.

2.1.2 Hippo pathway in vertebrates

As in *Drosophila*, Hippo signaling in vertebrates is a kinase cascade in which Mst1/2 (Hippo ortholog), in association with Salvador (also known as hWW45), phosphorylates and activates both mammalian copies of Warts, Lats1 and Lats2[37], in order to control tissue growth. At the same time, Mst1/2 also phosphorylates Mob1 (Mats ortholog) in order to enhance its interaction with Lats1/2[38]. In vertebrates, two different Yki orthologs were identified, YAP (Yes-associated protein) and TAZ (Tafazzin)[39,40]. The phosphorylation of these two transcriptional co-activators through Lats1/2, creates a 14-3-3 binding domain, leading to their cytoplasmic retention and functional inactivation[39–41] (Figure I2.2a). Several transcription factors, including TEAD (Scalloped homolog), ErbB4, Runx2, and p73, have been reported to interact with YAP or TAZ[42]. Nowadays, TEAD is the most potent YAP/TAZ DNA-binding partner. The complex YAP/TAZ-TEAD stimulates gene expression, cell growth and epithelial-mesenchymal transition (EMT)[43,44] (Figure I2.2b). Most of adult tissues express at least one TEAD member, and different TEAD members play different roles[42]. Despite the similarities between the two paralogs YAP and TAZ, the inhibition of these genes separately produces different phenotypes. Such differences can be explained by differential spatiotemporal regulation of YAP and TAZ activities, or different downstream targets[45]. In vertebrates, it was show that one of the most important targets of Hippo pathway is *CTGF*, at its downregulation blocks YAP-dependent cell growth[43]. YAP hyperactivation is also intimately related to the expansion of the stem cell compartment through the control of cell proliferation[14]. The presence of two effectors of Hippo pathway in vertebrates that have their own regulatory mechanisms and functions, confirms the complexity of this pathway.

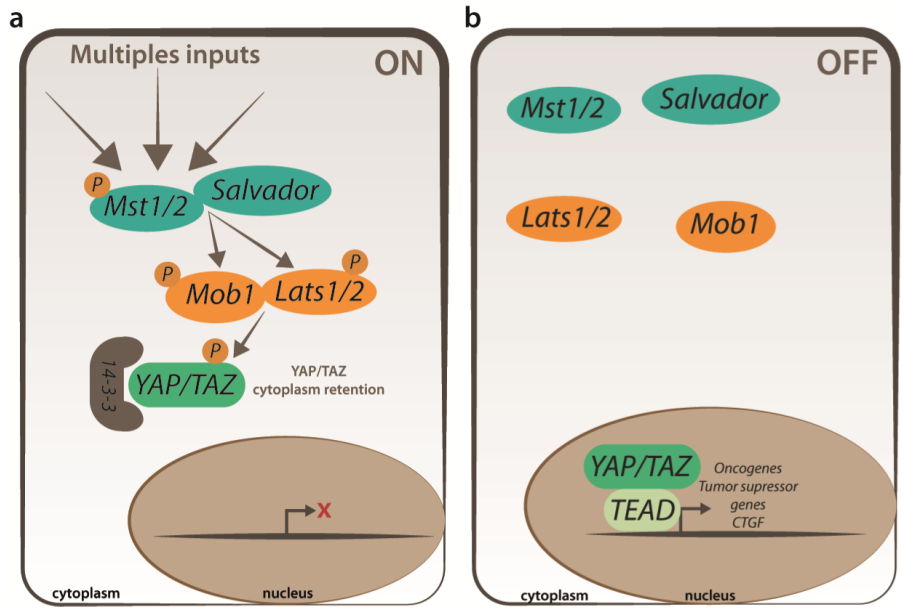

Figure I2.2: Hippo pathway in vertebrates.

(a) Mats1/2 phosphorylation by different extracellular inputs increases its affinity to Salvador. Together they phosphorylate Mob and Lats1/2, which form a complex that phosphorylates YAP/TAZ. YAP/TAZ phosphorylation leads to an increase in its affinity to 14-3-3 proteins. This interaction retains YAP/TAZ in the cytoplasm, avoiding the transcription of target genes. **(b)** When the Hippo pathway is silenced, the pathway core is inactive, allowing the entrance of YAP/TAZ in the nucleus where, in association with its DNA-binding partner TEAD to promote the transcription of target genes.

2.1.3 Other Hippo pathway elements

The Hippo pathway was named due to the *Drosophila hippo* gene (homologue of MST1/2), and *hippo* was considered the central regulatory molecule of the Hippo pathway during several years. However, in the last few years, Warts/Lats has emerged as the essential gene for Yki/YAP/TAZ regulation by virtually all signals tested, and Hippo/MST1/2 were granted a secondary role for Yki/YAP/TAZ regulation. So, a new definition of the 'Hippo pathway' should include all the proteins that specifically

influence Warts/Lats kinase activity, and the functional output of Yki/YAP/TAZ, even without the intervention of Hippo/MST1/2.

In the last years, novel elements of the Hippo pathway have been identified based on their direct role in Warts/Lats1/2 phosphorylation and activation. These elements are MAP4K family members – *Drosophila* Happyhour, homologues MAP4K1/2/3 in mammals, and *Drosophila* Misshapen, homologues MAP4K4/6/7 in mammals – that directly activate Warts/Lats1/2 independently of Hippo/Mst1/2, regulating the activity of Hippo pathway (Figure I2.3). It seems that MAP4Ks act in parallel to, and are partially redundant with, Hippo/Mst1/2 in the regulation of Warts/Lats1/2. Indeed, cytoskeleton stress restricts Yki/YAP/TAZ nuclear localization through MAPK4s when Hpo/Mst1/2 activity is compromised, providing an explanation for the Wts/Lats1/2-dependent but Hpo/Mst1/2-independent regulation of Yki/YAP/TAZ in certain contexts[46–48].

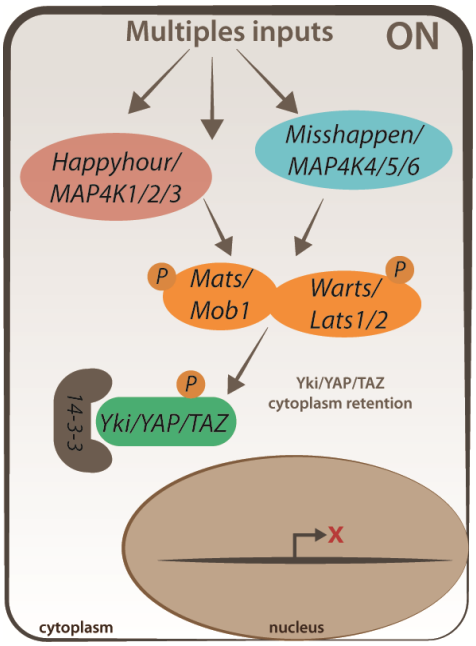

Figure I2.3: Other Hippo pathway elements. Multiple inputs activate Happyhour/MAP4K1/2/3 and Misshappen/MAP4K4/5/6, which in turn can activate the Mats/Mob1 and Warts/Lats1/2 leading to the sequestering of Yki/YAP/TAZ in the cytoplasm.

2.2 Hippo signaling regulation by multiple inputs

The up-stream regulation of Hippo signaling depends on a complex network of protein interactions and crosstalk between pathways essentially modulated by cell-cell contact, the cytoskeleton shift, and mechanical forces[41,49,50]. Thus, the Hippo pathway is considered to act as a regulator of growth in response to the cellular environment.

2.2.1 Physical cues: cell contact and mechanical forces

Tissue architecture physically restricts cell growth, and in many cases leads to cell quiescence. Cell-cell contact at high cell density produces a growth inhibitory signal mediated, in part, by the Hippo pathway. At high cell density Lats is activated, whereas at low cell density it is inactive. The increase of AJ and TJ in confluent cells contribute to activation of Lats and inactivation of YAP/TAZ, in order to control the number of cells within a tissue[41]. Indeed, different cellular models demonstrate that cells read ECM elasticity, cell shape and cytoskeletal forces, manipulating the mechanoresponde of YAP/TAZ levels according to the cell behavior. So, high levels of cytoskeletal contractility and internal cell resisting forces developed against the substratum, lead to YAP/TAZ nuclearization. On the other hand, when the external conditions impose small cell geometry and do not allow the development of actomyosin contractility, YAP/TAZ are inhibited[49–51] (Figure I2.4a). This regulation by mechanical forces requires Rho-GTPases and F-actin capping/severing proteins as mediators, and is proposed to function as a physical checkpoint of cell growth and a cell fate determination during stem cell differentiation[52]. Likewise, regulation of Hippo pathway by mechanical forces can occur by different mechanisms, such as: (1) high stretched cells can recruit core elements to adherent junctions through α-catenin or Jub, preventing the phosphorylation of Yki or YAP/TAZ[50] and (2) high stretching promotes the binding of Lasts – inhibitor to Lats1 – in a JNK-dependent manner, increasing the YAP/TAZ nuclear translocation[53] (Figure I2.4b).

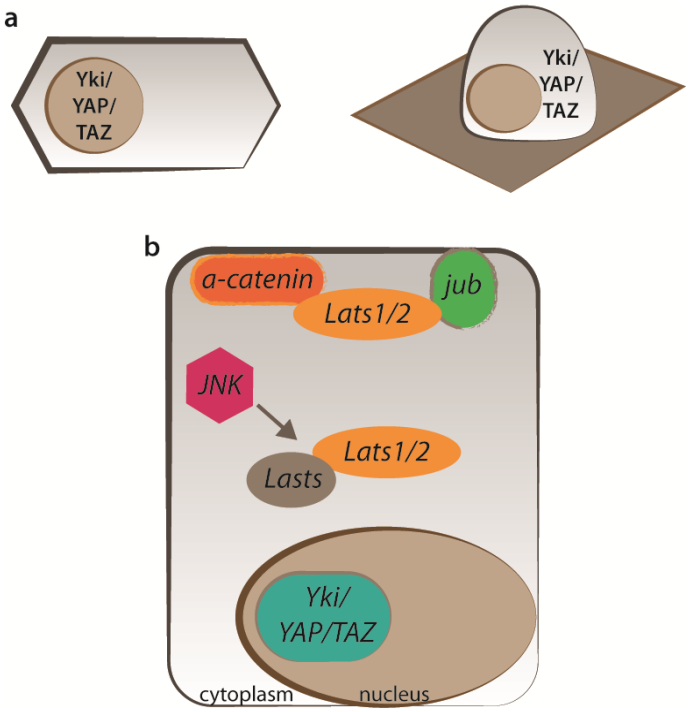

Figure I2.4: Physical cues: cell contact and mechanical forces in the control of the Hippo pathway.

(a) High levels of cytoskeleton tension leads to the Yki/YAP/TAZ nuclearization. In contrast, when the cytoskeleton tension is soft, Yki/YAP/TAZ became sequestered in cytoplasm. **(b)** In situations of high cell tension, α-catenin and Jub proteins recruit the core elements of pathway to the cell membrane, allowing the entrance of Yki/YAP/TAZ in the nucleus. At the same time, Jnk promotes the binding of Lats1/2 with its inhibitor Lasts.

2.2.2 Up-stream gene regulators

Epithelial cells usually adhere to one another through cell-cell junctions such as AJs, desmosomes, and TJs. AJs and TJs, together with different polarity complexes, divide the plasma membrane into an apical domain and a basolateral domain, and thereby establish an apical-basal polarity in epithelial cells[54]. Interestingly, many upstream regulators identified for the Hippo pathway are known components of TJs, AJs, or apical-basal polarity protein complexes.

One example of apical regulator of Hippo pathway is the Merlin/Expanded/Kibra protein complex. Merlin, (NF2 in mammals) functions as an adaptor protein with a FERM domain to transduce a growth-regulatory signal. In *Drosophila*, Merlin acts as a negative regulator of growth, where it functions with Expanded, a related FERM domain protein. Both are components of the Hippo signaling pathway that restrict cell and tissue growth through the control of cell cycle, proliferation, and cell death[55,56]. This complex is also formed by Kibra, a WW-domain-containing protein and Crumbs, a transmembrane protein. Kibra associates with Merlin and Expanded stabilizing the Merlin/Expanded interaction[57]. Crumbs has a large extracellular domain, and a short intracellular domain. The short intracellular domain contains a FERM-binding motif (FBM) that can interact with Expanded. This interaction modulates Expanded localization and stability, regulating the activity of Hippo pathway[58]. Merlin/Expanded/Kibra protein complex can be regulating the Hippo cascade from two different mechanisms: (1) through the direct binding to Hippo and Salvador, recruiting them to the apical domain, promoting its activation[59] (Figure I2.5a) or (2) though the binding to Warts, recruiting it to the plasma membrane promoting Warts phosphorylation by the complex Hippo/Salvador[60,61] (Figure I2.5b).

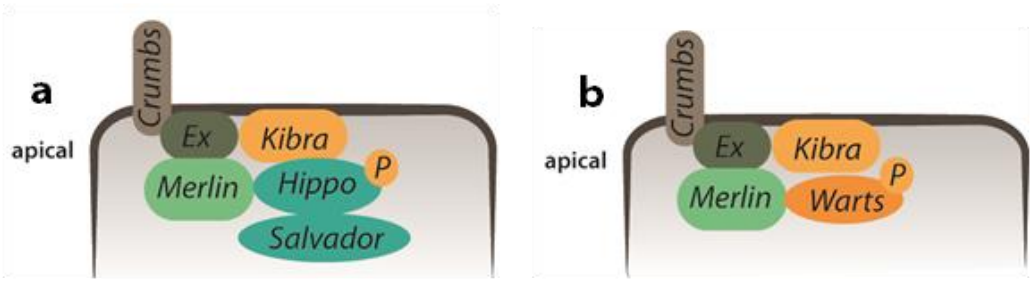

Figure I2.5: Up-stream regulators of the Hippo pathway.
Crumbs, Expanded (Ex), Merlin and Kibra form a regulator complex of Hippo pathway in the apical cell membrane. This complex can be regulating the Hippo pathway by two different paths: **(a)** They recruit Hippo and Salvador to the apical membrane, promoting its activation or **(b)** Recruiting Warts, facilitating its phosphorylation by Hippo and Salvador.

2.2.3 Negative Regulators

Hippo pathway regulation can also be done by direct negative regulators that inhibit the pathway core, promoting the activation of the effector Yki/YAP/TAZ. As referred to before, apicobasal cell polarity regulates Hippo pathway, thus Par apical complex – located in the apical domain of the cell – and the Scrib/Dlg/Lgl (Scribble/Discs large/Lethal giant larvae) complex – located in the basal domain – form a negative regulatory mechanism of Hippo pathway. Therefore, Par complex induces the activity of Yki by the inhibition of core elements of Hippo pathway. In turn, Scrib/Dlg/Lgl complex antagonizes the function of the Par complex, resulting in a decrease of Yki activation[58,62] (Figure I2.6a).

The Hippo pathway is also regulated by the mammalian Ajuba proteins (Ajuba, LIMD1, WTIP) or *Drosophila* dJub. These proteins are cytosolic adapters that exhibit the potential to communicate cell adhesive events with nuclear responses to remodel epithelia. It was shown that Ajuba/dJub proteins interact with Lats/Wts, inhibiting them and consequently, allowing the YAP/Yki nuclearization. There are two proposed

models by which Ajuba/dJub proteins can act (1) though the association of Ajuba/dJub with α-catenin promoted by cytoskeletal tension, recruiting and inhibiting Lats/Warts to junction in a tension-dependent manner and/or (2) through JNK phosphorylation, where Ajuba/dJub phosphorylated proteins increases their binding with Lats/Warts, thereby preventing their activation by Hpo/Mst1/2[63–65] (Figure I2.6b).

Another mechanism of Warts regulation is made through Fat (Ft), a protocadherin, and Dachsous (Ds), a related protocadherin. They bind each other acting as receptor (Ft) and ligand (Ds)[66]. Inhibition of Ft through Approximated (App) promotes the localization of atypical myosin Dachs to apical domains. This translocation promotes the binding Dachs/Zyxin (sub-apical protein) which increases the affinity of Zyxin to Warts. Finally, the interaction Zyxin/Warts promotes Warts degradation, increasing the activity of Yki[66–68] (Figure I2.6b).

RASSF family proteins are also involved in the inhibition of Hippo signaling. In this case the mammalian RASSF or *Drosophila* RASSF ortholog (dRASSF) restricts Hippo signaling activity binding to Hippo/Mst1/2. This interaction between RASSF and Hippo/Mst1/2 competes with the Salvador, preventing the phosphorylation of Warts/Lats1/2 and thus Yki inhibition[69] (Figure I2.6b).

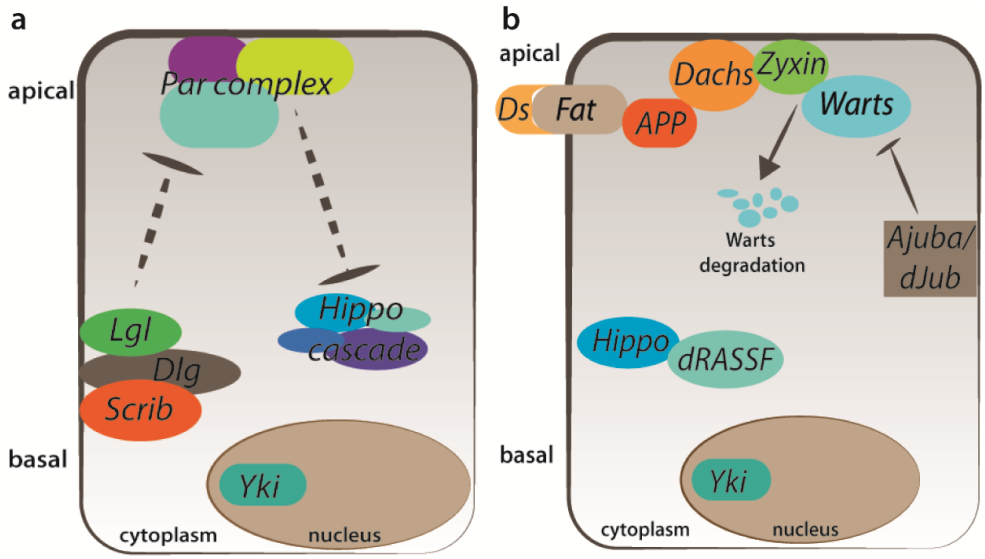

Figure I2.6: Negative regulators of the Hippo pathway.

(a) Par complex located in the apical membrane inhibit the core elements of Hippo pathway, allowing the entrance of Yorkie in the nucleus. Under different signals, the complex formed by Lgl/Dgl/Scrib inhibits the signal of Par complex, allowing the activation of Hippo pathway elements. **(b)** Fat/Ds complex is inhibited by APP, which recruits to the apical membrane Dachs. Dachs interacts with Zyxin, increasing its affinity to Warts, promoting its degradation. In the same direction, Ajuba/dJub can also inhibit Warts. dRASSF acts as a competitor of Salvador, binding to Hippo. In all these scenarios, Yorkie increase its nuclearization, promoting the transcription of its target genes.

2.2.4 Yorkie/YAP/TAZ specific-regulators

Direct regulators of Yki/YAP/TAZ have been described in a Hippo-independent manner, promoting or preventing its translocation to nucleus. One of the direct regulators of YAP/TAZ activity are the Angiomotin (AMOT) proteins, which interact extensively with multiple TJ components being important for TJ integrity and epithelial cell polarity. AMOT proteins recruit YAP/TAZ to TJs, which consequently results in reduced YAP/TAZ nuclearization and activity (Figure I2.7). In addition, AMOT proteins also induce YAP/TAZ phosphorylation at Lats target sites. An ortholog of

AMOT in *Drosophila* has not been identified; suggesting that regulation of AMOT on the Hippo pathway may be different between *Drosophila* and mammals[70]. Conversely to AMOT, zona occludens-2 (ZO-2) protein interacts with YAP using its PDZ-binding motif, promoting YAP nucleus translocation[71]. Intriguingly, ZO-2 is a negative regulator of TAZ, preventing is translocation to the nucleus[72] (Figure I2.7). This evidence reveals different regulation mechanisms between YAP and TAZ.

An inhibitory role of α-catenin on YAP activity has also been reported, and this is mediated by 14-3-3. Unlike AMOT, the phosphorylation of YAP at S127 is required for interaction with α-catenin because 14-3-3 only binds to phosphorylated YAP. The trimeric complex of α-catenin, 14-3-3 and YAP sequesters YAP to AJs and prevents YAP activation[73] (Figure I2.7). Another AJ component, protein tyrosine phosphatase 14 (PTPN14), has also been shown to be a regulator of the Hippo pathway. PTPN14 can directly interact with YAP, resulting in cytoplasmic localization of YAP and thus decreasing its activity[62] (Figure I2.7).

Surprisingly, Expanded also regulates Yki directly. Expanded binds to Yki at endogenous levels via WW-domain-PPxY interactions, independently of Yki phosphorylation at S168, which is critical for 14-3-3 binding. Expanded functions downstream of Warts, in concert with 14-3-3 proteins to sequester Yki in the cytoplasm, inhibiting growth activity of the Hippo pathway[74] (Figure I2.7).

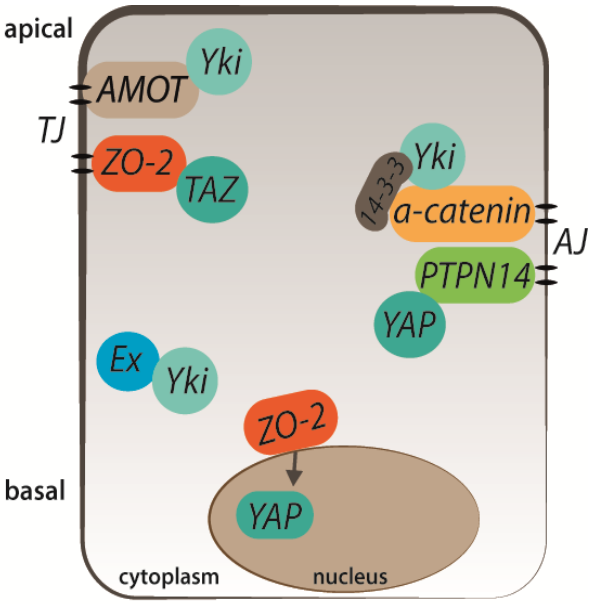

Figure I2.7: Yki/YAP/TAZ specific regulators.

In the apical cell membrane, AMOT and ZO-2 are recruited to the tight junctions (TJ) who in turn, recruit Yki or TAZ, respectively, inhibiting them. In the adherent junctions (AJ) α-catenin, together with 14-3-3 proteins, and PTPN14 recruit Yki or YAP, respectively, retaining them in the cytoplasm. Expanded (Ex) also interacts with Yki, inhibiting its nuclearization. Contrary to the function that plays with TAZ, ZO-2 promotes the nuclearization of YAP.

2.2.5 Other regulations (Stress signals, Soluble factors and G-protein-coupled receptors (GPCRs))

Control of cell death is one of the most important mechanisms regulated by Hippo signaling. Accordingly, Hippo pathway can be responsible for inducing cell death after DNA damage, preventing the accumulation of mutations that can give rise to tumoral progression. In this context, after ionizing irradiation, Hippo is phosphorylated in a p53-dependent manner in order to activate the pathway, and induces the cell death by the decrease of *Diap1*[75] (Figure I2.8a). In addition, energy stress caused by glucose deprivation rapidly induces YAP/TAZ phosphorylation due to Lats1/2 activation, in order to limit the cell proliferation in the absence of nutrients[50].

Soluble factors can also inhibit Hippo pathway signaling, namely the mitogenic growth factors. Epidermal Growth Factor Receptor (EGFR) inhibits the Hippo pathway through activation of PI3-kinase (PI3K) and phosphoinositide-dependent kinase (PDK1), but independent of AKT activity. The entire Hippo core complex dissociates in response to EGF signaling in a PI3K-PDK1–dependent manner, leading to Lats inactivation, YAP dephosphorylation, and transcriptional activation of its target gene, CTGF[76] (Figure I2.8b).

A series of studies further demonstrate that regulation of the Hippo pathway by GPCRs is indeed a universal response of cells to hormonal cues. Therefore, depending on the nature of downstream G proteins, GPCRs can both activate or inhibit the Lats kinase to stimulate or suppress YAP activity. For example, estrogen acts through G protein-coupled estrogen receptor (GPER) to inhibit Lats, promoting the activation of YAP/TAZ, indicating a possible role of YAP/TAZ activation through estrogen in breast cancer[77] (Figure I2.8b).

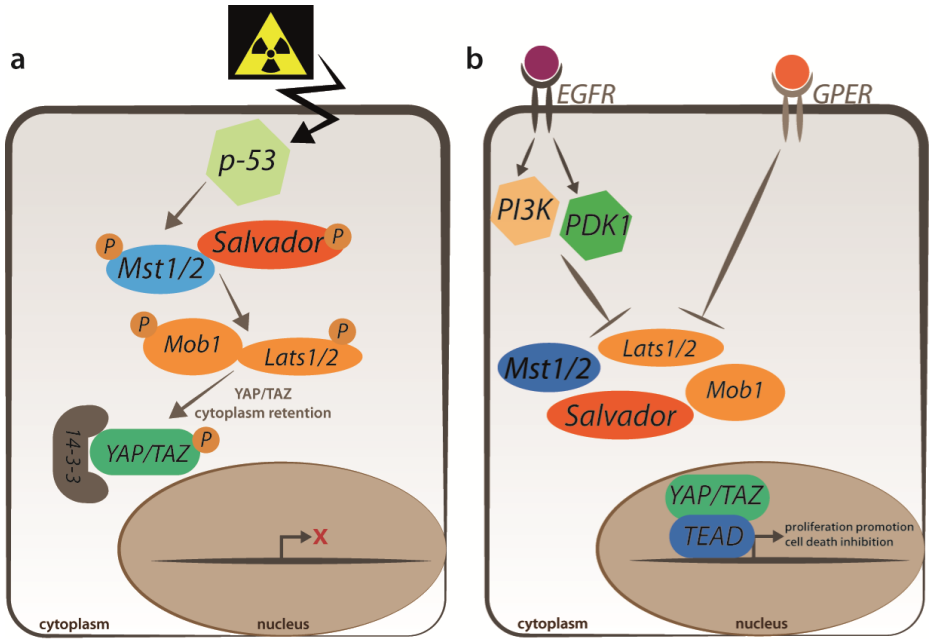

Figure I2.8: Other mechanisms of the Hippo pathway regulation.
(a) Irradiation activates p-53, which in turn activates the Hippo pathway core elements, retaining YAP/TAZ in the cytoplasm, promoting cell death. **(b)** Different signaling pathway as EGFR and GPER can inhibit the Hippo pathway cassette, increasing YAP/TAZ nuclearization.

Synopsis

Although some mechanisms by which these regulators control Hippo signaling are not totally clear, all these results indicate that cell-cell contact, integrity of cell junctions, and apical-basal polarity are important in regulation of the Hippo pathway. Apical-basal polarity can regulate the Hippo pathway by either recruiting the Hippo pathway kinases to the apical domain for activation, or sequestering Yki/YAP/TAZ at cell junctions, both resulting in inactivation of Yki/YAP/TAZ. Furthermore, cells have direct paths to control Yki/YAP/TAZ in a Hippo-independent manner, maybe in an exigent context where cells need to inhibit or translocate Yki/YAP/TAZ to nucleus in a very quick way.

2.3 Targets of the Hippo signaling pathway

The Hippo pathway is involved in a wide variety of physiological processes, such as cell death, proliferation, differentiation, and cell determination. To promote the transcription of specific genes for each process, cells need to acquire the proper transcriptional program. As described above, the interaction of Yki/YAP/TAZ with different DNA-binding partners will define the pathway target genes. This decision depends not only on the cell type, but also the spatiotemporal environment. The link of Yki/YAP/TAZ with different transcription factors can also occur within the same cell. Although how this association is modulated, and which factors can influence it, are not totally understood. One possibility is the context-dependent post-translational modifications of Yki/YAP/TAZ that allows a selective choice of interaction partner[44].

An important function of the Hippo pathway seems to be the inactivation of Yki/YAP/TAZ in differentiated cells to maintain cell quiescence. Upon tissue injury, the Hippo pathway is suppressed, and Yki/YAP/TAZ are activated to promote stem/progenitor cell self-renewal and tissue repair. Consistently, Yki/YAP/TAZ activity is required for injury-related proliferation of stem cells and cell migration to promote wound healing[50,78].

The coordination and balance between cell proliferation and apoptosis are crucial for normal development and tissue homeostasis. In the context of growth control by Hippo pathway, we can consider distinct types of down-stream target genes, autonomous, and non-autonomous. Autonomous growth promoting targets of Yki/YAP/TAZ include, genes that promote cellular growth (*Myc*, *bantam, CTGF*), genes involved in cell cycle progression (*CyclinB*, *CyclinD*, *CyclinE*, *E2F1*), and inhibitors of cell death (*Diap1, clap1*)[79]. Non-autonomous growth promoting targets include genes that encode ligands for other signaling pathways. In *Drosophila*, the Wnt pathway ligand Wg is regulated by Hippo signaling (namely by *Fat* and *Dachous*) in the proximal wing, where it is a major contributor to growth regulation[80]. Indeed, Notch and EGFR

signaling pathways can also be regulated by *Fat* in some contexts[81,82]. The importance of non-autonomous growth promoting targets in vertebrates has been emphasized by the discovery of YAP ability to transform breast epithelial cells though up-regulating the expression of the EGFR ligand amphiregulin, promoting cell proliferation, and migration[83]. Thus, the biological effects of Yki/YAP/TAZ on growth control *in vivo* appear to reflect a combination of autonomous and non-autonomous effects, which is cell type-dependent.

2.4 Role of the Hippo signaling during embryogenesis and regeneration

As referred to before, the Hippo pathway controls tissue growth in response to multiple inputs that depend on the tissue and organ context. Therefore, the Hippo signaling is essential during animal embryogenesis, regeneration, and homeostasis. In general, during embryonic development, Yki/YAP/TAZ activity is high, but soon declines to basal levels after birth. Similarly, after tissue injury, Yki/YAP/TAZ are immediately activated in a transient manner, promoting expansion of progenitors, or dedifferentiation of mature cells, to facilitate tissue regeneration. In the following sections, I will describe the function of the Hippo pathway during embryonic development and in regenerative contexts, in different model organisms, and organs.

2.4.1 Drosophila

During *Drosophila* nervous system development, neural stem cells (NSCs) remain quiescent at early larval stages, and proliferate at embryonic and adult phases. Hippo pathway has been shown to play an important role in the control of NSCs quiescence. Yki is silenced when NSCs are quiescent, but relocates to the nucleus to regulate NSCs proliferation and growth during NSCs reactivation[84]. Suppression of Hippo pathway upstream regulators leads to premature exit from quiescence and NSCs reactivation, demonstrating a role of Hippo pathway in the restriction of NSCs proliferation during postembryonic neurogenesis in *Drosophila*[84–86].

In the *Drosophila* midgut, Yki expression is largely restricted to intestinal stem cells (ISC). Under homeostatic conditions, Yki is mostly located in the cytoplasm, and seems to be inactive. Contrastly, in response to an injury, Yki nuclear localization and an increase on its activity, has an important and cell-autonomous role in ISC proliferation[87]. Interestingly, the Hippo pathway also has a non-autonomous function during regeneration. Loss of Hippo signaling in ISCs increases the production of multiple EGFR ligands that activate JAK-STAT and EGFR signaling pathways to stimulate their proliferation, revealing a unique non-autonomous role of Hippo signaling in blocking ISC proliferation[88]. In developing *Drosophila* imaginal discs, tissue ablation leads to Yki nuclear localization. Grusche *et al*. found that Yorkie plays a crucial role in the post-wounding proliferation, and that Yki was rate-limiting for wing regeneration. Yki hyperactivation is achieved through Warts inhibition in a Ft–Ds-dependent manner[89].

These data claim Hippo pathway as an essential mediator for proper development and tissue regeneration in *Drosophila*.

2.4.2 Mammalian intestine

Mice regenerating intestinal crypts express elevated YAP protein levels. Inactivation of YAP causes no obvious intestinal defects under normal homeostasis, but severely impairs intestinal regeneration[25]. Furthermore, transient activation of YAP after an intestine injury, reprograms Lgr5+ ISCs by inhibiting the Wnt homeostatic program, inducing a regenerative response by cell reprogramming[90]. In contrast, an inhibitory role for YAP in intestinal regeneration has been observed in another study: overexpression of YAP in the mouse intestine leads to the loss of proliferative crypts, and its knockout results in hyperplastic crypts. In this scenario, loss of YAP increases Wnt target genes, leading to expansion of ISCs and Paneth cells[91]. Considering the important role that Wnt signaling play in ISCs, the discrepancy between this study and

others may be due to the differences in the extent and duration of Wnt inhibition by YAP/TAZ.

2.4.3 Liver

During liver development, Hippo pathway modulates liver cell lineage specification and proliferation. Furthermore, hyperactivation of YAP/TAZ forces hepatoblasts to commit to the biliary epithelial cell (BEC) lineage. It increases BEC by up-regulating TGF-β signaling, but suppresses hepatoblast differentiation into hepatocyte by repressing *hnf4-α* expression[92].

During liver regeneration, YAP over activation drives to a clonal expansion, suppressing hepatocyte differentiation, and promoting a progenitor phenotype. Interestingly, YAP activation is insufficient to promote growth in the otherwise normal tissue. Using a mosaic mouse model, it was shown that YAP overexpression in a fraction of hepatocytes does not lead to their clonal expansion, as proliferation is counterbalanced by increased apoptosis. These results suggest that YAP activation is insufficient to promote growth in the absence of a second signal, thus coordinating tissue homeostasis and repair[93].

These results demonstrate that Hippo pathway is important for a proper liver development, regeneration, and homeostasis.

2.4.4 Skin

During early mouse embryonic stage, YAP is highly activated in the early embryonic epidermal progenitors, playing an essential role in the expansion of progenitor's population and the development of the epidermis. Deletion of YAP at early embryonic stage causes lethality, the skin of these mice is thinner and deficient in epidermal tissue, and a reduction of both progenitor cells and proliferative basal cells are also observed[94]. Conversely, YAP hyperactivation significantly increased proliferation of basal epidermal progenitors, a thicker epidermis, and hyperkeratinization of skin[73].

Epidermal wound healing, and differentiation of epidermal progenitors, are also affected by high levels of YAP nuclear protein. YAP silencing leads to a reduction of cell growth, inhibition of keratinocyte differentiation, and delay in wound healing. On the other hand, terminal differentiation of keratinocytes is blocked in cells with high YAP activity[73,94].

Thus, these studies demonstrate that YAP activity is crucial for the formation of the skin during embryogenesis, as well as to maintain epidermal homeostasis and its wound healing.

2.4.5 Heart

Heart growth is strictly restricted, and can be generally divided into two phases: 1) fetal heart growth, which is mainly due to the proliferation of cardiomyocytes; and 2) soon after birth, in which cardiomyocytes stop proliferating, and heart size is principally controlled by the size of cardiomyocytes. During embryonic development, depletion of YAP blocks cardiomyocyte proliferation, causing myocardial hypoplasia and lethality. In contrast, YAP overexpression increases cardiomyocyte number and heart size[95].

Several studies have shown that the Hippo pathway plays an important role in maintaining basal heart homeostasis, and regulating cardiomyocyte proliferation and cardiac regeneration[78]. A couple of studies define Hippo signaling as an endogenous repressor of adult cardiomyocyte renewal and regeneration. Forced expression of a constitutively active form of YAP in the adult heart stimulates cardiac regeneration through adult mouse cardiomyocytes proliferation, and also improves contractility after myocardial infarction. In contrast, cardiac-specific deletion of YAP impedes neonatal heart regeneration, resulting in a default fibrotic response[96,97]. Postnatal cardiac-specific activation of YAP drives cardiomyocytes proliferation, improving the heart function and survival after myocardial infarction. Surprisingly, long-term YAP

activation did not cause cardiac hypertrophy[98]. Conversely, cardiomyocyte-specific inactivation of YAP in the postnatal heart increase myocyte apoptosis and fibrosis, dilated cardiomyopathy, and leads to premature death[99]. These findings reveal that YAP is a critical factor for embryonic heart development, and basal heart homeostasis.

2.4.6 Nervous system

Neural stem cells (NSCs) are capable of self-renewal, and generate multiple neuronal and glial lineages, in both fetal and adult nervous systems in mammals. It was shown that YAP is undetectable in neurons, but selectively expressed NSCs and astrocytes, being required for astrocytic proliferation. In homeostatic conditions, YAP hyperactivation decreases neuronal differentiation and drives to an expansion of the neural progenitor cell population, which in part is due to the up-regulation of stemness genes such as cyclin D1. In the opposite direction, repression of either YAP or TEADs in the neural tube causes a significant increase in cell death, cell cycle exit, and differentiation of neuronal cells[15,100].

2.4.7 Lung

The importance of the Hippo pathway in the cell fate, and the maintenance of cell determination, has been highlighted in the last few years, namely in mammalian lung. During mouse development in the airway progenitors, YAP is required for *sox2* expression, which is essential for progenitor's response to TGF-β and initiation of the airway epithelial fate. However, to complete the differentiation process into distinct cellular phenotypes, YAP should be retained in cytoplasm[28]. Also in lung, but in differentiated airway secretory cells, YAP overexpression causes a partially reprogramming of these cells, inducing them to adopt a stem cell-like identity[101].

2.4.8 Mammary gland

The spatiotemporal regulation of Hippo pathway depends on stage-specific requirements of the tissue or organ. One clear example occurs during mammary

development. Hippo pathway is dispensable in virgin mammary glands, but specifically required during pregnancy, when mammary epithelia undergo rapid growth and terminal differentiation. In this scenario, YAP hyperactivation fails to induce hyperplasia, but mammary epithelial cells fail to undergo terminal differentiation. Interestingly, although inactivation of YAP causes no obvious defects in virgin mammary glands, it potently suppresses tumor growth and metastasis[102].

2.4.9 Cell culture

Several studies performed in cell cultures described the Hippo pathway as a novel barrier to reprogramming cells into the pluripotent stem cell state. It was shown that the inhibition of Lats1/2 enhances the generation of fully reprogrammed induced pluripotent stem cells (iPSCs), increasing the expression of pluripotency markers: Oct4, Sox2 and Nanog[103]. A more complex scenario was observed in mouse embryonic stem cells (mESCs) cell culture depleted from Lats1/2. In this case, cells are not able to properly acquire the transcriptional program, and retain bivalent chromatin marks for developmental genes and stem cell-genes, when exposed to differentiated signals. In mESCs Lats-dependent resolution of bivalency and maintenance of epigenetic order is crucial to avoid "confuse" developmental messages and cell plasticity[104]. Furthermore, recent studies suggest that YAP is dispensable for self-renewal, but required for differentiation of embryonic stem cells (ESCs). Moreover, knockdown or knockout of YAP does not alter ESC self-renewal, but impairs their differentiation[105,106]. Together, these results reveal a potent role for Hippo signaling in the control of cell fate and cell reprogramming.

Synopsis

A tight relationship between stem cell proliferation, the proper differentiation of progenitor cells, and cell death is a challenging issue during embryogenesis, regeneration and homeostasis. In the last years, Hippo pathway has been emerging as an essential mechanism in the control of progenitor's differentiation towards differentiated cells. In the most of described cases, Yki/YAP/TAZ nuclearization is necessary for the expansion of stem cells, promoting the transcription of genes involved in proliferation, and then Yki/YAP/TAZ phosphorylation and citoplasmatic retention is necessary and crucial for a proper cell differentiation[23,28,29,102,104]. In addition, a proper spatiotemporal location of Yki/YAP/TAZ is essential for the control of cell fate and acquisition of correct transcriptional program. Furthermore, it was shown that hyperactivation of Yki/YAP/TAZ boosts the regenerative ability. Overall, these evidences confirm Hippo signaling as a crucial pathway in the control of stem cell population, its proper differentiation into progenitors by the acquisition of correct transcriptional program, and to terminally differentiate into the different cell populations through the spatiotemporal nuclearization of Yki/YAP/TAZ (Figure I2.9).

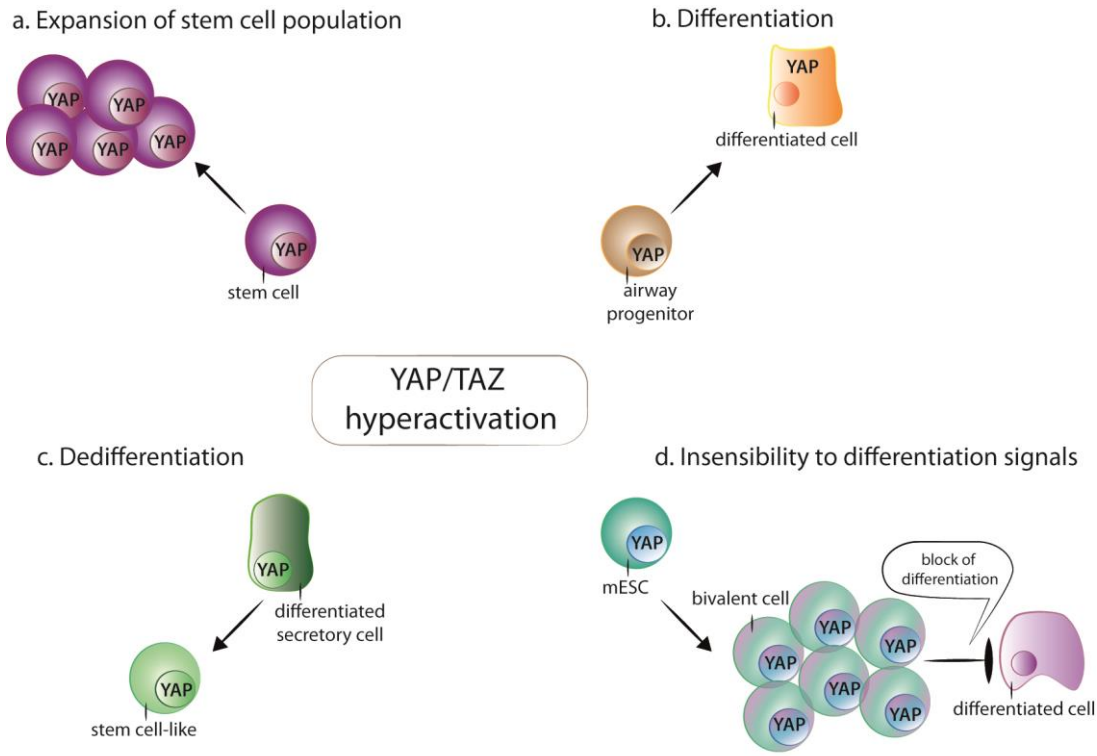

Figure I2.9: Hippo pathway outputs.

(a) Overexpression of YAP in the stem cell nucleus increases cell proliferation, leading to the expansion of this population. **(b)** Airway progenitors present high levels of YAP nuclearization crucial to initiate the differentiation process. During this process, YAP should be translocated to the cytoplasm to allow a correct differentiation. **(c)** Differentiated secretory cells submitted to high levels of YAP are able to de-differentiate and acquire stem cell markers. **(d)** Mouse epithelial stem cells (mESC) depleted from Lats1/2 do not recognize properly the differentiation signals, giving rise to a poorly committed population that express stem cell, progenitors and differentiation markers. In this scenario the differentiation is compromised.

2.5 Role of Hippo Signaling in Cancer

The Hippo signaling is controlled by a wide range of mechanisms such as cell-cell contact, ECM, and the microenvironment within the tissue or organ. Therefore, this pathway is able to sense and respond to the physical organization of cells, and changes in the environment promote different responses. As referred to before, nuclearization of Yki promotes the expansion of the stem cell population, enables dedifferentiation, and controls specific cell fates. These outputs are intimately related to tumoral transformation and involve the Hippo pathway with the most of human cancers[107] . Tumoral transformation generates niches that are different to those found in non-neoplastic tissues in which cell-cell communication is loss[108]. In this scenario YAP/TAZ translocates to nucleus promoting principal cancer features such as cancer stem cell (CSCs) properties, increase of genomic instability, EMT, increased migration, resistance to anoikis (apoptosis induced by insufficient attachment of cells to a substrate) and increased potential for metastasis, promoting the development and sustainability of neoplasia[107,109–112]. Inactivation of YAP/TAZ in a variety of cancer revert the principal features of cancer cells, providing evidences for the therapeutic benefits of YAP and TAZ inhibition in cancer[107]. In breast cancer, TAZ has been shown to be a potent stimulator of CSCs. TAZ activation, but not YAP, in non-CSCs could reactivate their self-renewal potential, suggesting that TAZ levels may regulate cell plasticity during cancer development[110]. However, the role of YAP in promoting cancer-like properties in non-transformed mammary epithelial cells was also reported[113]. Given that YAP and TAZ promote pluripotency in other stem cell contexts it is likely that their hyperactivation also contributes to stem cell expansion, survival and self-renewal in other malignancies.

Although YAP behaves as an oncogene in several cancers, recent data suggest an interesting hypothesis that YAP also has tumour suppressor functions in certain contexts. As referred to above, loss of YAP during mouse intestine regeneration led to WNT hypersensitivity with subsequent stem cell expansion and hyperplasia, whereas

transgenic overexpression of YAP restricts WNT signals and decreases proliferation[91]. DNA damage also confers pro-apoptotic characteristics to YAP. After a damage, activated YAP interacts with p73 through JNK-dependent manner supporting the transcription of pro-apoptotic genes, such as BAX and PUMA, ensuring genomic estability[45,107]. A possible explanation for the conflicting cancer-related functions of YAP is that it can form complexes with various transcription factors. These selective modulation produces distinct functions, which might be differentially altered in distinct types of cancers. More speculatively, YAP and TAZ may differentially contribute to tumorigenesis by binding to various partners, depending on the cellular context. This flexibility adds an extra level of complexity to the regulation of cancer by YAP and TAZ in different tissues.

As mentioned before, YAP/TAZ protein levels and nuclear localization are elevated in many human cancers, and YAP/TAZ hyperactivation mainly drive to the acquisition of several important cancer cell phenotypes. However, the mechanism of Hippo pathway de-regulation and YAP/TAZ activation in human cancers is not well understood. Surprisingly, mutations in Hippo pathway core genes were found in few cancers. In contrast, there is increasing evidence implicating epigenetic silencing as a prevalent mechanism of inactivating Hippo pathway tumor suppressor genes. Besides the frequent hypermethylation of RASSF family genes in human cancers, hypermethylation of Mst1/2 (in soft tissue sarcoma) and Lats1/2 (in astrocytoma and breast cancers) leading to a decrease in their expression has also been reported[42]. In addition, YAP/TAZ hyperactivation during tumorogenesis can also be due to mutations in proteins that are implicated in regulation of the Hippo pathway, such as Ajuba (in head and neck squamous carcinoma), or GPCRs and their cognate G proteins[114,115]. Hence, current evidence suggests that multiple mechanisms contribute to the deregulation of YAP and TAZ in human cancers, including hypermethylation and amplification, rather than specific mutations in the Hippo pathway core elements.

Therefore, direct or indirect attenuation of YAP and/or TAZ represents a rational and novel targeted approach for treatment and prevention of human malignancies

.

3.Planarians as a model organism to study growth control

3. Planarians as a model organism to study growth control

Planarians are bilaterally symmetric platyhelminthes, members of the superphylum lophotrochozoa. There are terrestrial, marine, and freshwater planarians. They prey predominantly upon injured insects, insect larvae, and other invertebrates. Planarians are tripoblastic and acoelomated animals that lack circulatory, skeletal, and respiratory systems. These animals have the amazing ability to restore any missing part of their body after an amputation in a few days[116,117]; and to grow and degrow depending of the environmental conditions and food availability[118]. These characteristics are due to the presence of an adult stem cell population – called neoblasts – that is able to give rise to any planarian cell type[116,117]. The high regenerative capacity of planarians, with the presence of a unique totipotent stem cell system, provides an ideal model for studying cell renewal, regeneration, and stem cell regulation.

In the last years, considerable progress has been made in understanding the biology of planarian stem cells, their progeny, and the fundamentals of the regenerative process. Nowadays, there are clear clues about how early events in neoblast differentiation and maintenance are controlled, as well as working models of how axial polarity and fate might be determined during planarian regeneration. Nonetheless, detailed mechanistic descriptions are still missing. One emerging theme from planarian research is the continuous relationship between the stem cell, the postmitotic cell compartment, and the differentiated cells. The pathways and signals that underlie the coordination between these three cell populations remain largely unknown.

3.1 Schmidtea mediterranea

The specie of study in the present work is *Schmidtea mediterranea*, which is a freshwater planarian. Normally freshwater planarians reproduce either asexually by transverse fission, or sexually, as cross-fertilizing hermaphrodites[119]. However, some

species present only one type of reproduction, and others can alter their reproduction depending of the year season[120,121]. *Schmidtea mediterranea* is the most common planarian used in molecular biology to perform regeneration and stem cell studies, because it presents special features that optimize research. Within these characteristics we have found: (1) some strains can reproduce both sexual and asexually, allowing the study of the genetic basis that regulates both types of reproduction; (2) there is a strain that only reproduces asexually, and shows a extremely good regenerative ability, which is the one mainly used for regeneration studies; (3) it is easy to maintain a stable clonal line due to their robust ability to regenerate, allowing a uniform genetic background minimizing the experiment's variability; (4) the genome is available[122], although it is not completely annotated, as well as several transcriptomes, facilitating the search of homolog genes [123–126] and (5) different molecular techniques as interference RNA (RNAi)[127], gene expression analysis by *in situ* hybridization[128,129] and fluorescence-activated cell sorting (FACS) to separate different cell populations[130] have been developed.

During this PhD thesis, I used the asexual strain of *S. mediterranea* as model animal, since the main aim of this work was the study of adult development. Animals from this specie present a brownish color, and measure between 3-8 mm in longitude. In special circumstances of low temperature they can reach 20-25 mm. They have two eyes in the most anterior-dorsal part, and a mouth in the middle part of the ventral region, which is the only digestive orifice (Figure I3.1a). Planarians use their mouth either to feed or to expulse waste. When they feed, a pharynx is extended from its gastrovascular cavity to capture the food (Figure I3.1b). Planarian reproduction depends of several factors such as; population density, temperature, animal size, and light/darkness cycles[131–133]. During the process of asexual reproduction, animal tail clings to the substrate, and the anterior part moves in the opposite direction, until fission occurs, giving rise to two new fragments.

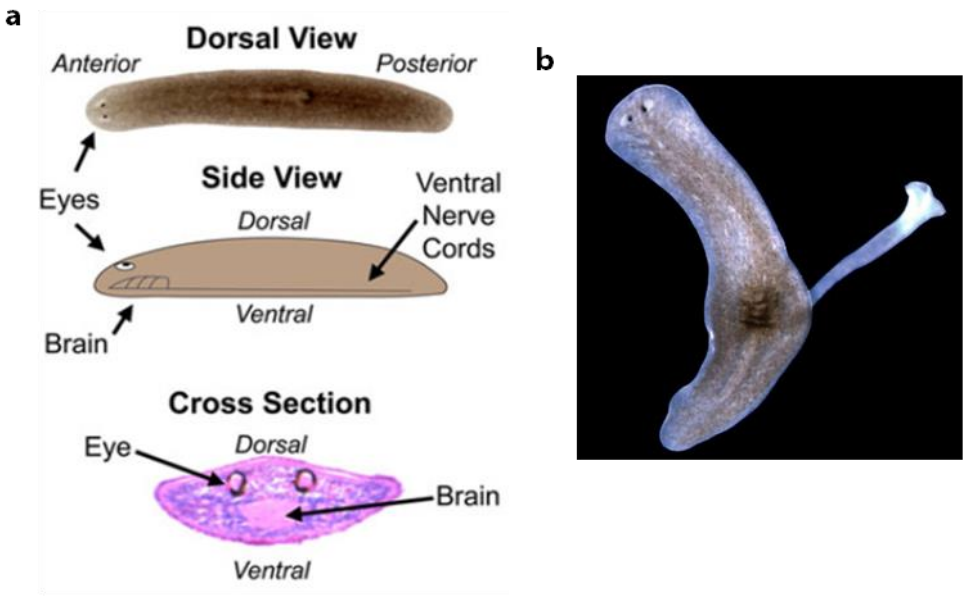

Figure I3.1: *Schmidtea mediterranea* anatomy.
(a) *Schmidtea mediterranea* present two eyes in the most anterior-dorsal part, and a pharynx in the middle of the body. The central nervous system is located in the ventral part, and the brain is below the eyes. Adapted from Deochand *et al.*, 2016[134]. **(b)** Planarians are able to evaginate their pharynx to capture the food from the medium and ingest it. Adapted from Rossant, 2014[135].

3.2 Planarian anatomy

3.2.1 Epidermis

Planarian epidermis consists of a monolayer of cells, composed by differentiated multi-ciliated and non-ciliated cells based in a basal lamina[136]. Planarians use cilia beating at the surface of this ventral epidermis for gliding along substrates. Furthermore, in the apical domain there are secretor structures – called the rhabdites – and the connectors of several secretory cells present on the parenchyma[137]. The mucus secretion is essential for planarians since it forms a protector layer against external aggressions.

3.2.2 Mesenchyme

The mesenchyme, or parenchyma, is a connective tissue that fills the space between the epidermis and the internal organs. The mesenchyme contains multiple types of secretory and pigment cells, and a mix of several differentiated cell types and stem cells[119].

3.2.3 Muscle

The body-wall musculature of adult planarians is formed by intricately organized muscle fibers, formed by elongated muscle cells that coat all the animal body. These fibers are organized in four main layers: circular, longitudinal, diagonal, and longitudinal fibers (from outside to inside). The inner longitudinal fibers are thicker than the outer ones. These layers are compressed within a region of 7–12µm thick below the epidermis[138,139]. In addition, there are dorsoventral fibers that cross the mesenchyme, and coat the digestive system and the pharynx[140]. These fibers are more abundant in the tips and margins of the animal, than in the central region of the body, forming a dense, compact muscle net[138] (Figure I3.2). Planarian body-wall muscle plays important roles during homeostasis and regeneration, being essential for supporting, since planarians lack skeletal structures, and also for wound closure and proper regeneration of missing structures[138,141]. In addition, muscle cells provide positional instructions for the regeneration by sending signals to the neoblasts[142].

3.2.4 Central nervous system

The planarian central nervous system (CNS) consists mainly of an anterior brain, or cephalic ganglia, and a pair of ventral nerve cords (VNC) that run along the length of the animal (Figure I3.3). The brain is organized as a central neuropil surrounded by an outer layer of neuronal cell bodies, and it displays a typical spongy texture, as it is traversed by muscles and processes from secretory cells. Furthermore, planarians have nervous plexus in the subepidermal region, intestine, and pharynx[143]. Even with

its apparent simplicity, planarian CNS is a complex net where a large number of different sensory nerves leave the brain, and connect with the margins and sensory organs of the head[143–146]. Despite the apparent simplicity of planarians, neurotransmitters, axon guidance signals, and neurogenic genes are mainly conserved between planarian and vertebrates[144].

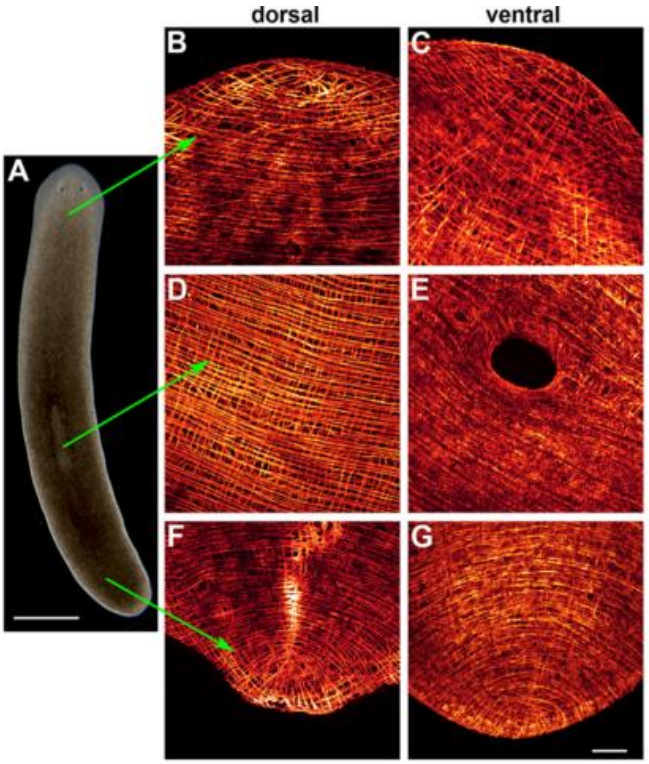

Figure I3.2: Planarian body-wall musculature.

(a) Planarian live animal. **(b-g)** Immunostaining with T-MUS anti-body, which labels the myosin heavy-chain (MHC) protein. Images show the different organization of the muscle fibers in the anterior pole, middle of the animal, mouth and posterior pole. Scale bar: 1mm for (a) and 50µm for (b-g). Adapted from Cebrià, 2016[139].

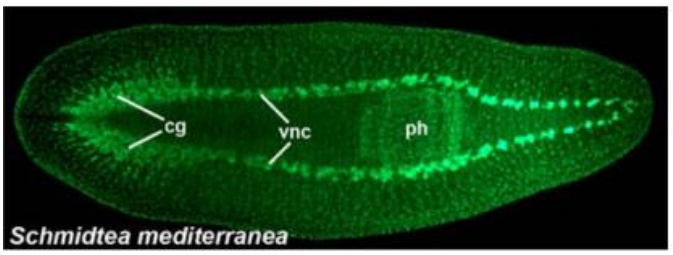

Figure I3.3: Planarian Central Nervous System.
Whole-mount immunostaining using anti-synapsin (3C11) antibody. A bi-cephalic ganglia (cg) is observed in the more anterior part of the animal body, and two ventral nerve cords (vnc) elongate along the planarian body. Nervous connections are also labeled in the pharynx (ph). Adapted from Cebrià, 2007[143].

3.2.5 Sensory organs

Several types of sensorial cells were described in planarians – photoreceptors, mechanoreceptors, and chemoreceptors – mostly located in the cephalic domain. The visual system is the sensory organ most well studied[119,136]. The planarian eye is composed only by two cell types: photoreceptor cells (phc) and pigment cells (pc). The pigment cells form a semi-lunar pattern on the proximal side of a transparent optic cup. The bipolar photoreceptor neurons project their dendrites into the optic cup, forming stacks of photosensitive microvilli called rhabdomeres. Their axons, in turn, innervate the underlying brain both contralaterally and ipsilaterally via a true optic chiasm[147] (Figure I3.4).

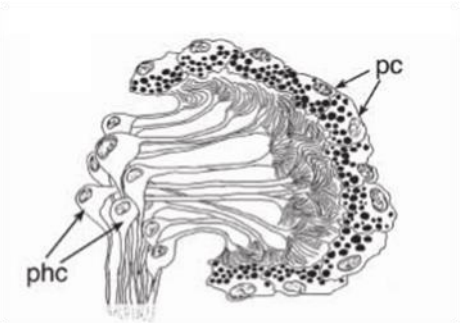

Figure I3.4: Planarian eye.
Draw of the planarian eye. Optic cup view showing the two eye tissue types: pigmented cells (pc) and photoreceptor cells (phc). Adapted from Pineda *et al.*, 2002[147].

3.2.6 Digestive system

Planarians present a blind digestive system composed by one anterior and two posterior main gut branches (Figure I3.5a), which ramify into secondary, tertiary, and quaternary branches (Figure I3.5b) throughout the entire animal. This widely ramification allows an uniform distribution of nutrients, acting as a vascular system[148]. The intestine cells are organized in a monolayer surrounded by the basal lamina and the muscular plexus, and they can be divided in phagocytes and goblet cells[149]. The collection of nutrients from digestive lumen is done by phagocytes and goblet cells, which producs and releases enzymes to the lumen, facilitating the digestion. The three main gut branches converge to the pharynx. The pharynx is a cylindrical organ located in the central part of the animal, surrounded by the muscular and nervous plexus[150]. Through muscular contraction, the pharynx is able to extend and contract through the mouth in order to capture the food[151].

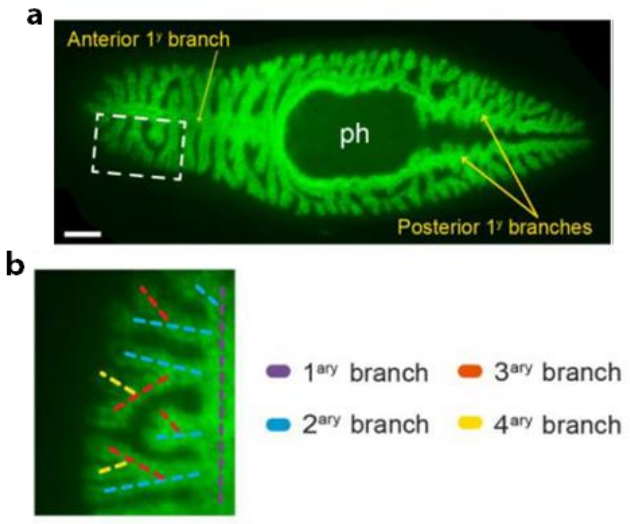

Figure I3.5: Planarian digestive system.

(a) Fluorescence *in situ* hybridization using *pk1* which labels the digestive system. Planarians digestive system is composed by one anterior, and two posterior main branches. White box is amplified in **(b)**. Gut branches can ramify into secondary, tertiary, and quaternary branches throughout the all the animal body. ph = pharynx. Adapted from Barberán *et al.*, 2016[152].

3.2.7 Excretory system

The planarian excretory system consists of an extensive net of protonephridia, along the lateral body margins and their ciliated side branches. Protonephridia are located below the muscular plexus, and are composed of blind tubules ending in a terminal cell in which beating cilia generate negative pressure, allowing filtration from the extracellular space into the tubule lumen through membrane fenestrations[153]. Three cell types were described in planarians excretory system: non-ciliated cells – which are the more distal –, followed by the ciliated tubular cells and the flame cells – that are also ciliated and are located in the tubules extreme[153] (Figure I3.6). Planarians protonephridial architecture, and the concomitant identification of specific markers for flame cells, proximal and distal tubule cells, reveal a complex, branched epithelial organ composed by multiple cell types[153].

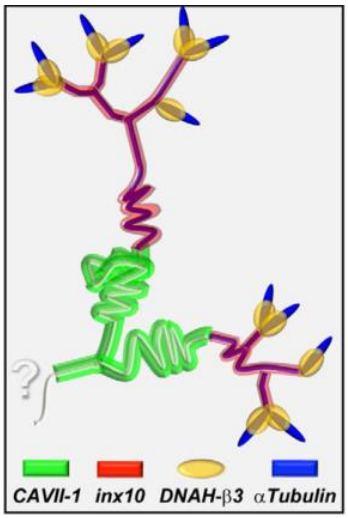

Figure I3.6: Planarian protonephridial molecular anatomy.
Non-ciliated cells are represented in green, followed by the ciliated tubular cells in purple, and the flame cells in yellow and blue on the tip. Adapted from Rink *et al.*, 2011[153].

3.3 Neoblasts

As referred to before, the incredible ability of planarians to grow/degrow and regenerate, is due to the presence of an adult pluripotent stem cell population called neoblats[154]. These cells are the only cells in planarians with mitotic ability and therefore, the only source of new cells during both homeostasis and regeneration[155,156]. They can be identified morphologically because they are small cells of 6-10 µm diameter with a high nucleus-to-cytoplasm ratio (Figure I3.7a). The cytoplasm is strongly basophilic, rich in free ribosomes and with few mitochondria, and contains chromatoid bodies close to the nucleus[157,158]. Neoblasts are distributed homogenously throughout the animal body surrounding the organs, with exception of the pharynx and in front of the eyes[158,159] (Figure I3.7b-c). Depending on the adult size, they account for 20-30% of the total cell number. This percentage corresponds to the pluripotent stem cells and the progeny cells that retain neoblast-like features.

Planarian tissue renewal and regeneration is fueled by the stem cell population. Although in other organisms it has been observed that dedifferentiation can occur in response to an injury or damage, to amplify the cycling population, and initiate the regenerative response[12], in planarians these phenomena has never been observed. Indeed, in 1989 Baguñà and others observed that the injection of differentiated cells into an irradiated host (depleted of neoblasts) is not enough to recover planarian stem cell population, demonstrating that dedifferentiation is not occurring in planarians[158].

Different experimental approaches have demonstrated that neoblasts are very similar to mammalian embryonic stem cells, as they share genes important for pluripotency, including regulators as well as targets of OCT4[160]. Furthermore, as any cell with mitotic ability, neoblasts are sensible to irradiation by gamma-rays[154] (Figure I3.7b). The finding of several neoblast markers in the last years, as members of Piwi/Argonaute family[161,162] or the *histone 2b*[163], has enabled a deeper study of this population in planarians. Other tools commonly used to study the planarian cycling population are

the histone-3 phosphorylated antibody (H3P)[131], to detect neoblasts in M phase, and the BrdU incorporation[159], a thymidine analogue which is incorporated in DNA during replication.

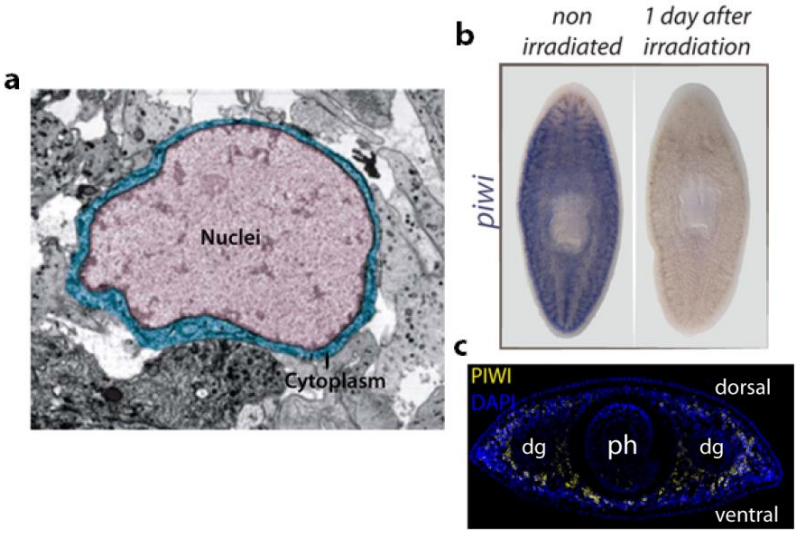

Figure I3.7: Planarian stem cells, the neoblasts.

(a) Electron micrograph of a neoblast. Nuclei-cytoplasm ratio is very high. Adapted from Reddien & Sanchéz Alvarado, 2004[116]. **(b)** *In situ* hybridization using *piwi* which labels all planarian neoblasts. They present a uniform distribution through the animal body, with the exception of the anterior part of the head and the pharynx. After one day of gamma irradiation, the expression of *piwi* completely disappears, since the animal is depleted of neoblasts. **(c)** Immunostaining, showing the PIWI protein distribution in a planarian transverse section. PIWI is located mainly in the planarian mesenchyme. ph=pharynx; dg=digestive.

3.3.1 Neoblasts heterogeneity

One of the central questions about planarian neoblasts was, for a long time, whether they are a homogeneous, or a heterogeneous population of pluripotent cells. In 2011, Wagner and colleagues demonstrated that, at least a part of neoblasts were pluripotent, and can give rise to all the planarian structures. They used ionizing radiation and single-cell transplantation to identify neoblasts that can form large

descendant-cell colonies *in vivo*. These neoblasts were called clonogenic neoblasts (cNeoblasts), and are distributed throughout the body being able to produce cells that differentiate into all cell types[164].

In addition to cNeoblasts, it was shown that the neoblasts population can be divided at least in four main classes: sigma-class "σ-class"; gamma-class "γ-class"; zeta-class "ζ-class" and nu-class "ν-class", based on their gene expression profiles (Figure I3.8). The σ-class is composed by pluripotent neoblasts that are able to restore all the cell populations and mediate the early regenerative responses to injury (proliferation and migration). This class of neoblasts give rise to lineage-specific neoblasts that are committed to different cell populations: the ζ-neoblasts that give rise to epidermal lineage; γ-neoblasts which are committed to the gut, and ν-neoblasts that are committed to neuronal lineage.

It was found that early wound response remained unaltered following elimination of the ζ-neoblasts. However, the maintenance and/or differentiation of epidermal cell type is severely affected after its silencing, demonstrating that this neoblast-class is related to the epidermal specification[165]. The γ-neoblasts are characterized by high expression of *hnf4* and *gata4/5/6,* genes linked to the planarian intestine. This evidence strongly suggests that γ-neoblasts represent an intestinal progenitor state[165]. Finally, ν-neoblasts express neural genes and were found adjacent to the brain, suggesting that they could be determined to neural population[166] (Figure I3.8).

Thus, the neoblasts are a highly heterogeneous population composed by pluripotent stem cells and lineage-specific progenitors. Lineage-specific stem cells express specific transcription factors to give rise to specific lineages. Some examples of these transcription factors are *six-3* or *pax6A/B* as neural progenitors, *hnf4* or *gata4/5/6* as gut progenitors and *agat* or *nb21/32* as epidermal progenitors[167] (Figure I3.8).

Recently, it was proposed that cNeoblasts are not a stable stem cell population

present in planarians, but rise sporadically from a larger population of fate-restricted or committed neoblasts. According to this hypothesis, self-renewal becomes a conceptual property not possessed by a discrete population, but transiently held by a small number of cells and arising probabilistically depending on the demands of the animal. If stem cells express progenitor markers for specific lineages, perhaps injury induces changes in the transcriptional program, allowing the loss of the lineage-restriction markers, its proliferation as pluripotent cells, followed by its differentiation into the required cell type. Such a model allows us to take a new concept about the remarkable plasticity of planarian in terms of dynamic cell states, rather than statically defined cell types[168].

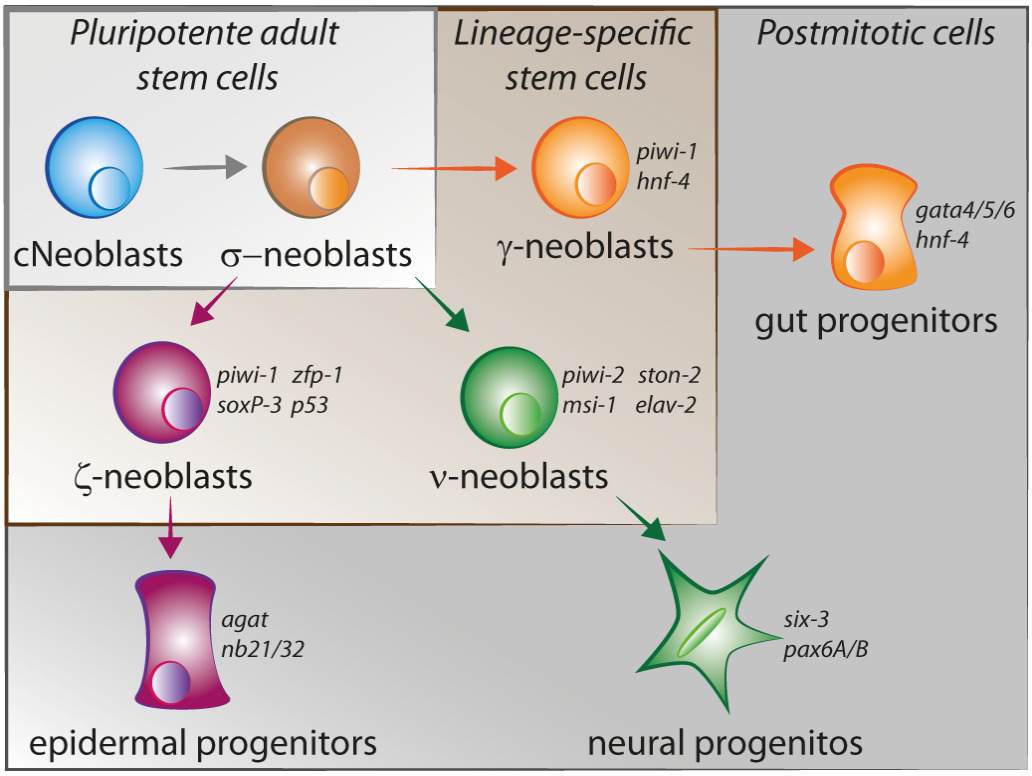

Figure I3.8: Neoblast classes.

cNeoblasts give rise to a population of pluripotent σ-neoblasts. σ-neoblasts, in turn, are able to specialize into different lineage-specific neoblast such as γ-neoblasts, ν-neoblasts, and ζ-neoblasts. γ-neoblasts acquire markers specific for planarian gut cells, while ν-neoblasts express markers to neural progenitors, and the ζ-neoblasts become committed to the epidermal lineage.

3.3.2 Neoblasts migration and differentiation – the epidermal lineage

During cell turnover, the dying cells should be replaced by the new cells formed. As mentioned earlier, neoblasts are the only planarian cells with proliferative ability, and are located in the mesenchyme. To replenish the old cells, neoblasts residing deep in the mesenchyme must produce new cells that mobilize, undergo multiple determination steps, intercalate in the tissue, and finally differentiate in the proper cell type.

The specific spatiotemporal coordination of changes in gene expression produces the diverse number of differentiated cell types. For example, in *Drosophila*, the sequential expression of the transcription factors *hunchback – krüppel – pdm – castor* in the neural stem cells is critical for proper formation of the developing CNS[169]. The spatiotemporal transition from a stem cell to a differentiated cell is well studied in the planarian epidermal lineage. The planarian epidermis is a simple, monostratified tissue composed by multiple differentiated multi-ciliated and non-ciliated cell types. Individual epidermal cells must continuously be replaced due to aging, damage from environmental insults or exogenous wounds[170]. As referred before, ζ-neoblasts give rise to the epidermal lineage since *zfp-1* – a ζ-neoblasts marker – *(RNAi)* animals can regenerate tissues including the gut, brain and muscle, but fail to generate cells expressing epidermal markers[165]. Therefore, in the very beginning σ-neoblasts give rise to ζ-neoblasts, which are already committed to the epidermal lineage. Then ζ-neoblasts start to express *nb21/32,* and these cells lose the proliferative ability. At the same time, cells start to move through the mesenchyme towards the epidermis. Thereafter, the sequential expression of *agat – zpuf – vim* gives rise to differentiated epidermal cells, located in the sub-epidermal or epidermal layer (Figure I3.9). Once in epidermis, *vim*+ cells terminally differentiate into multiple epidermal cell types[171,172]. This data reveals the pivotal role of the changes in gene expression to specify different cell types during the migration of stem cell descendents from the mesenchyme towards epidermis.

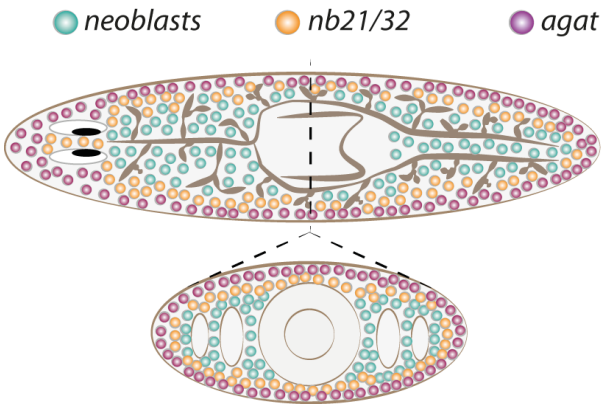

Figure I3.9: Epidermal lineage distribution.
Neoblasts are located in the most internal part of the planarian mesenchyme. During differentiation, epidermal progenitors express specific determinants in a spatiotemporal manner and migrate towards the epidermis.

3.4 Planarian plasticity

As mentioned earlier, planarians present a high plasticity, allowing them to grow and degrow maintaining the proportions and organs functionality throughout their lives, and also to regenerate any missing part of their body. Nevertheless, regeneration and homeostatic state require different biological responses. Thus, depending on the context, stem cells will acquire different transcriptional programs and cellular characteristics.

3.4.1 Planarians regeneration

Regeneration is accomplished by a complex network of signals from the wound site, in order to trigger the appropriate regenerative response according to the nature of the injury. As referred to previously, planarians are able to regenerate from essentially any type of body piece. This impressive regenerative power was firstly illustrated in the experiments of T.H. Morgan, who showed that a tiny fragment, 1/297 of a planarian, was able to regenerate a complete organism within two weeks[173]. After an

amputation, planarians pull away from the wounding agent, possibly reflecting a predator avoidance reflex. A strong muscular contraction at the site of wounding occurs within seconds, to minimize the surface area of the wound[131,174]. A thin layer of old epidermis, covers the wound in the first thirty minutes of regeneration, is formed by the extension and fusion of dorsal and ventral epithelia. The contact between both epithelia is essential to trigger the regeneration process[141,175–177]. The molecular mechanisms that underlie the wound closure are still unknown. However, it was shown that ROS signaling is necessary for the induction of regeneration after planarian injury, and that the expression of *runt-1* and *egr-1* is rapidly induced after wounding[178,179].

After wound closure, the surrounding neoblasts proliferate, and its progeny migrates to the healing epithelia forming an undifferentiated structure called blastema. At the same time, the pre-existing tissues readapt their size to the new body[176]. Blastema size increases by the proliferation and migration of additional neoblasts from the pos-blastema region, thus no mitotic activity occurs within the blastema[174,176]. After that, blastema cells differentiate in order to restore the missing structures, and in 7-10 days the regenerative process is complete[174] (Figure 3.10a).

Both proliferation of neoblasts – as a source of new cells to restore the missing tissues – and the cell death of differentiated cells – to allow the rescaling of pre-existence tissues – are essential for the regenerative process[176,180,181]. Moreover, both mechanisms should be under a tight control. Proliferative response after an amputation shows a bimodal distribution[181], presenting a first general mitotic peak 6 hours after the lesion, followed by a decrease in mitotic rates at 18 hours, and then a local mitotic peak at 48 hours after amputation (Figure I3.10b). The second mitotic peak is observed only when tissue is lost, but not after a mild incision[181]. Apoptotic response after an injury is also bimodal. The first peak is observed close to the wound 4 hours after amputation, followed by a general cell death through animal body three

days after amputation (Figure I3.10b). This apoptotic dynamic is not altered after irradiation, demonstrating that only differentiated cells are affected by cell death[180]. In some animals, as *Hydra* and *Drosophila*, it has been described that a proliferative response is coordinated by apoptotic cells in order to restore the dying cells in a compensatory mechanism[182,183]. In planarians it is not known whether apoptosis triggers the proliferative response. However, it has been reported that JNK is required to coordinate both responses[184].

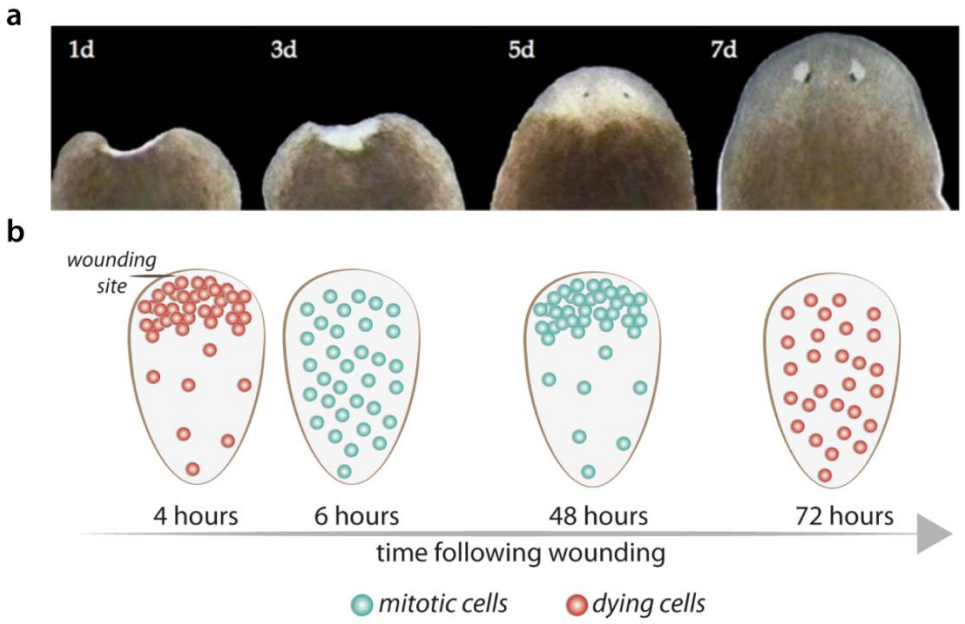

Figure I3.10: Planarian regeneration.

(a) Time course of planarian regeneration in vivo. 1 day after amputation, the wound is already closed. At 3 days of regeneration, the blastema is formed, and at 5 days of regeneration, the eye appears in the blastema. At 7 days of regeneration, the missing structures are almost recovered. Provided by Susanna Fraguas. **(b)** Apoptotic and mitotic response during planarian regeneration. 4 hours after amputation, an apoptotic response is observed in the area close to the wound. At 6 hours of regeneration, a general mitotic peak is observed followed by a second mitotic response in the wound area 48 hours after amputation. A general apoptotic response is observed 72 hours after amputation.

Thanks to the coordination between the proliferative and the apoptotic responses, after amputation new committed and/or differentiated cells appear within the blastema and also in the pre-existent tissue, which is remodeling. Thus, at 3 days of regeneration the brain primordia and the eyes appear within the blastema, and at 7 days they appear almost regenerated and properly integrated in the new-sized animal[123,144,185].

A crucial aspect of the regeneration process is the determination and differentiation of progenitors in order to reestablish the missing body pattern. After an amputation, pre-existing stem cells in the body must recognize the organs absent, and subsequently, initiate expression of the appropriate lineage genes. It was shown that muscle cells from the planarian body wall are able to signal neoblasts in order to acquire the proper identity[142]. These positional coordinates are given by the expression of secreted factors, like Wnts and Bmp, which determine the AP and DV axis, respectively[186].

3.4.2 Planarians homeostasis

Cell renewal is a complex mechanism based on three processes: (a) the elimination of selected differentiated cells by cell death; (b) the replacement of eliminated cells through cell division, typically involving adult stem cells and their descendants; and (c) the differentiation of newly generated cells and their integration with preexisting tissue[187,188].

In planarians, cell renewal must be coordinated continuously, since they growth and degrowth depending on food availability and temperature[118]. It is known that the changes in size result mainly from changes in cell number, rather than in cell size, so the ratio of dying/proliferating cells is controlled by environmental conditions[188]. Planarians are able to tolerate long starvation periods, and during this time, they degrow up to minimum sizes. Under these stressful conditions, food reserves from gastrodermis and mesenchyma are the firsts to be used, and at more extreme points, the sexual strains digest the sexual organs, and become asexual[188,189]. When food is available, planarians are able to grow back, and in the sexual strains, the reproductive organs reappear. These cycles of grow and degrow occur during all planarian lives without damage to the animal. Several signaling pathways control the body axis and proportions during planarians growth and degrowth. Thus, the Wnt and BMP pathways, are not only essential during regeneration, but are also required to maintain the AP and the DV axis in intact animals[190].

During planarian starvation, cell death increases to re-organize the organs and structures, and neoblast self-renewal is maintained at basal levels, resulting in a decrease of planarian body size (Figure I3.11a-b)[191]. The tissue remodeling is critical during planarian starvation because it maintains a proportioned planarian body. It was shown that JNK signaling, and *Gtdap-1* are controlling the planarian body re-scaling during degrowing through the modulation of apoptotic cell death[184,192].

In contrast, after feeding there is a high increase in proliferation, which is

accompanied by minimum levels of cell death (Figure I3.11a-b). This results in the increase of cell number and thus, planarian body size[191]. The Insulin and TOR pathways were described as important mechanisms in the control of planarian body size after feeding, through the modulation of cell proliferation. Also, the silencing of both pathways leads to a reduction in the planarians body size – similarly to starved animals – despite these animals being fed[189,193].

Despite the importance of the tight control of cell renewal that planarians require during all their lives, the mechanisms, pathways and signals that underlie it, remain largely unknown.

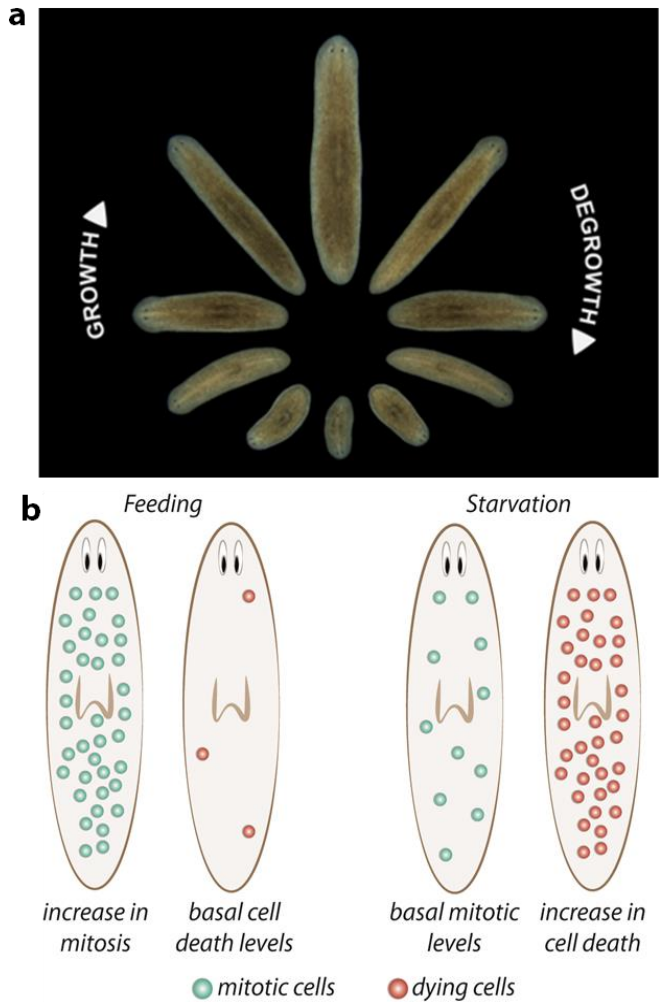

Figure I3.11: Planarian homeostasis.

(a) Planarians are able to growth and degrowth during their lives, maintaining their body proportions and functionality. Provided by Gustavo Rodriguez-Esteban. **(b)** After a stimulus, proliferation and/or cell death can change in planarians. After feeding, neoblast proliferation increases throughout planarian body, and cell death is reduced to minimum levels, resulting in the increase of animal's size. Conversely, when planarians are in starvation, neoblast proliferation is maintained at basal levels and cell death increases, mainly to reorganize the tissues.

Objectives

The main objective of this thesis was the study of the role of the Hippo signaling during planarian homeostatic cell turnover and tissue regeneration.

The specific objectives of this thesis were:

1. Identify the Hippo pathway core elements of *Schmidtea mediterranea* and characterize their function during planarian homeostasis and regeneration.

2. Identify the up- and down-stream elements of the Hippo pathway in *Schmidtea mediterranea* and study their function in planarians.

Results

The Hippo pathway has been extensively studied in the last decade in a wide range of animals, organs and in cell culture. Although in most contexts the Hippo pathway controls apoptosis, proliferation and the stem properties of the cells, its precise function appears highly dependent on the tissue and organism studied. To gain further insight into the role of this pathway during cell renewal and regeneration, we boarded its study in planarians, a stem-cell based system that provides the opportunity to understand the control of cell proliferation/differentiation and cell death in a complete *in vivo* organism.

First, the Hippo pathway core elements (*hippo*, *salvador*, *warts*) were identified in *Schmidtea mediterranea*. Their inhibition by interference RNA (RNAi) revealed that all those elements performed similar functions, confirming that they were taking part of the same cassette. Therefore, only the function of *Smed-hippo* (*hippo*, for simplicity) was studied in detail. Furthermore, elements reported to be up-stream regulators or inhibitors in other models and possible targets of Hippo were also studied. These results will be described in detail in the following sections.

Chapter 1

Role of the Hippo pathway core elements during planarian homeostasis

Role of the Hippo pathway core elements during planarian homeostasis

Hippo kinase cassette elements are conserved in planarians

Four genes of the Hippo pathway core were identified in the *Schmidtea mediterranea* transcriptomes (PlanMine[126]): *Smed-hippo*, *Smed-salvador*, *Smed-warts* and *Smed-yorkie* (for simplicity, *hippo*, *salvador*, *warts* and *yorkie*) (Annex 1). *In situ* hybridization (ISH) showed that the four genes were ubiquitously expressed (Figure R1.1a). Furthermore, an *in silico* search in a single-cell transcriptomic database of planarians[194] also corroborates that they are present in several planarian cell types (Figure R1.1b).

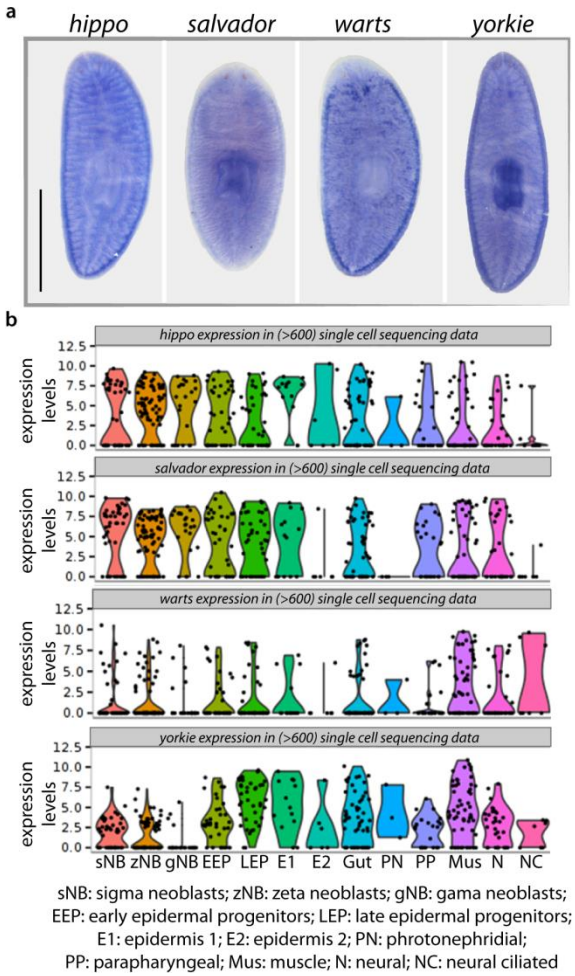

Figure R1.1: Hippo pathway core genes are ubiquitously expressed. **(a)** ISH of *hippo, salvador, warts* and *yorkie* shows their ubiquitous expression pattern. **(b)** *hippo, salvador, warts* and *yorkie* expression levels in different cell types according to a single-cell RNAseq[194]. Scale bar: 1mm.

To decipher the possible function of the Hippo core genes during homeostatic cell renewal in planarians, we injected dsRNA of the four genes into animals during two or three weeks (see materials and methods and Figure R1.2a). After the inhibition of *hippo*, *salvador* or *warts*, which integrate the kinase cassette, animals present unpigmented regions, mainly around the body margin, which became bigger or evolved into unpigmented overgrowths (Figure R1.2b). On the other hand, inhibition of *yorkie* (*yki)*, which signals to the nucleus when it is dephsphorylated, leads to edema formation, mainly in the posterior region of the planarian body (Figure R1.2b). During the inhibition process, we fund that *yki (RNAi)* animals did not survive longer than two weeks due their severe phenotype.

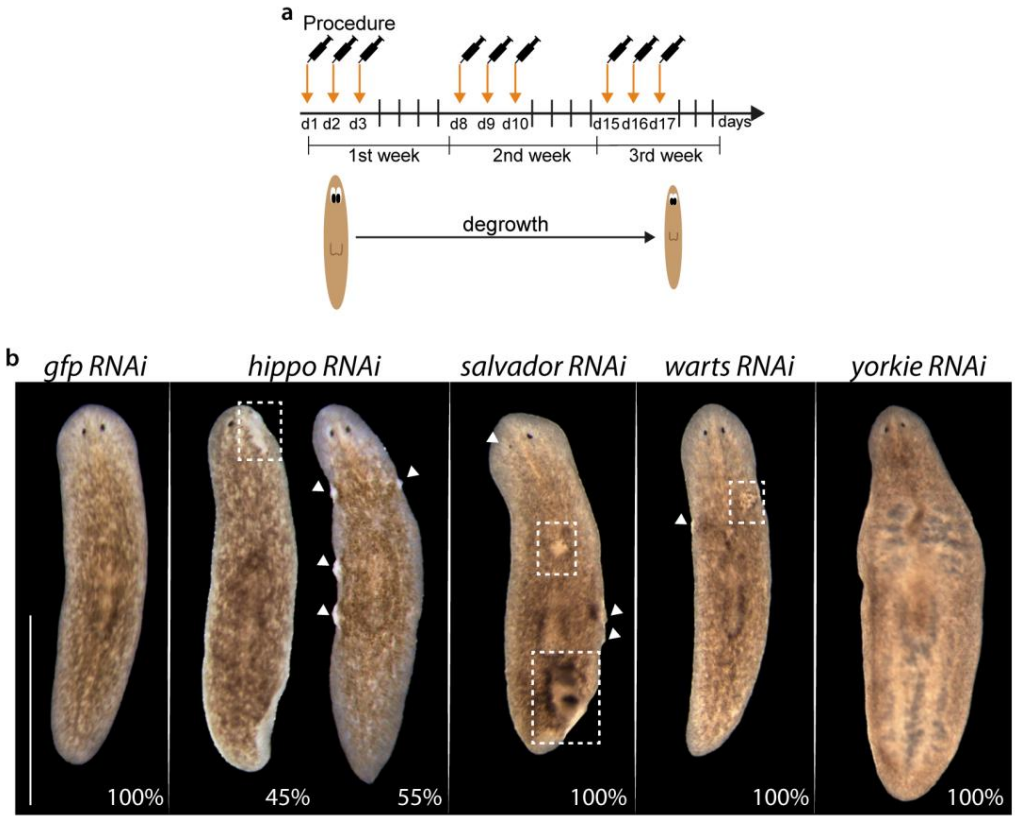

Figure R1.2: Inhibition of Hippo pathway elements produces overgrowths or edemas.
(a) Cartoon illustrating the experimental design during planarians homeostasis. Animals were starved one week before the experiment, and then were injected during three consecutive days during two or three weeks. During the experiment animals were maintained in starving conditions. **(b)** Stereomicroscopic view of *hippo, salvador, warts* and *yorkie (RNAi)* live animals. *hippo*, *salvador* and *warts (RNAi)* animals show the formation of overgrowths and unpigmented regions in the marginal part of the body. White arrows indicate unpigmented overgrowths and white boxes unpigmented regions. *yorkie (RNAi)* animals show the formation of edemas. (n=15) Scale bar: 1mm.

The analysis of differentiated structures revealed that *hippo*, *salvador* and *warts (RNAi)* animals are not able to properly maintain differentiated structures as the visual and the digestive system. The eyes of these animals are smaller, the optic chiasm is thinner, and the digestive system is not properly patterned. *yki (RNAi)* animals, in turn, present an aberrant projection of the optic nerves and the digestive system is impaired (Figure R1.3a). The edemas observed in *yki (RNAi)* animals could be due to the loss of osmotic regulation as a result of defects in the protonephridia. To address this question we quantified the number of nephridial clusters through a ISH with *carbonic anhydrase* (*ca*) probe. A significant reduction of nephridial clusters in *yki (RNAi)* animals was found, as well as an aberrant distribution, showing zones without protonephridia (Figure R1.3b). In contrast, *hippo*, *salvador* and *warts (RNAi)* animals showed a normal distribution of protonephridia (Figure R1.3b).

To test the possible role of the Hippo genes in the control of cell proliferation we quantified the mitotic activity by anti-pH3 immunostaining (H3P). Mitotic activity was found increased after three weeks of *hippo*, *salvador* and *warts* inhibition. The inhibition of *yorkie* also produced an increase in the mitotic activity (Figure R1.3c). According to the reported role of the Hippo-Yki signal in other organisms[14,24], the increase in mitotic cells was expected after inhibition of the integrants of the kinase cassette but not after *yki* inhibition. This observation can be a consequence of the

blotted phenotype after several days of *yki* inhibition or due to an unknown role of *yorkie* in planarians. These hypotheses will be discused later.

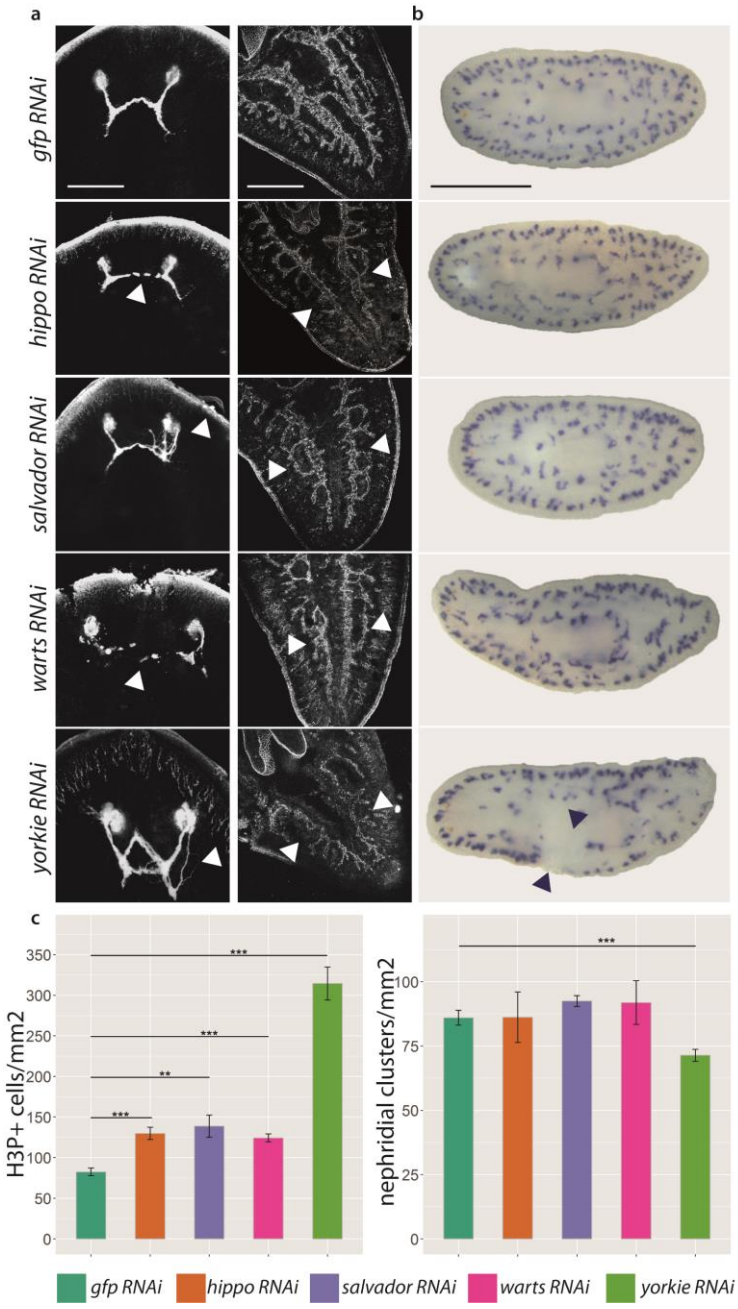

Figure R1.3: The Hippo pathway controls mitotic activity and is essential to properly maintain the differentiated structures. **(a)** Immunostaining using anti-arrestin antibody (VC1) labeling the photoreceptors and the digestive system labeled using the anti-Bcat2 antibody. Photoreceptors and digestive branches are aberrant in all *(RNAi)* conditions. White arrows indicate the improper patterned structures. **(b)** ISH for *carbonic anhydrase* (*ca*) for all (RNAi) conditions and respective quantification of nephridial clusters (n≥10). **(c)** Quantification of mitotic cells (H3P+) after two or three weeks of inhibition (n≥10). Error bars represent standard deviation. Data was analyzed by Student's t-test. **p<0.01; ***p<0.001. Scale bar: 50µm and 150µm **(a)**; 1mm **(b)**.

The observation that inhibition of the Hippo kinase cassette integrants (*hippo*, *salvador* and *warts*) produces a similar phenotype, suggest that they are acting together in planarians, as observed in other models. The finding of an increase in mitotic cells after their inhibition, which agrees with the literature[30,195,196], points to the functional conservation of the Hippo kinase cascade in planarians. For that reason, in the following studies we focused in the in deep functional analysis of *hippo*.

Chapter 2

Functional characterization of hippo during planarian homeostasis

Functional characterization of hippo during planarian homeostasis

hippo controls the number of apoptotic and mitotic cells in planarians, but not the total cell number.

To decipher the possible function of *hippo* during homeostatic cell renewal in planarians, we proceed to the same protocol referred to before, three weeks of *hippo* inhibition. To validate the *hippo (RNAi)* inhibition we performed a qPCR to quantify the decrease in the transcript. The result confirms that there is a significant decrease of *hippo* mRNA levels from the first week of treatment (Figure R2.1a).

To test whether the appearance of overgrowths could be caused by an imbalance between cell death and cell proliferation, we performed TUNEL and Caspase-3 assays, and quantified mitotic activity by anti-pH3 immunostaining (H3P). After two weeks of inhibition, *hippo (RNAi)* animals showed a reduction in cell death that became more evident after three weeks of inhibition (Figure R2.1b-c). The changes in cell death observed in *hippo (RNAi)* animals were also confirmed by the differential expression of apoptotic genes observed by RNAseq of *hippo (RNAi)* animals (Table R2.1)[197]. After three weeks of *hippo* inhibition, animals showed fewer apoptotic cells and increased mitotic activity (Figure R2.1b-d). Nevertheless, measurement of the body area revealed no differences between *hippo (RNAi)* planarians and controls (Figure R2.1e). Quantification of the total number of cells through fluorescence-activated cell sorting (FACS) also showed no difference in cell number between *hippo (RNAi)* and control planarians (Figure R2.1f). Thus, our results indicate that Hippo promotes apoptotic cell death and controls mitotic activity, leading to the formation of unpigmented regions and overgrowths without affecting animal size or cell number.

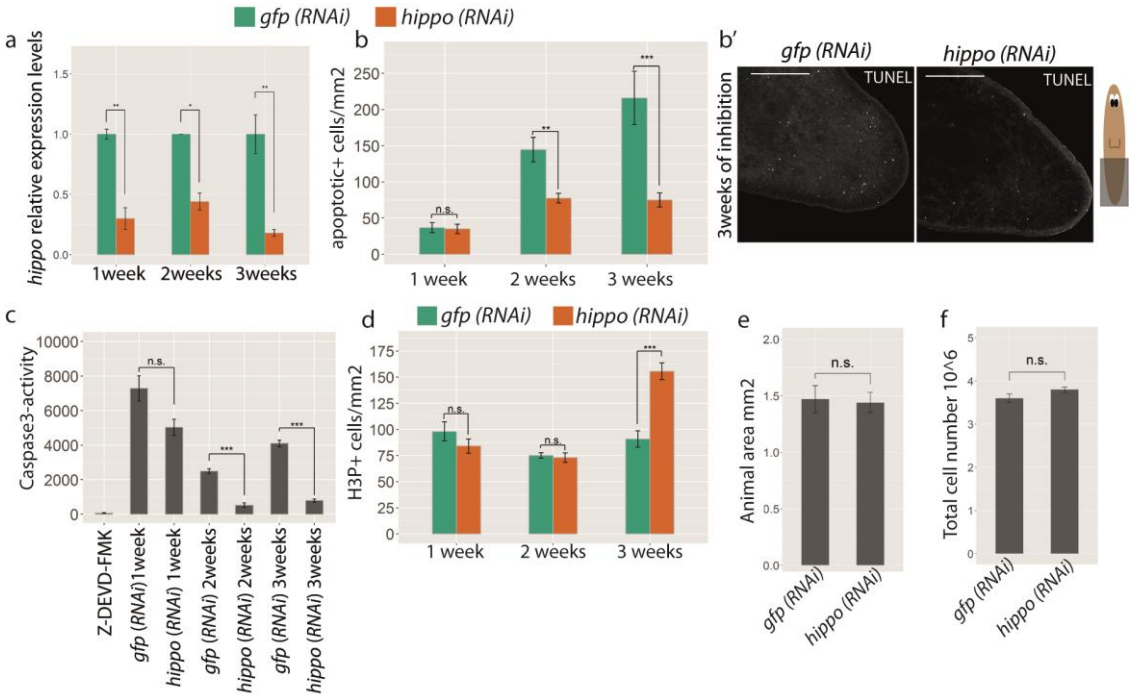

Figure R2.1: Inhibition of *hippo* decreases apoptosis and increases mitotic rates but does not affect cell number.

(a) Relative expression level of *hippo* mRNA after *hippo (RNAi)* by qRT-PCR. Values represent the means of three biological replicates. **(b)** Quantification of apoptotic cells (TUNEL+) after one, two and three weeks of *hippo* inhibition (n≥5). **(b')** TUNEL images from *gfp* and *hippo (RNAi)* animals at three weeks of inhibition. **(c)** Quantification of Caspase3-activity at one, two and three weeks of *hippo* inhibition. The results are presented as units of caspase-3 activity per µg of protein. Experiments were performed using three biological replicates. **(d)** Quantification of mitotic cells (H3P+) after one, two and three weeks of *hippo (RNAi)* inhibition (n≥10) **(e)** Area quantification of three weeks *hippo (RNAi)* animals with respect to the controls (n≥8) **(f)** Graph showing the total cell number of the three weeks *hippo (RNAi)* animals analyzed by FACS. 3 biological replicates were analyzed for each condition. Bars correspond to the mean of the three replicates. Error bars represent standard deviation. Data was analyzed by Student's t-test. *p<0.05; **p<0.01; ***p<0.001; n.s.: not significant. Scale bar: 150µm **(b')**.

Table R2.1: Up-regulated genes in the *hippo (RNAi)* RNAseq involved in cell death.

Selected up-regulated genes in *hippo (RNAi)* RNAseq involved in apoptosis. Each column contains the following information: Gene Ontology (GO) code, gene name, gene symbol, p-value and fold change. References showing that those genes are involved in apoptosis are included.

GO code	Gene	Symbol	p-value	FoldChange	Literature
GO:0070374	Mitogen Protein Kinase Kinase 2-like	MAP2K2	8,26E-73	0,659	198
GO:0006309	Deoxyribonuclease II family protein	Dnase2	0,0003	0,263	199
GO:1904714	Cathepsin A	CTSA	0,0004	0,197	200
GO:0042981	Actinin Alpha 1	ACTN1	0,0101	0,140	201
GO:0042536	Growth Hormone Secretagogue Receptor	GHSR	1,61E-07	0,781	202
GO:0006915	Phospholipid scramblase 1	PLSCR1	2,69E-07	0,658	203

Hippo controls G2/M transition and mitotic exit

It has been reported in other animal models that *hippo* deregulation causes defects in cell cycle progression[204–206]. Such an effect could therefore provide a plausible explanation for our observation that the decrease in cell death and increase in mitotic activity in *hippo (RNAi)* animals does not lead to changes in cell number. To test this hypothesis, we performed a EdU incorporation assay followed by an anti-H3P immunostaining to analyze the proportion of cells in M and S phase in *hippo (RNAi)* animals and the respective controls (Figure R2.2a). We found that 16h after EdU incorporation, *hippo (RNAi)* animals have the same number of EdU+ cells as controls, indicating that the same number of cells enter the cell cycle in both conditions (Figure R2.2b-c). In addition, an increase in the number of EdU+/H3P+ double-positive cells in *hippo (RNAi)* animals with respect to controls was observed (Figure R2.2b-d). This suggests that cells either transit faster from S to M phase in *hippo (RNAi)* animals or that they cannot complete M phase, or both. The finding that *hippo (RNAi)* animals have a high number of EdU-/H3P+ cells with respect to controls (Figure R2.2b-e) indicates that there is an increase in the number of cells that are in M phase but have not passed through S phase in the previous 16 hours in *hippo (RNAi)* animals. Thus, *hippo (RNAi)* leads to cells trapped in M phase but does not affect the number of cells entering the cell cycle (Figure R2.2f). This explains why the increased number of H3P+ cells is not translated into an increase in cell number. We cannot rule out the possibility that there is also a faster transit of cells from S to M phase after *hippo* inhibition. The finding that several genes related to cell cycle are differentially expressed in the *hippo* RNAseq database further supports a role for *hippo* during cell cycle progression (Table R2.2).

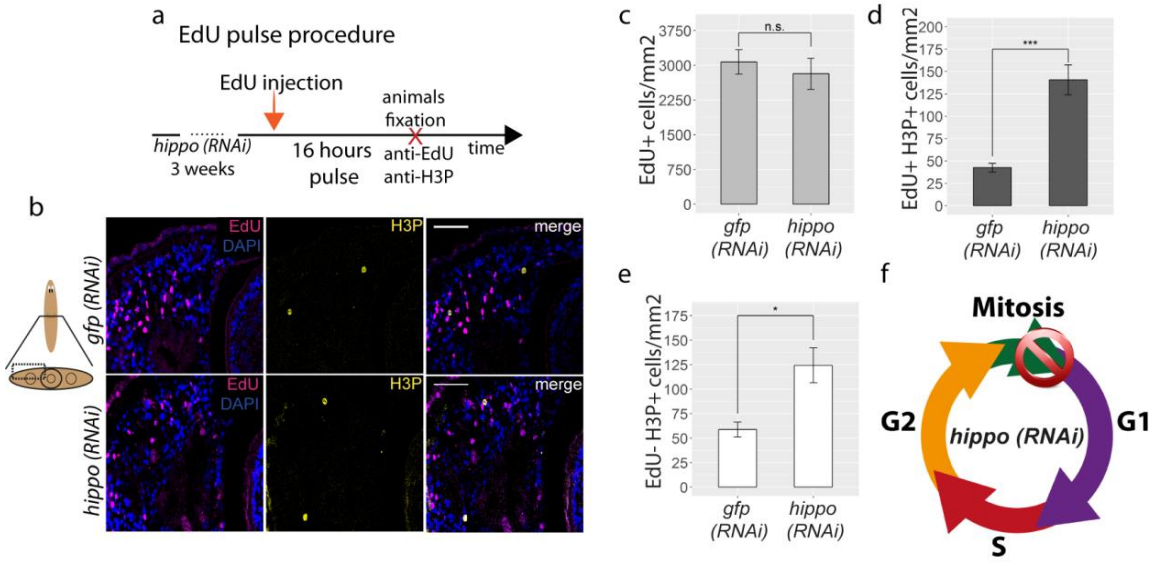

Figure R2.2: *hippo* plays a pivotal role during cell cycle.

(a) Cartoon illustrating the EdU pulse procedure. Animals were starved one week, injected during three weeks with *hippo* dsRNA, then injected with EdU and fixed 16 hours later. **(b)** EdU labeling in transverse sections combined with immunostaining of anti-H3P antibody in the pharynx region in three weeks *hippo (RNAi)* animals and their controls. Scale bar: 25µm. **(c)** Quantification of EdU+ cells in *hippo (RNAi)* animals and the respective controls. **(d)** Quantification of double positive Edu+/H3P+ cells in *hippo (RNAi)* animals and the respective controls. **(e)** Quantification of EdU-/H3P+ cells in *hippo (RNAi)* animals and the respective controls. All the graphs correspond to three weeks *hippo (RNAi)* animals (n≥8). Error bars represent standard deviation. Data was analyzed by Student's t-test. *p<0.05; ***p<0.001; n.s.: not significant. **(f)** Scheme showing the proposed function of *hippo* during cell cycle in planarians: *hippo* attenuates G2/M progression and ensures successful mitotic exit.

Table R2.2: Up- or down-regulated genes in the *hippo (RNAi)* RNAseq involved in cell cycle.

Selected up- or down-regulated genes in *hippo (RNAi)* animals RNAseq involved in apoptosis. Each column contains the following information: Gene Ontology (GO) code, gene name, gene symbol, p-value and fold change. References demonstrating the function of those genes in cell cycle are included.

GO code	Gene	Symbol	p-value	FoldChange	Literature
GO:0007049	Septin 4	SEPT4	0,0004	0,163	207
GO:0007017	Alpha-Tubulin1A	TUBA1A	0,001	0,187	208,209
GO:0045840	Insulin Growth Factor	IGF	7,99E-112	0,751	210
GO:0008283	Progranulin	PGRN	3,96E-193	0,877	211
GO:0008017	Dynamin	DYN1	9,66E-46	0,873	212
GO:0044770	Protein Tyrosine Phosphatase	PTPase	6,74E-36	0,779	213,214
GO:0007049	Muscarinic Acetylcholine Receptor	mAChR	2,36E-06	0,726	215
GO:0001558	Serine proteinase inhibitor Kazal-type 1	SPINK1	3,03E-135	-0,660	216
GO:0008283	Lysosomal Acid Lipase	LAL	2,97E-28	-0,966	217
GO:0000086	Centriolin	CNTRL	0,001	-0,181	218
GO:0051297	Ciliary Rootlet	CROCC	0,012	-0,107	219

Hippo is required to maintain the differentiated cell population

A detailed analysis of the overgrowths caused by *hippo* inhibition (Figure R2.3a) revealed that they are due to the accumulation of cells in the subepidermal region (Figure R2.3b) and that in some cases they arise from the submuscular plexus region (Movie R2.1). In agreement with their unpigmented appearance, which indicates that epidermal cells cannot produce pigment and thus are not terminally differentiated, we observed that the epidermal cells above the overgrowths do not display correct distribution of β-catenin2, a component of adherens junctions[220] (Figure R2.3c). The finding of PIWI+ cells accumulated in the subepidermal overgrowths and in the

corresponding epidermis (Figure R2.3b) indicates that they are mainly composed by undifferentiated cells.

Besides the specific regions of the overgrowths, broader unpigmented areas were also observed in *hippo (RNAi)* animals (Figure R2.3a). Analysis with specific markers revealed that differentiated structures such as the nervous system, the eyes and the digestive system failed to be properly renewed or maintained in those unpigmented areas, (Figure R2.3d-f). Furthermore, *hippo (RNAi)* animals had a poorly developed digestive system, smaller pharynx, brains and eyes (which in some cases almost disappeared), consistent with general defects in the maintenance of differentiated structures (Figure R2.3g). Note that the smaller brains appeared to be surrounded by ectopic mitotic cells (Figure R2.3g), indicating that the loss of differentiated tissues is not caused by a lack of cycling cells. Analysis of the *hippo (RNAi)* RNAseq further indicated that most of the markers associated with terminal differentiation of multiple cell types (*opsin, pantothenate kinase1, synapsin, tropomyosin*) are downregulated (Figure R2.3h), consistent with a general problem in the process of cell differentiation or maintenance of the differentiated state. Quantification of the number of dopaminergic and serotonergic neurons by ISH with the corresponding markers (*tyrosine hydroxylase* and *tryptophan hydroxylase 1*) further confirmed the general decrease in the number of differentiated neurons in *hippo (RNAi)* planarian heads (Figure R2.3i). Taken together, these data indicate that Hippo plays an important role in the maintenance or renewal of differentiated tissues and that its inhibition leads to the appearance of extensive regions of undifferentiated cells that accumulate in overgrowths.

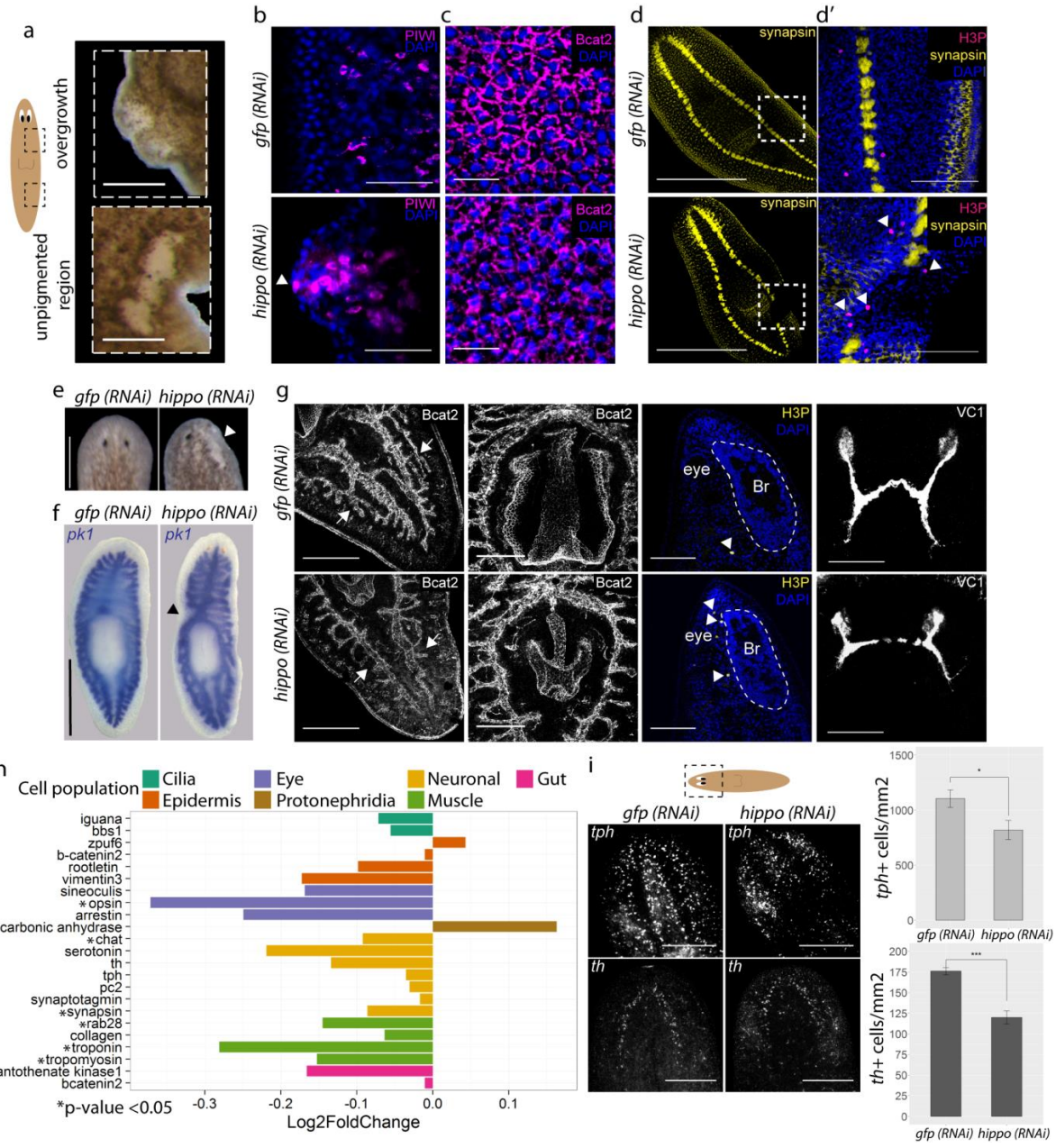
a
overgrowth
unpigmented region
b
c
d
d'
PIWI
DAPI
Bcat2
synapsin
H3P
gfp (RNAi)
hippo (RNAi)
e
gfp (RNAi) hippo (RNAi)
f
pk1
g
eye
Br
VC1
h
Cell population
Cilia
Epidermis
Eye
Protonephridia
Neuronal
Muscle
Gut
genes
iguana
bbs1
zpuf6
b-catenin2
rootletin
vimentin3
sineoculis
*opsin
arrestin
*carbonic anhydrase
*chat
serotonin
th
tph
pc2
synaptotagmin
*synapsin
*rab28
collagen
*troponin
*tropomyosin
*pantothenate kinase1
bcatenin2
*p-value <0.05
Log2FoldChange
i
tph
th
tph+ cells/mm2
th+ cells/mm2

Figure R2.3: *hippo* inhibition yields overgrowths and extensive areas composed by undifferentiated cells.

(a) Cartoon illustrating the regions affected by overgrowths or unpigmented regions. Stereomicroscopic view of an overgrowth and an unpigmented region generated after *hippo* inhibition. **(b)** Immunostaining using anti-PIWI antibody in an overgrowth region in *hippo (RNAi)* animals. Images correspond to confocal Z-projections. White arrows indicate a PIWI+ cell in the epidermis of the overgrowth. **(c)** Staining of the epithelia nuclei with DAPI combined with the immunostaining with anti-β-catenin-2 antibody (Bcat2). **(d)** Immunostaining using anti-Synapsin antibody in an unpigmented region in *hippo (RNAi)* animals. White box represents the magnified region. **(d')** Detail of an unpigmented region showing a double immunostaining using anti-Synapsin and anti-H3P antibodies. Nuclei are labeled with DAPI. Images correspond to confocal Z-projections. White arrows indicate the H3P+ cells surrounding the undifferentiated region. **(e)** Stereomicroscopic view of anterior region showing the disappearance of anterior structures in *hippo (RNAi)* animals. White arrow indicates the region where anterior structures disappear. **(f)** ISH staining with pantothenate kinase 1 (*pk1*) showing the disappearance of the gut in an unpigmented region after *hippo* inhibition. Black arrow indicates the region with no digestive. **(g)** Immunostaining using different markers. From left to right: Digestive system labeled using anti-Bcat2 antibody. White arrows indicate the gut branches. Immunostaining using anti-Bcat2 antibody labeling the pharynx. Brain region stained with DAPI (nuclei) combined with immunostaining with anti-H3P antibody in sagittal sections. Br=brain. White arrows correspond to H3P+ cells. Discontinuous line delimits the brain. Immunostaining using anti-arrestin antibody (VC1) labeling the photoreceptors. All the experiments were performed in three weeks *hippo (RNAi)* animals. All the images correspond to confocal Z-projections. **(h)** Graph showing the relative expression levels of cell markers for differentiated cells in the RNAseq of *hippo (RNAi)* animals. **(i)** FISH staining of serotonergic and dopaminergic neurons (*tph* and *th*, respectively), and the corresponding quantification. Images correspond to confocal Z-projections (n≥5). All the experiments were performed in three weeks *hippo (RNAi)* animals. Error bars represent standard deviation. Data were analyzed by Student's t-test. *p<0.05; ***p<0.001. Scale bars: 150µm **(a)**; **(d')** and **(c)**; 100µm **(b)**; 1mm **(d)** and **(f)**; 200µm **(e)** and **(i)**; **(g)** from left to right: 100µm; 250µm; 150µm; 150µm, 100µm.

hippo defines the expression boundaries of epidermal markers.

The epidermal lineage is the most abundant in planarians and its progression and determination is well understood[171]. Epidermal maturation requires temporally correlated transition states in planarians, in which stem cells (*piwi*+) became postmitotic and start to sequentially express *nb21/32*, *agat* and *vimentin* (*vim*)[171,172]. In parallel, epidermal precursors migrate from the inner parenchyma towards the epidermis[171]. Thus, proliferating cells are mainly found in the inner part of the animal and postmitotic epidermal cells are found in the periphery. Interestingly, a large number of mitotic cells were observed in the animal periphery of *hippo (RNAi)* planarians, where overgrowths and unpigmented regions are mainly found (Figure R2.4a). Since this region should mainly contain postmitotic epidermal precursors[171], we reasoned that the process of differentiation and/or cell fate maintenance of the epidermal lineage could be impaired in *hippo (RNAi)* animals. In agreement with this hypothesis, we found that *hippo* is expressed in all epidermal lineage cells (Figure R1.1b and Figure R2.4b).

To gain further insight into cell fate progression in *hippo (RNAi)* animals, we analyzed the number and distribution of mitotic cells (H3P+), stem cells (*piwi*+) and postmitotic epidermal cells (*nb21/32*+, *agat*+ or *vim*+). First, we quantified H3P+ cells in four different regions defined from the inner to the outermost in transverse sections of the animals (Figure R2.4c). There was a significant increase in the number of mitotic cells (H3P+) in the two outer regions of *hippo (RNAi)* animals compared with controls (Figure R2.4c).

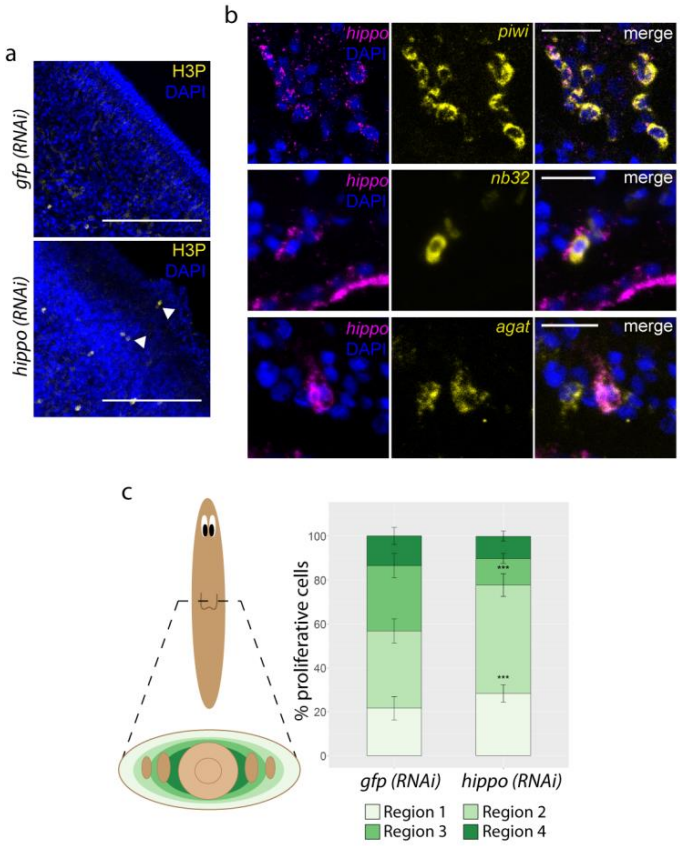

Figure R2.4: *hippo* (RNAi) animals present mitotic activity in postmitotic regions.
(a) Immunostaining with anti-H3P of the subepidermal region of hippo *(RNAi)* animals and their controls. Nuclei are labeled in blue. White arrows indicate H3P+ cells. **(b)** FISH showing the colocalization of *hippo* with *piwi*, *nb32* and *agat*. **(c)** A scheme indicating the different regions quantified, from the more external part (light green) to the more internal (dark green), is shown. Corresponding quantification of the number of H3P+ cells in the different regions along the medio-lateral axis of the animals (n≥6). Scale bars: 150 µm (**a**); 25µm (**b**).

vim+ cells were mainly found in the epidermis (fully differentiated cells) of control animals, whereas they were mainly in the mesenchyme of *hippo (RNAi)* animals (Figure R2.5a-R2.5a'). This indicates that *hippo (RNAi)* causes a problem in the acquisition or maintenance of epithelial fate or in the migration process of epidermal cells. There was an increase in *vim*+/PIWI+ cells in the mesenchyme of *hippo (RNAi)* animals, whereas these cells were virtually absent in the mesenchyme of control animals (Figure R2.5a- R2.5a''). This result, together with the presence of ectopic mitotic cells, suggests that epidermal cells have a problem in the process of differentiation or fate maintenance but not in migration.

Quantification of double-positive cells for the different epidermal markers revealed an increase in *piwi*+/*agat*+, *nb*+/*agat*+ and *agat*+/*vim*+ cells in *hippo (RNAi)* animals compared to controls (Figure R2.5b). This increase in poorly committed cells in *hippo (RNAi)* animals is consistent with a failure of epidermal cells to progress appropriately through the hierarchical transitions that occur during epidermal lineage specification and suggests that they are unable to maintain a defined fate. Interestingly, double labeling of H3P+/*agat*+, H3P+/*nb32*+ or H3P+/*piwi*+ showed that mitotic cells are always *piwi*+ but never *agat*+ or *nb32*+ in both *hippo (RNAi)* animals and in controls (Figure R2.5c). Although we cannot exclude the possibility that ectopic mitotic cells could arise from a different lineage or from aberrant migration of stem cells, our findings suggests that mitotic cells never express postmitotic markers.

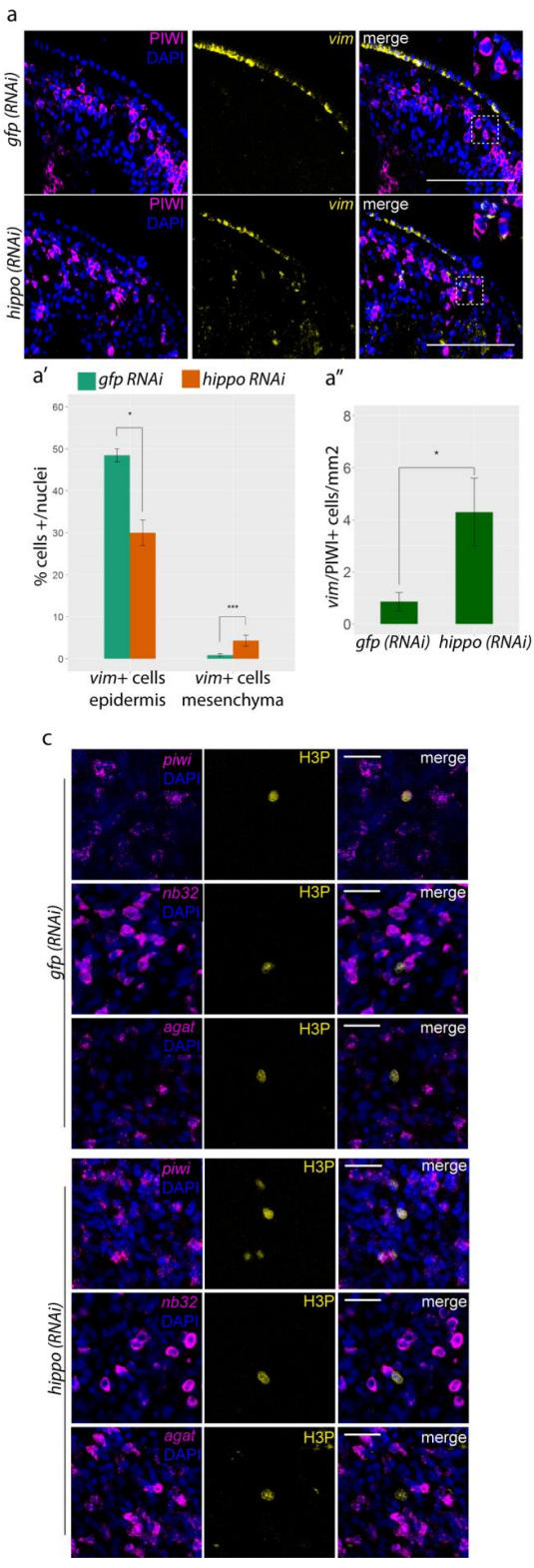
a
gfp (RNAi)
hippo (RNAi)
PIWI
DAPI
vim
merge
a'
gfp RNAi
hippo RNAi
% cells +/nuclei
vim+ cells epidermis
vim+ cells mesenchyma
a''
vim/PIWI+ cells/mm2
gfp (RNAi)
hippo (RNAi)
b
piwi
nb32
vim
agat
DAPI
merge
gfp (RNAi)
hippo (RNAi)
+ cells/mm2
piwi+/agat+
agat+/nb+
agat+/vim+
c
piwi
nb32
agat
DAPI
H3P
merge
gfp (RNAi)
hippo (RNAi)

Figure R2.5: *hippo* defines the boundaries of expression of epidermal markers.
(a) FISH staining for *vim* combined with immunostaining of anti-PIWI antibody in transverse sections of *hippo (RNAi)* animals and their controls. **(a')** Corresponding quantification of *vim*+ cells in the epidermis and the mesenchyme (n≥6). **(a'')** Corresponding quantification of *vim*+/PIWI+ cells (n≥6). (**b**) Double FISH staining with markers of different epidermal cell progenitors: *piwi/agat*, *agat/nb32* and *agat/vim* and corresponding quantification (n≥6). **(c)** FISH with *piwi*, *nb32* and *agat* combined with immunostaining using anti-H3P antibody. Nuclei are stained with DAPI. Error bars represent standard deviation. Data were analyzed by Student's t-test. *p<0.05; **p<0.01; ***p<0.001. Scale bars: 50 µm **(a)**; 25µm **(b)** and **(c)**.

In agreement with a problem in the specification of the epidermal lineage after *hippo* inhibition, we observed an increase in markers of ζ-neoblasts (*zfp-1* and *p53*), which are precursors of the epidermal lineage[221], in *hippo (RNAi)* RNAseq (Figure R2.6a). This increase could be caused by an increase in the number of ζ-neoblasts. However, we found that, while the levels of *piwi*—a general marker of stem cells—decreases in the transcriptome (Figure R2.6a), the number of cells that express it does not change in *hippo (RNAi)* animals (Figure R2.6b). Thus, the increase in the expression levels of ζ-neoblasts markers could also be due to an increase in the expression levels of those markers in ζ-neoblasts or the incorrect acquisition of its expression by other cell types. Overall, our analysis of the epidermal lineage shows an increase in the population of cells that co-express cell markers that define different epidermal cell lineages in *hippo (RNAi)* animals, as well as its improper location (Figure R2.6c). Thus, precursors and differentiated epidermal cells are neither properly defined nor located. Together these results indicate that *hippo* is essential for the acquisition and/or maintenance cell fate decisions in the epidermal lineage.

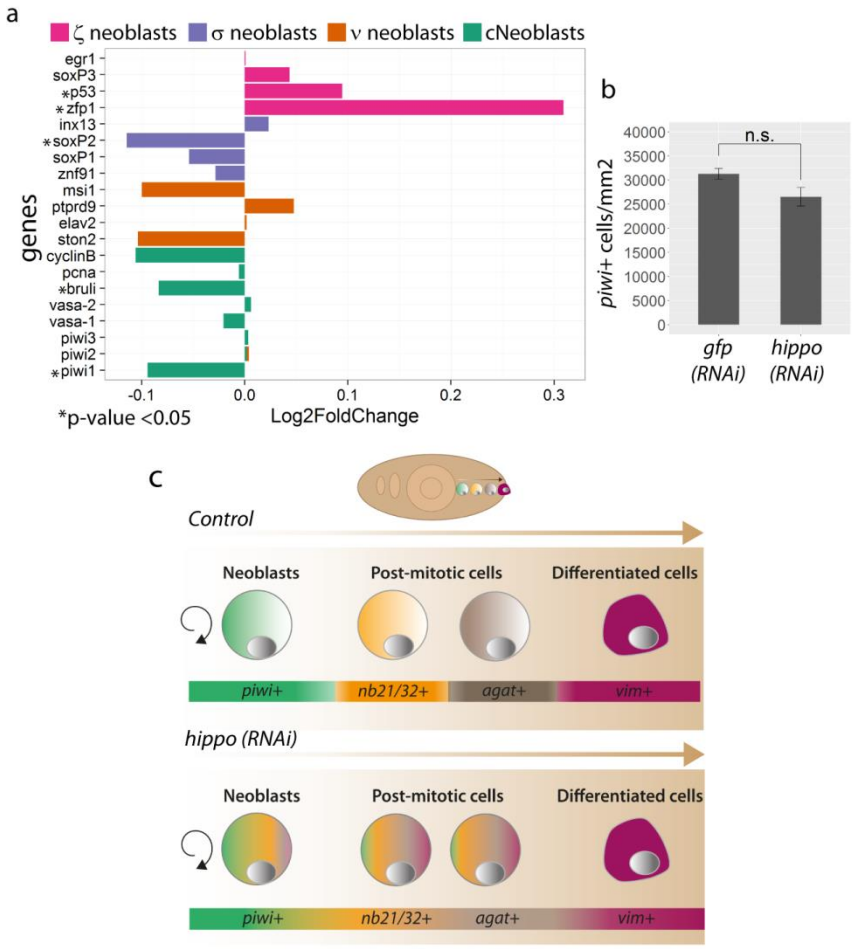

Figure R2.6: Epidermal specific-neoblasts are increased in *hippo (RNAi)* animals.

(a) Graph showing the relative expression levels of different neoblasts markers in the RNAseq of *hippo (RNAi)* animals. **(b)** Graph showing the quantification of *piwi*+ cells in control and *hippo (RNAi)* animals. n≥7. Error bars represent standard deviation. Data were analyzed by Student's t-test. n.s.: not significant *p<0.05; **p<0.01; ***p<0.001. **(c)** Scheme exemplifying the consequences of *hippo* inhibition in the epidermal lineage. In wild type animals, the onset of differentiation of stem cells causes the loss of *piwi* expression and the acquisition of post-mitotic genes in a sequential manner (*nb32 – agat – vim*) to reach the fully differentiated state in the epidermis (*vim*+ cells). In *hippo (RNAi)* animals the spatiotemporal transition of post-mitotic epidermal cells is loss: *piwi*, *nb32*, *agat* and *vim* co-express in the same cell and there is a decrease in the number of fully differentiated cells.

The Hippo pathway maintains the differentiated state in planarians

The presence of large numbers of undifferentiated cells and overgrowths following *hippo (RNAi)* could be explained either by problems in the differentiation of stem cells towards a specific fate or by a dedifferentiation process in which postmitotic cells are unable to maintain the committed state and start to express stem-cell markers. To investigate the possibility that postmitotic cells undergo dedifferentiation, we depleted the stem-cell population in planarians through *h2b (RNAi)*[163] and analyzed whether it recovered after *hippo* inhibition (Figure R2.7a). qPCR analysis using specific primers for *h2b* and *hippo* confirmed the inhibition of both genes (Figure R2.7b). ISH for *piwi* revealed no differences between *hippo (RNAi)* animals and controls (named "piwi WT" phenotype in Figure R2.7c), whereas in *h2b (RNAi)* animals *piwi* expression was completely absent (named "no *piwi*" phenotype in Figure R2.7c) (5/11) or reduced to a few scattered cells (named "disperse *piwi*+ cells" phenotype in Figure R2.7c) (6/11), which correspond to stem cells that escape from *h2b* inhibition (Figure R2.7c). Strikingly, we found several animals in the *h2b/hippo (RNAi)* group that had clusters of *piwi*+ cells in the marginal part of the animal (named "*piwi* clusters" phenotype in Figure R2.7c) (7/12) (Figure R2.7c). Interestingly, this corresponds to the region where ectopic mitosis and overgrowths were located. Moreover, we also observed that, despite the presence of *piwi* clusters, *h2b/hippo (RNAi)* animals had the same number of H3P+ cells as *h2b (RNAi)* animals, which, as expected, was very low compared to controls (Figure R2.7d). This indicates that the clusters of *piwi*+ cells found in *h2b/hippo (RNAi)* animals do not arise from proliferation of remaining stem cells that escape from *h2b* inhibition but from dedifferentiation of postmitotic cells that regain the expression of stem cell markers. The lack of proliferation caused by the inhibition of *h2b* explains the death of both *h2b/gfp* and *h2b/hippo (RNAi)* animals 15-17 days after the first *h2b* dsRNA injection.

Since our previous results demonstrate that *hippo* is required to properly maintain epidermal fate and that there is an increase in the expression of ζ-neoblast markers

after *hippo (RNAi)*, we analyzed whether the *piwi*+ clusters observed in *h2b/hippo (RNAi)* animals expressed the ζ-neoblasts marker *zfp1*. ISH showed that *h2b/hippo (RNAi)* animals were mostly depleted of *zfp1*, as were *h2b (RNAi)* animals (Figure R2.7e). This result does not allow us to determine whether *piwi*+ clusters arise from dedifferentiation of epidermal cells. It could be that *piwi*+ clusters arise from a different lineage or, alternatively, that during dedifferentiation epidermal cells do not maintain the lineage restriction. Nevertheless, our results indicate that Hippo is essential to maintain the postmitotic state in planarians and that its absence induces the dedifferentiation of post-mitotic cells towards a stem-cell identity.

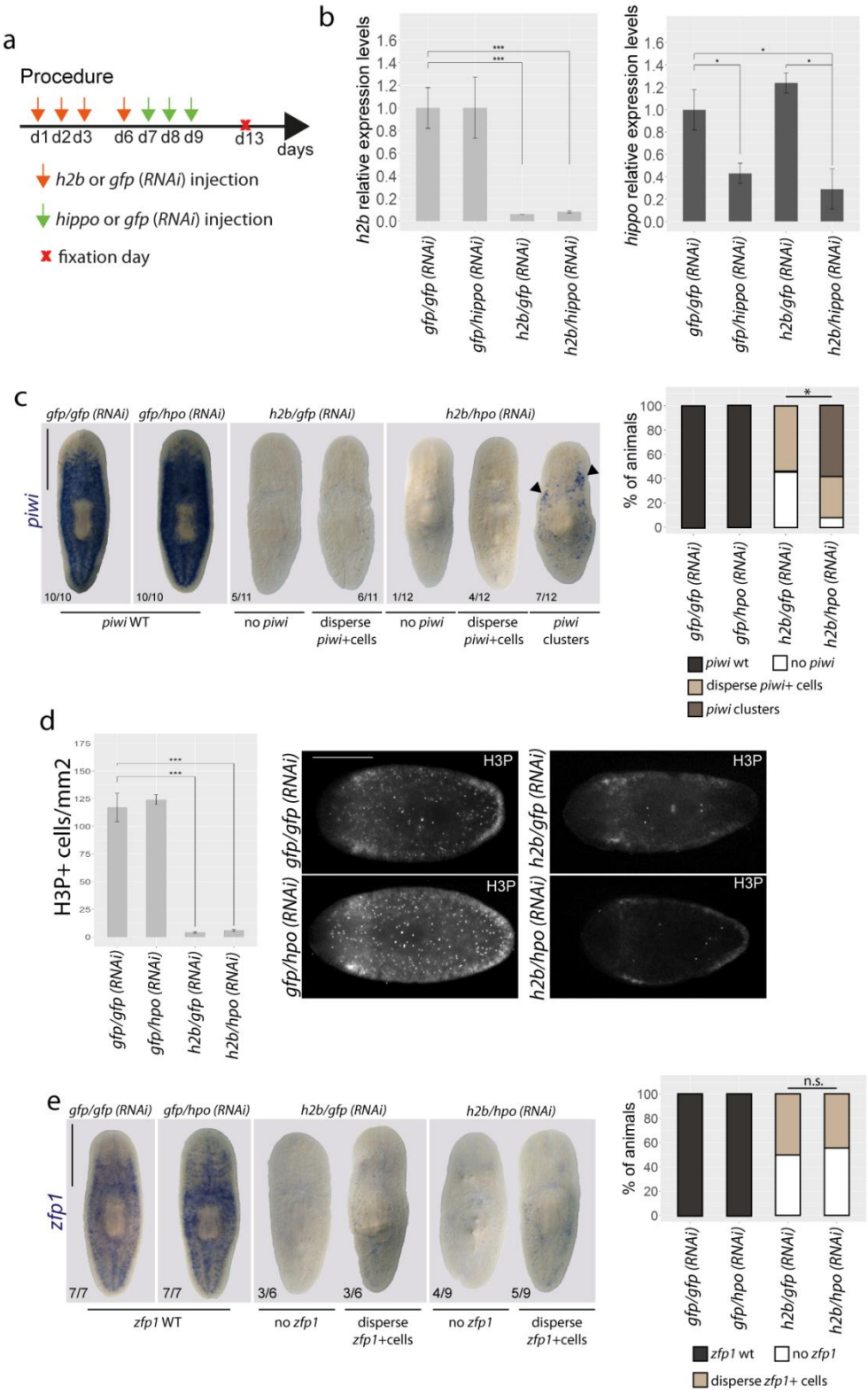
a
Procedure
d1 d2 d3
d6 d7 d8 d9
d13
days
h2b or gfp (RNAi) injection
hippo or gfp (RNAi) injection
fixation day
b
h2b relative expression levels
hippo relative expression levels
gfp/gfp (RNAi)
gfp/hippo (RNAi)
h2b/gfp (RNAi)
h2b/hippo (RNAi)
c
gfp/gfp (RNAi)
gfp/hpo (RNAi)
h2b/gfp (RNAi)
h2b/hpo (RNAi)
piwi
10/10
10/10
5/11
6/11
1/12
4/12
7/12
piwi WT
no piwi
disperse piwi+cells
no piwi
disperse piwi+cells
piwi clusters
% of animals
piwi wt
no piwi
disperse piwi+ cells
piwi clusters
d
H3P+ cells/mm2
H3P
e
zfp1
7/7
7/7
3/6
3/6
4/9
5/9
zfp1 WT
no zfp1
disperse zfp1+cells
no zfp1
disperse zfp1+cells
n.s.
zfp1 wt
no zfp1
disperse zfp1+ cells

Figure R2.7: *hippo* maintains the differentiated state in planarians.
(a) Cartoon illustrating the experimental design of the *hippo (RNAi)* experiment in neoblast depleted animals. **(b)** Relative expression of *h2b* and *hippo* in four days post-injection animals determined by qRT-PCR. Values represent the means of three biological replicates. **(c)** ISH staining for *piwi* in the four *(RNAi)* conditions and the corresponding quantification of *piwi* expression distribution according to the 4 categories assigned (n≥10). Black arrows indicate the *piwi*+ clusters. **(d)** Immunostaining of *h2b/hippo (RNAi)* animals and the respective controls with anti-H3P antibody. The corresponding quantification is shown (n≥14). **(e)** ISH staining for *zfp1* in the four *(RNAi)* conditions and the corresponding quantification of *zfp1* expression according to the 4 categories assigned (n≥10). Error bars represent standard deviation. Data were analyzed by Student's t-test: **(b)** and **(d)** or Chi-square test, applying Bonferroni correction **(c)** and **(e)**. *p<0.05; ***p<0.001; n.s., not significative. Scale bars: 1mm **(c)**; **(d)**; **(e)**.

Chapter 3

Functional characterization of the Hippo pathway during planarian regeneration

Functional characterization of the Hippo pathway during planarian regeneration

A Hippo-Yorkie signaling controls cell differentiation during planarian regeneration

Although Yki/YAP is a highly evolutionary conserved downstream element of the Hippo pathway[24], the unexpected phenotype observed after *yki* inhibition in planarians lead to the proposal that in planarians Yki does not act downstream of Hippo[222]. To test the possible conservation of a Hippo-Yki signal in the control of cell renewal in planarians we generated a specific anti-Yki antibody with the aim to check its expression levels and pattern. We found that Yki levels decrease in *yki (RNAi)* animals, both in western blot and in immunohistochemical analysis, as expected (Figure R3.1a-b). In contrast, Yki protein levels are up-regulated specifically in the nucleus in *hippo (RNAi)* planarians (Figure R3.1a-b), supporting that a Hippo-Yki signal is conserved in planarians.

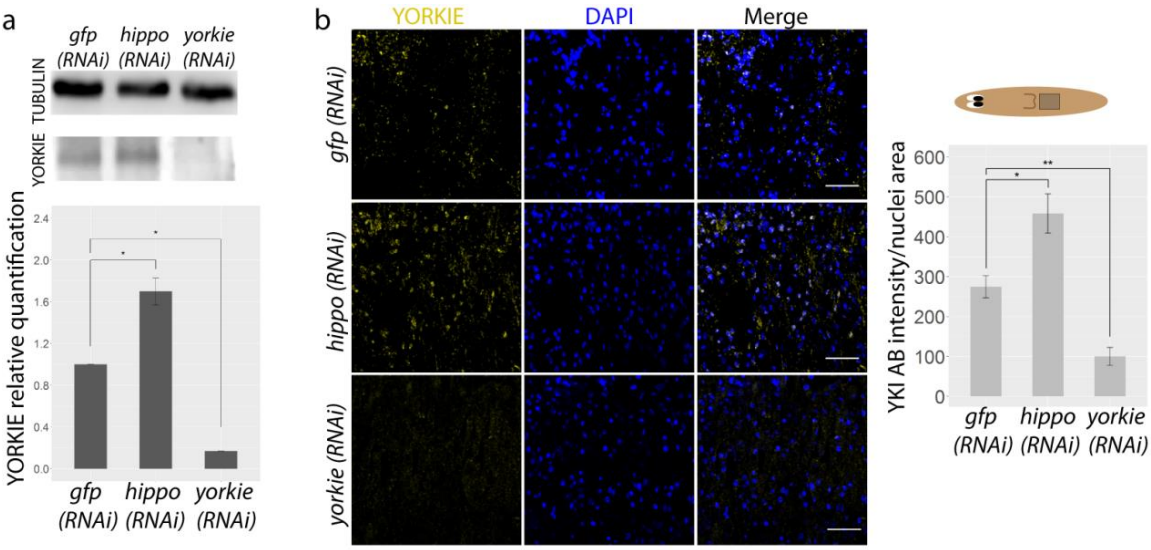

Figure R3.1: Yorkie is one of the Hippo pathway targets in planarians.

(a) Western-Blot of protein extracts from *hippo (RNAi)*, *yorkie (RNAi)* and controls immunoblotted with the anti-YORKIE and anti-α-TUBULIN antibodies. Extracts correspond to intact animals after three weeks (*hippo (RNAi)*) or one week (*yorkie (RNAi)*) of inhibition. The corresponding quantification of YORKIE versus TUBULIN signal is shown. Bars show the mean of three biological replicates. **(b)** Immunostaining with anti-YORKIE antibody in longitudinal sections of *hippo (RNAi)*, *yorkie (RNAi)* and control animals. *hippo* was inhibited during three consecutive weeks and *yorkie* during one week. Nuclei were stained with DAPI. The corresponding quantification of the nuclear signal in the post-pharyngeal region is shown. Yorkie nuclear signal intensity was measured using the integrated density (RID) and then normalized with the respective nuclear area (see materials and methods). n≥3. Error bars represent standard deviation. Data were analyzed by Student's t-test. *p<0.05; **p<0.01. Scale bar: 50μm.

To deep into the knowledge of the Hippo-Yki role in planarians we performed some experiments during planarian regeneration, since during homeostasis *yki* inhibition produces the blotted phenotype which leads to animal dead, preventing further studies. We analyzed the effect of *hippo* inhibition in planarians in which the head and tail were amputated (Figure R3.2a). ISH shows that both *hippo* and *yki* are expressed in the wound region at five days after amputation revealing a possible role of these genes during planarian regeneration (Figure R3.2b). Our results demonstrated that *hippo (RNAi)* regenerating animals show an increase in the mitotic rates but regenerate smaller blastemas (Figure R3.2c-d), in which the new tissues as the brain or digestive system do not differentiate properly (Figure R3.2e). Accordingly, quantification of the number of differentiated neural cell types as dopaminergic neurons (*th+)* or differentiated eye cells (*ovo*+ cells in the eye)[123] appear reduced after *hippo* inhibition (Figure R3.2f-g). Interestingly, despite the increase in mitotic rates and the problems in differentiation, *hippo (RNAi)* regenerating animals never show the formation of overgrowths. Conversely, our results show that *yki* inhibition in regenerating animals produces the opposite phenotype, which is the increase of differentiated neurons and photoreceptors (Figure R3.2f-g). In agreement with our results, a general increase in the number of several types of differentiated cells in *yki (RNAi)* animals has been recently reported[223].

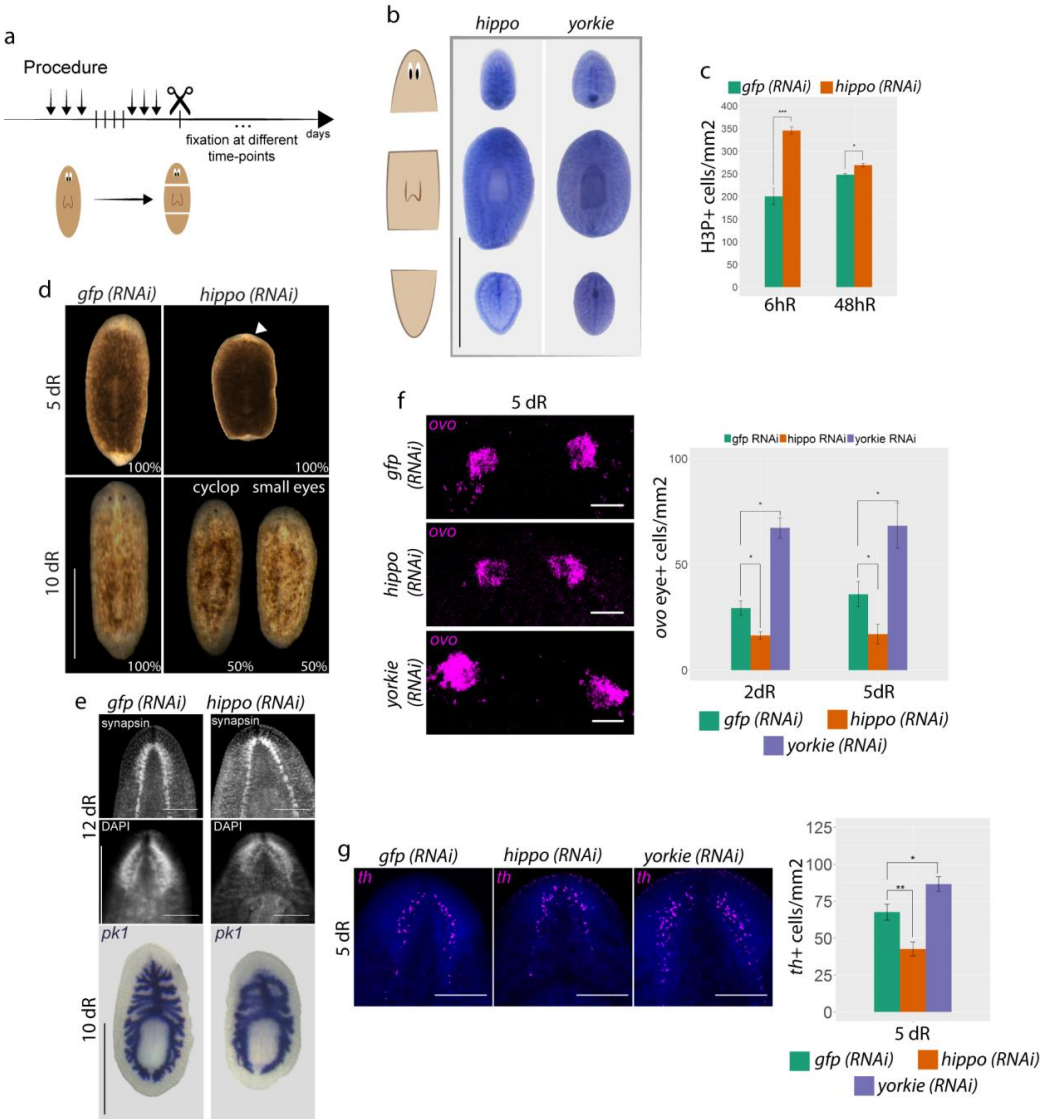
a
Procedure
fixation at different time-points
days
b
hippo
yorkie
c
gfp (RNAi)
hippo (RNAi)
H3P+ cells/mm2
6hR
48hR
d
gfp (RNAi)
hippo (RNAi)
5 dR
10 dR
100%
cyclop
small eyes
50%
e
gfp (RNAi)
hippo (RNAi)
12 dR
10 dR
synapsin
DAPI
pk1
f
5 dR
ovo
gfp (RNAi)
hippo (RNAi)
yorkie (RNAi)
gfp RNAi
hippo RNAi
yorkie RNAi
ovo eye+ cells/mm2
2dR
5dR
g
gfp (RNAi)
hippo (RNAi)
yorkie (RNAi)
th
5 dR
th+ cells/mm2

Figure R3.2: A Hippo-Yki *signal* is essential for proper planarian regeneration.
(a) Cartoon illustrating the procedure of *(RNAi)* inhibition in regenerating conditions. Animals were starved one week before the experiment and then injected during three consecutive days for two weeks, then were cut and fixed at different time points. **(b)** ISH showing the expression pattern of *hippo* and *yorkie* at five days of regeneration. **(c)** Quantification of H3P+ cells at 6 and 48 hours of regeneration (hR) in *hippo (RNAi)* animals and the corresponding controls (n≥8). **(d)** Stereomicroscopic view of control and *hippo (RNAi)* 5-10 days regenerating (dR) live animals (n=10). White arrow indicates the smaller blastema. **(e)** Anti-synapsin immunostaining of the brain region of *hippo (RNAi)* and control animals. Nuclei are stained with DAPI. Images correspond to 12 days regenerating animals. ISH staining with *pk1* (digestive system) in *hippo (RNAi)* and control animals. Images correspond to 10 days regenerating animals. **(f)** FISH staining of the eyes with *ovo* in *hippo (RNAi)*, *yorkie (RNAi)* and control animals. Images correspond to 5 days regenerating animals. The corresponding quantification is shown (dR, days of regeneration). **(g)** FISH staining of dopaminergic neurons (*th*+) in 5 days regenerating control, *hippo* (*hpo*) *(RNAi)* and *yorkie* (*yki*) *(RNAi)* animals. Nuclei are stained with DAPI. The corresponding quantification is shown (n≥5). Error bars represent standard deviation. Data was analyzed by Student's t-test. *p<0.05; **p<0.01. Scale bars: 500µm **(d)**; 250µm **(e)**; 50µm **(f)**; 150 µm **(g)**.

These results indicate that a conserved Hippo-Yki signal regulates cell differentiation during planarians regeneration. In regenerative contexts, it has been reported that Yki/YAP nuclearization induced after *hippo* inhibition or Yki/YAP direct hyperactivation is associated to an increase in the proliferative rates and an improvement of the regenerative abilities[27,224]. In contrast, in planarians, *hippo* inhibition, and thus Yki nuclearization, blocks differentiation and decreases the regenerative response.

Chapter 4

Up-stream regulators and inhibitors of the Hippo pathway

Up-stream regulators of Hippo pathway

lgl2 is an up-stream regulator of the Hippo pathway in planarians

To understand whether the up-stream signals identified in other organisms also regulate Hippo function in planarians we proceed to the identification of some potential up-stream regulators of the pathway[62]. Thus, we identified *Smed-lgl1*, *Smed-lgl2*, *Smed-expanded*, *Smed-merlin* and *Smed-scribble* (for simplicity: *lgl1*, *lgl2*, *ex*, *mer* and *scrib*) (Annex 1). ISH show that they present a rather ubiquitous, although *mer* is specially enriched in the pre-pharyngeal regionand *lgl1* is also expressed in the CNS *In silico* searches in the single-cell trasncriptomic database[194] show that these genes, except *mer*, are expressed in several planarian cell types (Figure R4.1a-b).

To test the function of these genes during planarian homeostasis we proceed to their silencing through *(RNAi)* during three consecutive weeks. At the third week, we observed that animals exhibit unpigmented regions and overgrowths in the most marginal part of the body (Figure R4.2a). Although the phenotype was milder, it resembled the phenotype observed after *hippo* inhibition. Since these genes are directly related with cell-cell contact and cell junctions[62] we checked the organization of adheren junctions after their silencing through the analysis of B-catenin2[220]. Our results demonstrate that in all *(RNAi)* animals β-catenin2 is not propperly organized when compared with controls (Figure R4.2b), although the defect was more evident in *lgl2* and *scrib (RNAi)* animals. These results suggest that *lgl1*, *lgl2*, *ex*, *mer* and *scrib* could be up-stream regulators of Hippo in planarians, and that they play an important role in the organization of cell junctions.

To check the role of these genes in the control of cell proliferation we performed an analysis of mitotic activity using anti-H3P. We observed that there is a general tendency in increasing in the mitotic rate, although only in *lgl2 (RNAi)* animals this increase was significant (Figure R4.2c).

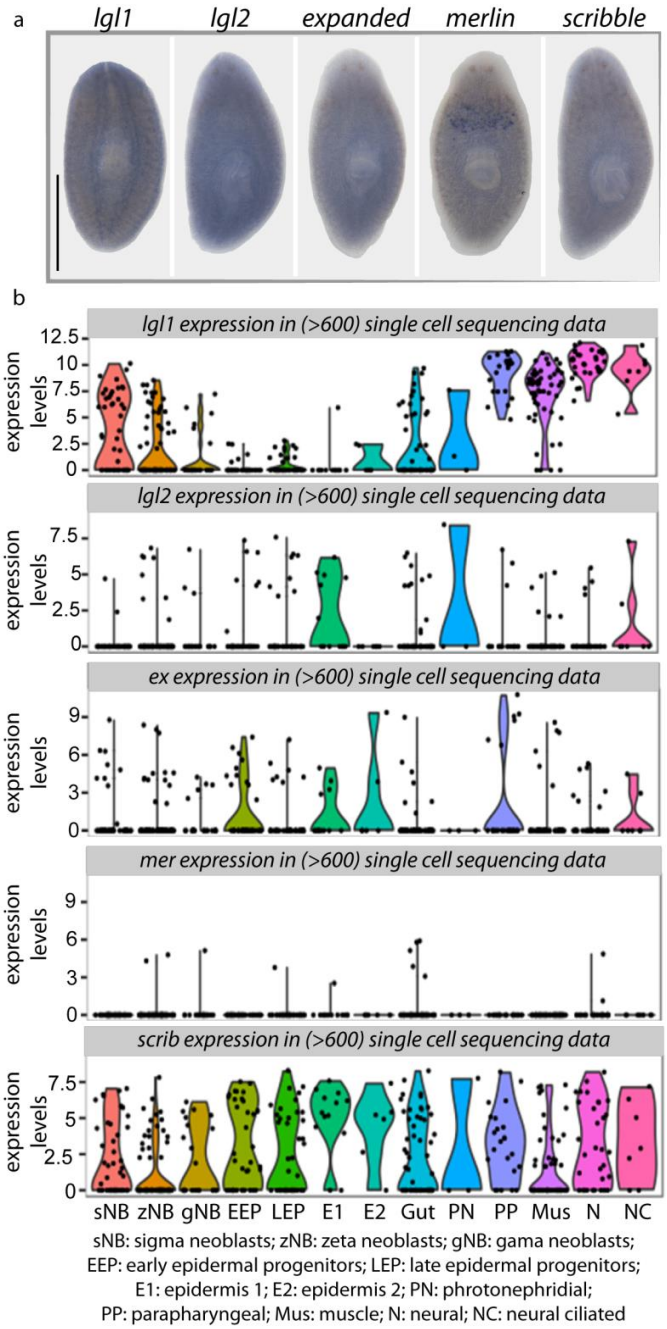

Figure R4.1: Hippo pathway up-stream regulators expression pattern.

(a) ISH of *lgl1*, *lgl2*, *expanded*, *merlin* and *scribble* showing their expression pattern. **(b)** *lgl1*, *lgl2*, *expanded*, *merlin* and *scribble* expression levels in different cell types according to a single-cell RNAseq[194]. Scale bar: 1mm.

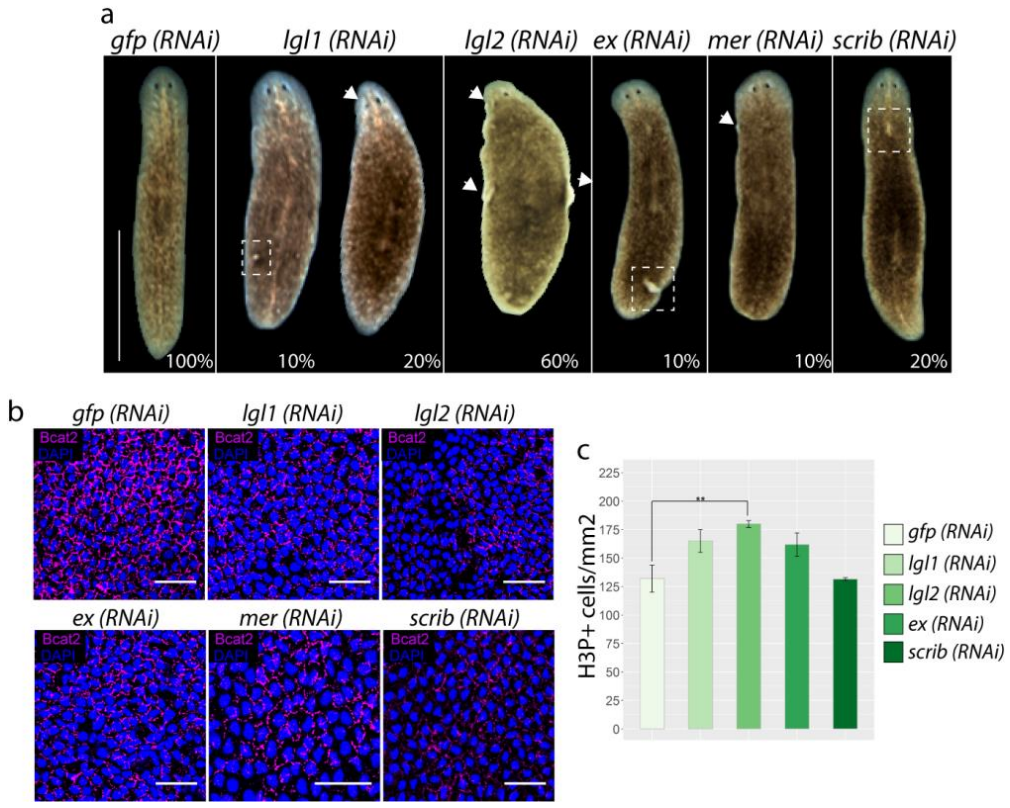

Figure R4.2: Inhibition of putative Hippo pathway up-stream regulators leads to overgrowths.

(a) Stereomicroscopic view of control, *lgl1, lgl2, expanded, merlin* and *scribble (RNAi)* live animals. *(RNAi)* animals show the formation of overgrowths and unpigmented regions in the marginal part of the body (n=12). **(b)** Immunostaining using β-catenin2 of the planarian epidermis in control and *(RNAi)* animals. White arrows indicate overgrowths or undifferentiated regions and white boxes unpigmented regions. **(c)** Quantification of mitotic activity (H3P+ cells) (n≥8). Error bars represent standard deviation. Data was analyzed by Student's t-test. **p<0.01. Scale bars: 1mm **(a)**; 50µm **(b)**.

Since *lgl2 (RNAi)* animals are the ones that present a more similar phenotype to *hippo (RNAi)* animals, we proceed to a deeper analysis of this gene. Thus, analysis of the population of undifferentiated cell through PIWI expression shows that PIWI+ cells

accumulated in the subepidermal overgrowths and in the epidermis itself (Figure R4.3a). Furthermore, analysis of the differentiated tissues demonstrated that the muscular layer and the visual system are not properly structured or maintained, suggesting a problem in cell differentiation (Figure R4.3b).

Together these results suggest that *lgl2* could be an important up-stream regulator of Hippo, playing an essential role in the maintenance of the differentiated structures.

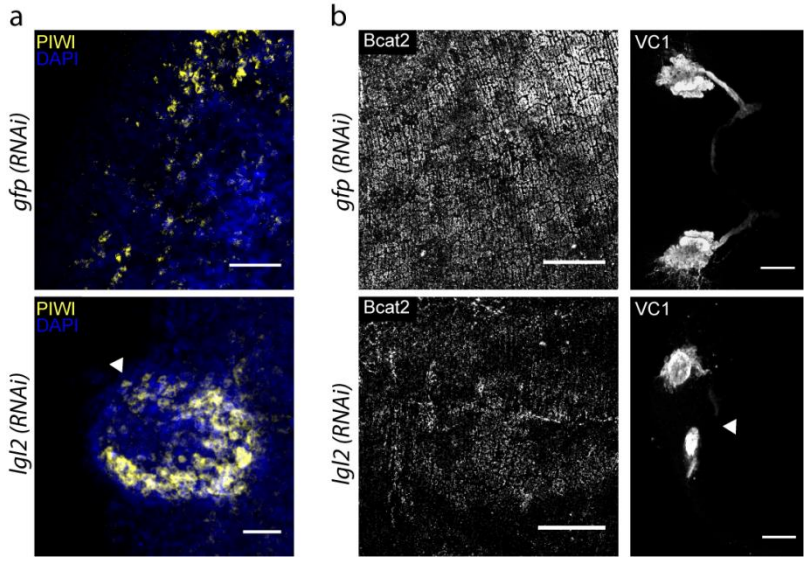

Figure R4.3: *lgl2* inhibition yields overgrowths and affects differentiated structures.
(a) Immunostaining using anti-PIWI antibody in an overgrowth region in *lgl2 (RNAi)* animals. Images correspond to confocal Z-projections. White arrow indicates a PIWI+ cell in the epidermis of the overgrowth. **(b)** Immunostaining using anti-β-catenin2 from the planarian muscular layer (unspecific signal that is usefull to visualize the muscular layer). Immunostaining with VC1 (anti-arrestin) in control and *lgl2 (RNAi)* animals. White arrow indicates aberrant optic chiasm. Scale bars: 50µm **(a)**; 100 µm **(b)**.

As described in *Drosophila*, the inhibition of *lgl2* in planarians could be inhibiting Hippo and, therefore, promoting the entrance of Yorkie in the nucleus in a Par-complex-dependent manner (Figure R4.4c and reviewed in the chapter 2 of the Introduction). To further understand the relationship between *lgl2* and *hippo*, we proceed to the inhibition of both genes simultaneously. We observed that double *lgl2/hippo (RNAi)* animals present a more severe phenotype than *lgl2* or *hippo (RNAi)* alone (Figure R4.4a). In addition, mitotic rates are higher in double *(RNAi)* animals than in single inhibited animals (Figure R4.4b). These results indicate that *lgl2* and *hippo* act synergistically, although we can not demonstrate with the current datathat both genes are acting through the same cascade.

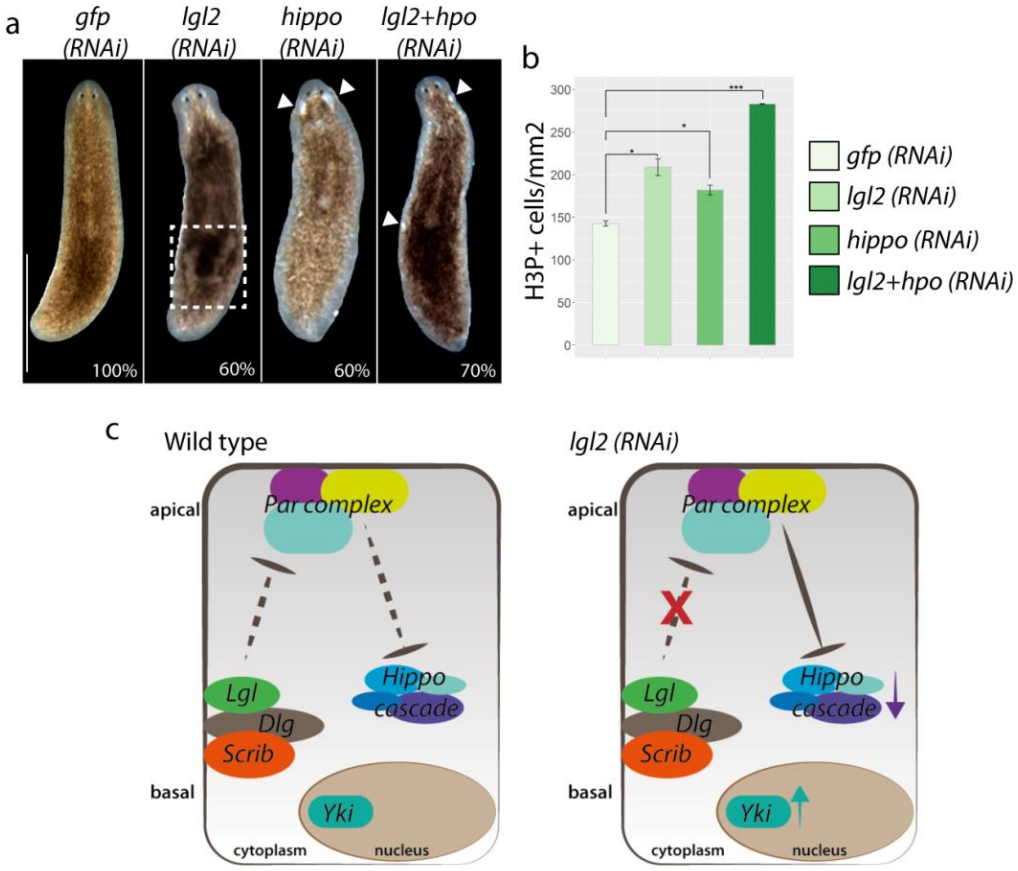

Figure R4.4: Lgl2 is an up-stream regulator of the Hippo pathway

(a) Stereomicroscopic view of control, *lgl2*, *hippo*, and *lgl2/hippo (RNAi)* live animals. *(RNAi)* animals show the formation of overgrowths and unpigmented regions in the marginal part of the body (n=10). White arrows indicate overgrowths and white boxes unpigmented regions. Scale bar= 1mm **(b)** Quantification of mitotic activity (H3P+ cells) (n≥7). Error bars represent standard deviation. Data was analyzed by Student's t-test. *p<0.05; **p<0.01. **(c)** Cartoon illustrating the possible role of *lgl2* in planarians. In wild-type conditions, the complex formed by Lgl/Scribble/Dlg inhibits the Par complex in order to activate the Hippo pathway. In *lgl2 (RNAi)* conditions, the Par complex inhibits the Hippo kinase cassette, promoting Yorkie nuclearization.

Inhibitors of the Hippo pathway

Ajuba proteins and Zyxin are putative Hippo pathway inhibitors

As referred in the introduction of this thesis, Ajuba proteins and Zyxin are well known Hippo pathway inhibitors in *Drosophila*[63,64,67]. To check if these genes act as Hippo pathway inhibitors in planarians, we identified and inhibit these genes by (RNAi).

We found two Ajuba proteins in planarians that we named *Smed-jub* and *Smed-jub B* (for simplicity, *jub* and *jub B)*, in which Jub B is shorter than Jub but conserves the three LIM domains (Annex 1), and one single copy of the ortholog Zyxin, *Smed-Zyxin* (for simplicity, *zyxin*). ISH shows that these genes present a ubiquitous expression throughout the planarian body. *in silico* searches in the single-cell transcriptomic database [194] show that *jub* is mainly expressed in the neoblasts and in the epidermal lineage while *jub b* and *zyxin* are expressed in muscle cells (Figure R4.5a-b).

To decipher if these genes are inhibitors of the Hippo pathway we silenced them through *(RNAi)* during three consecutive weeks. No *in vivo* phenotype was observed after this time of inhibition (Figure R4.6a). To assess the role of these genes in the control of cell proliferation and cell death we analyzed the mitotic activity through anti-H3P and cell death by measuring Caspase-3 activity. Our results show that inhibition of *jub* does affect neither cell proliferation nor cell death (Figure R4.6b-c). Conversely, inhibition of *jub B* and *zyxin* leads to a decrease in cell proliferation but also in cell death (Figure R4.6b-c). The decrease in mitosis could indicate that those genes act as inhibitors of Hippo. However, in *hippo (RNAi)* animals cell death decreases, as in *jub B* and *zyxin (RNAi).* An explanation could be that those genes inhibit the proliferative response exerted by *hippo*, but not the apoptotic. In this case, a compensatory mechanism, in which planarians sense less proliferating neoblasts, could lead to cell death inhibition. This issue will be debated in more detail in the discussion chapter. Although more experiments should be done, these results

suggest that *jub B* and *zyxin* could be Hippo pathway inhibitors in planarians (Figure R4.6d).

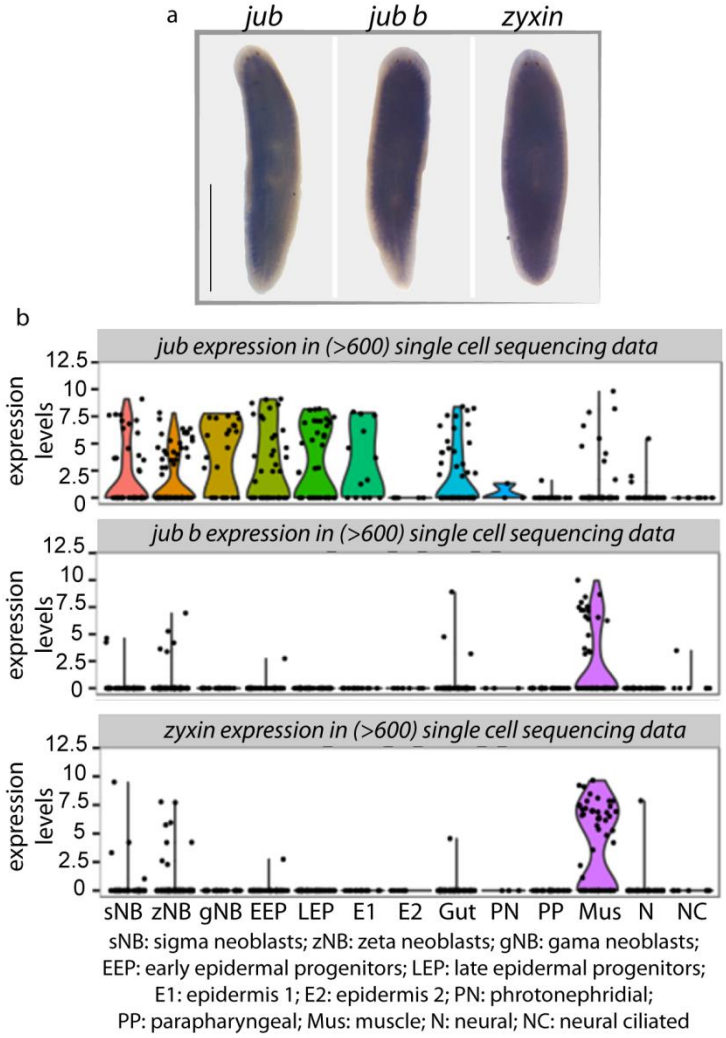

Figure R4.5: Hippo pathway inhibitors are mainly expressed in muscle cells.

(**a**) ISH showing the ubiquitous expression pattern of *jub*, *jub B* and *zyxin*. (**b**) *jub*, *jub B* and *zyxin* expression levels in different cell types according to a single-cell RNAseq[194]. Scale bar: 1mm.

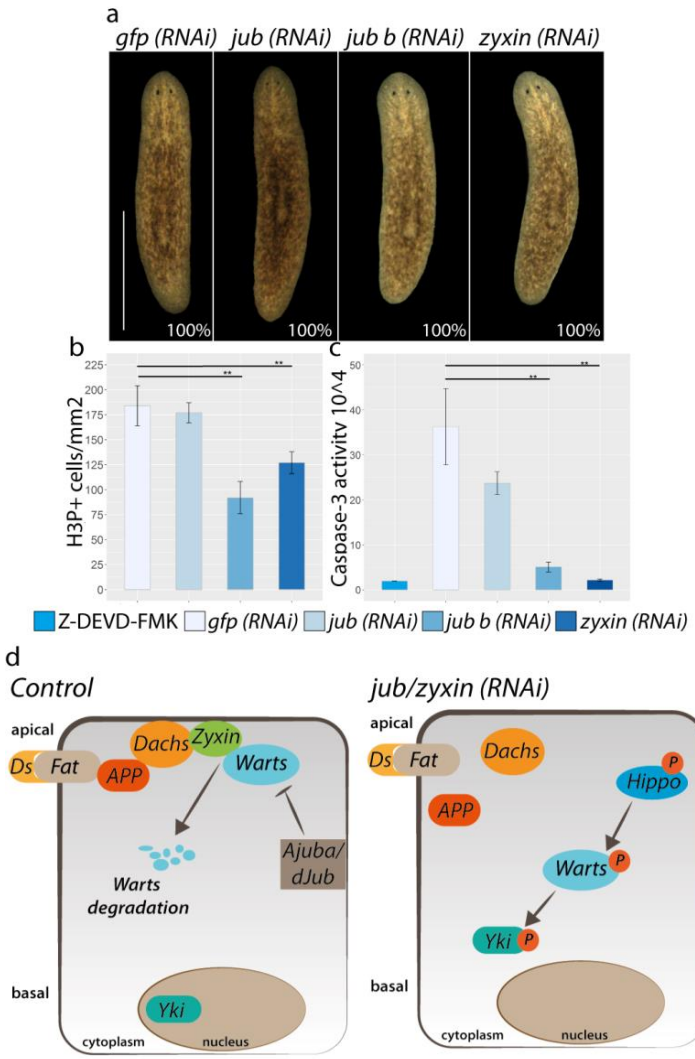

Figure R4.6: Hippo inhibitors regulate cell proliferation and cell death.

(a) Stereomicroscopic view of control, *jub, jub B* and *zyxin (RNAi)* live animals. *(RNAi)* animals do not present any *in vivo* phenotype (n=10). Scale bar =1mm. **(b)** Quantification of mitotic cells (H3P+) (n>8). **(c)** Quantification of Caspase3-activity. The results are presented as units of caspase-3 activity per µg of protein. The experiments were performed using three biological replicates. Error bars represent standard deviation. Data was analyzed by Student's t-test. **p<0.01. **(d)** Cartoon illustrating the possible role of *jub b* and *zyxin* in planarians. In wild-type conditions, the complex formed by Ds/Fat initiate a cascade of events that result in the interaction between *zyxin* and *warts*, promoting its degradation. On the other hand, *jub* proteins direct inhibit *warts*. In both situation, Yorkie nuclearization increases. In *jub b* and *zyxin (RNAi)* conditions, the Hippo pathway is active, preventing Yorkie nuclearization.

Chapter 5

Hippo targets in planarians

Hippo targets in planarians

Identification of Hippo targets in planarians

During this project we performed an RNAseq of *hippo (RNAi)* animals after one, three and four weeks of inhibition. The aim was to identify putative targets of the Hippo pathway in planarians out of the genes differentially expressed after one week of *hippo* inhibition and also identify genes involved in the onset of the phenotype.

To identify putative targets of Hippo in planarians we selected the first eleven downregulated genes in the *hippo (RNAi)* animals RNAseq (Table R5.1 and Annex 1). *In silico* searches in the single-cell transcriptomic database[194] show that most of these genes are expressed in several planarian cells types (Figure R5.1). However, *med17* is expressed only in neoblasts and *hyprot* is mainly expressed in the epidermal lineage (Figure R5.1).

Table R5.1: Down-regulated genes selected as putative Hippo targets.
Selected down-regulated genes in *hippo (RNAi)* RNAseq after one week of inhibition. Each column contains the following information: gene name, gene symbol, fold change and p-value.

Name	Symbol	Log2FoldChange	p-value
Mediator of RNA polymerase II transcription subunit 17	med17	-0,53	1,07E-9
Spondin	spon	-0,58	1,4E-4
Coilded-coil domain containing protein 96	ccdc96	-0,40	2,1E-4
Isoform 2 of centromere-associated protein E	cenpe	-0,52	2,3E-4
Synaptonemal complex protein 1	sycp1	-0,29	2,7E-4
Abnormal spindle-like microcephaly-associated protein	aspm	-0,34	3,4E-4
Isoform 3 of dystonin	dst3	-0,41	5,6E-4
Hypothetical Protein	hyprot	-0,40	6,8E-4
Mucin	muc	-0,57	1,2E-3
Musashi homolog 2b	msi2b	-0,24	2,3E-3
X-ray radiation resistance-associated protein1	xrra1	-0,24	1,4E-2

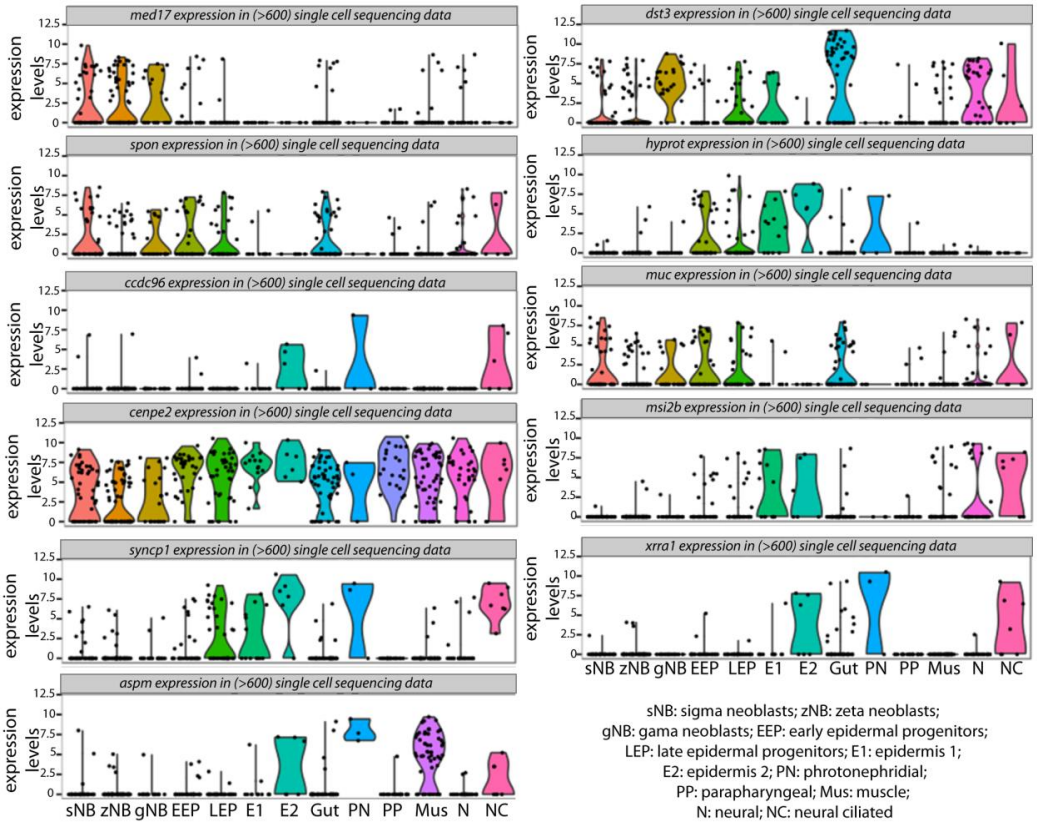

Figure R5.1: Expression levels of candidate Hippo targets.
Expression of the eleven putative targets of Hippo pathway selected from the *hippo (RNAi)* RNAseq in Planaria SC.

To achieve if these genes are targets of Hippo in planarians we inhibited them through *(RNAi)* to assess if it reproduces the *hippo (RNAi)* phenotype. After three weeks of inhibition we observed that four of the putative Hippo targets (*ccdc96*, *cenpe2*, *aspm* and *xxra1*) do not present any in vivo phenotype (Figure R5.2a). The inhibition of six putative target genes (*spon*, *syncp1*, *dst3*, *hyprot*, *muc* and *msi2b*) promotes the formation of small overgrowths or unpigmented regions (Figure R5.2a). However, the inhibition of *syncp1*, *dst3* and *msi2b* produces the phenotype in a very low penetrance and expressivity. Finally, *med17 (RNAi)* animals presented a strong phenotype that

lead to head regression (Figure R5.2a), which is consistent with the phenotype observed with other genes expressed in the neoblasts[161]. To perform a deeper characterization, we selected the genes that presented a stronger phenotype: *med17, spondin*, *hypothetical protein* and *mucin*.

First, we analyzed the role of these four genes in the control of cell proliferation and cell death. Mitotic activity was analyzed through anti-H3P and cell death by measuring Caspase-3 activity. Our results show that the inhibition of *spon* and *muc* increases the mitotic rates compared to control animals. *med17 (RNAi)* animals present a decrease in mitosis, and *hyprot (RNAi)* animals do not show changes in the mitotic activity compared to controls (Figure R5.2b and Table R5.2). An increase in the cell death is observed after the inhibition of *med17*, *spon* and *hyprot,* but remains unaltered in *muc (RNAi)* animals (Figure R5.2c and Table R5.2).

As described to before, Hippo plays a pivotal role in the control of cell differentiation and maintenance of differentiated state in planarians. To check if these genes are involved in the differentiation process in planarians we quantified the number of dopaminergic neurons by FISH using *th*. Our results demonstrate that *(RNAi)* animals have the same number of neurons than control animals (Figure R5.3a-b and Table R5.2). Analysis of the epidermal progenitors (*nb32* and *agat*) reveal that *med17 (RNAi)* animals show a drastically reduction of the epidermal precursors in the head region which fits with the neoblast-loss phenotype observed *in vivo* (Figure R5.3c and Table R5.2). The inhibition of *spon*, *hyprot* and *muc* does not affect the number of epidermal progenitors.

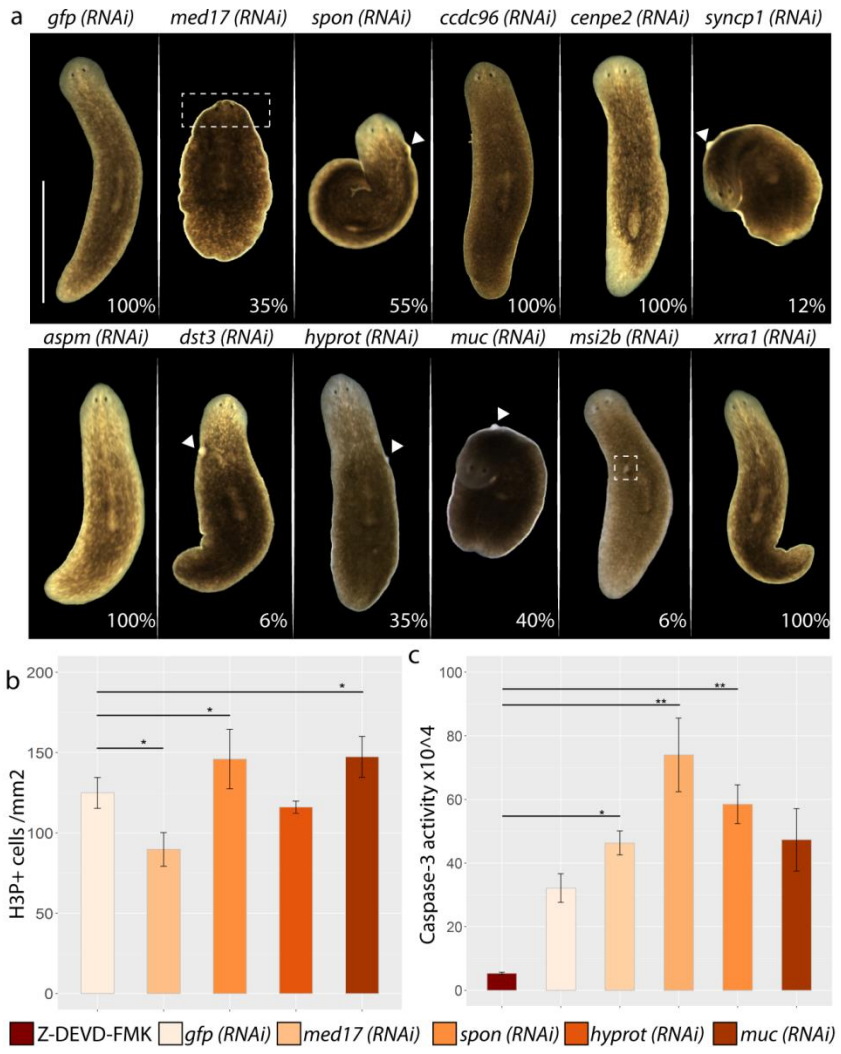

Figure R6.2: Hippo targets affect cell turnover.

(a) Stereomicroscopic view of control, *med17*, *spon*, *ccdc96*, *cenpe2*, *syncp1*, *aspm*, *dst3*, *hyprot*, *muc*, *msi2b* and *xrra1 (RNAi)* live animals (n=10). White arrows indicate overgrowths and white boxes head regression (*med17 (RNAi)*) or unpigmented regions (*msi2b (RNAi)*). Scale bar = 1mm. **(b)** Quantification of mitotic cells (H3P+) (n>8). **(c)** Quantification of Caspase3-activity. The results are presented as units of caspase-3 activity per µg of protein. The experiments were performed using three biological replicates. Error bars represent standard deviation. Data was analyzed by Student's t-test. *p<0.05; **p<0.01; ***p<0.001.

Although a detailed analysis of the phenotypes of those RNAi's should be performed, the phenotypes resulting from the inhibition of the candidate genes obtained through our experimental approach suggest that they could be Hippo target genes. The fact that none of them reproduces the strong phenotype observed after *hippo* inhibition, neither the mitotic and apoptotic behaviour could indicate that *hippo* is controlling the function of several targets that exert specific functions with respect to cell proliferation, differentiation and cell death. Only the inhibition of these genes together would lead to the *hippo (RNAi)* phenotype.

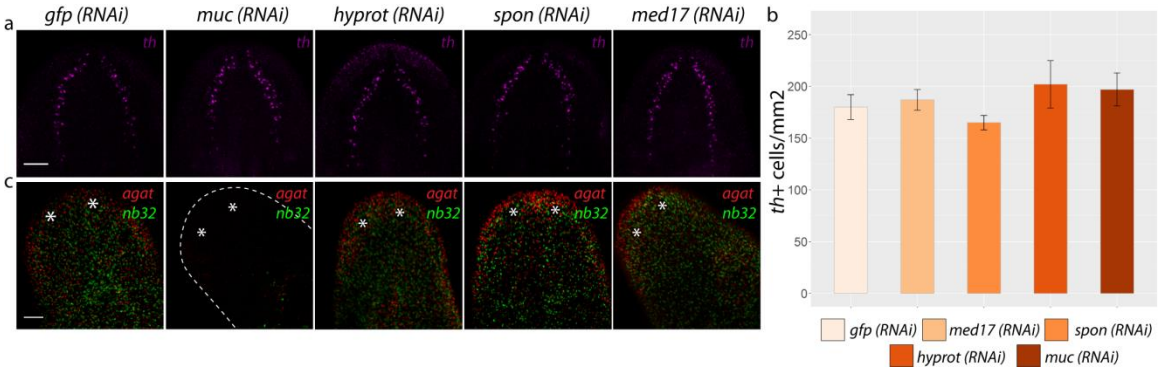

Figure R6.3: Hippo targets do not affect differentiation

(a) FISH staining for dopaminergic neurons (*th*), and the corresponding quantification (n≥5). Error bars represent standard deviation. Data were analyzed by Student's t-test. **(b)** FISH staining for epidermal progenitors (*nb32* and *agat*). Images correspond to confocal z-projections. Scale bars: 100µm.

Table R6.2: Summary of observed phenotypes.

Symbol	Phenotype				
	in vivo	**Proliferation**	**Cell death**	**Progenitors**	**Differentiated cells**
med17	Head regression	↓	↑	↓	=
spon	Small overgrowths (55%)	↑	↑	=	=
hyprot	Small overgrowths (35%)	=	↑	=	=
muc	Small overgrowths (40%)	↑	=	=	=

Discussion

The results found in the present study demonstrate that the main role of the Hippo pathway in a stem cell-based system, such as planarians, is not to regulate the size of the animal or the stem-cell population, as found in other systems[14,112,225], but is required for the maintenance of the differentiated fate. Nevertheless, *hippo* inhibition promotes the formation of overgrowths, and the appearance of extensive areas composed by undifferentiated cells. As follows, we will discuss the specific roles that Hippo exerts in planarians that have been found in the present study.

Hippo holds the differentiated state in planarians

Hippo activation and/or Yki/YAP/TAZ citoplasmatic retention are essential for a proper cell differentiation in several model organisms. Nowadays it is known that ectopic over activation of Yki/YAP/TAZ in progenitors/differentiated cells leads to reprogramming and acquisition of a stem cell-like state[28,226]. During this study we found that the severe inhibition of *hippo* affects the maintenance of differentiated structures as the CNS, the eyes, and the digestive system. The inability to maintain the differentiated structures after *hippo* inhibition could be caused by problems in cell differentiation, or by the dedifferentiation of postmitotic cells. Our finding that planarians depleted of neoblasts restore the expression of stem cell markers (*piwi)* after *hippo* inhibition, suggests that dedifferentiation is occurring in *hippo (RNAi)* animals. However, it should also be considered that the process of differentiation of progenitor cells in *hippo (RNAi)* animals could also be affected, giving rise to cells that are improperly determined, which are the ones that co-express markers of stemness and differentiated cells. Therefore, in a stem cell based system, such as planarians, the Hippo pathway is essential to maintain the differentiated state of cells (Figure D1).

The imbalance between apoptosis and mitotic cells after hippo inhibition does not lead to changes in planarian body size, nor in cell number

In the present study, we have shown that *hippo* is required to regulate the apoptosis and mitotic exit in degrowing starved planarians. Importantly, the imbalance between apoptotic and mitotic cells observed following *hippo* inhibition does not lead to changes in planarian body size, nor in cell number, as described in other organisms[14,112,225]. One explanation is the finding that the increase in the number of cells in M phase in *hippo (RNAi)* animals is not accompanied by an increase of cells in S phase, since we have found that *hippo* is required to successfully complete the cell cycle. The role of core Hippo signaling elements in critical mitotic events, namely in centrosomal duplication, chromosomal alignment, spindle formation, and cytokinesis completion, was also reported in *Drosophila* and vertebrates[204,206,227–230]. Despite the failure in mitotic exit, *hippo (RNAi)* animals do not show a regression of the tissues, which is the phenotype associated with the loss of the cycling population in planarians[161]. Indeed, the total population of stem cells or neoblasts (*piwi*+ cells) is maintained in *hippo (RNAi)* animals. This result suggests that just a fraction of the cells that enter the cell cycle become arrested in M phase after *hippo* inhibition. This result is also corroborated by the observation of an increase of mitotic cells only three weeks after *hippo* inhibition, suggestting that it could be a cumulative effect of the cells that became trapped in M phase during this period (Figure D1).

A second explanation for the finding that the imbalance between apoptosis and mitosis in *hippo (RNAi)* animals does not lead to changes in the total cell number, is that a fraction of the cells found in M phase could arise from dedifferentiation of postmitotic cells. This possibility is supported by the finding of ectopic mitotic cells in the periphery of the animals, a region where postmitotic cells are normally located. These mitotic cells are unlikely to result from incorrect migration of stem cells, which are normally located in the inner part of the animal, since they also show aberrant co-expression of committed epidermal cell markers. Moreover, the finding that the

boundaries of expression of the epidermal markers corresponding to the entire lineage are not conserved, together with the finding that *hippo* inhibition promotes the expression of *piwi* in neoblast-depleted planarians, indicates that *hippo* inhibition causes problems in the maintenance of cell identity (Figure 1D).

Hippo silencing gives rise to overgrowths

Although *hippo* silenced planarians do not present an increase in cell number, they show overgrowths, as described in other models studied[225,231,232]. Previous studies on the Hippo pathway attributed the appearance of tumors, to the imbalance between cell death and proliferation[231,232]. However, our results indicate that an underlying mechanism for the appearance of the overgrowths, composed of undifferentiated cells, could be the inability of cells to maintain the differentiated state when *hippo* is inhibited. In agreement with this hypothesis, the onset of the overgrowths was preceded by the appearance of large areas in which different tissues, such as the neural, digestive and visual system, lose differentiated cell types. Those results agree with recent studies supporting an essential role for *hippo* in restricting cell plasticity in the liver or in the intestine[29,90], which has been linked to its role in the recruitment of chromatin-remodeling complexes[104,233]. Thus, rather than pluripotency, nuclear Yki/YAP could exert a critical role in conferring cell plasticity, which is a crucial property of tumor cells[110].

Not only the increase in cell plasticity but also the inhibition of apoptosis observed after *hippo (RNAi)* could underlie the formation of overgrowths. In wild-type animals, senescent cells and cells with DNA disarrangements are eliminated by apoptosis. However, in *hippo (RNAi)* animals, they will not be eliminated, contributing to the acquisition of additional genetic or epigenetic changes. Furthermore, the number of cells with DNA rearrangements and aneuplodies is probably increased in *hippo (RNAi)* planarians, since those animals show a deregulation of critical cell cycle mitotic regulators, and impaired cytokinesis completion, as already shown in LATS2 knockout

mouse embryos[204]. Importantly, the control of apoptosis is known to be intrinsically linked to genomic instability and malignant transformation[234].

Thus, two main roles of Hippo could contribute to the tumoral transformation: (1) it is required to successfully complete the cell cycle and to promote apoptosis; deregulation of these processes could favor the accumulation of genomic errors and instability since the failure to exit M phase is linked to DNA damage, and the inhibition of the apoptotic response hampers the elimination of damaged and old cells, and (2) *hippo* is necessary to acquire and maintain the cell fate and thus, to restrict cell plasticity. Consequently, long-term Hippo pathway inhibition leads to the inability to renew tissues and to the generation of overgrowths (Figure D1).

Although our results indicate that the overgrowths formed after *hippo (RNAi)* are not promoted by the unbalance between cell death and proliferation, it is interesting to comment that an increase in proliferation and a decrease in cell death, also promotes the formation of tumors in planarians (Annex 2, Figure A2.1). Thus, we found that the inhibition of *Smed-blitzschenell* (for simplicity, *bs),* a novel gene which is currently under study in our group, leads to an increase in proliferation and a decrease in cell death, yielding to overgrowths in the planarian marginal part, very similar to the ones observed in the *hippo (RNAi)* animals (unpublished) (Annex 2, Figure A2.1). However, *bs (RNAi)* animals present a higher cell number and an increase of differentiated cells, conversely to *hippo (RNAi)* animals (Annex 2, Figure A2.2). Furthermore, the overgrowths produced after *bs (RNAi)* are composed of cells which retain some markers of differentiated cells, in contrast to the overgrowths observed after *hippo* inhibition. These results demonstrate that changes in cell turnover are enough to yield overgrowths and that the overgrowths observed after *hippo* inhibition arise from a more complex deregulation mechanism beyond cell turnover.

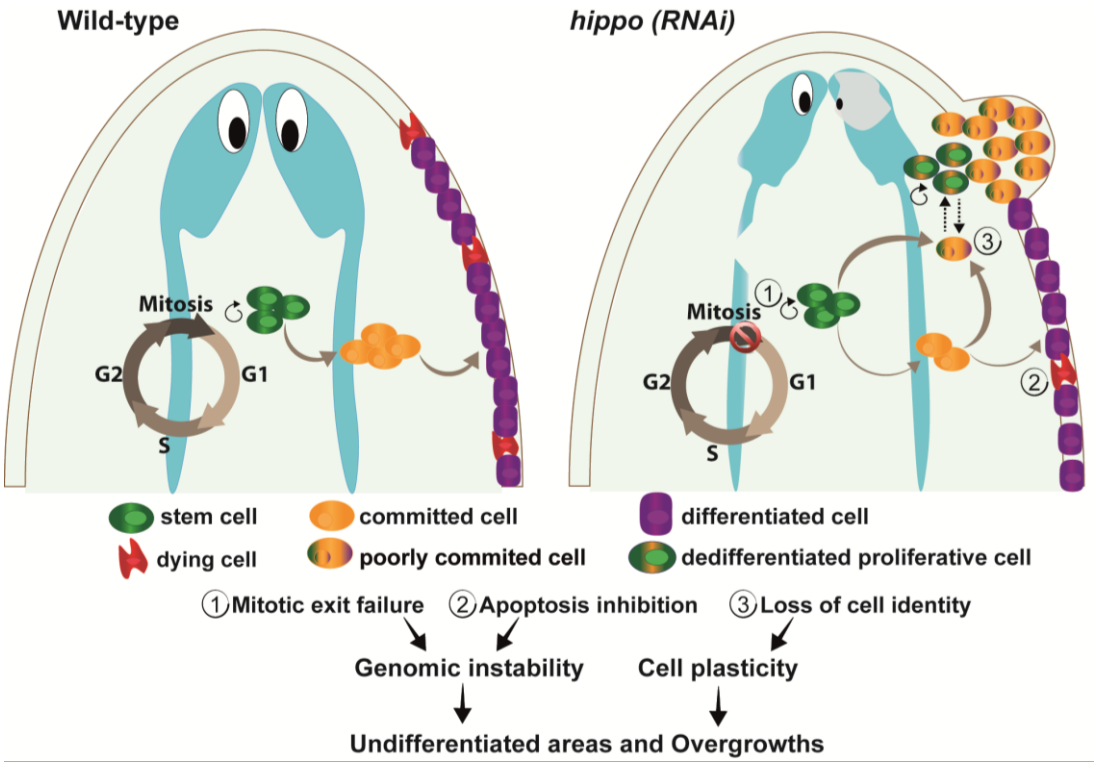

Figure D1: Model of the function of *hippo* in planarians

In wild-type animals, stem cells or neoblasts can proliferate or be committed and differentiate into specific cell types. Committed cells exit the cell cycle to carry on the differentiation process. The health and number of postmitotic cells is also controlled by programmed cell death. In *hippo (RNAi)* planarians, some proliferating stem cells or neoblasts became trapped in M phase (1), and furthermore, they show a decrease in the number of dying cells (2). Both alterations could lead to genomic instability. *hippo* inhibition also promotes cell plasticity and facilitates cell dedifferentiation (3). Both genomic instability and cell plasticity could promote the appearance of undifferentiated areas and overgrowths.

Cellular origin of the overgrowths

Taking into account the position of the overgrowths in the subepidermal region, which is abundant in epidermal precursors, and also correlates with the location of the ectopic mitotic cells, it is tempting to speculate that the origins of the cell accumulations in *hippo (RNAi)* animals relies on cells from the epidermal lineage. The epidermal cell plasticity promoted by *hippo* inhibition could allow the appearance of poorly committed cells that are susceptible to tumoral transformation. Furthermore, although the total number of stem cells is not altered after *hippo* inhibition, there is an important increase in the markers of ζ-neoblasts, the precursors of the epidermal cells, which supports the important role of the pathway in restricting the fate of this specific lineage. However, we have shown that the *piwi*+ cell clusters generated in planarians depleted of cycling cells (or neoblasts) after *hippo* inhibition do not express the ζ-neoblast marker *zfp1*, which does not support the hypothesis that their origin is in the epidermal lineage. A deep analysis of the molecular features of those *piwi*+ cells is required to clarify whether they arise from a non-epidermal cell type or, alternatively, that dedifferentiation leads cells into a more pluripotent state. Nevertheless, the finding that almost all markers of differentiation appear downregulated in the *hippo (RNAi)* transcriptome, and the appearance of undifferentiated areas affecting neuronal, epithelial and digestive cells in *hippo (RNAi)* animals indicates that *hippo* controls the fate of several cell types, and that different cell lineages could contribute to the overgrowths observed. It will be necessary to analyze whether the aberrant co-expression of precursor cell markers also takes place after *hippo* inhibition in different cell lineages, to understand whether *hippo* exerts a predominant role in specific tissues. To clarify the origin of the overgrowths, it would also be required to analyze the expression of markers from different lineages in the cells that compose it.

Yorkie is an effector of the Hippo pathway in planarians

Yorkie was described for the first time in 2005, and was named like this because the small size phenotype of the *Drosophila yki*-mutant tissues was reminiscent of Yorkshire Terriers, one of the smallest breeds of dog. Known as the main effector of the Hippo pathway, *yki* inhibition reduces cell proliferation, and increases apoptosis in a similar manner to the gain of function of *hippo/warts* activity in *Drosophila* and mammals[14,24]. Conversely to these observations, we and other group[222] observed that the inhibition of *yki* in planarians increases mitotic activity, and animals present severe defects in the excretory system which leads to their blotting and death. Because of this unexpected phenotype, it was proposed that the presence of an Arginine (R), instead of a Lisine (K) in the conserved Warts/Lats phosphorylation motif, HxRxxS, could interfere with Yki phosphorylation[222]. Thus, the authors proposed that in planarians Yki function was independent on Hippo[222]. However, the Arginine to Lisine substitution is conservative. To analyze whether Yki could be the target of Hippo in planarians, we checked whether *hippo* inhibition resulted in an increase in *yki* nuclearization, and, since the main role of *hippo* is to maintain the differentiated fate in planarians, we analyzed the role of *yki* in cell differentiation. Our results showed that, in fact, *hippo* silencing promotes Yki nuclearization. We also found that the inhibition of *yki* increases the number of differentiated cells, the opposite phenotype observed in *hippo (RNAi)* animals. The increase in the differentiated cell population, namely muscle cells, after *yki* silencing was also recently described by Li & Pearson (2016), supporting our results. Taking into account that the phosphorylation of Yki depends not only on Hippo, but also on the core elements of the kinase cassette[195], the finding that *warts* and *sav (RNAi)* produces the same phenotype than *hippo (RNAi),* further supports the conservation of the pathway in planarians.

The Hippo-Yorkie signaling is essential for planarian regeneration

In the last few years, Hippo signaling modulation has emerged as an important mechanism to improve regeneration in several organs and tissues[27,96,235]. Taking advantage of the amazing ability of planarians to regenerate, we modulated the activity of the Hippo pathway during planarians regeneration. Conversely to what is found during heart and liver regeneration, where the inactivation of the Hippo pathway and the increase in YAP nuclearization improves regeneration[27,96,235], we found that the inhibition of *hippo* leads to severe defects in planarian regeneration, with a decrease of differentiated cells, and the impairment of the regeneration of the missing organs.

Although YAP nuclearization promotes regeneration in the heart and the liver[27,96,235], it was shown that YAP can play a growth restrictive role in intestine stem cells (ISCs). The underlying mechanism could be that loss of YAP during intestinal stem cells regeneration causes a de-repression of WNT signaling, resulting in the expansion of the ISCs and related progenitors[91]. In this case, YAP is controlling proliferation in a non-autonomous manner, dependent of the Wnt pathway. However, it was also shown that transient activation of YAP after an intestine injury, reprograms ISCs by inhibiting the Wnt homeostatic program, inducing a regenerative response by cell reprogramming[90]. Considering the pivotal role that Wnt signaling plays in ISCs, the discrepancy between these studies may be due to the differences in the extent and duration of Wnt inhibition by YAP/TAZ. Although there specific relationship between the Hippo pathway and the Wnt signaling in planarians is not clear, Lin & Pearson (2014) demonstrated that *yki* is required to restrict the expression domains of posterior Wnts and anterior Wnt inhibitors[222].

Overall, these results indicate that *hippo* inhibition in planarians does not promote regeneration, possibly because in planarians the regenerative response does not rely on cell dedifferentiation, like in the heart or the liver, but on the increase in stem cells

proliferation. The context found in planarians could be more similar to the one described in the gut, in which cell renewal and the regenerative potential relies on the activity of existent stem cells. Furthermore, it would be necessary to understand the relationship between Hippo and Wnt signaling in planarians, since it could be also important to regulate the regenerative response.

Lgl2 could be an up-stream of the Hippo pathway

On the present study we identified five new genes that are orthologs of well known up-stream regulators of the Hippo pathway in other organisms[62]. These genes encode membrane proteins, essential for the cell-cell contact and environmental networking[54,236]. Consistently, after its silencing, we observed that cell-cell contact is disrupted (β-catenin2 delocalization), suggesting that cell communication is not properly occurring. Focusing on *lgl2*, we found that *lgl2 (RNAi)* caused an increase in the mitotic rates, the inability to maintain differentiated structures and overgrowths composed by non-differentiated cells, phenocopying the *hippo (RNAi)* phenotype. Although the increase in the number of mitotic cells observed after the silencing *lgl2* could be occurring in a non-autonomous way, since this gene is not expressed by stem cells, an interesting possibility is that *lgl2* inhibition leads to intercellular uncommunication and to cell dedifferentiation, as proposed in *hippo* (*RNAi*) animals. Thus, as discussed earlier, in the *hippo (RNAi)* animals, the overgrowths observed in the *lgl2 (RNAi)* animals could be caused by the accumulation of cells that cannot maintain the differentiated fate. Nevertheless, a detailed study should be done to understand if the overgrowths arise from an increase in neoblast proliferation, from an increase in cell plasticity, or a combination of both processes.

The double inhibition of *hippo* and *lgl2* showed that both genes act synergistically. It is possible that *lgl2* is responsible to activate Hippo in planarians, but the results indicate that it could also exert a Hippo-independent role in the control of cell proliferation and differentiation. Overall, our findings suggest that Lgl2 could be

acting as a Hippo pathway regulator in planarians, and that an important input of the pathway is cell-cell contact, as described in other models[237], which in fact is one of the most important cancer hallmarks[108].

Jub b and Zyxin are putative inhibitors of the Hippo pathway

Ajuba proteins and Zyxin inhibit the Hippo pathway in *Drosophila* by sequestering and degrading Warts in order to promote Yki nuclearization[62]. Thus, the inhibition of these genes should produce a high Yki citoplasmatic retention, promoting the decrease in mitosis and an increase in cell death. In planarians, we found that *jub b* and *zyxin* are mainly expressed in the muscle cells, which also present high levels of *warts* and *yorkie* expression. Although no apparent phenotype was observed after their inhibition, a high decrease in the mitotic rates is observed in both *jub b* and *zyxin (RNAi)* animals, which fits with the possible role of these genes in the control of Warts activity. It was described that during planarian regeneration, muscle cells play an essential role in the signaling of neoblasts to maintain a stable stem cell population[186]. Thus, in parallel with Warts inactivation, the inhibition of *jub b* and *zyxin* could be affecting the ability of muscle cells to properly signal the neoblasts to proliferate, decreasing its mitotic activity.

Interestingly, the decrease in proliferation in *jub b* and *zyxin (RNAi)* animals is accompanied by a significant decrease in cell death. This observation could be explained by a compensatory mechanism in order to maintain the cell number. In this case, *jub b* and *zyxin* would be mainly controlling mitosis and not the apoptotic process.

Putative targets of Hippo in planarians

Out of the eleven more differentially expressed genes found in *hippo (RNAi)* RNAseq corresponding to one week of inhibition, we selected four to perform a deeper analysis. We found that *Mediator of RNA polymerase II transcription subunit 17 (med17)*

is a gene specific of neoblasts, and that its inhibition produces the typical phenotype observed after the silencing of genes essential for neoblast maintenance (e.g. *piwi*[161] and *h2b*[163]), that is head regression. Consistently, *med17 (RNAi)* animals show a reduction in the mitotic activity, accompanied by a reduction in the population of epidermal progenitors in the head region. All these features are also found in planarians with a compromised neoblast population. *med17 (RNAi)* animals also show an increase in the apoptotic rates, which could be a general feature in animals that suffer tissue regression due to the inability to renew the tissues. This result could be further analyzed in other types of neoblast-depleted animals.

On the other hand, the inhibition of *spondin, mucin* and *hypothetical protein* produces overgrowths. When we analyze mitosis and cell death, we found that in the case of *spondin* there is an increase in the mitotic activity and also an increase in cell death, which could indicate that it exerts a role in controlling mitosis as a *hippo* target, and that apoptosis increases as a compensatory mechanism. In the case of *mucin* we found an increase in mitosis but no affectation of cell death, which again could indicate that it controls mitosis as a *hippo* target. In the case of *hyprot*, its inhibition does not produce any change in mitotic rates but an increase in apoptosis, which does not explain the appearance of overgrowths and thus requires further analysis. An interesting issue that also deserves further analysis is the finding that in some RNAi phenotypes (*spon*) changes in mitotic rates lead to changes in apoptosis, suggesting the existence of compensatory mechanisms, but not in others (muc). A possibility could be that in the first situation the increase in mitotic rates implies an increase in proliferation and S phase entrance, but not in the second situation, as described after *hippo (RNAi)*.

Overall, these data indicates that the formation of overgrowths can arise just after an impairment of the mitotic activity, and that a concomitant decrease in cell death, that is what occurs after *hippo* silencing, is not necessary for tumoral transformation. It

would be interesting to analyze if the increase in mitotic rates in those cases is accompanied by problems in cell differentiation. Although we observed that the number of dopaminergic neurons, after the inhibition of these genes, is not affected, a more in depth analysis would be required to clarify it.

Finally, these observations suggest that the role of *hippo* in planarians relies on the activation of multiple targets, which exert specific functions in relation to the control of mitosis, cell death, and cell differentiation. Thus, the inhibition of any of them alone, partially reproduces the phenotype observed after *hippo* inhibition.

Conclusions

The main conclusions of this thesis are:

1. The Hippo cascade elements are functionally conserved in planarians and they are expressed in planarian stem cells (neoblasts) and differentiated cells.

2. Loss of *hippo* promotes the appearance of large areas of undifferentiated cells and the formation of overgrowths, although the total number of cells is not increased.

3. Hippo is controlling the mitotic exit. Inhibition of *hippo* leads to accumulation of cells in M phase while the number of cells that enter in cycle is maintained.

4. Hippo is controlling cell death. Inhibition of *hippo* decreases the number of apoptotic cells.

5. Hippo is controlling the differentiation process. Inhibition of *hippo* results in a decrease in the number of differentiated cells and the loss of the hierarchical transitions between cell states.

6. Hippo is required to maintain the differentiated fate. Neoblast-depleted planarians regain the expression of neoblast markers after *hippo (RNAi)*, indicating that *hippo* inhibition promotes dedifferentiation of planarian cells.

7. The overgrowths observed after *hippo* inhibition, mainly composed of non-differentiated cells, could be due to problems in the maintenance of the differentiated fate – increase in cell plasticity – and less cell death.

8. In contrast to published results, Yorkie appears as a down-stream effector of Hippo in planarians.

9. The silencing of the Hippo pathway up-stream regulators (*merlin, expanded, scribble* and specially *lgl1* and *lgl2*) phenocopy the overgrowths produced after *hippo* inhibition. The integrity of the cell-cell contacts appears as a conserved input of the *hippo* control in planarians.

10. Jub b and Zyxin could act as Hippo inhibitors in the control of mitosis.

11. Transcriptomic analysis of *hippo (RNAi)* animals allowed us to identify 11 putative target genes of Hippo in planarians. The inhibition of 4 of them produces overgrowths, as *hippo* inhibition, although the mitotic and apoptotic rates are affected in a different manner. Hippo could control the function of individual targets that only in conjunction lead to a complete *hippo* response.

Materials and methods

Planarian culture

Asexual planarians from a clonal strain of *S. mediterranea* BCN-10 were maintained at 20ºC in artificial water as described[238]. Animals were fed with veal liver and starved for at least 1 week before starting the experiments.

Cloning

To amplify the genes of interest we followed set of primers:

Gene	*Forward 5'-3'*	*Reverse 5'-3'*
hippo	CGAGCACTGTTTATGATTCCTTC	CTCGGCTTGCAAGTCTGAGTC
salvador	GAGGTTAAATCTATGCTTTACAACG	AGAGCCGAAATTTCTTTAAGATTGT
warts	ACAGCTCGTTCACAATGGCTAC	GCCGTCCGCTATTTCTCACA
yorkie	GTTTGGATGAATTATTCGAAGTGG	CACAATACAAAAGAAACCACATGG
lgl1	TTCGCTAGCCAAATTTTCGT	CTCATGTCGAATTACCCGCT
lgl2	TTATTGGACACGGTGATGGA	CCATGTTGCGATGATAATCG
expanded	CCCGTTCGAGATCAAACATT	TTGGAAATGCACGAAATGAA
merlin	CCTTCAATCGAGAACCGAAG	CAAACCCTTCGTCTCATTCG
scribble	TTGCCACAATCAGGAATTGA	TGAAATTCCGGGTGTCTTCT
jub	CACTTCTAAAAATTTCCATCCAA	CCAATTTGGATGAAAAATGC
jub b	CTCGCATTTCATTGGTG	GTATTGCGGTTTTCAACAAAG
zyxin	CGGAGGCTGAAGTAGACG	CGGCAGTTTCAACTTCATC
med17	GCTGAATGGAATTACTTTGGA	CCACCATTTTCTGGAAATAATG
spon	GCAAAGAGAAGCCGGTATTG	CGTTTCTTTTTCTCCGCATC
ccdc96	GGTCTGAATTTCCCAGCAT	CGTCGAAACTCGCTTGG
cenpe2	GCAGTCAGGCGGAGATT	CGCGGAGAACTGTGATGATA
sycp1	CCAGCAATAACACGTTAGAAAT	CGTCGGTTTTGGTAGCAG
aspm	GGTGCATTTTAACCATGAATTC	CCAAAGTCTTTGTCACCG
dst3	CCAATTTTCATTGCACCTT	GGCCAATTGAAGAGACTCC
hyprot	GCCTCTCGAGAATCAATCA	CCATTGGGTCCGGTAAA
muc	CCACTGAATCTTCCGCA	CGTAATGATGACAGGTTTGTAGA
msi2b	GGAAAACTTAGCGACTCGAG	GGAAAACTTAGCGACTCGAG
xrra1	GCCGTGATCAATGTCAGTTT	GCTTTTCCATCGTCGCC

PCR fragments were cloned into the pCRII (Life Technologies) and pGEM-T Easy (Promega) vectors to synthesize dsRNA or ssRNA, as required.

RNA interference analysis

dsRNA was synthetized by in vitro transcription (Roche) and microinjection performed as previously described[127], following the standard protocol of 3x32nl injection of dsRNA for three consecutive days. For the studies in homeostatic conditions, starved planarians were injected with *hippo*, *warts* or *salvador* dsRNA during three consecutive weeks with the standard protocol (see scheme in Figure R1.2a). *yorkie (RNAi)* animals were injected only one week. Experiments in regenerating animals were performed in animals injected with *hippo* or *yorkie* dsRNA for two weeks prior to amputation of the head and tail (see scheme in Figure R3.2a). Animals were fixed at different times after dsRNA injection or amputation depending on the experiment. Control animals were injected with dsRNA for green fluorescence protein (GFP), a gene not present in planarians.

In the *h2b/hippo* (RNAi) experiment, animals were injected with *gfp* or *h2b* on three consecutive days and, after two days, another injection of *gfp* or *h2b* was performed. On the next day, animals were injected with *gfp* or *hippo* on three consecutive days. Animals were fixed four days after the last injection (see scheme in Figure R2.7a).

Quantitative real-time PCR

Total RNA was extracted from a pool of 5 planarians each for *hippo (RNAi); gfp (RNAi); h2b/gfp (RNAi); h2b/hippo (RNAi); hippo/gfp (RNAi)* and. *hippo/h2b (RNAi)*. Quantitative real-time PCR was performed as previously described[163], and data was normalized based on the expression of EF2 or URA4 as internal control. All the experiments were performed using three biological replicates. The following sets of specific primers were used:

hippo mRNA, 5′-:TTTGGTCTTTGGGAATCAC-3′ and 5′-:TGGAGGAGGTTGAGAAGG-3′;

h2b mRNA, 5′-GAGAAAGTTGAACGGCCC-3′ and 5′-AAGATAATACGTACTTCAACGACG-3′.

Whole-mount in situ hybridization and immunohistochemistry

RNA probes were synthesized in vitro using Sp6 or T7 polymerase (Roche) and DIG-, FITC- or DNP-modified nucleotides (Perkin Elmer). RNA probes were purified and precipitated with ethanol and 7.5 M ammonium acetate. For ISH and FISH, animals were fixed and processed as previously described[128,129]. After probe development, neoblasts were visualized with the rabbit anti-SMEDWI-1 antibody (kindly provided by Kerstin Bartscherer, Max Plank Institute for Molecular Biomedicine, Münster, Germany; 1:1000)[239]. Nuclei were stained with Dapi (1:5000) and mounted with 70% glycerol in PBS.

Whole-mount immunostaining

Immunostaining was performed as described[240]. The following antibodies were used: mouse anti-synapsin (anti-SYNORF-1; 1:50; Hybridoma Bank); rabbit anti-phospho-histone-H3-Ser10 (anti-H3P) (1:500; Cell Signaling Technology); rabbit anti-SMEDWI-1 antibody (1:1000); mouse anti-arrestin (anti-VC1) (kindly provided by Prof. K. Watanabe; 1:15000); rabbit anti-β-catenin2 (anti-Bcat2) ([220]; 1:2000). Nuclei were stained with Dapi (1:5000) and mounted with 70% glycerol in PBS. To avoid technical variance and obtain a reliable quantification of H3P+cells, at least two independent experiments were performed.

In situ hybridization and immunohistochemistry in paraffin sections

For ISH and immunohistochemistry, animals were killed and processed as previously described[152]. The antibodies used were rabbit anti-SMEDWI-1 (1:1000), rabbit anti-phospho-histone-H3-Ser10 (anti-pH3) (1:500; Cell Signaling Technology), rat anti-

phospho-histone-H3-Ser10 (anti-pH3) (1:1000; Millipore), and rabbit anti-YORKIE (1:200).

Whole-mount TUNEL and Caspase3-activity

For TUNEL analysis, animals were fixed and treated as described[187] using the ApopTag Red in Situ Apoptosis Detection Kit (Merck-Millipore Ref.S7165). To avoid technical variance at least two independent TUNEL experiments were performed. For the Caspase-3 assay, total protein was extracted from a pool of five planarians and processed as described[241]. Enzyme activity was measured in a luminescence spectrophotometer (Perkin-Elmer LS-50) (1 excitation, 380 nm). A unit of caspase-3 activity was defined as the amount of active enzyme necessary to produce an increase of 1 arbitrary luminescence unit after the 2 h incubation. The results are presented as units of caspase-3 activity per µg of protein. All experiments were performed using five biological and three technical replicates for each condition. To avoid technical variance at least two independent experiments were performed.

Flow cytometry

Dissociation of planarians, cell labelling and isolation of cells by FACS were performed as described previsously[242]. Absolute cell counts were done by adding beads with a known concentration to the sample. Beads and cells were detected simultaneously and absolute counts of the cells were calculated from bead numbers (absolute counts by indirect method). Flow-Check Fluorospheres Polystyrene Fluorescent Microspheres (Beckman Coulter Inc, Indianapolis, US) were adjusted at $1x10^6$fluorospheres/mL. A 1:100 dilution of the bead solution was applied to each sample to obtain a final concentration of $1x10^4$beads/mL. Beads and cells were identified according to their different pattern of scatter and fluorescence.

Edu staining on paraffin sections

32 nl of F-ara Edu (Sigma) was injected in *gfp* and *hippo (RNAi)* animals at a concentration of 60µg/mL (diluted in 10%DMSO/planarian artificial water). After 16 hours, animals were processed and stained with EdU Click-555 kit (Baseclick Gmbh; BCK-Edu555), following the manufacturer's recommendations, and adding a pre-treatment of proteinase K (20µg/mL) 10 min RT. Samples were immunostained with anti-H3P, stained with DAPI, and mounted with 70% glycerol in PBS.

Generation of the anti-YORKIE polyclonal antibody

The complete coding sequence of *yorkie* cDNA was cloned into a p-GEMT vector Easy (Promega). Subcloning, protein expression and antibody production were performed using ProteoGenix (ProteoGenix, France). Briefly, 200µg of recombinant protein was used as immunogen to produce polyclonal IgGs in two rabbits. The post-immunization serum was purified using Protein A affinity purification then precipitated in sodium azide buffer and stored at 4ºC.

Western blot assay

Protein extracts were obtained as previous described[243]. After incubation with rabbit anti-YORKIE (1:2000) and anti-α-TUBULIN (Sigma, 1:10000) antibodies, signal was developed using Clarity™ Western ECL Substrate (Bio-Rad) and chemiluminescence was detected using a C-DiGit Chemiluminescent Western Blot Scanner (LI-COR). Quantifications were performed with Image Studio Lite and normalized to anti-α-TUBULIN signal.

Transcriptomic analysis

To perform the transcriptomic analysis, total RNA was extracted from *gfp (RNAi)* and *hippo (RNAi)* animals after one, three and four weeks of inhibition. Three replicates were generated per condition from a pool of five organisms each. RNA was extracted with Trizol® (Invitrogen) following the manufacturer's instructions. RNA was

quantified with a Nanodrop ND-1000 spectrophotometer (Thermo Scientific) and quality check was performed by capillary electrophoresis in an Agilent 2100 Bioanalyzer (Agilent Technologies) prior to library preparation. cDNA libraries were prepared using the Illumina® TruSeq Stranded mRNA Library Prep Kit and sequenced as paired-end reads in an Illlumina® HiSeq 2000 sequencer. Quality check of the reads was performed with the FastQC suite. Transcript abundances were calculated with kallisto v0.43.0[244] on the *S. mediterranea* dd_Smed_v6 transcriptome assembly[126]. Differential expression analysis was carried out with the sleuth[245] and DESeq2[246] statistical packages. Raw sequencing data in FASTQ format as well as the transcript abundances have been deposited at NCBI Gene Expression Omnibus (GEO)[247] and are accessible through GEO Series accession number GSE95130[197].

Imaging

FISH and immunostaining samples were imaged using a MZ16F stereomicroscope (Leica) equipped with a ProgRes C3 camera (Jenoptik) or an SP2 confocal laser-scanning microscope (Leica). Images were processed using Fiji and Photoshop CS5 (Adobe) software. Brightness/contrast and color balance adjustments were always applied to the entire image. Quantifications were performed by hand using the "multi-point selection" tool of Fiji. Co-localization quantification was performed using the equivalent areas using the "roi-manager" tool in Fiji. Nuclei area in Edu experiments was measured using the "threshold" tool with the "moments" mask for all samples. Signal quantification of Yorkie antibody immunostaining was processed using Fiji software. Two planes were used to build the Z-projection. Nuclear-stained (DAPI) images were transformed into a mask using the "threshold" tool with the "moments" mask. The mask was used to obtain the nuclear signal with the Image calculator process. The nuclear signal obtained from the resulting image was measured to obtain the raw integrated density (RID). The nuclear area was obtained from the mask. Then, the RID was normalized with the respective nuclear area. Animals were averaged and significant differences determined by two-tailed Student t tests.

References

1. Clevers, H., Loh, K. M. & Nusse, R. Stem cell signaling. An integral program for tissue renewal and regeneration: Wnt signaling and stem cell control. *Science (80-.).* **346,** 1–9 (2014).
2. Leblond, C. P. , Walker, B. Renewal of cell population. **36,** 255–276 (1956).
3. Roostaee, A., Benoit, Y. D., Boudjadi, S. & Beaulieu, J. F. Epigenetics in Intestinal Epithelial Cell Renewal. *J. Cell. Physiol.* **231,** 2361–2367 (2016).
4. Ito, K. & Ito, K. Metabolism and the Control of Cell Fate Decisions and Stem Cell Renewal. *Annu. Rev. Cell Dev. Biol.* **32,** (2016).
5. Simons, B. D. & Clevers, H. Strategies for homeostatic stem cell self-renewal in adult tissues. *Cell* **145,** 851–862 (2011).
6. Yang, Y., Akinci, E., Dutton, J. R., Banga, A. & Slack, J. M. W. Stage specific reprogramming of mouse embryo liver cells to a beta cell-like phenotype. *Mech. Dev.* **130,** 602–612 (2013).
7. Merrell, A. J. & Stanger, B. Z. Adult cell plasticity in vivo: de-differentiation and transdifferentiation are back in style. *Nat. Rev. Mol. Cell Biol.* **17,** 413–25 (2016).
8. Worley, M. I., Setiawan, L. & Hariharan, I. K. Regeneration and transdetermination in Drosophila imaginal discs. *Annu. Rev. Genet.* **46,** 289–310 (2012).
9. Raff, M. Adult Stem Cell Plasticity: Fact or Artifact? *Annu. Rev. Cell Dev. Biol.* **19,** 1–22 (2003).
10. Takahashi, K. & Yamanaka, S. Induction of Pluripotent Stem Cells from Mouse Embryonic and Adult Fibroblast Cultures by Defined Factors. *Cell* **126,** 663–676 (2006).
11. Tapscotr, S. J. *et al.* MyoDi: A Nuclear Phosphoprotein Reqiring a Myc Homology Region to Convert Fibroblasts to Myoblasts. *Science (80-.).* **242,** 405–411 (1988).
12. Jopling, C., Boue, S. & Izpisua Belmonte, J. C. Dedifferentiation, transdifferentiation and reprogramming: three routes to regeneration. *Nat. Rev. Mol. Cell Biol.* **12,** 79–89 (2011).
13. Tsonis, P. A., Madhavan, M., Tancous, E. E. & Del Rio-Tsonis, K. A newt's eye view of lens regeneration. *Int. J. Dev. Biol.* **48,** 975–980 (2004).
14. Camargo, F. D. *et al.* YAP1 Increases Organ Size and Expands Undifferentiated Progenitor Cells. *Curr. Biol.* **17,** 2054–2060 (2007).
15. Cao, X. *et al.* YAP regulates neural progenitor cell number via the TEA domain transcription factor. *Genes Dev.* **22,** 3320 (2008).
16. Tapon, N. *et al.* salvador promotes both cell cycle exit and apoptosis in Drosophila and is mutated in human cancer cell lines. *Cell* **110,** 467–478 (2002).
17. Zhao, B., Tumaneng, K. & Guan, K. L. The Hippo pathway in organ size control, tissue regeneration and stem cell self-renewal. *Nat. Cell Biol.* **13,** 877–883 (2011).
18. Wilson, M. R., Close, T. W. & Trosko, J. E. Cell population dynamics (apoptosis, mitosis, and cell-cell communication) during disruption of homeostasis. *Exp. Cell Res.* **254,** 257–268 (2000).
19. M. Phipps, J. Phipps, J.F. Whitfield, A. Ally, R.L. Somorjai, S. A. N. Carcinogenic Implications of the Neighborhood Coherence Principle (NCP). **31,** 289–301 (1990).
20. Xin, T., Greco, V. & Myung, P. Hardwiring Stem Cell Communication through Tissue Structure. *Cell* **164,** 1212–1225 (2016).

21. Lai, E. C. Notch signaling: control of cell communication and cell fate. *Development* **131,** 965–973 (2004).
22. Alberts B, Johnson A, Lewis J, et al. *Molecular Biology of the Cell.* (2002).
23. Hong, J.-H. et al. TAZ, a Transcriptional Modulator of Mesenchymal Stem Cell Differentiation. *Science (80-.).* **309,** 1074–1078 (2005).
24. Huang, J., Wu, S., Barrera, J., Matthews, K. & Pan, D. The Hippo signaling pathway coordinately regulates cell proliferation and apoptosis by inactivating Yorkie, the Drosophila homolog of YAP. *Cell* **122,** 421–434 (2005).
25. Cai, J., Zhang, N. & Zheng, Y. The Hippo signaling pathway restricts the oncogenic potential of an intestinal regeneration program. *Genes Dev.* 2383–2388 (2010). doi:10.1101/gad.1978810
26. Ramos, A. & Camargo, F. D. The Hippo signaling pathway and stem cell biology. *Trends Cell Biol.* **22,** 339–346 (2012).
27. Loforese, G. *et al.* Impaired liver regeneration in aged mice can be rescued by silencing Hippo core kinases MST1 and MST2. *EMBO Mol. Med.* 1–15 (2016). doi:10.15252/emmm.201506089
28. Mahoney, J. E., Mori, M., Szymaniak, A. D., Varelas, X. & Cardoso, W. V. The Hippo Pathway Effector Yap Controls Patterning and Differentiation of Airway Epithelial Progenitors. *Dev. Cell* **30,** 137–150 (2014).
29. Yimlamai, D. *et al.* Hippo pathway activity influences liver cell fate. *Cell* **157,** 1324–1338 (2014).
30. Wu, S., Huang, J., Dong, J. & Pan, D. hippo encodes a Ste-20 family protein kinase that restricts cell proliferation and promotes apoptosis in conjunction with salvador and warts. *Cell* **114,** 445–456 (2003).
31. Wei, X., Shimizu, T. & Lai, Z.-C. Mob as tumor suppressor is activated by Hippo kinase for growth inhibition in Drosophila. *EMBO J.* **26,** 1772–1781 (2007).
32. Goulev, Y. *et al.* SCALLOPED Interacts with YORKIE, the Nuclear Effector of the Hippo Tumor-Suppressor Pathway in Drosophila. *Curr. Biol.* **18,** 435–441 (2008).
33. Peng, H. W., Slattery, M. & Mann, R. S. Transcription factor choice in the Hippo signaling pathway: Homothorax and yorkie regulation of the microRNA bantam in the progenitor domain of the Drosophila eye imaginal disc. *Genes Dev.* **23,** 2307–2319 (2009).
34. Chen, H.-J. *et al.* The Hippo pathway controls polar cell fate through Notch signaling during Drosophila oogenesis. *Dev. Biol.* **357,** 370–379 (2011).
35. F. Ren, L. Zhang, J. J. Hippo signaling regulates Yorkie nuclear localization and activity through 14-3-3 dependent and independent mechanisms. *Dev. Biol.* **337,** 303–312 (2010).
36. Oh, H. & Irvine, K. D. In vivo analysis of Yorkie phosphorylation sites. *Oncogene* **28,** 1916–27 (2009).
37. Chan, E. H. Y. *et al.* The Ste20-like kinase Mst2 activates the human large tumor suppressor kinase Lats1. *Oncogene* **24,** 2076–2086 (2005).
38. M. Praskova, F. Xia, J. A. MOBKL1A/MOBKL1B Phosphorylation by MST1 and MST2 Inhibits Cell Proliferation. *Curr Biol* **18,** 583–592 (2008).
39. Lei, Q.-Y. *et al.* TAZ Promotes Cell Proliferation and Epithelial-Mesenchymal Transition and Is Inhibited by the Hippo Pathway. *Mol. Cell. Biol.* **28,** 2426–2436 (2008).
40. Hao, Y., Chun, A., Cheung, K., Rashidi, B. & Yang, X. Tumor suppressor LATS1 is a

negative regulator of oncogene YAP. *J. Biol. Chem.* **283,** 5496–5509 (2007).
41. Zhao, B. *et al*. Inactivation of YAP oncoprotein by the Hippo pathway is involved in cell contact inhibition and tissue growth control. *Genes Dev.* **21,** 2747–2761 (2007).
42. Pan, D. Review The Hippo Signaling Pathway in Development and Cancer. *Dev. Cell* **19,** 491–505 (2010).
43. Zhao, B. *et al*. TEAD mediates YAP-dependent gene induction and growth control. *Genes Dev.* **22,** 1962–1971 (2008).
44. Halder, G. & Johnson, R. L. Hippo signaling: growth control and beyond. *Development* **138,** 9–22 (2011).
45. Zhao, B., Lei, Q. Y. & Guan, K. L. The Hippo-YAP pathway: new connections between regulation of organ size and cancer. *Curr. Opin. Cell Biol.* **20,** 638–646 (2008).
46. Meng, Z. *et al*. MAP4K family kinases act in parallel to MST1/2 to activate LATS1/2 in the Hippo pathway. *Nat. Commun.* **6,** 8357 (2015).
47. Zheng, Y. *et al*. Identification of Happyhour/MAP4K as Alternative Hpo/Mst-like Kinases in the Hippo Kinase Cascade. *Dev. Cell* **34,** 642–655 (2015).
48. Li, S., Cho, Y. S., Yue, T., Ip, Y. T. & Jiang, J. Overlapping functions of the MAP4K family kinases Hppy and Msn in Hippo signaling. *Cell Discov.* **1,** 15038 (2015).
49. Dupont, S. *et al*. Role of YAP/TAZ in mechanotransduction. *Nature* **474,** 179–183 (2011).
50. Meng, Z., Moroishi, T. & Guan, K. Mechanisms of Hippo pathway regulation. *Genes Dev.* **30,** 1–17 (2016).
51. Dupont, S. Role of YAP/TAZ in cell-matrix adhesion-mediated signalling and mechanotransduction. *Exp. Cell Res.* **343,** 42–53 (2015).
52. Aragona, M. *et al*. A mechanical checkpoint controls multicellular growth through YAP/TAZ regulation by actin-processing factors. *Cell* **154,** 1047–1059 (2013).
53. Codelia, V. A., Sun, G. & Irvine, K. D. Regulation of YAP by mechanical strain through Jnk and Hippo signaling. *Curr. Biol.* **24,** 2012–2017 (2014).
54. Martin-Belmonte, F. & Perez-Moreno, M. Epithelial cell polarity, stem cells and cancer. *Nat. Rev. Cancer* **12,** 23–38 (2011).
55. Pellock, B. J., Buff, E., White, K. & Hariharan, I. K. The Drosophila tumor suppressors Expanded and Merlin differentially regulate cell cycle exit, apoptosis, and Wingless signaling. *Dev. Biol.* **304,** 102–115 (2007).
56. Hamaratoglu, F. *et al*. The tumour-suppressor genes NF2/Merlin and Expanded act through Hippo signalling to regulate cell proliferation and apoptosis. *Nat Cell Biol* **8,** 27–36 (2006).
57. Genevet, A., Wehr, M. C., Brain, R., Thompson, B. J. & Tapon, N. Kibra Is a Regulator of the Salvador/Warts/Hippo Signaling Network. *Dev. Cell* **18,** 300–308 (2010).
58. Grzeschik, N. A., Parsons, L. M., Allott, M. L., Harvey, K. F. & Richardson, H. E. Lgl, aPKC, and Crumbs Regulate the Salvador/Warts/Hippo Pathway through Two Distinct Mechanisms. *Curr. Biol.* **20,** 573–581 (2010).
59. J. Yu, Y. Zheng, J. Dong, S. Klusza, W. Deng, P. D. Kibra functions as a tumor suppressor prote. *Clin. Lymphoma* **18,** 288–299 (2010).
60. F. Yin, J Yu, Y. Zheng, Q. Chen, N. Zhang, D. P. Spatial organization of Hippo signaling at the plasma membrane mediated by the tumor suppressor Merlin/NF2. *Cell* **154,** 1–24 (2013).
61. Sun, S., Reddy, B. V. V. G. & Irvine, K. D. Localization of Hippo signalling complexes and

Warts activation in vivo. *Nat. Commun.* **6,** (2015).
62. Yu, F. X. & Guan, K. L. The Hippo pathway: Regulators and regulations. *Genes Dev.* **27,** 355–371 (2013).
63. Thakur, M. Das *et al.* Ajuba LIM Proteins are Negative Regulators of the Hippo Signaling Pathway. *Curr Biol* **20,** 657–662 (2010).
64. Sun, G. & Irvine, K. D. Ajuba family proteins link JNK to Hippo signaling. *Sci Signal* **6,** 1–17 (2013).
65. Rauskolb, C., Sun, S., Sun, G., Pan, Y. & Irvine, K. D. Cytoskeletal tension inhibits Hippo signaling through an Ajuba-Warts complex. *Cell* **158,** 143–156 (2014).
66. Willecke, M. *et al.* The Fat Cadherin Acts through the Hippo Tumor-Suppressor Pathway to Regulate Tissue Size. *Curr. Biol.* **16,** 2090–2100 (2006).
67. Rauskolb, C., Pan, G., Reddy, B. V. V. G., Oh, H. & Irvine, K. D. Zyxin links fat signaling to the hippo pathway. *PLoS Biol.* **9,** (2011).
68. Matakatsu, H., Blair, S. S. & Fehon, R. G. The palmitoyltransferase Approximated promotes growth via the Hippo pathway by palmitoylation of Fat. *J. Cell Biol.* **216,** 1–13 (2017).
69. Polesello, C., Huelsmann, S., Brown, N. H. & Tapon, N. The Drosophila RASSF Homolog Antagonizes the Hippo Pathway. *Curr. Biol.* **16,** 2459–2465 (2006).
70. Zhao, B. *et al.* Angiomotin is a novel Hippo pathway component that inhibits YAP oncoprotein. *Genes Dev.* **25,** 51–63 (2011).
71. Oka, T., Schmitt, a P. & Sudol, M. Opposing roles of angiomotin-like-1 and zona occludens-2 on pro-apoptotic function of YAP. *Oncogene* **31,** 128–134 (2012).
72. Remue, E. *et al.* TAZ interacts with zonula occludens-1 and -2 proteins in a PDZ-1 dependent manner. *FEBS Lett.* **584,** 4175–4180 (2010).
73. K. Schlegelmilch, M. Mohseni, O. Kirak, J. Pruszak, R. Rodriguez, D. Zhou, B. kreger, V. Vasioukhin, J. Avruch, T. Brummelkamp, F. C. Yap1 acts downstream of α-catenin to control epidermal proliferation. *Cell* **144,** 782–795 (2011).
74. Badouel, C. *et al.* The FERM-Domain Protein Expanded Regulates Hippo Pathway Activity via Direct Interactions with the Transcriptional Activator Yorkie. *Dev. Cell* **16,** 411–420 (2009).
75. Colombani, J., Polesello, C., Josué, F. & Tapon, N. Dmp53 Activates the Hippo Pathway to Promote Cell Death in Response to DNA Damage. *Curr. Biol.* **16,** 1453–1458 (2006).
76. Fan, R., Kim, N.-G. & Gumbiner, B. M. Regulation of Hippo pathway by mitogenic growth factors via phosphoinositide 3-kinase and phosphoinositide-dependent kinase-1. *Proc. Natl. Acad. Sci. U. S. A.* **110,** 2569–74 (2013).
77. Zhou, X. *et al.* Estrogen regulates Hippo signaling via GPER in breast cancer. *J. Clin. Invest.* **125,** 2123–2135 (2015).
78. Y. Wang, A. Yu, F. Y. The Hippo pathway in tissue homeostasis and regeneration. *Protein Cell* (2017). doi:10.1007/s13238-017-0371-0
79. Oh, H. & Irvine, K. D. Yorkie: the final destination of Hippo signaling. *Trends Cell Biol.* **20,** 410–417 (2010).
80. Cho, E. & Irvine, K. D. Action of fat, four-jointed, dachsous and dachs in distal-to-proximal wing signaling. *Development* **131,** 4489–4500 (2004).
81. Mao, Y. *et al.* Dachs: an unconventional myosin that functions downstream of Fat to regulate growth, affinity and gene expression in Drosophila. *Development* **133,** 2539–2551 (2006).

82. Garoia, F. *et al.* The tumor suppressor gene fat modulates the EGFR-mediated proliferation control in the imaginal tissues of Drosophila melanogaster. *Mech. Dev.* **122,** 175–187 (2005).
83. Zhang, J. *et al.* YAP-dependent induction of amphiregulin identifies a non-cell-autonomous component of the Hippo pathway. **11,** 1–16 (2009).
84. Ding, R. & Berger, C. Hippo pathway regulates neural stem cell quiescence. *Cell Cycle* **15,** 1525–1526 (2016).
85. Keder, A. *et al.* The Hippo pathway core cassette regulates asymmetric cell division. *Curr. Biol.* **25,** 2739–2750 (2015).
86. Poon, C. L. C., Mitchell, K. A., Kondo, S., Cheng, L. Y. & Harvey, K. F. The Hippo Pathway Regulates Neuroblasts and Brain Size in Drosophila melanogaster. *Curr. Biol.* **26,** 1034–1042 (2016).
87. Karpowicz, P. *et al.* The Hippo tumor suppressor pathway regulates intestinal stem cell regeneration. *Development* **137,** 4135–4145 (2010).
88. Ren, F. *et al.* Hippo signaling regulates Drosophila intestine stem cell proliferation through multiple pathways. *Pnas* **107,** 21064–21069 (2010).
89. Grusche, F. A., Degoutin, J. L., Richardson, H. E. & Harvey, K. F. The Salvador/Warts/Hippo pathway controls regenerative tissue growth in Drosophila melanogaster. *Dev. Biol.* **350,** 255–266 (2011).
90. Gregorieff, A., Liu, Y., Inanlou, M. R., Khomchuk, Y. & Wrana, J. L. Yap-dependent reprogramming of Lgr5+ stem cells drives intestinal regeneration and cancer. *Nature* **526,** 715–718 (2015).
91. Barry, E. R. *et al.* Restriction of intestinal stem cell expansion and the regenerative response by YAP. *Nature* **493,** 106–110 (2013).
92. Lee, D.-H. *et al.* LATS-YAP/TAZ controls lineage specification by regulating TGFβ signaling and Hnf4α expression during liver development. *Nat. Commun.* **7,** 11961 (2016).
93. Su, T. *et al.* Two-signal requirement for growth-promoting function of yap in hepatocytes. *Elife* **2015,** 1–21 (2015).
94. Elbediwy, A. *et al.* Integrin signalling regulates YAP/TAZ to control skin homeostasis. *Development* **143,** 1674–1687 (2016).
95. Xin, M. *et al.* Regulation of Insulin-Like Growth Factor Signaling by Yap Governs Cardiomyocyte Proliferation and Embryonic Heart Size. *Sci Signal* **4,** 1–15 (2012).
96. Xin, M. *et al.* Hippo pathway effector Yap promotes cardiac regeneration. *Proc. Natl. Acad. Sci.* **110,** 13839–13844 (2013).
97. Heallen, T. *et al.* Hippo signaling impedes adult heart regeneration. *Development* **140,** 4683–4690 (2013).
98. Z Lin, A von Gise, P Zho1, F Gu, Q Ma, J Jiang, A Yau, J Buck, K. Gouin, P van Gorp, B Zhou, J Chen, J Seidman, D. W. and W. P. Cardiac-Specific YAP Activation Improves Cardiac Function and Survival in an Experimental Murine MI Model. *Circ. Res.* **115,** 354–363 (2014).
99. Del Re, D. P. *et al.* Yes-associated protein isoform 1 (Yapl) promotes cardiomyocyte survival and growth to protect against myocardial ischemic injury. *J. Biol. Chem.* **288,** 3977–3988 (2013).
100. Huang, Z. *et al.* YAP stabilizes SMAD1 and promotes BMP2-induced neocortical astrocytic differentiation. *Development* **143,** 2398–2409 (2016).

101. Zhao, R. *et al.* Yap Tunes Airway Epithelial Size and Architecture by Regulating the Identity, Maintenance, and Self-Renewal of Stem Cells. *Dev. Cell* **30,** 151–165 (2014).
102. Chen, Q. *et al.* A temporal requirement for Hippo signaling in mammary gland differentiation , growth , and tumorigenesis. **28,** 432–437 (2014).
103. Qin, H. *et al.* Transcriptional analysis of pluripotency reveals the hippo pathway as a barrier to reprogramming. *Hum. Mol. Genet.* **21,** 2054–2067 (2012).
104. Aylon, Y., Sarver, A., Tovy, A., Ainbinder, E. & Oren, M. Lats2 is critical for the pluripotency and proper differentiation of stem cells. *Cell Death Differ.* **21,** 624–633 (2014).
105. Azzolin, L. *et al.* YAP/TAZ incorporation in the b-catenin destruction complex orchestrates the Wnt response. *Cell* **158,** 157–170 (2014).
106. Chung, H. *et al.* Yap 1 is dispensable for self-renewal but required for proper differentiation of mouse embryonic stem. **17,** 1–11 (2016).
107. Moroishi, T., Hansen, C. G. & Guan, K.-L. The emerging roles of YAP and TAZ in cancer. *Nat. Rev. Cancer* **15,** 73–9 (2015).
108. Hanahan, D. & Weinberg, R. A. Hallmarks of cancer: The next generation. *Cell* **144,** 646–674 (2011).
109. Maugeri-Saccà, M. & De Maria, R. Hippo pathway and breast cancer stem cells. *Crit. Rev. Oncol. Hematol.* **99,** 115–122 (2016).
110. Cordenonsi, M. *et al.* The hippo transducer TAZ confers cancer stem cell-related traits on breast cancer cells. *Cell* **147,** 759–772 (2011).
111. Janse van Rensburg, H. J. & Yang, X. The roles of the Hippo pathway in cancer metastasis. *Cell. Signal.* **28,** 1761–1772 (2016).
112. R. Johnson, G. H. The two faces of Hippo: targeting the Hippo pathway for regenerative medicine and cancer treatment. *Nat Rev Drug Discov* **144,** 724–732 (2014).
113. Overholtzer, M. *et al.* Transforming properties of YAP, a candidate oncogene on the chromosome 11q22 amplicon. *Proc. Natl. Acad. Sci. U. S. A.* **103,** 12405–12410 (2006).
114. Kandoth, C. *et al.* Mutational landscape and significance across 12 major cancer types. *Nature* **503,** 333–339 (2013).
115. M O'Hayre, JVázquez-Prado, I Kufareva, E Stawiski, T. Handel, S Seshagiri, J. G. The Emerging Mutational Landscape of G-proteins and G-protein Coupled Receptors in Cancer. *Nat Cell Biol* **13,** 412–424 (2013).
116. Reddien, P. W. & Alvarado, A. S. Fundamentals of Planarian Regeneration. *Annu. Rev. Cell Dev. Biol.* **20,** 725–757 (2004).
117. Saló, E. The power of regeneration and the stem-cell kingdom: Freshwater planarians (Platyhelminthes). *BioEssays* **28,** 546–559 (2006).
118. Baguñá, J. & Romero, R. Quantitative analysis of cell types during growth, degrowth and regeneration in the planarians Dugesia mediterranea and Dugesia tigrina. *Hydrobiologia* **84,** 181–194 (1981).
119. Hyman, L. H. The invertebrates: Vol. II. Platyhelminthes and Rhynchocoela; the acelomate Bilateria. 572 (1951).
120. Kobayashi, K. & Hoshi, M. Switching from asexual to sexual reproduction in the planarian Dugesia ryukyuensis: change of the fissiparous capacity along with the sexualizing process. *Zoolog. Sci.* **19,** 661–6 (2002).
121. Kobayashi, K., Arioka, S., Hase, S. & Hoshi, M. Signification of the Sexualizing

Substance Produced by the Sexualized Planarians. *Zoolog. Sci.* **19,** 667–672 (2002).
122. S Robb, K Gotting, E Ross, and A. S. A. SmedGD 2.0: The Schmidtea mediterranea genome database Sofia. *Genesis* **53,** 535–546 (2015).
123. Lapan, S. W. & Reddien, P. W. Transcriptome Analysis of the Planarian Eye Identifies ovo as a Specific Regulator of Eye Regeneration. *Cell Rep.* **2,** 294–307 (2012).
124. Rodríguez-Esteban, G., González-Sastre, A., Rojo-Laguna, J. I., Saló, E. & Abril, J. F. Digital gene expression approach over multiple RNA-Seq data sets to detect neoblast transcriptional changes in Schmidtea mediterranea. *BMC Genomics* **16,** 1–23 (2015).
125. Abril, J. F. *et al.* Smed454 dataset: unravelling the transcriptome of Schmidtea mediterranea. *BMC Genomics* **11,** 1–20 (2010).
126. Brandl, H. *et al.* PlanMine - A mineable resource of planarian biology and biodiversity. *Nucleic Acids Res.* **44,** 764–773 (2016).
127. Sanchez Alvarado, A. & Newmark, P. A. Double-stranded RNA specifically disrupts gene expression during planarian regeneration. *Dev. Biol.* **96,** 5049–5054 (1999).
128. Currie, K. W. *et al.* HOX gene complement and expression in the planarian Schmidtea mediterranea. *Evodevo* **7,** 1–23 (2016).
129. King, R. S. & Newmark, P. A. In situ hybridization protocol for enhanced detection of gene expression in the planarian Schmidtea mediterranea. *BMC Dev. Biol.* **13,** 1–32 (2013).
130. Hayashi, T., Asami, M., Higuchi, S., Shibata, N. & Agata, K. Isolation of planarian X-ray-sensitive stem cells by fluorescence-activated cell sorting. *Dev. Growth Differ.* **48,** 371–380 (2006).
131. Newmark, P. A. & Alvarado, A. S. Not Your Father'S Planarian: a Classic Model Enters the Era of Functional Genomics. *Nat. Rev. Genet.* **3,** 210–219 (2002).
132. Morita, M. & Best, J. B. Effects of photoperiods and melatonin on planarian asexual reproduction. *J. Exp. Zool.* **231,** 273–282 (1984).
133. Best, J. B., Goodman, a B. & Pigon, A. Fissioning in planarians: control by the brain. *Science* **164,** 565–566 (1969).
134. Deochand, M. E., Birkholz, T. R. & Beane, W. S. Temporal regulation of planarian eye regeneration. *Regeneration* **28,** 209–210 (2016).
135. Rossant, J. Genes for regeneration. *Elife* **3,** (2014).
136. Rieger, R. M., Tyler, S., Smith, J. P. S. III., and Rieger, G. E. *Platyhelminthes: Turbellaria. A Microscopic Anatomy of Invertebrates, Vol. 3: Platyhelminthes and Nemertinea.* (Wiley-Liss, 1991).
137. Skaer, R. J. the Origin and Continuous Replacement of Epidermal Cells in the Planarian Polycelis Tenuis (Iijima). *J. Embryol. Exp. Morphol.* **13,** 129–139 (1965).
138. Cebria, F., Vispo, M., Newmark, P., Bueno, D. & Romero, R. Myocyte differentiation and body wall muscle regeneration in the planarian Girardia tigrina. *Dev. Genes Evol.* **207,** 306–316 (1997).
139. Cebrià, F. Planarian Body-Wall Muscle: Regeneration and Function beyond a Simple Skeletal Support. *Front. Cell Dev. Biol.* **4,** 1–10 (2016).
140. Cebria, F., Bueno, D., Reigada, S. & Romero, R. Intercalary muscle cell renewal in planarian pharynx. *Dev. Genes Evol.* **209,** 249–253 (1999).
141. CHANDEBOIS, R. the Dynamics of Wound Closure and Its Role in the Programming of Planarian Regeneration. *Dev. Growth Differ.* **22,** 693–704 (1980).
142. Witchley, J. N., Mayer, M., Wagner, D. E., Owen, J. H. & Reddien, P. W. Muscle Cells

Provide Instructions for Planarian Regeneration. *Cell Rep.* **4,** 633–641 (2013).
143. Cebrià, F. Regenerating the central nervous system: How easy for planarians! *Dev. Genes Evol.* **217,** 733–748 (2007).
144. Cebrià, F., Nakazawa, M. & Mineta, K. Dissecting planarian central nervous system regeneration by the expression of neural-specific genes. *Dev. Growth Differ.* **44,** 135–146 (2002).
145. März, M., Seebeck, F. & Bartscherer, K. A Pitx transcription factor controls the establishment and maintenance of the serotonergic lineage in planarians. *Development* **140,** 4499–509 (2013).
146. Okamoto, K., Takeuchi, K. & Agata, K. Neural Projections in Planarian Brain Revealed by Fluorescent Dye Tracing. *Zoolog. Sci.* **22,** 535–546 (2005).
147. Pineda, D. *et al*. The genetic network of prototypic planarian eye regeneration is Pax6 independent. *Development* **129,** 1423–1434 (2002).
148. D Forsthoefela, A Parka, and P. N. Stem cell-based growth, regeneration, and remodeling of the planarian intestine. *Dev. Biol.* **356,** 445–459 (2011).
149. Kobayashi, C., Kobayashi, S., Orii, H., Watanabe, K. & Agata, K. Identification of Two Distinct Muscles in the Planarian Dugesia japonica by their Expression of Myosin Heavy Chain Genes. *Zoolog. Sci.* **15,** 861–869 (1998).
150. Kobayashi, C., Watanabe, K. & Agata, K. The process of pharynx regeneration in planarians. *Dev. Biol.* **211,** 27–38 (1999).
151. Lőw, P., Molnár, K. & Kriska, G. *Atlas of Animal Anatomy and Histology*. (Springer International Publishing, 2016). doi:10.1007/978-3-319-25172-1
152. Barberán, S., Fraguas, S. & Cebrià, F. The EGFR signaling pathway controls gut progenitor differentiation during planarian regeneration and homeostasis. *Development* **143,** 2089–2102 (2016).
153. Rink, J. C., Vu, H. T.-K. & Sánchez Alvarado, A. The maintenance and regeneration of the planarian excretory system are regulated by EGFR signaling. *Development* **138,** 3769–3780 (2011).
154. Woff, F. S.-D. Sur la migration de les celules de regeneration chez de planarias. *Rev Suisse Zol* **55,** 218–227 (1948).
155. Morita, M. & Best, J. B. Electron microscopic studies of planarian regeneration. IV. Cell division of neoblasts in Dugesia dorotocephala. *J. Exp. Zool.* **229,** 425–436 (1984).
156. Saló, E. & Baguñà, J. Regeneration and pattern formation in planarians. II. Local Origin and Role of Cell Movements in Blastema Formation. *Development* **107,** 69–76 (1989).
157. Coward, S. J. Chromatoid bodies in somatic cells of the planarian: Observations on their behavior during mitosis. *Anat. Rec.* **180,** 533–545 (1974).
158. Baguñà, J., Saló, E. & Auladell, C. Regeneration and pattern formation in planarians \nIII. Evidence that neoblasts are totipotent stem cells and the source of blastema cells. *Development* **107,** 77–86 (1989).
159. Newmark, P. a & Sánchez Alvarado, a. Bromodeoxyuridine specifically labels the regenerative stem cells of planarians. *Dev. Biol.* **220,** 142–53 (2000).
160. Önal, P. *et al.* Gene expression of pluripotency determinants is conserved between mammalian and planarian stem cells. *EMBO J.* **31,** 2755–2769 (2012).
161. Reddien, P. W. SMEDWI-2 Is a PIWI-Like Protein That Regulates Planarian Stem Cells. *Science (80-.).* **310,** 1327–1330 (2005).
162. Palakodeti, D., Smielewska, M., Lu, Y.-C., Yeo, G. W. & Graveley, B. R. The PIWI proteins

SMEDWI-2 and SMEDWI-3 are required for stem cell function and piRNA expression in planarians. *RNA (New York, NY)* **14,** 1174–1186 (2008).
163. Solana, J. *et al.* Defining the molecular profile of planarian pluripotent stem cells using a combinatorial RNAseq, RNA interference and irradiation approach. *Genome Biol.* **13,** 1–23 (2012).
164. Wagner, D. E., Wang, I. E. & Reddien, P. W. Clonogenic Neoblasts Are Pluripotent Adult Stem Cells That Underlie Planarian Regeneration. *Science (80-.).* **811,** 1–48 (2011).
165. J van Wolfswinkel, D Wagner, and P. R. Single-cell analysis reveals functionally distinct classes within the planarian stem cell compartment. *Cell Stem Cell* **15,** 326–339 (2014).
166. Molinaro, A. M. & Pearson, B. J. In silico lineage tracing through single cell transcriptomics identifies a neural stem cell population in planarians. *Genome Biol.* **17,** 87 (2016).
167. Scimone, M. L., Kravarik, K. M., Lapan, S. W. & Reddien, P. W. Neoblast specialization in regeneration of the planarian schmidtea mediterranea. *Stem Cell Reports* **3,** 339–352 (2014).
168. Adler, C. E. & Sanchez Alvarado, A. Types or States? Cellular Dynamics and Regenerative Potential. *Trends Cell Biol.* **25,** 687–696 (2015).
169. Isshiki, T., Pearson, B., Holbrook, S. & Doe, C. Q. Drosophila neuroblasts sequentially express transcription factors which specify the temporal identity of their neuronal progeny. *Cell* **106,** 511–521 (2001).
170. P Rompolas, R. Patel-King, S. K. An Outer Arm Dynein Conformational Switch Is Required for Metachronal Synchrony of Motile Cilia in Planaria. *Mol. Biol. Cell* **21,** 3669–3679 (2010).
171. Eisenhoffer, G. T., Kang, H. & Alvarado, A. S. Molecular Analysis of Stem Cells and Their Descendants during Cell Turnover and Regeneration in the Planarian Schmidtea mediterranea. *Cell Stem Cell* **3,** 327–339 (2008).
172. Tu, K. C. *et al.* Egr-5 is a post-mitotic regulator of planarian epidermal differentiation. *Elife* **4,** 1–27 (2015).
173. Morgan, T. H. Experimental studies of the regeneration of Planaria maculata. *Entwickelungsmechanik der Org.* **7,** 364–397 (1898).
174. J. Baguñá, E Saló, R Romero, J Garcia-Fernández, D Bueno, A Muñoz-Marmol, J Bayascas-Ramirez, A. C. Regeneration and Pattern Formation in Planarians: Cells, Molecules and Genes. *Zoolog. Sci.* 781–795 (1994).
175. Baguñà, J. Mitosis in the Intact and Regenerating Planarian Dugesia mediterranea n. sp. *J. Exp. Zool.* **195,** 53–64 (1976).
176. Saló, E. & Baguñà, J. Regeneration and pattern formation in planarians. *J. Embryol exp. Morph.* **83,** 63–80 (1984).
177. Kato, K., Orii, H., Watanabe, K. & Agata, K. The role of dorsoventral interaction in the onset of planarian regeneration. *Development* **126,** 1031–1040 (1999).
178. Sandmann, T., Vogg, M. C., Owlarn, S., Boutros, M. & Bartscherer, K. The head-regeneration transcriptome of the planarian Schmidtea mediterranea. *Genome Biol.* **12,** 1–19 (2011).
179. Pirotte, N. *et al.* Reactive oxygen species in planarian regeneration: An upstream necessity for correct patterning and brain formation. *Oxid. Med. Cell. Longev.* 1–19 (2015). doi:10.1155/2015/392476

180. Pellettieri, J. *et al*. Cell death and tissue remodeling in planarian regeneration. *Dev. Biol.* **338,** 76–85 (2010).
181. Wenemoser, D. & Reddien, P. W. Planarian regeneration involves distinct stem cell responses to wounds and tissue absence. *Dev. Biol.* **344,** 979–991 (2010).
182. Fan, Y. & Bergmann, A. Distinct Mechanisms of Apoptosis-induced Compensatory Proliferation in Proliferating and Differentiating Tissues in the Drosophila Eye. *Dev Cell* **14,** 399–410 (2008).
183. Chera, S. *et al*. Apoptotic Cells Provide an Unexpected Source of Wnt3 Signaling to Drive Hydra Head Regeneration. *Dev. Cell* **17,** 279–289 (2009).
184. Almuedo-Castillo, M. *et al*. JNK Controls the Onset of Mitosis in Planarian Stem Cells and Triggers Apoptotic Cell Death Required for Regeneration and Remodeling. *PLoS Genet.* **10,** 1–15 (2014).
185. Matsuo, R., Yamagishi, M., Wakiya, K., Tanaka, Y. & Ito, E. Target innervation is necessary for neuronal polyploidization in the terrestrial slug Limax. *Dev. Neurobiol.* **73,** 609–620 (2013).
186. Witchley, J. N., Mayer, M., Wagner, D. E., Owen, J. H. & Reddien, P. W. Muscle Cells Provide Instructions for Planarian Regeneration. *Cell Rep.* **4,** 633–641 (2013).
187. Pellettieri, J. & Sánchez Alvarado, A. Cell turnover and adult tissue homeostasis: from humans to planarians. *Annu. Rev. Genet.* **41,** 83–105 (2007).
188. González-Estévez, C. & Saló, E. Autophagy and apoptosis in planarians. *Apoptosis* **15,** 279–292 (2010).
189. Miller, C. M. & Newmark, P. A. An insulin-like peptide regulates size and adult stem cells in planarians. *Int. J. Dev. Biol.* **56,** 75–82 (2012).
190. Adell, T., Cebrià, F. & Saló, E. Gradients in planarian regeneration and homeostasis. *Cold Spring Harb. Perspect. Biol.* **2,** 1–13 (2010).
191. González-Estévez, C., Felix, D. A., Rodríguez-Esteban, G. & Aziz Aboobaker, A. Decreased neoblast progeny and increased cell death during starvation-induced planarian degrowth. *Int. J. Dev. Biol.* **56,** 83–91 (2012).
192. González-Estévez, C., Felix, D. a, Aboobaker, A. a & Saló, E. Gtdap-1 promotes autophagy and is required for planarian remodeling during regeneration and starvation. *Proc. Natl. Acad. Sci. U. S. A.* **104,** 13373–13378 (2007).
193. Peiris, T. H. *et al*. TOR signaling regulates planarian stem cells and controls localized and organismal growth. *J. Cell Sci.* **125,** 1657–1665 (2012).
194. Wurtzel, O. *et al*. A Generic and Cell-Type-Specific Wound Response Precedes Regeneration in Planarians. *Dev. Cell* **35,** 632–645 (2015).
195. Harvey, K. & Tapon, N. The Salvador-Warts-Hippo pathway an emerging tumour-suppressor network. *Nat Rev Cancer* **7,** 182–191 (2007).
196. Justice, R. W., Zilian, O., Woods, D. F., Noll, M. & Bryant, P. J. The Drosophila Tumor-Suppressor Gene Warts Encodes a Homolog of Human Myotonic-Dystrophy Kinase and Is Required for the Control of Cell-Shape and Proliferation. *Genes Dev.* **9,** 534–546 (1995).
197. No Title. Available at: https://www.ncbi.nlm.nih.gov/geo/query/acc.cgi?acc=GSE95130.
198. Cagnol, S. & Chambard, J. C. ERK and cell death: Mechanisms of ERK-induced cell death - Apoptosis, autophagy and senescence. *FEBS J.* **277,** 2–21 (2010).
199. Enari, M. *et al*. A caspase-activated DNase that degrades DNA during apoptosis, and

its inhibitor ICAD. *Nature* **391,** 43–50 (1998).
200. Repnik, U., Stoka, V., Turk, V. & Turk, B. Lysosomes and lysosomal cathepsins in cell death. *Biochim. Biophys. Acta - Proteins Proteomics* **1824,** 22–33 (2012).
201. Vandamme, D. *et al.* ??-Skeletal muscle actin nemaline myopathy mutants cause cell death in cultured muscle cells. *Biochim. Biophys. Acta - Mol. Cell Res.* **1793,** 1259–1271 (2009).
202. Iglesias, M. J. *et al.* Growth hormone releasing peptide (ghrelin) is synthesized and secreted by cardiomyocytes. *Cardiovasc. Res.* **62,** 481–488 (2004).
203. Frasch, S. C. *et al.* Regulation of phospholipid scramblase activity during apoptosis and cell activation by protein kinase C?? *J. Biol. Chem.* **275,** 23065–23073 (2000).
204. Yabuta, N. *et al.* Lats2 is an essential mitotic regulator required for the coordination of cell division. *J. Biol. Chem.* **282,** 19259–19271 (2007).
205. Hergovich, A. & Hemmings, B. A. Hippo signalling in the G2/M cell cycle phase: Lessons learned from the yeast MEN and SIN pathways. *Semin. Cell Dev. Biol.* **23,** 794–802 (2012).
206. Hergovich, A. Hippo Signaling in Mitosis: An Updated View in Light of the MEN Pathway. *Mitotic Exit Netw. Methods Protoc. Methods Mol. Biol.* **1505,** 265–277 (2017).
207. Dobbelaere, J., Gentry, M. S., Hallberg, R. L. & Barral, Y. Phosphorylation-dependent regulation of septin dynamics during the cell cycle. *Dev. Cell* **4,** 345–357 (2003).
208. Schedl, T., Burland, T. G., Gull, K. & Dove, W. F. Cell cycle regulation of tubulin RNA level, tubulin protein synthesis, and assembly of microtubules in Physarum. *J. Cell Biol.* **99,** 155–165 (1984).
209. Zhou, J., Shu, H. B. & Joshi, H. C. Regulation of tubulin synthesis and cell cycle progression in mammalian cells by γ-tubulin-mediated microtubule nucleation. *J. Cell. Biochem.* **84,** 472–483 (2001).
210. Jones, J. I. & Clemmons, D. R. Insulin-like growth factors and their binding proteins: Biological actions. *Endocrine.Rev.* **16,** 3–34 (1995).
211. He, Z., Ismail, A. & Kriazhev, L. Progranulin (PC-Cell-derived Growth Factor / Acrogranin) Regulates Invasion and Cell Survival Progranulin (PC-Cell-derived Growth Factor / Acrogranin) Regulates Invasion and. 5590–5596 (2002).
212. M Bonner, A. S. Cell divisions screens and dynamin. *Biochem Soc Trans* **36,** 431–435 (2008).
213. Tonks, N. K., Cicirelli, M. F., Diltz, C. D., Krebs, E. G. & Fischer, E. H. Effect of microinjection of a low-Mr human placenta protein tyrosine phosphatase on induction of meiotic cell division in Xenopus oocytes. *Mol Cell Biol* **10,** 458–463 (1990).
214. Walton, K. M. & Dixon, J. E. Protein Tyrosine Phosphatases. *Annu. Rev. Biochem.* **62,** (1993).
215. Arredondo, J. *et al.* Muscarinic acetylcholine receptors regulating cell cycle progression are expressed in human gingival keratinocytes. *J. Periodontal Res.* **38,** 79–89 (2003).
216. Ozaki, N. *et al.* Serine protease inhibitor Kazal type 1 promotes proliferation of pancreatic cancer cells through the epidermal growth factor receptor. *Mol. Cancer Res.* **7,** 1572–81 (2009).
217. Yan, C., Ding, X., Dasgupta, N., Wu, L. & Du, H. Gene profile of myeloid-derived suppressive cells from the bone marrow of lysosomal acid lipase knock-out mice. *PLoS One* **7,** 1–13 (2012).

218. Schweitzer, J. K. & D'Souza-Schorey, C. Finishing the job: Cytoskeletal and membrane events bring cytokinesis to an end. *Exp. Cell Res.* **295,** 1–8 (2004).
219. Yang, J. *et al.* Rootletin, a novel coiled-coil protein, is a structural component of the ciliary rootlet. *J. Cell Biol.* **159,** 431–440 (2002).
220. Chai, G. *et al.* Complete functional segregation of planarian β-catenin-1 and -2 in mediating Wnt signaling and cell adhesion. *J. Biol. Chem.* **285,** 24120–24130 (2010).
221. Van Wolfswinkel, J. C., Wagner, D. E. & Reddien, P. W. Single-cell analysis reveals functionally distinct classes within the planarian stem cell compartment. *Cell Stem Cell* **15,** 326–339 (2014).
222. Lin, A. Y. T. & Pearson, B. J. Planarian yorkie/YAP functions to integrate adult stem cell proliferation, organ homeostasis and maintenance of axial patterning. *Development* **141,** 1197–1208 (2014).
223. Lin, A. Y. T., Pearson, B. J. & Biology, S. C. Yorkie is required to restrict the injury responses in planarians. *bioRxiv* 1–30 (2016). doi:doi.org/10.1101/092353
224. Zhou, Q., Li, L., Zhao, B. & Guan, K. The hippo pathway in heart development, regeneration, and diseases. *Circ. Res.* **116,** 1431–47 (2015).
225. Demircan, T. & Berezikov, E. The Hippo pathway regulates stem cells during homeostasis and regeneration of the flatworm Macrostomum lignano. *Stem Cells Dev.* **22,** 2174–85 (2013).
226. Panciera, T. *et al.* Induction of Expandable Tissue-Specific Stem/Progenitor Cells through Transient Expression of YAP/TAZ. *Cell Stem Cell* **19,** 725–737 (2016).
227. Gao, T. *et al.* Hippo Signaling Regulates Differentiation and Maintenance in the Exocrine Pancreas. *Gastroenterology* **144,** 1543–1553 (2014).
228. Oh, H. J. *et al.* MST1 Limits the Kinase Activity of Aurora B to Promote Stable Kinetochore-Microtubule Attachment. *Curr. Biol.* **20,** 416–422 (2010).
229. Yabuta, N. *et al.* N-terminal truncation of Lats1 causes abnormal cell growth control and chromosomal instability. *J. Cell Sci.* **126,** 508–520 (2013).
230. Ganem, N. J. *et al.* Cytokinesis failure triggers hippo tumor suppressor pathway activation. *Cell* **158,** 833–848 (2014).
231. Udan, R. S., Kango-Singh, M., Nolo, R., Tao, C. & Halder, G. Hippo promotes proliferation arrest and apoptosis in the Salvador/Warts pathway. *Nat. Cell Biol.* **5,** 914–920 (2003).
232. Dong, J. *et al.* Elucidation of a Universal Size-Control Mechanism in Drosophila and Mammals. *Cell* **130,** 1120–1133 (2007).
233. Skibinski, A. *et al.* The Hippo Transducer TAZ Interacts with the SWI/SNF Complex to Regulate Breast Epithelial Lineage Commitment. *Cell Rep.* **6,** 1059–1072 (2014).
234. Zhivotovsky, B. & Kroemer, G. Apoptosis and genomic instability. *Nat. Rev. Mol. Cell Biol.* **5,** 752–762 (2004).
235. Fan, F. *et al.* Pharmacological targeting of kinases MST1 and MST2 augments tissue repair and regeneration. *Sci. Transl. Med.* **8,** 352ra108-352ra108 (2016).
236. Grusche, F. A., Richardson, H. E. & Harvey, K. F. Upstream regulation of the Hippo size control pathway. *Curr. Biol.* **20,** 574–582 (2010).
237. Sun, S. & Irvine, K. D. Cellular Organization and Cytoskeletal Regulation of the Hippo Signaling Network. *Trends Cell Biol.* **xx,** 1–11 (2016).
238. Cebrià, F. & Newmark, P. a. Planarian homologs of netrin and netrin receptor are required for proper regeneration of the central nervous system and the maintenance

of nervous system architecture. *Development* **132,** 3691–3703 (2005).
239. Guo, T., Peters, A. H. F. M. & Newmark, P. A. A bruno-like Gene Is Required for Stem Cell Maintenance in Planarians. *Dev. Cell* **11,** 159–169 (2006).
240. Ross, K. G. *et al.* Novel monoclonal antibodies to study tissue regeneration in planarians. *BMC Dev. Biol.* **15,** 2 (2015).
241. González-Estévez, C., Felix, D. A., Aboobaker, A. A. & Saló, E. Erratum: Gtdap-1 and the role of autophagy during planarian regeneration and starvation (Autophagy). *Autophagy* **3,** 640–642 (2007).
242. Moritz, S. *et al.* Heterogeneity of planarian stem cells in the S/G2/M phase. *Int. J. Dev. Biol.* **56,** 117–125 (2012).
243. Sureda-Gómez, M., Martín-Durán, J. M. & Adell, T. Localization of planarian βCATENIN-1 reveals multiple roles during anterior-posterior regeneration and organogenesis. *Development* dev.135152 (2016). doi:10.1242/dev.135152
244. Bray, N. L., Pimentel, H., Melsted, P. & Pachter, L. Near-optimal probabilistic RNA-seq quantification. *Nat. Biotechnol.* **34,** 525–527 (2016).
245. Pimentel, H. J., Bray, N., Puente, S., Melsted, P. & Pachter, L. Differential analysis of RNA-Seq incorporating quantification uncertainty. *bioRxiv* (2016). doi:10.1101/058164
246. Love, M. I., Huber, W. & Anders, S. Moderated estimation of fold change and dispersion for RNA-seq data with DESeq2. *Genome Biol.* **15,** 550 (2014).
247. Barrett, T. *et al.* NCBI GEO: Archive for functional genomics data sets - Update. *Nucleic Acids Res.* **41,** 991–995 (2013).

Annexes

Annex 1

Core elements of the Hippo pathway

Hippo

RNLYKSYMMEKLLDDDLQKEPSEVFQIESKLGKGSYGSVYKAKHKKNGFTVAAKLVPVDSELSD
IVKEISIMQQCKSDYIVQYYGSFYDSHDLWIVMEYCGAGSVSDIMRLRNKTCNEEEIAIILQGS
LKGLEYIHQLKKIHRDIKAGNILLTEEGNAKLADFGVAGQLSDTLAKRNTVIGTPYWMAPEVIQ
EIGYHYSADIWSLGITAIEMADGKPPYADIHPMRALFMIPSQPPPTLLNPSIWSPSFVNFITQC
LVKNPDQRPSASQLLLNCEFIINASSPDHLIATIKQANEIRENRQHEEDTIQSRGSVTEEERTT
DNGTMVRCSGDTATSLSSESSMIVRDSLSSSVEAPTMLINATDDDSEAGGDTLTEQPHKSNKSP
SQFAHQKKLQENGVKESAAQSPCGPLNPNAFVNVEEIYRNLETKSYNELQQLLSRIDSDLQAEL
NNLEIRYLHKRQPILDAISEKSKPIAASVNSK

Domains prediction

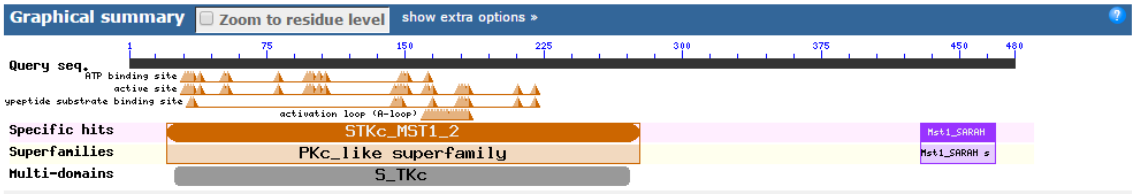

Salvador

MSKIKHENDIILLSIDANWMPYNFNSTYFSRYLSVDNSLDLIFYSSEVLNMLDKNICAEFEISY
ELPKGWFEIRSSRGRMCFLDTINKISTWTNPTNNFIIPFGWERIDSETEGIYYHHIFLNHCQRY
NPNLWIQIDCKRPEITQRNFFAYFKNIKNKNIEMNMLFFAFLIFKNDNNFTEVKSMLYNDLISL
YEALEMVMYLKIKDIFTKYEKLRAEISLRLFLESSSKQV

Domains prediction

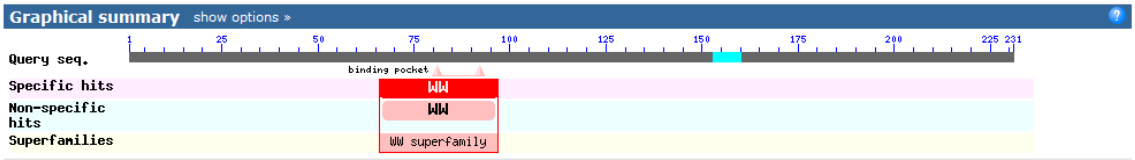

Warts

LRHFEIFNWIIILIENVSLITKTASFPMYPMSNILKMRPIGQNSLNFSEAFLNKTTGCRLDNNN
MCPSFLSNAAIHKRPNYLSPNFHPNEYNHAFTNEVMFNSSPIDSVYSSPAYGMRLFPNNEIYAP
PLPPKLSPQPSLQPSLEELSSSNNRRMYNECFPTPSYEPTQIRAQLILSKSAVFQQTARSQWLP
KNIQRGQAFAINCDSNQPYGASPGGQQMMVNNRDCNSNNRMRPMDTNNHQIMSENVGELIQSGQ
SKAFVSVDEMLLKSFACDSSRPLFLTNIYKDPIIFQQMDEHTNRNYILPSVQNPPPIPPKPTRS
LSHANPPTLPPRQPITTTTETNDCADCIKPNSEDIENETKSSVLVSPDDNSAVPEHQSKDGYLN
IRKVDAAAYKRFMENRMEQVERTHKERYDRMQQLEYEMDKMGLDSNYKEQMRQLLLQKESNYLR
MKRQKMNKSMFERIKLLGVGAFGEVALVRKKDNKQLYAMKKLKKRNVVERRQTAHVRAERDILA
EADNDWVVKLFFSFQDQTSLYLVMEYIPGGDMMSLLIKKGIFEEDLGRFYAAEMTLALESVHSL
GFVHRDIKPDNILLTKDGHIKLTDFGLCTGFRWTHMAQYYKHWDPSATSSYHISQDSEGFQEIV
ADGQTNPDLNKPLIRRKNRFKNRKFMRSLVGTPNYIAPEILKREKYNKSCDWWSVGVIVYEMLV
GQPPFLAPSAAHTQYRVINWESFLNIPAHANLDPNAEDIIRRFCCNPANRLSDPSEIKQHPFFI
SIDWKNLINQDAPYKPYIRDELDTSNFDSVEDDIGSSSDSNSSQDDDNPTSKSRLNNNNTDIPF
FNFTFKRFFDHGNS

Domains prediction

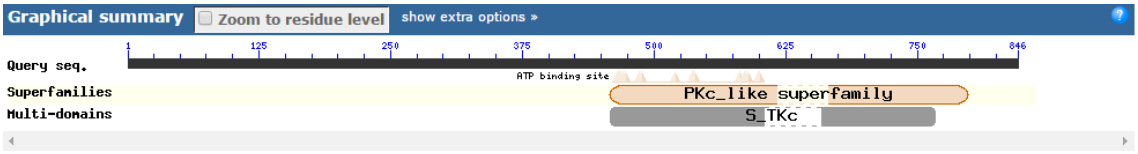

Yorkie

MSFSSASNNVVLKTSDAMNNSLDELFEVVINKSSSRQKPLTERQLPRSFFVPPSGNSNCPSVSH
FKAFSSPATLEETYRAGPGQQNINHFKQRSLDSQNGNQHFSDLTSVPNIEMKSHSPALERKPHL
NIEIKELPVGYEMAINGNCQVYFLNHNTKETTWFDPRLPETIQKWGMTLNDLQELHIRYINMMS
NNNAKSLSQTQHPMNVLRSPQTQQSHSGSSDQTNSFNDPKSQTHFRSCSQPVSSSGTSLGGGVV
DSSSATLNNFQMKPVGNLQYFVNQVSGGGSMLGNYQDLCRLHPHCSSSVQGSLSHSNNSSCSNL
STCLNGLNLSPLPSSQNSGNSILLNHSPYTGHASPGLNVVAYSHSHQDSLDSGVGQSVVSQSQL
SSNTLNQTNDPSKSFDYSIKYEEADNFDSCTSKLDDFMDIDFRQLNY

Domains prediction

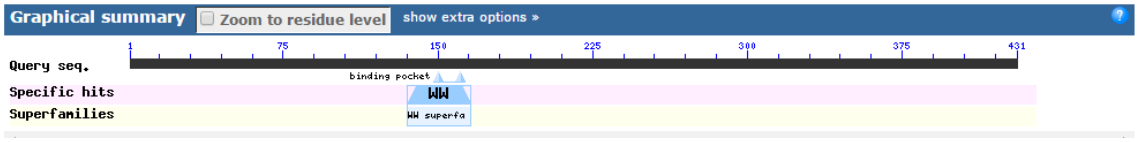

Up-stream regulators of the Hippo pathway

Merlin

MPKNINVNVTTVDAELQFSIQSNAIGKTLFDQIIKTIGLRETWYFGLLYIDVKGNLCWLNLEKK
VSHINVLSKTEMEFQFRIKFYPEDVSEELIQEITIKFFYLQVRESILGSDIFCPPEPALLLASY
ACQVKFGDYDPSVQKPGFLSDERILPPRILNQHKWSNQQWESKIVKWYSEYRGMLRVEAMLEYL
KIAQDLEMYGVSYFEIKNKKGSQLYIGIDALGLNIYKFKDKLTPQVGFPWGEIRNISFKDKRFV
IKSIDKKAPDFVFFVNKLRVNKTILALCAGNHELFVRRRNEDSIDVQQMKTQAQEDKINKKNEK
ERLFREKLAREAAEKRLVSIEKKLKQETQEHAETNKTLLTVRQSFSLIQEQLEAECKQRKALED
RQQEILKEKKLLEERNLEETDCYKNILTENSEIQRVLDEQNSILIRKKREMITQTEHIKNEEPD
IPSEHIPDSDISIESENLCNVDLDKSLKFYHHELEVLENGDYKPSIENRRTIIEADEDLHNKLS
DLGEELKEARNSKGFDEIDTIHENNKAKGLDKFQTLRLIRQGNTKKRIDEFESM

Domains prediction

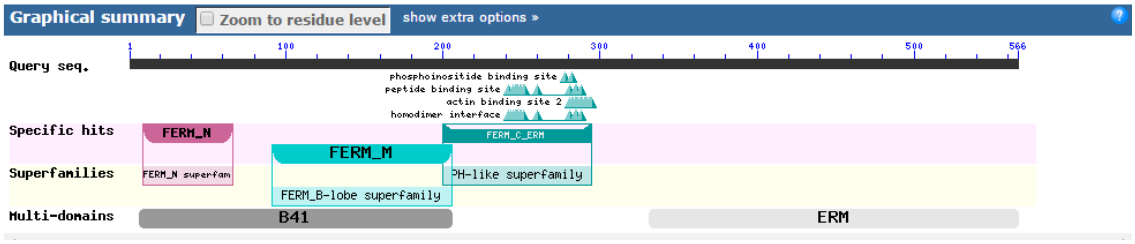

Expanded

MNDLYPNLFKNLTRSPITIILLDNRKQTMVYDKTTKLSSLFEATCDLCYVDCDNLFGFAILMDD
YYAFLDLDSKVCKLNFKEFAKKSQSNVLFKPLGSNISPIHQSVDENRRHSQILNNHTNHRLQNS
TASTKSAPVFHQKSNYIPNEDDTPVIYFRVKSYVHTYCLRDRMTKMLYFQQLMRNVLDYKLQCA
DEIYLQLGAYAIQAFYGDYELLLSNDDSISMSSTNTESSATYSPTLVKLSRSSDRYQNFTREMV
QTGRYFEPKKFFPSWIITKYSSEYLYKEISQLHKSLTGLSRFDAEFSYIRMASAQYSNFNMHLF
PVRDQTLTGHSGTGTFPTFTSNGKANGIKTLKNKLWLGLGPAGLEMHEMKNSDFLIHLSTLKWS
DIVEVTQKPYRINVRVGGRNLKLHTNTKMQADHLFWLTRHMHIYQTKAKLNAICTPEALDTVER
QKYREKYVYMDLEDLKQNGFQFVDTNEISSENMFTEEIVRYSIPKSMPAVNTPAVPPRRNPSKA
RPLKMKDLMKISNPPKESVTDNVQVKPEINKRYIKKTNPSNQSNTYTNAIQKGIKSPEIIVKDH
IEVPQGLISRGFKENYIEIQSFQSDIDSDQNTSKAYETMDESDFASSLNESESRSPGQFGLKHA
GRFISLSQEINHFDEFPSELQSLKDLLPPKEFREPSQSLTHITKSISFDNHDISLQKPSGISPR
QMSEPVLFNANLYRSLPMIMGLCHEFHDSKLIGDIKLTKLPNALEKHQSKTSVGMKSWKSDILC
NLNNCLDNDEEEDSVVINNSISSVDIAPPQFESHLSRRNSLPQCPSSYRDIISSSSTLDTANDD
SVDISSLSSFDFDYMNYSRYNRSNSSKGQNPHVAII

Domains prediction

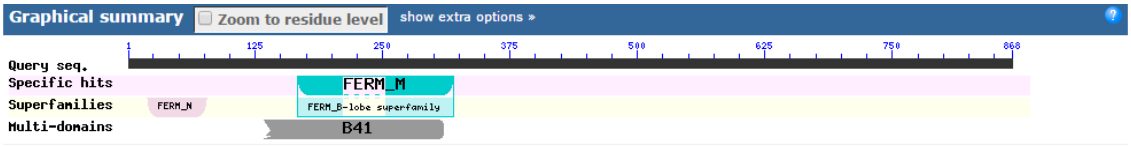

Scribble

MKKCFPFLTTCGSQLEVIDKRHSNLLYVPDEVIRNARSIEECFLDANQIKDLPKNFFKLSKLRV
LTLSDNELTYIPESIGNFNHLVELDVSRNHIDSVHYNIKFCNELRSLDLSNNPINRLPEGFSSL
RNLIVLNLNDNSLTELPNDFGNLSLLQKLELRDNCLKTLPNSFSKFVHLEILDLGGNEFQEFPK
SLAKLSALRELSLDNNELQNLPQELGTLKNLQQLDVSENFLEVICEEIGNLEQLTDFALSQNSL
DSLPNNIGNLKELTILKVDQNKLMSLTTHIGSCSKLQELYLTENLLTKLPGSLGRLSKLVHLNV
DRNNLNSIPPELSKCNELSIMSFRDNHIRRLPDEIGNMKKLHVLDISINQIDRLPLSIAQCPLK
ALWLSENQSQSMVKLQRDKDDNTNEEYLTCYLLPQSGIDAELNHNQNIIDTQDYVNEFAAGDRN
SLVLSGTDNDSMKFRVSSGTSETKVKFNEDEQTPSIRMSKELPKTRHPKFDKKAVDGHIIPKDI
HVNKEIKFAPNRFSPENDQVDSRINGKVPPKRTKKISAPPSMAPNISIQLVENIENQFEESRLR
SHSDAGLRPGEITAITEEDCIEKPNAHSSRSASQSSSSSYSDHSAKKHNETVQIVKEPVEIEEV
SPEVKTRKTKFGVKLTDHVREICPNDDNRFLEVSSRISSREQAGYSSGGEEIDGIARHVGFSEE
VEDNEEATDLKLIRRDTPHYTKKSKIQQITADGVKNEDVVKQIMEKLRSPSVGSSHSVTVVNQK
TEKLRDNEQDQMSVQMRHMDSLQIMPTYDQVVSASALARGSDVPPGMNSATSEAEEVHVIIERN
ENEPLGMSIAGGKGSCPYQPVFVSRVTDNGAANRCGLRVNDKIISVNNQSMNDVDHSVAVSALK
TAGNYIDLLVLREVVIAPPPLSSSDNYLANMDQNTDNVDVKFEAIKCEVVRDENGLGFSIAGGK
GSMRKDFCDQRWAFLESIYICKITPNGAADKSKRLQVGDKIIKINGIDVSDARHDQAVVLLSGS
EPIIHLEVQRQIIISKNSFDQIDHSMELSKPISPVSKNSICGTKYNNSEIVKIIKTGAQLGLCI
CGGIDHYSHPFGINDPGVFISKISPKGAAKATGKLRIGDRIISVNGHDITKATHDEAILLIVQA
NNDILLEVVHEPPPPGLKELTIYKEINEKLGINIQGGNDGLFMNPDDSKDRGIFITKIIPGGAI
HRDGKLKVGDRVLEVNRRSFMGLSISAANKVLGSVTTQLEVLVCDGISPEKIDQVLSSSHLLPP
NLSISERKSPTVSSPGTSHINISPYDSMQNSPNLQEDNAHNYENQDYLSNINKNHALINEREHL
SFRSKKQFFEKEIEQRKN

Domains prediction

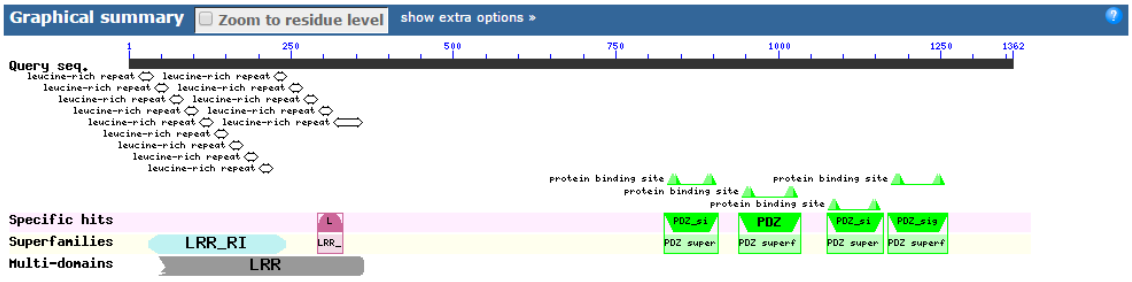

Lgl1

MASKLFAPFKKFPQQLPIFKKSSDKFKDASMANYNSICGMLDDVTCNCFDNELYLFAVGTKKGE
IKIYGSPGIAYTLINSPLKPIKFLKFLKGQGRLISVNIENEISLWEYKIELSTWEMISSISLSA
YINTGKITAIDISQSFSWKTTSDDLLELLVVGSSTNKIFQILIIGNRFHFYDGDDLSIDSDHVI
SKIQDLDKTYDLGGVDKIQFNPDQNSLFYISYSNGMLLILESKVKEEKDENKENEVTETKSHDE
KLIVTGTTEEESEKPSEATNELKLPESEDITSSEVPKIDENKEQGEKTDEAEEVAKSEIVKSKA
DDEIQKLDEAKPEVQKSEDIKPEIKKLKESTQVPYAHVELPAITKYVFSGKKILAVNWANDKIA
VAQEDSESICFYDIGSDNFKISESEKTVTIPENFQTSLAKFSFCNLKNFNLTILMAHSNEKNIL
IVLKDDSKSTEIKTPSNIVDFVLTTNNFSELSKQSHTLLILCESQLIAIDIESEDLIEIDCPYL
SLNNTSHITSLTSIIQVPPSLFPNASTVNELFKNWPFRNENCANEKHEDELLIDIFGSGHADGT
IKIWQVLPSGVLNLLIKVESSEIFHQAVSEVNACSQSNGISKQVGCHLTDSEDNLLQITNIQLM
LHSTNSFSEPSANELFCLTGNSCGTVLVFKYDGTDNKGDLTEISANFDKEGIIWNDCEIPELLS
STDISEKLQNLNYIVKLNPSLPVTALAFQPAWEFLSVGCTNGLVLVDFHQNKCVFSHLTIQRIS
KASNAGQAPLTVGQQLKKSIRQSFRKLKKLKPATKHTYTVNEEKAKDKEEAKSAEKEEEKEIVK
PDDKEENLKETQQEDGENIEEKDKEEVKEHVD

Domains prediction

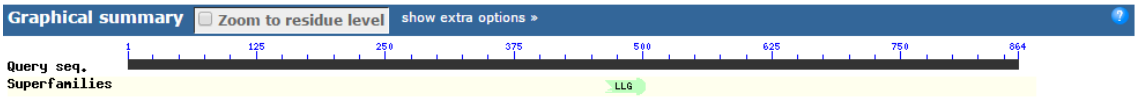

Lgl2

MTQSIFNSVRKLNFYNFKTKYINQNESIGEFYKKQSIEDFGSIPEPSCIDYDHKLSLLGIASKK
GLIKIFGCPGVCYSTRLEGQDEIWNIKFIPGTNFFVTLTADNKLILWLISTLTNELFKVDVISN
LNVVNSARTSAHNQSDYNNNNENSIEQNITAIEVNDLTSSIIMGNGSGSLIQVKLDLLKMRKQA
NNYKTVPPGNTIWQMPTKSDVIDRDRIISKLPIGSQNRVIIDAVIHISARPGSRKHLLIGYRSG
NSIIYNVQKDSVDFLLSAKSTLNALSWCPPDPIVQDNFMVAPNRNEPQYYSSMKLHSCHEDGSI
ITWNLPQNSDEFLVLDFQIFSPYKKDQKCLPISKILWKRYKQDYLIVFSGGLPRSDYMTKSTIT
IMNNSCLDSSKANNEHLVLDLTSQLIDFTTIDDNDSGSVEYLLVLTEEEFFIVDLTKESWPILH
DRQPYLNCLHNSPITAYQFLSEVKSDWFQKLNEMSSNKEDCNISFSDWPIKGYAQKVRNDEIWQ
NDLLIIGHGDGTIVFWKFGMGGCMKKISTVKSSSLFKMADELHLNEVSYEDDEIPLRRTGQFDP
CCDDNRLAIQLIHYTGKHLLIGGYGGQIVLWGFQENKYEKHLLDVDLTTHLSNFKWKGCQPFQH
IEGSIKTGSNFQVMMSMCIFPPSQITALDILEDNNCNGYVIIACGTLHGLVIVSCPKETNLEAL
VLTTHCTVPRNTLASQEASLGEGWARRRTRELKKSLRSSFRRLRRRSTKRMEHPSVSRHLSDNN
DKTMRVELVENEVEFEERAIEDRPKDTANDGLIRSIRINVSLIKRKGSNGPHEKLLNLFAGCYG
GLLLWFQSDYSVENILKNSPINLRLIKQYQFQHRAPILHFNMLSPESGLSKLNENTDADFDLDP
NRKPDHLVVLTEEQVRLYAFPSFTLKCKIRVTAHDGFRLKNGSLIVFSDDRLTTQNNSKEPLIC
ATNNGGQFLLLNCVNLKRKDVVQFVDKTDLMALNFMSLAKNANLSNARTLCPYGICYSGQGQVT
LFEIISKTKTIGTHSSGYFWSRNNSS

Domains prediction

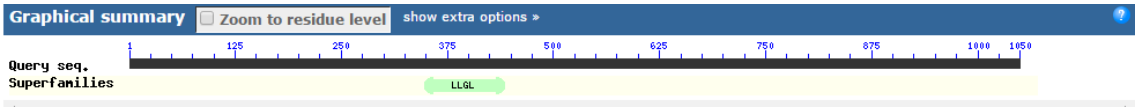

Inhibitors of theHippo pathway

Jub

MSSIKDYTSKNFHPNCIDDIITQYDSLSLSSSETDNITLDSGIYFDSKSDITKQSSNPVSKETL
PPPPPPPYNSCHNIISSILDSPEIDIPFQCENFDNTTSTNKSNLDEKCSTKNLILTQNLPTNFS
GFGNQFSMSRLLAEDKLFQIKENQSNESIDQKPNSVHSNQLINKLNKQSYLMKKLQNHCQSTNN
FAVDTKILGTCNKCQCLITDSEGACIALGNLYHSNCFTCCYCNRSLRGRVFYKDQEKIYCENDY
MVFGFHKSVKVCFACGHIVTETILEALGKDFHPRCFKCSICHKCLDGIPFTVDRNNNIYCIIDY
HNTFAPKCAICLQPIIPRKNSDEVVRIVVNDRDFHVECYRCQNCLRLLSNESNCFVWATDRSET
NIKLLCRKCYVNQIREISRLN

Domains prediction

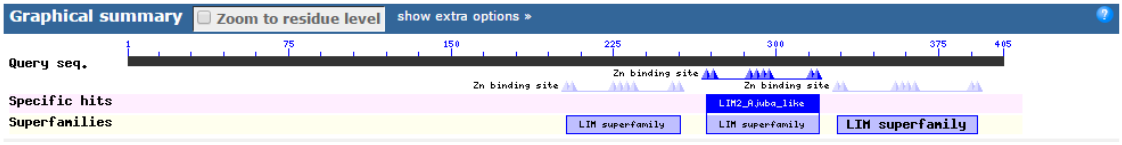

Jub B

MSFNSINGSVLCCQCSGLINKAEDACQAMGMLFHNNCFSCCYCYRQLKGKIFYKDHGKLFCEED
YLYCGFQQSADRCKICGHMITNKILKADGNYYHVDCFRCTICNECLDGAPFTLDKDGKILCIKD
YYLSHSSNCESCNQPIIPEKNSLSTKKVVVLEKEFHFACFQCEECQMNLTIESDSSCYPKYDSV
GNLHLYCRRCFVKSPHISRSLTSSSSSSSLASTNPKKFQSSTKVTSTFR

Domains prediction

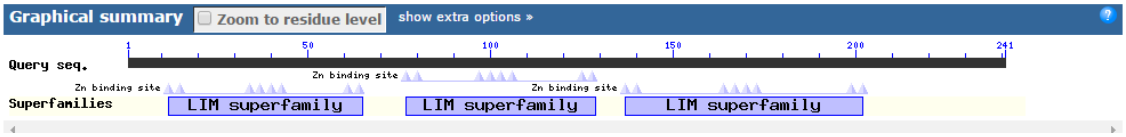

Zyx

MHYNHPFRRVFDLDSAFNERASPRAKLFSDLYGLLDMNQSTFPHSRLYNFTLDARDREPYPLDN
RLSKTNYPKYTDEMTTATLIPVVHLPSNNNSDYSTSTRKSTSFNDPPKSNLSQVRKNSEAEVDA
LTNILIKSIANKTENKDSNPRSYTSSTYLPNQPYSSKRVSNTSSQPAVSTSSNSTTGSISRQSS
LSSNECHRCRKPFELANGKSSVGQINGPLNTVFHQTCFNCYRCEANLNVDSFFYAQKRLLCSRC
VHESLEKCTVCNFIINDRIIRVLGHPYHPKCFTCTVCNCCLDGKAFTVDVHERMFCLEDFHKRY
APRCDACGEPIRPQNGGQENKRIISGDKTFHLECSGITIKN

Domains prediction

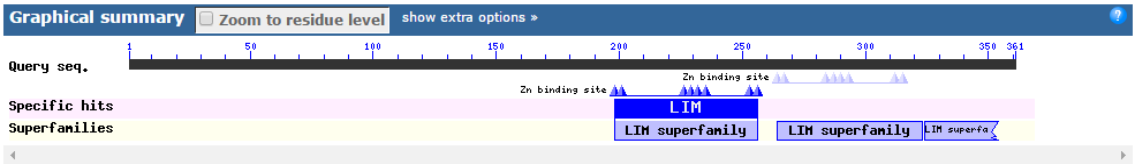

Putative targets of Hippo

Mediator of RNA polymerase II transcription subunit 17

IFDFYLLMNRYKLIAFEPISENEIASYNFEGVENQEKPLNPNEEFIQLTSKIDFKKLNGITLDY
TSPDYQCMDEESEPSETVQLNLTETLKKHITTSLNEINALIDILQVSKDNTYMNLKKIVKESHE
DNVTSYVAAKKMGLAASSSTLLNSAVRLSKTLSSVKDQISQNSFYLDLAILRKEWRIKWFQKNL
IGDLGLQSCGSLFPENGGFQILEMEDDSERSDNSFENDLRSLKIILMNNQEGEPILKVNVKDSS
FPSTVEFKSFQELPEAKTCQSQIEKLNRAQNLLYLHEIFSTLCWESRLLDNPIIVKENRLIVNI
NGVMNLEVDFIILPEKHWFGYKEKETDELLKTRHQNELIIKQHSLLSDALIVFLRELLREKHRS
NSCAHFSLANPIAGPVQIPLNHRYRGTQFYRAIDYSTSERSSVVFLLPLLIDGVIFHKARTDLM
FVLDKISIMPNGSIFVRNHIQLTQSMLNCSVSVVIGCSTYNSLQHFFTLNLSVSKETVYLTIIS
DQLRHDLIYESIDVELLTSFFKNQIWNFKIDVINKLATIKHNWRLIDLRLSNSPNSIKQNDIEI
IVISNDGRWLLSFGGTKNSDSYQLSVKHSQVECQKVTEWKSINLLMFQKKLIKNDLETIDVLLT
AWR

Domains prediction

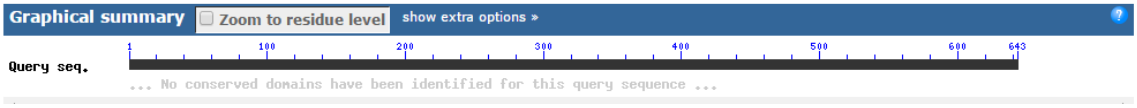

Spondin

SWDAQKENQQKKSQQQYRTQTPTVTGTGSSSQSISSTTTGTTTSRITGCKEKPVLISTEEYVKE
IVVPKNGTSETSLITEIWNTTVIRTEPKFEIKFYKPVIITKIRFENIVNIETFNVLVLYENEKE
YKPFETGLVVTYMKEYEEIEKTVEKVSAIKITFTLSSTKEKVSLKVIIEGCGEKETTTQRSTTI
SISIPTVSSTTESTTTGTTTTGXXXXLQRLDLXXXXTTGTTTTGTTTTGSTSTGNTTTVSSSST
SSESSSSPSTTNGVHTTSSLIGCVEVLRLSTFDYVEKTLEKTFTSSMINFEIPILGRWESWKND
SNPSIQIIFKRNLFITQIELDKTNNIRKYSVFVQYGEKDSWYSIAETNLLNPNSQGTVNVSLLV
SAVKIEIDKENIDESVRAFLLIFGCEKQVISTEPSSISTTTEHTESTPLNVTTVSEQRSTTETT
LTTTQPIKKENCSFVSESKSKIKHLNCVSVEEIEIGHCAGGCPSRSSIDYFTGFVDSKCLCCHP
VKIKKTLRFFCDPGYKSVEVYIISGCQCNSCQQTVIDKCET

Domains prediction

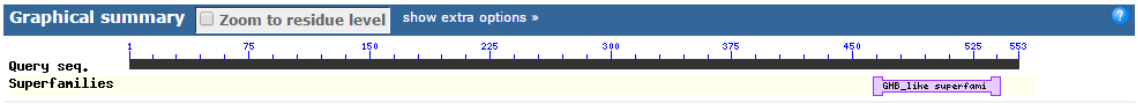

Coiled-coil domain-containing protein 96

IIKIQDKDVNLEEYQDLTKEINENLADEIKKEIPSEEIENQITEDSEDHLSPKTSKEVENFIET
IIDFILEKIFDKKMEQDKTEENEYPSNENFIEYHEVGRIDEAAEPEEIKEDYDSQLNDEEELHH
DENFNANKENEDANEWVEEEKEEEEEEEEEEEEEEEIKLSREELIQELKNAQIEEKSLFEINTS
IQHKIGDFLRKKKVEQTSAAIAEEKGIVDFEQKYNKQMETLRDLIRQYEQENIDFKFRIEELQE
ETKNLEEKVKEDKTKFQNYRFAISQKAINTRTGKPISPKDLEIISLNEEKKETQVVETRLVCIK
LQNEVNKIDSILKSKEELADGLHLIDFEQFKIENQSYNEKLEERTEDLLKLRKKITTNVHILTH
VKEKLEFVKYECDLEQKILKETEEKLSTNRDQLTSLKQNRDRLRSSNQKLKKSCGMLGNSDLLR
NYEDCVDTVEIQKQKMNEMKNKQIKLTLRNQGLQMKIENTRIGSSNG

Domains prediction

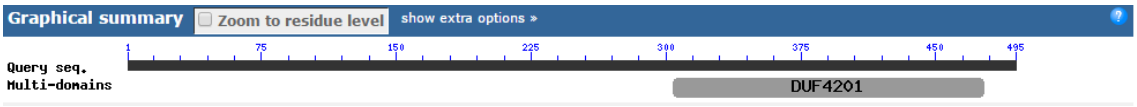

Isoform 2 of Centromere-associated protein E

FHSELSEIITIKHFNENLEVLTKTSLSIYEQLHSCLTRISDVENQLQGVLHDRNDLQIQMRRME
LDHSQILENKDKEFCELKELISEYEFALSNEKLISKNGTDFENSFQQMEHEEPVINYETLPFRK
SKNETEPKIQVQNYVLNKLTDTFSMNTSEIRGDLENDFENSFVNYLQIIKNSIPHQYSIKDMKN
VEIQTDMDLTYLQKLETEITQSLYEWQNLNEFSIANELIPEDFIGNIILYNRAMEIMNDKVIKL
QKDLEIEELQKCEMSDKFEQIITELESACDAEVEKLKLNNEFLKQELEFLKCEREEQNSSMNLL
KNQIFSLQLESTRQNLDFDTNHLIDAAVDTNEGDLSWMSNLNDALKQTISEKEDQVTELMKKLN
ESISKLKEAKLQEESCRLEIQNLNEKLNVICEEIKLKDRSIQDNFEVINELEVICIEKENRVNS
LEKELADINSQLEQYISAVCSMQARLEASKPNIESMLNKIGSRSNNLQLLNLIDQLEKDYADEL
EQSEIAKSKIELKLNKAIQVINKLKKQLKQSHARVLNLNDEIKSLKTPDPFHKILEEKECHIDK
DSTTVDVSTQTNFELDNIALCKEENVDLKGLMENLNVNNFILLRELDKMQNNDRTSRGSSLPPT
STGSLHTGKGFHVGSERSLSPVSQISSNSFDGGDSINLNQIKDLQRKLQRTNQQLNQMRIERNR
IHQEYTRIRQMKEEADQKALELSRLIDSNLNQDDILHEKDQLIEMNNKYSVTIVELKAETEMTN
VRNSILETKCKKMEWKLNNQRRKYDQLILKLDEKEQDIDNISDELRKNLSIFEKERIDWLKERK
ELKLLNKNKDNKIVEFRKKLSNKTNETTENTENDYVIEIEQHKNQISQLKQENKQFLAQHREEI
NKYKGQLEELIDDNKQLKRKLTLDQKDNKMFFVENRVNNPLMHIIDEVSENSDSLWSSNTESNA
ILAKVVLEKEHLLCQLSETEKQLNDEKQKSSEYQFKTSILNESKIVNSISQFTQYEELFSKNNN
NTNLKCGETQTYSSHHPIHQSTETSENYELEKIKQINSIMTKNDVNQNIQTEHNFDKEIINNYR
LALINRLNIHKYPQIECTDLPVKVEIGVQTDPTLNSSTYHVIHQSTETSESYELEIMKQVKSKI
TGKNVNQNIQTEHNFDKKVINDYRSALINRLDIHRFPQIECTNLPVTVDIDVQTDPNKQLQIFY
SKGTQISHSVGIQTVDDELTNELIKEIKMKTKIIEDSSRQIRTLENQMDRINYELNETGKRIAL
LENENLDYQETIGKLQLDSIEVEKKYKQCLGELNLEIGNYKELNDNKNKLVVQSENEESQVNEL
QLADGWDMEWEYEKIANDIQNATQPSDKNVNNLQNSPENCLSKFLIELDHIFNHYSDSSAALAE
IKNLISSYKSAENCDDICNSELSNNSGSVLNLVAILREEITQLKQGLNEKNNEIGHLKCLRNQL
QADLLESGQQIKDSNMEFLNLKENIQAINAEKNMLRQKLEDLEIRFRQFVNFVRMLGVDLRRLR
DSSQIIAESPPDCNVLDEQNVSLVTQSMEHELHKLLEKIYEKDIDLHKSINQIEQMTCALQRLQ
LTQKSQIFTEHNIIDGNPVNSKYNNNLSESNSHEECENFLTELSELLEKKQSEIEELKSRLFLA
TDQLIHFRAFYADPDFKLKSEYLNPNKNISPKWSSFNNEIEDGHHQPHIKVLVESEDDQFSDSD
DQLMVSHAGSTVIKVEKSDRIRTPSSKTLFTRICGQMRNKKILNNIKSAMSADRGSLFFFRSQP
RFNFKTLLTLYIMLIHVLLFHCMSS

Domains prediction

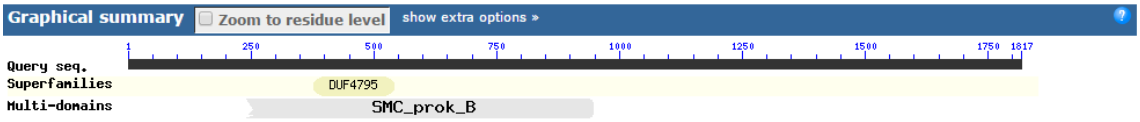

Synaptonemal complex protein 1

KMISVNLIKLCLIFGLTMSMRNIPVGNQNPIALGTXXXXXXXXXXXASLKEYNEKAKKIAMESI
SLNKMNLEYLSNNQEEERERIMNLTSSTYKEKIESDLAKVFEHQHHDLISQLKIKENLDMEKLK
LTQEELLNSQLNDLYLSAVKEILKNSENNKNLEGISAESASELIKNYLDWQQQLQSIKEKEKIR
QLGRLDYIFQKRNNFIKLKENEINDTNEVMEKKNEFFVEMINNLKDREELDGRVCETILLDYEK
YKKDLFKEMDTSRRDQNDKMLSLLNQKRNEKLNDLKNQHDNEIVNLLASHSADNNIKSLSDDLK
NIESKYYEKVLNEENSHDAEGVNEIIKIHNEISTQTKEKLDSEIILXTKSLKSEGVDSGDIRSI
LDSYDKRFKSLKNTQNKERERQLMEMNEKIRKFKENIDKNVEKQINEKDQLFQSENNIVEELIN
IQKTLSEDDRDYILKEYNKHKISTQNSIANSFLEQKRKMEEALALRKAKQLKEIDDKHDLKVEE
LINRKMRVKTKRTQQEIKEESEKELMLDYVNQKLQLSSVGNSKDDLDKELEIIRNELLAERAAL
VKKKEEEYVALILKVQMLKAKESAELKDQEEKIFKLQLAXFDEQ

Domains prediction

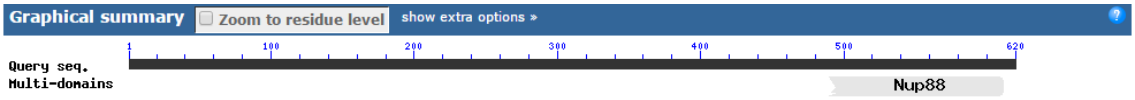

Abnormal spindle-like microcephaly-associated protein

ETKWKNQEPTNENKDKEIEKAVITIQAGFRGYRIRNSLKVRDKAAQRIQAGFRGYQTRRILKQN
NQKKQENDNNKEEAAKRIQAGFRGFKTRKEIKNKEKKNQENAAIKIQAGFRGYKTRKEFVMKVK
SAEKIQAGFRSYKTRKEISEKPVTKPKSLSPEEQAQERNDAAAKIQAAFRGHVYRRDHS

Domains prediction

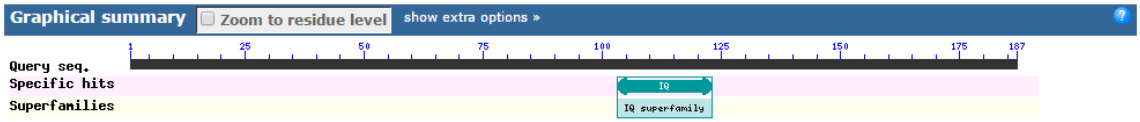

Isoform 3 of Dystonin

RMLNEIKNYEESDIRNTIEEIENQFSLFVNNVQQRSKSLQESLQLAKEFNSKLNELDVWLRKAE
KLLKIKSLPKFQNEADLVELIEKHEFLVKQVKEMKTTMTNFNNIGKVILTNCHPMATNYVNRLI
FKTGSRWNQINSRSEDRSKKLNESLGSLRGSTALIEELIYKVGECLNKIQNEIRIEIPCDMQNV
NDIINKHLIFINELSEIDSQIKSLIKDFKLQNPSSFHKAPTKRYHDRVEFYKNIWRNSKDSLNK
STDDLSTNTRPNFLNTQFNKLWKLSIEHKVALQNHLMDLNEKEQLRRFDFNTWKKDFLTYIKVK
GLRLTDLFRRQQSRRPGYHVLEEFTNCIIKSGFPTNKYLLQQVFNIFNKNNNNEIPYQDFIDSL
RPERRSQVDKNINLNDKKVVTLIIHDIIEKEVAVCTCTLRYYVKREGDNKYRFGQNSKLYMVRY
LNSTVMVRIGGGWQTITEFLKKNDPCRIANSLDLQKSKSMKMSFSTVTKVVKTLKKTDEKPTVK
KSIQYQKASSLSSRIPTGLSKK

Domains prediction

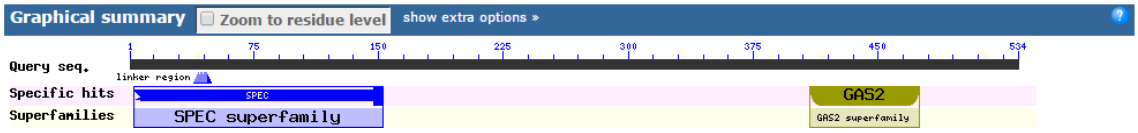

Hypothetical protein

LITSFSISDNLDLKINLIKNFETTSIDQVKMSKFEEIQNQLQIQKTIVTNLMYMNQEFEVKNQI
KKVNLFHEMIKRSIAIFEETSTKINENKTIINKIEKWIINAKSILQTKQNSEHNLKELKINVEN
LFEEFSKLNGEIDIEKFVITSVLSSENVEPFFNILSNNLSNINQLKSEMEIISKDIERRLKQIQ
IEEEIQNKFLENSERFYLFANEINVNIDEFDLQSINNFNQIDTINNKIIEIQKLFENIKETSVK
QINQTKDLQMENDVKLARKKLSELNEKYENLFRYVKKKFIQENFISYSISNTTLFAAERDVKTN
ANKLQTVFDSCNFMAVKSRLLTKDLRISSTSDLYLQIFTENLMRIIQDSCKKIFLKREFSQSSS
FYEMSTHNLRKSKTTNAEFINVINRNREREMAIFNNYLTHQRLSRPPD

Domains prediction

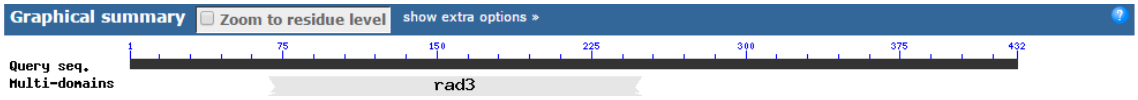

Mucin

TGTTTTGTTTTGTTTTGSTTTGSTTTETTSTGSTTTPSSIVTTTESSATTTQTPTVTGTGSSSQ
SISSTTTGTTTSRITGCKEKPVLISTEEYVKEIVVPKNGTSETSLITEIWNTTVIRTEPKFEIK
FYKPVIITKIRFENIVNIETFNVLVLYENEKEYKPFETGLVVTHMKEYEEIEKTVEKVSAIKIT
FTLSSTKEKVSLKVIIEGCGEKETTTQRSTTISISSPTVSSSSTSSESSSSLSTTSSLIGCVEV
LRLSTFDYVEKTFTSSMINFEIPILGRWESWKNDSNPSIQIIFKRNLFITQIELDKTNNIRKYS
VFVQYGEKDSWYSIAETNLLNPNSQGTVNVSLLVSAVKIEIDKENIDESVRAFLLIFGCEKQVI
STEPSSISTTTEHTESTPLNVTTVSEQRSTTETTLTTTQPIKKENCSFVSESKSKIKHLNCVSV
EEIEIGHCAGGCPSRSSIDYFTGFVDSKCLCCHPVKIKKTLRFFCG

Domains prediction

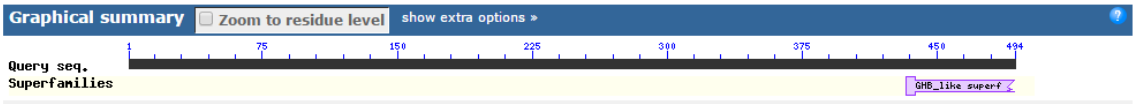

Musashi homolog 2b (Drosophila)

IMTLEIACHDESNSEYETENSSPICNDPGKMFIGGLSPTTSPETMRDYFRKYGDIKEFMIMRDP
VTKRSRXXXXXXXXXXXXXXXXXXXXXXXXXXXXXXXXXXXNCDTSIDCLGINGYSSGKLSDSSLN
NAKTKKVFIGGISTNTTKQELEEYFSQFGILETCELMMDKATSRHRGFGFVTFENEDSAEKVCD
IHFHDLNNKTVEAKKALPKEIIGNNGVLKQRNQWIRTSLPLISNQLQNNYALNALSAIAALLGS
VIHS

Domains prediction

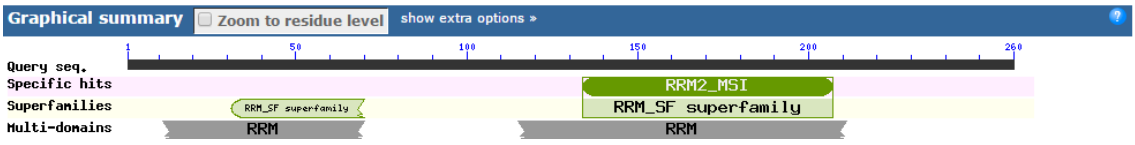

X-ray radiation resistance-associated protein 1

FKMNYLPVRPLIKCNSDDGAWVIAQKADQRKRFKAIICNLKVTEGFNQSNRIKYDHESNANANN
FKFSKEFILENCKTVDPDKIAVINVSFKDLESSEDEFYEFSSVYKIDASSNRLTLDDFITFIPL
IELNLSSNNVRNININPQDFENLEILDLSFNNXCSEDILMLGLLRKLKILNLTGNNLQALPLDM
AHPYMGDDGKAYRKFESLEELHIEYNQLHSSSSFSALGGLPKLRILKLAHNNFESIPMLKCIKL
KTNSNNNQINNYEIDYEEEEEMEDYQNSFFTKNMELRIPSTLHEVEEETTYRTTIDTKSSNEYS
PKIVSKEAKVIKEILDEIIDKIDLQQHQESKDEELEAETEDANSNYRTEINLNAEERNDEEIQP
EFINKSEDFTGTSEKNYFEENNAQVFPSAKKTYILEIKENIEIPINESPSEEDFNDNYQHETFS
EKKETINPNLDELNIDIQSNQSNNLKKNLTEDPEDKINTENTDPFKQEPNFIVIQVKENEINLS
NENKEQSDQKSRSNNNNKIMIDKQNSKIKIPKENNKENDIENSGELIPYQEENEDRNQNKENRI
AKDNEEDSNKFETLETFDEMKWMSLSQDEENSYHSLIIVNDFMKSSSVSDIIRQLSISSFNENS
PKPFPALEFLDLSFNQIKSERVLIPVIAWLNLKMLSIFNNPISMKKSQKSSFIKVLLENTFKIK
VEWLPPISKEKPNPTIKKSKLRVVDTVPNVPLNCRKSNAFHTGLIKTEENELNLPKMMPLPNIL
KQSHPTVHENNSLAIISEMNKPDDDLENDLKEGQSFKLLGRNKTFLMRALQYKIDHPITYFERN
VDLFEKQNSLQSIKKRTYQIDERKMGKSENIVLVLKQQKNRVNQSEMSLDKVLSTEFLTLNRKN
TQESAIASKALKNMQKKYNQVRLESLNKEY

Domains prediction

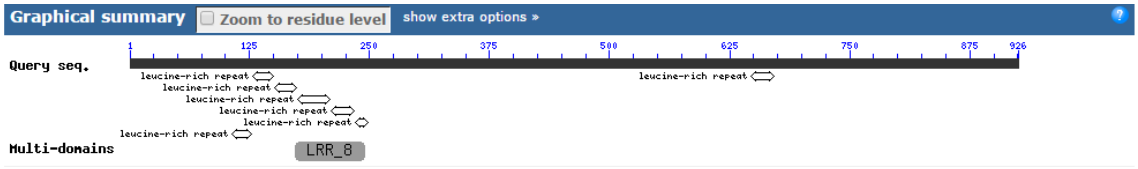

Note: All the domains prediction were made using the tool CDD: NCBI's conserved domain database.

Annex 2

Smed-Blitzschnell is a novel gene that controls cell number in planarians

Introduction

Cell number and cell size are the two main mechanisms by which animals determine their growth. Cell number is determined by the balance between cell proliferation and cell death. When proliferation overtakes cell death, cell number increases and the tissue grow. Cell size increases by the duplication of cellular components without cell division[1,2]. Planarians are flatworms that, due the presence of an adult pluripotent stem cell population, are able to regenerate any missing part and to grow and degrow depending of the environmental conditions and food availability[3–5]. Therefore, the amazing planarian plasticity based in the continuous activation of the signaling cues that coordinate cell turnover coverts plaarians in a perfect model to uderstand tissue growth.

Here, we describe a novel secreted peptide *Smed-Blitzschnell* (for simplicity, *bs*), which controls the total cell number during planarian homeostasis. *bs* encodes a polypeptide of 156Aa with a predicted molecular weight of 17,69 kDa. This peptide shows a signal peptide, suggesting that it could be secreted. A homologous is found in *S. Polychroa*, but not in more distant planarian species neither in other animals.[6].

Results

bs controls planarian cell turnover

To decipher the possible function of *bs* during homeostatic cell renewal in planarians, we proceed to inhibition of *bs* through *(RNAi)* during three consecutive weeks (Figure A2.1a). After this time, we observed that *bs (RNAi)* animals show overgrowths mainly around the body margin (Figure A2.1b). To analyze the possible role of *bs* in the control of cell death and cell proliferation we performed TUNEL and quantified the mitotic activity through anti-pH3 immunostaining (H3P) at three weeks of inhibition. Our results show that the inhibition of *bs* results in a a decrease in cell death and a significant increase of mitotic activity (Figure A2.1c-d). Thus, *bs* inhibition results in less apoptotic cells and more mitotic activity. Then, we checked whether the unbalance between cell death and mitotic activity results in an increase in body size or in cell number. Measurement of the body area shows no difference between *bs (RNAi)* planarians and controls (Figure A2.1e). Quantification of the total number of cells using a Neubaeur chamber shows that *bs (RNAi)* animals have more cells than control animals (Figure A2.1f). This result is also confirmed by the increase in the epidermal cell density observed in the *bs (RNAi)* animals (Figure A2.1g).

Altogether our results demonstrate that *bs* is essential for the control of cell number in planarians. Its inhibition results in an increase in cell number and cell density which is translated in the appearance of overgrowths in the marginal part of planarians body.

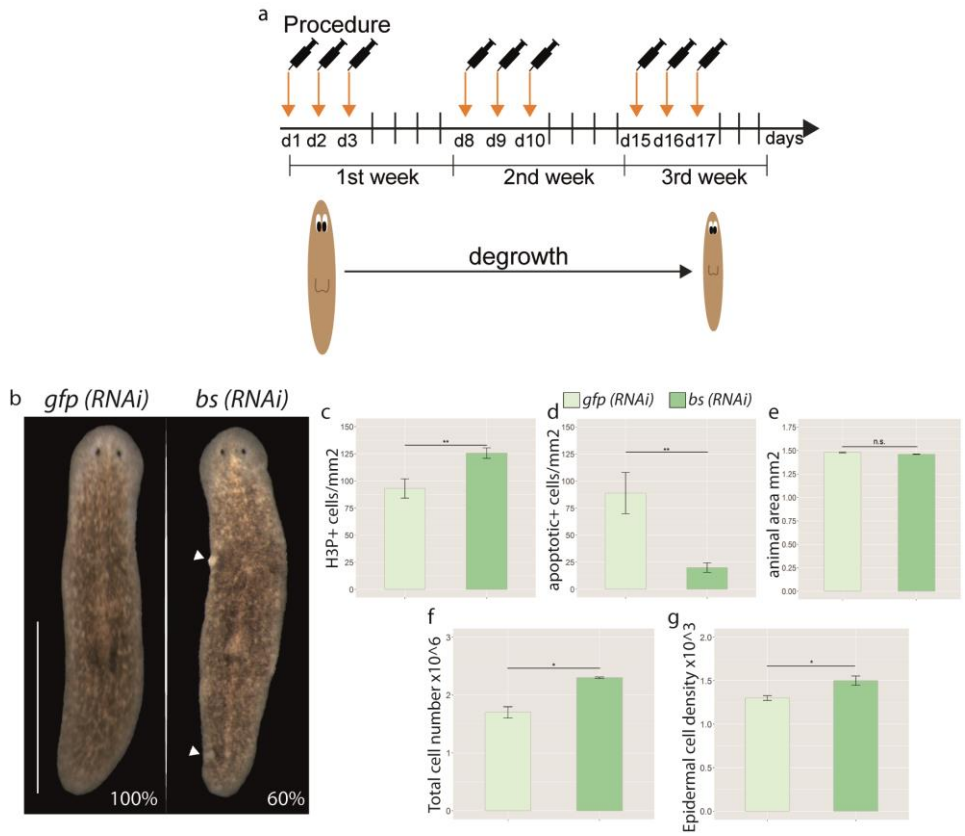

Figure A2.1: bs inhibition disrupts cell turnover leading to overgrowths.

(a) Cartoon illustrating the experimental design during planarians homeostasis. Animals were starved one week before start the experiment, and then were injected during three consecutive days during two or three weeks. During the experiment animals were maintained in starving conditions. **(b)** Stereomicroscopic view of control and *bs (RNAi)* animals. White arrows indicate overgrowths. Scale bar: 1mm. **(c)** Quantification of mitotic cells (H3P+) (n≥10). **(d)** Quantification of apoptotic cells (TUNEL+) (n≥5). **(e)** Area quantification *bs (RNAi)* animals respect to the controls (n≥5) **(f)** Graph showing the total cell number of *bs (RNAi)* animals analyzed in a Neubaeur camber. Three biological replicates were analyzed for each condition. **(g)** Quantification of epidermal cell density. All the experiments were performed in three weeks *bs (RNAi)* animals. Error bars represent standard deviation. Data was analyzed by Student's t-test. *p<0.05; **p<0.01; n.s.: not significant.

Bs controls the number of differentiated cells in planarians

To understand whether the increase in cell number observed in *bs (RNAi)* animals is translated to an increase in the number of differentiated cells we quantified the number of epidermal cells (*vim*+) and octopaminergic neurons (*tbh*+). Epidermal precursors migrate from the inner parenchyma towards the epidermis[7], thus the *vim*+ found in the epidermal layer but not the ones in the mesenchyme are totally differentiated. We quantified both, *vim*+ cells in the mesenchyme and in the epidermis in *gfp* and *bs (RNAi)* animals. Our results demonstrate that the inhibition of *bs* increases the number of *vim*+ cells in both compartments, mesenchyme and epidermis (Figure A2.2a-b). *bs (RNAi)* animals also present an increase in the number of octopaminergic neurons (Figure A2.2c).

Overall our results demonstrate that *bs (RNAi)* animals exhibit an increase in the number of differentiated cells.

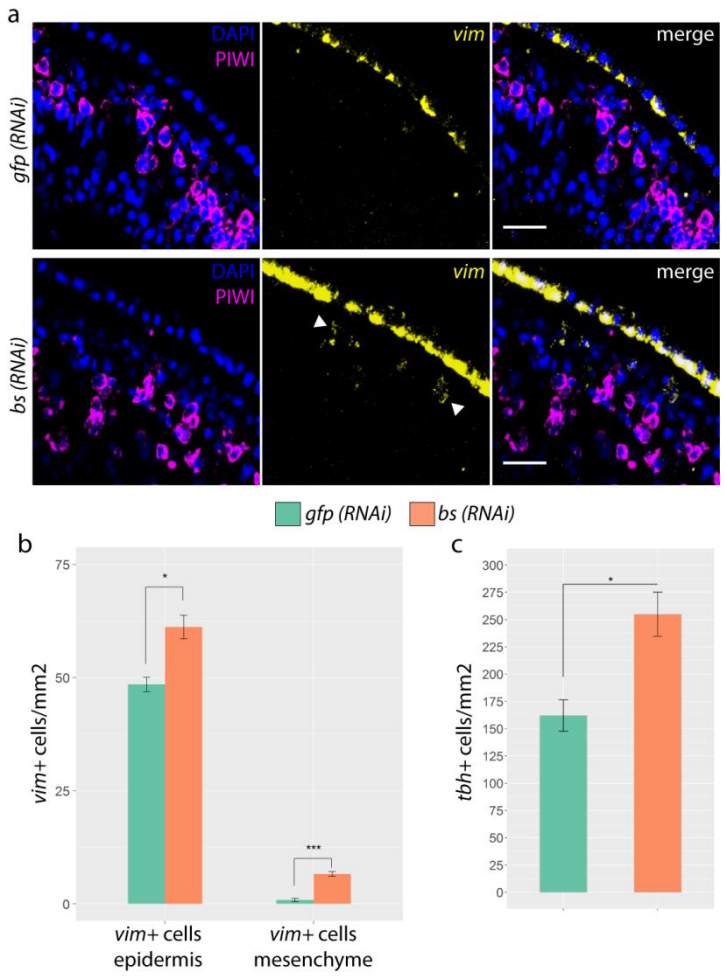

Figure A2.2: Inhibition of *bs* increases differentiated cells.

(a) FISH of *vim* combined with immunostaining of PIWI. White arrows indicate *vim*+ cells in the mesenchyme. Scale bar: 25 µm. **(b)** Quantification of *vim*+ cells in the mesenchyme and in the epidermis. **(c)** Quantification of octopaminergic neuros labeled with *tbh* by FISH. Error bars represent standard deviation. Data was analyzed by Student's t-test. *p<0.05; ***p<0.001.

Discussion

Cell turnover is a complex mechanism based on three integral processes: (a) the elimination of selected differentiated cells by cell death, that could be through apoptosis or autophagy; (b) the replacement of eliminated cells through cell division, typically involving adult stem cells and their descendants; and (c) the differentiation of newly generated cells and their integration with preexisting tissue[5,8–10]. In the present study we present *bs* as a novel peptide that controls cell turnover in planarians. Cell turnover disruption through the inhibition of *bs* results in the increase of cell number but not to the increase in the animal's size. Thus, *bs* inhibition leads to an increase in cell density that has as consequence the formation of overgrowths, located in the marginal part of the animals. The increase in total cell number is translated to an increase of differentiated cells, suggesting that *bs (RNAi)* animals is not playing any role in the differentiation process. Maybe for that reason, these overgrowths are not lethal, contrary to the phenotype observed with other genes that promote the appearance of overgrowths[11].

To conclude, we have found a novel peptide, only present in some planarian species, which controls the balance between cell death and cell proliferation, thus ensuring the proper cell number, without affecting cell differentiation. Further studies are required to understand the biological significance of this finding in the context of evolution, regeneration and cancer.

Materials and methods

Planarian culture

Asexual planarians from a clonal strain of *S. mediterranea* BCN-10 were maintained at 20ºC in artificial water as described[12]. Animals were fed with veal liver and starved for at least 1 week before starting the experiments.

RNA interference analysis

dsRNA was synthetized by in vitro transcription (Roche) and microinjection performed as previously described[13], following the standard protocol of 3x32nl injection of dsRNA for three consecutive days. To achieve a stronger inhibition for *bs*, we performed the same protocol during three consecutive weeks in starved planarians.

Whole-mount in situ hybridization and immunohistochemistry

RNA probes were synthesized in vitro using Sp6 or T7 polymerase (Roche) and DIG-, FITC- or DNP-modified (Perkin Elmer) nucleotides. RNA probes were purified and precipitated with ethanol and 7.5 M ammonium acetate. For ISH and FISH, animals were fixed and processed as previously described[14,15]. After probe development, neoblasts were visualized with the rabbit anti-SMEDWI-1 antibody (kindly provided by Kerstin Bartscherer, Max Plank Institute for Molecular Biomedicine, Münster, Germany; 1:1000)[16]. Nuclei were stained with Dapi (1:5000) and mounted with 70% glycerol in PBS.

Cell counting using Neubaeur Chamber

Planarians were dissociated as described[17]. 10µl of planarians dissociation were loaded in the Neubaeur chamber. Using a microscope several squares were counted and then normalized. Three biological replicates were used, each composed by five planarians.

Whole-mount immunostaining

Immunostaining was performed as described[18]. The following antibodies were used: rabbit anti-phospho-histone-H3-Ser10 (anti-H3P) (1:500; Cell Signaling Technology); rabbit anti-SMEDWI-1 antibody (1:1000). Nuclei were stained with Dapi (1:5000) and mounted with 70% glycerol in PBS.

Whole-mount TUNEL

For TUNEL analysis, animals were fixed and treated as described[8] using the ApopTag Red in Situ Apoptosis Detection Kit (Merck-Millipore Ref.S7165).

Imaging

FISH and immunostaining samples were imaged using a MZ16F stereomicroscope (Leica) equipped with a ProgRes C3 camera (Jenoptik) or an SP2 confocal laser-scanning microscope (Leica). Images were processed using Fiji and Photoshop CS5 (Adobe) software. Brightness/contrast and color balance adjustments were always applied to the entire image.

References

1. Goss, R. J. Hypertrophy versus hyperplasia. Science **153**, 1615–20 (1966).
2. Jopling, C., Boue, S. & Izpisua Belmonte, J. C. Dedifferentiation, transdifferentiation and reprogramming: three routes to regeneration. Nat. Rev. Mol. Cell Biol. **12**, 79–89 (2011).
3. Saló, E. The power of regeneration and the stem-cell kingdom: Freshwater planarians (Platyhelminthes). BioEssays **28**, 546–559 (2006).
4. Reddien, P. W. & Alvarado, A. S. Fundamentals of Planarian Regeneration. Annu. Rev. Cell Dev. Biol. **20**, 725–757 (2004).
5. Baguñá, J. & Romero, R. Quantitative analysis of cell types during growth, degrowth and regeneration in the planarians Dugesia mediterranea and Dugesia tigrina. Hydrobiologia **84**, 181–194 (1981).
6. E Pascual, N Sousa, M Marin, E. S. & T. A. Cell number regulation in Planarians. Prep. (2017).
7. Eisenhoffer, G. T., Kang, H. & Alvarado, A. S. Molecular Analysis of Stem Cells and Their Descendants during Cell Turnover and Regeneration in the Planarian Schmidtea mediterranea. Cell Stem Cell **3**, 327–339 (2008).
8. Pellettieri, J. & Sánchez Alvarado, A. Cell turnover and adult tissue homeostasis: from humans to planarians. Annu. Rev. Genet. **41**, 83–105 (2007).
9. González-Estévez, C. & Saló, E. Autophagy and apoptosis in planarians. Apoptosis **15**, 279–292 (2010).
10. Baguñà, J. Mitosis in the Intact and Regenerating Planarian Dugesia mediterranea n. sp. J. Exp. Zool. **195**, 53–64 (1976).
11. González-Estévez, C. et al. SMG-1 and mTORC1 act antagonistically to regulate response to injury and growth in planarians. PLoS Genet. **8**, (2012).
12. Cebrià, F. & Newmark, P. a. Planarian homologs of netrin and netrin receptor are required for proper regeneration of the central nervous system and the maintenance of nervous system architecture. Development **132**, 3691–3703 (2005).
13. Sanchez Alvarado, A. & Newmark, P. A. Double-stranded RNA specifically disrupts gene expression during planarian regeneration. Dev. Biol. **96**, 5049–5054 (1999).
14. Currie, K. W. et al. HOX gene complement and expression in the planarian Schmidtea mediterranea. Evodevo **7**, 1–23 (2016).
15. King, R. S. & Newmark, P. A. In situ hybridization protocol for enhanced detection of gene expression in the planarian Schmidtea mediterranea. BMC Dev. Biol. **13**, 1–32 (2013).
16. Guo, T., Peters, A. H. F. M. & Newmark, P. A. A bruno-like Gene Is Required for Stem Cell Maintenance in Planarians. Dev. Cell **11**, 159–169 (2006).
17. Moritz, S. et al. Heterogeneity of planarian stem cells in the S/G2/M phase. Int. J. Dev. Biol. **56**, 117–125 (2012).
18. Ross, K. G. et al. Novel monoclonal antibodies to study tissue regeneration in planarians. BMC Dev. Biol. **15**, 2 (2015).

Annex 3

Transcriptomic analysis of Planarians under 8g and simulated μg demonstrates that alteration of gravity induces genomic alterations and facilitates tumoral transformation

Nídia de Sousa[1], Gustavo Rodriguez-Estevez[2,3], Emili Saló[1], Teresa Adell[1], Jack J.W.A. van Loon[4] & Gennaro Auletta[5,6]

[1] Department of Genetics, Microbiology and Statistics. Institute of Biomedicine, University of Barcelona (IBUB), Barcelona, Spain.

[2] CNAG-CRG, Centre for Genomic Regulation (CRG), Barcelona Institute of Science and Technology (BIST), Barcelona, Spain

[3] Universitat Pompeu Fabra (UPF), Barcelona, Spain

[4] DESC (Dutch Experiment Support Center), Dept. Oral and Maxillofacial Surgery / Oral Pathology, VU University Medical Center & Academic Centre for Dentistry Amsterdam (ACTA), Gustav Mahlerlaan 3004, 1081 LA Amsterdam, The Netherlands.

[5] Pontifical Gregorian University, Piazza della Pilotta 4, 00187 Roma, Italy

[6] University of Cassino, Via Zamosch, 43, 03043 Cassino (FR), Italy

Introduction

Earth gravity is a constant parameter in living organisms which has had to be an essential environmental parameter along evolution. Accordingly, microgravity has been shown to alter the structure of cells, as well as their apoptotic and mitotic responses[1]. However, the cellular effects of microgravity and hypergravity are poorly understood. With the increase of Human activity of humans in the Space the precise influence of sustained changes in gravity needs to be addressed.

Planarians are flatworms with the ability to change their size depending of food availability or environmental conditions and to regenerate any missing body part in few days[2,3]. This amazing characteristic is due their population of adult stem cells – called neoblasts – which can give rise to any planarian cell type[4,5]. Planarians plasticity converts them in an ideal system to investigate the action of gravity in cell behaviour in an '*in vivo*' context being more informative than *in vitro* cell culture. The objective of the present study was to analyse the changes in the transcriptome during planarians regeneration due to the alteration of gravity forces.

Results and Discussion

Quality check and Mapping

Sequences were produced in different steps since the requested amount of reads was not reached in a single run. The quality was extremely good indicating that the rate of erroneous base call is very low. Raw sequences were also scanned for presence of contamination from rRNA by using riboPicker. The amount of putative rRNA was very low. Filtered reads were mapped to the reference transcriptome by using bowtie2. Alignments were fed to the Express program for the estimation of read effectively mapping to a given transcript (Table A3.1).

Table A3.1: Estimated number of fragments within transcripts calculated by Express

Sample	Effective fragments from express
Cont 8g 13d_1	31,042,667
Cont 8g 13d _2	34,362,055
Cont 8g 6d _1	29,081,210
Cont 8g 6d _2	29,675,276
Cont µg 13d _1	29,571,618
Cont µg 13d _2	29,647,290
Cont µg 6d _1	30,083,239
Cont µg 6d _2	26,693,556
8g 13d _1	34,845,858
8g 13d _2	33,896,332
8g 6d _1	34,840,003
8g 6d _2	35,269,747
µg 13d _1	32,549,792
µg 13d _2	37,708,629
µg 6d _1	34,482,939
µg 6d _2	32,219,794

Differential expression analysis

Effective read counts were rounded and fed to the DESeq2 pipeline and log2transformed after normalization for total number of mapped tags. The distance between samples was calculated by using the Pearson correlation (Figure A3.1). As shown the two main groups are present depending from the stage of planarians (6 days and 13 days). We also observed that within the 6 days group the biological replicates fall within the same cluster (PL5_1 and PL5_2, PH5_1 and PH5_2 and a single cluster for the 4 controls). Two main groups related to the day of treatments can be observed as indicated also from the dendrogram the presence of a sample far from the others (PL_1) (Figure A3.2). The fold change between the treatments and the controls was calculated and estimated an adjusted p-value by using the DESeq2 pipeline. Table A3.2 shows the number of genes found to overcome the indicated adjusted p-value (padj) threshold when comparing the treatment against the corresponding control.

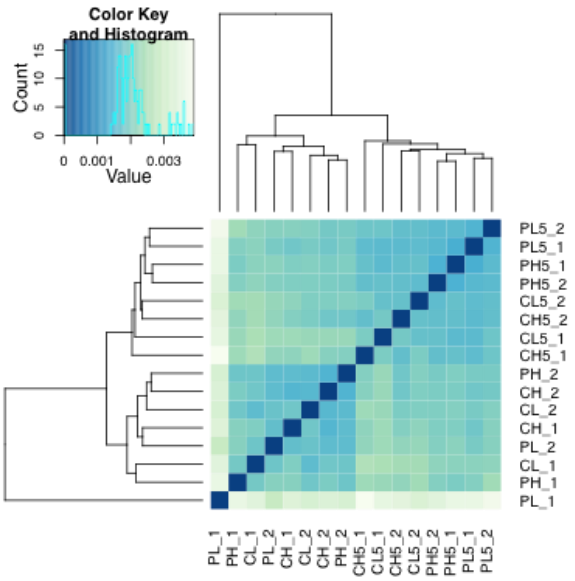

Figure A3.1: Distance between different samples

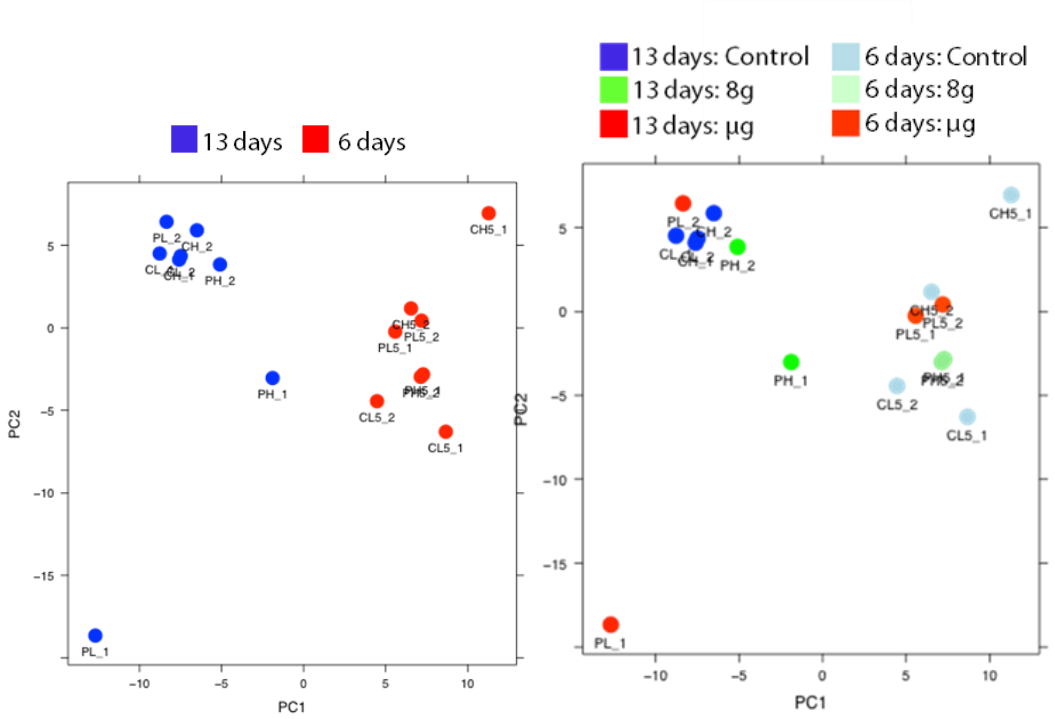

Figure A3.2: PCA Analysis of sample replicates. On the left the colour code indicates different days of treatment, while on the right, the colours indicate also the kind of treatment.

Results show that at 6 days of experiment in the simulated conditions there are almost no differences between samples (Table A3.2 and A3.3). This result agrees with our previous observations[1], in which we found correct regeneration of the structures and no changes in proliferation levels at early stage. Conversely, at 13 days there are high genetic differences (Table A3.2 and A3.3). Moreover, at simulated µg there are much more differences than at 8g.

We observed that at simulated µg there are up-regulated genes related with ribosomal activity and transcription/translation of proteins, as well as mitochondrial proteins. In the same conditions, genes related with ECM (morphogenesis, cell differentiation), actin cytoskeleton (cell migration, proliferation), and transposable

elements are down-regulated. We observe also less Piwi proteins (related with proliferation). It is interesting to note that when ribosome biogenesis is upgraded, the amount of ribosomes available to the cell increases, and therefore the translational capacity of the cell is increased dramatically. For that reason, this feature is a hallmark of cancer cells, which are able to maintain much higher proliferation rates[6,7]. Thus, our results suggest that at simulated µg cells are prepared to proliferate more, and eventually predisposed to cancer, which is an essential observation regarding human missions. Surprisingly, at this stage we do not see higher proliferative rates in planarians[1]. It could be explained by different reasons: 1- we have stopped the experiment at day 13, and a longer exposure would be necessary to increase mitotic rates; and/or 2- planarians are very resistant to tumorogenesis and even more during regeneration[8], because of their plasticity.

Table A3.2: Number of genes Down-regulated (padj<=0.05) and Up-regulated (padj<0.05).

	Down-regulated (padj<0.05)	**Up-regulated (padj<0.05)**
8g_d13	60	31
8g_d6	11	2
µg_d13	348	372
µg_d6	2	2

Table A3.3: Summary of the number of genes found, and the main classes.

Gs	Days of experiment	Down-regulated	Up-regulated
8g	**13d**	**45** genes, **15** unknown Metabolic process Mitotic cycle	**21** genes, **10** unknown Cellular processes
	6d	**11** genes	**2** genes Pair rule-like
µg	**13d**	**348** genes Cellular process Cellular response Cell organization ECM Cell contact	**372** genes Ribosome biogenesis Mitocondrial DNA and RNA binding Transcription
	6d	**2** genes DNA repair protein RAD50	**2** genes Pair rule-like

At 8g there are few genes up-regulated and, interestingly, many of them cannot be annotated to any known class. There are also very few genes down-regulated, which are related to microtubules, cell communication (slit, JNK) and cell cycle. Finally, Dynein, which is a protein required for axonal transport and is involved in neurodegenerative diseases as Alzheimer, is found significantly down regulated in simulated µg and at 8g.

Taking into account that at the end of the experiment planarians appeared completely regenerated[1], it should be considered that some of the up- and down- regulated

genes found in the transcriptome could be the result of a compensatory response of planarians in order to regenerate properly even under such strong inputs.

Validation of candidate genes found in the differential expression analysis

A second simulation was performed in order to validate the results of the transcriptome. For that aim, head fragments which must regenerate the rest of the body were loaded in the same conditions than in the previous experiment. In this experiment head, and not trunk fragments were included, with the aim to increase the differences between conditions, since head fragments are smaller and regeneration is more challenging. At 6 at 13 days regenerated animals were fixed for *'in situ'* hybridization analysis, in order to analyse the levels of expression of selected candidate genes from the transcriptome. Five candidate genes were selected from the group of genes down-regulated in simulated µg with respect to 1g at 13 days of the simulation (Table A3.4).

Table A3.4: Candidate genes selected for the validation

µg_13d_vs_ctrl_13d_padj0.05_down	**Result**
>lcl|dd_Smed_v4_840_0_1 collagen alpha	Down-regulated
>OX_Smed_1.0.02247 ADAMTS-like protein 1	Not differentially regulated
>OX_Smed_1.0.12860 antigen ki-67	Not detected
>OX_Smed_1.0.03172 piwi-2 smed	Down-regulated
>OX_Smed_1.0.13125 piwi-like protein 1 smed	Down-regulated

In situ results show that out of the 5 genes analysed, 3 appear down-regulated in µg (collagen and 2 Piwi genes) and behave as predicted from the transcriptomic analysis (Figure A3.3). One of them (ADAM) was not found differentially regulated with this methodology and another (KI-67) was not detected, probably due to its low levels of

expression. This result could be explained by the poor sensitivity of the 'in situ' with respect to the transcriptomic approach.

These results demonstrate the validity of our experimental approach. Moreover, the finding that Piwi genes are down-regulated indicates that the population of neoblasts and their progenitors, which are the planarian stem cells that underlie their regenerative properties, are somehow affected, although mitotic activity is found not altered in simulated µg.

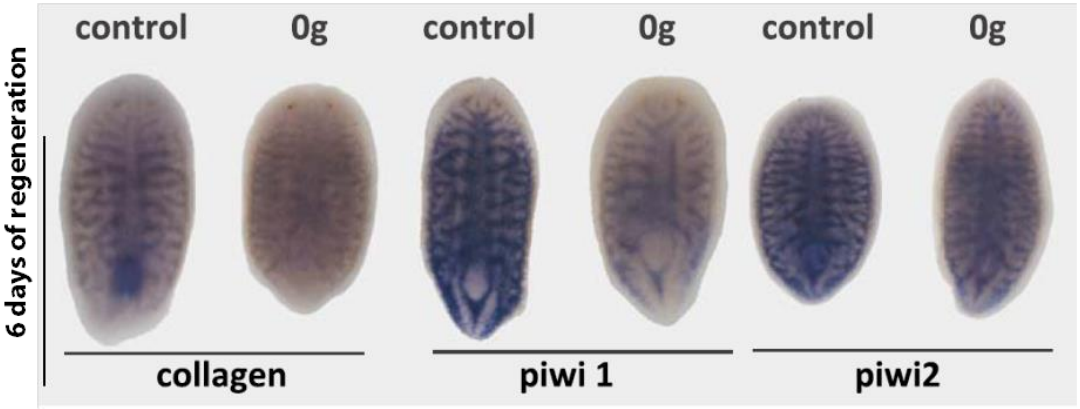

Figure A3.3: In situ hybridization showing the expression pattern and levels of some candidate genes at 6 days of regeneration. Scale bar: 0,5mm.

Effect of hippo suppression in simulated µg and 8g treated planarians

Although in previous experiments we did not observe a great effect of hypo- or hyper-gravity in proliferation in planarians[1], in our transcriptomic data the expression of metabolic and ribosintesis genes is up-regulated under simulated µg conditions. Since metabolic reprogramming has been recognized as one of the ten cancer hallmarks[9], these data suggests that alteration of microgravity could facilitate the tumour transformation. To test this hypothesis, in the simulation experiment presented in the above section, we included uninjured planarians in which the Hippo pathway had

been previously silenced by RNAi. It is well described the role of Hippo pathway in the control of cell proliferation according to cell-cell contact (an underlying mechanism of tumoral transformation)[10]. The inhibition of Hippo pathway induces overgrowths in model organisms as mouse and *Drosophila*[10,11] and is found down-regulated in several human cancers[12]. Results from our laboratory indicate that this signalling pathway also induces tumoral transformation in planarians[13].

In this experiment we analysed the tumorous formation and the proliferative rates in control (*gfp* dsRNA injected) and *hippo* (*hippo* dsRNA injected) planarians which were maintained during 13 days in simulated µg and 8g conditions. The respective controls at 1 g were also included. Our results show that at 13 days planarians showed the phenotype observed in our laboratory (at 1g) after silencing *hippo*, which is appearance of regions of undifferentiated cells and formation of small overgrowths in the strongest phenotypes (data not shown). These effects are due to the uncontrolled proliferation accompanied by an impairment of cell differentiation, which are cellular mechanisms underlying the tumoral transformation[13]. A quantification of mitotic activity by anti-pH3 immunostaining (H3P) showed that, as observed in previous simulations, planarians at 8g show a significant increase of the mitotic activity with respect to their control[1]. However, planarians in simulated µg show a mitotic activity comparable to controls[1]. Moreover, *hippo (RNAi)* animals at 1g show an increase of the mitotic activity with respect to the *gfp (RNAi)* (control) planarians, according to the role of Hippo as a tumour suppressor. The most important result observed was that when *hippo* was silenced in animals at simulated µg or 8g, proliferation was increased with respect to the *hippo (RNAi)* animals maintained at 1g (Figure A3.4). This result demonstrates that maintenance of planarians in sustained hypo-or hyper-gravity conditions sensitize cells in front of a situation of uncontrolled proliferation and growth.

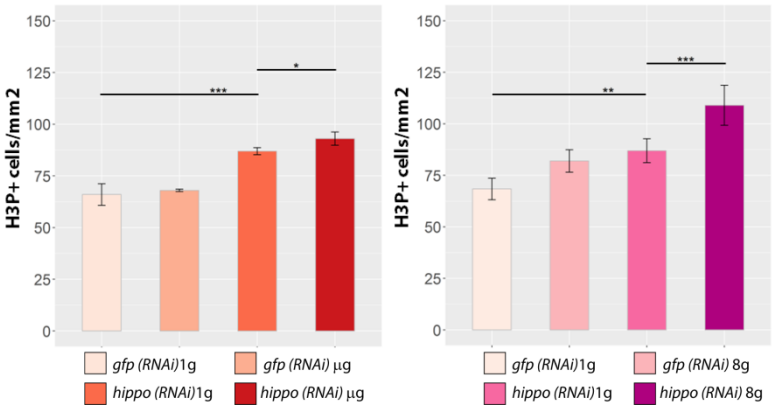

Figure A3.4. Quantification of pH3 in simulated hypo- and hyper- gravity when the Hippo pathway is silenced.

Conclusions

The general conclusions of the present study are:

At simulated µg using RPM, which allows apparently perfect regeneration of animals, several genetic alterations are shown, which demonstrates the potential of transcriptomic approaches.

This observation is essential for space missions. Apparently organisms behave perfectly, but they show important genetic alterations that may cause after longer exposures several diseases, for instances cancer, since we see a clear up-regulation of ribosomes biosynthesis, and neurodegeneration, since the axonal transport mechanisms seem affected.

At 8g, which is 8 times more gravity than we have on Earth, planarians also regenerate correctly. They show genetic alterations at 13 days, although not so many as planarians at simulated µg.

At simulated µg we find down-regulation of cytoskeleton and matrix proteins, as reported in several studies from other animal species. However, at 8g we do not find significant alteration of cytoskeleton or matrix proteins. This is surprising, since one could hypothesize that supporting higher forces requires strength of the cell cytoskeleton to maintain the shape.

Our results demonstrate that the data obtained is reliable, since we have been able to validate the down-regulation of several candidates found in the transcriptome in samples from an independent simulation (6 days regenerating head fragments)

Taking into account that genetic alterations are much higher at simulated µg than 8g, and that those alterations appear after long exposures, our results suggest that astronauts should be careful when planning long stages at low gravity, which is usual, but not so much to the high gravity suffered during short periods, for instances when taking off.

Alteration of the proliferative response after Hippo pathway inhibition is increased in simulated hypo- and hyper-gravity with respect to 1g, suggesting that gravity alteration could facilitate tumorous transformation of cells.

We want to stress again that the microgravity in these studies was provided by simulation using the Random Positioning Machine. The effects reported should be confirmed under real microgravity conditions.

Material and Methods

Simulations were performed in ESTEC (ESA). Planarians were loaded in the Random Positioning Machine (RPM) to simulate µg, or in the Large Diameter Centrifuge (LDC) to simulate hypergravity (8g). Control planarians at 1g were also loaded for each condition. For the transcriptomic analysis, one day after loading, heads and tails were amputated and trunk fragments were re-loaded in the same devices (Figure A3.5 and A3.6). At 6 and 13 days after loading (5 and 12 days of regeneration), RNA was extracted with in Trizol (Figure AIII5). Three 50 ml falcons with 10 planarians each were analysed in each condition.

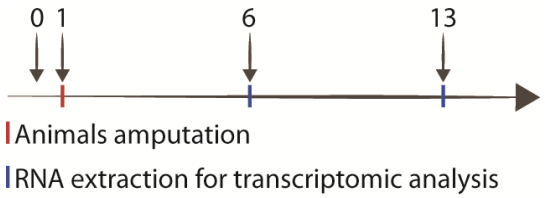

Figure A3.5: Graphical representation of the experiment

Four different conditions
. Control simulated µg
. Simulated µg
. Control 8g
. 8g

RNA was sequenced in the Genomics Unit of 'Centre de Regulació Genòmica' CRG and analyzed in the Bioinformatics Unit of the CRG and the Centro Nacional de Análisis Genómico (CNAG). Since no reference genome was available for *S. mediterranea* species, the comprehensive transcriptome recently published was used (http://www.biomedcentral.com/content/supplementary/1471-2164-14-797-s2.zip). Table A3.5 shows some information about the samples.

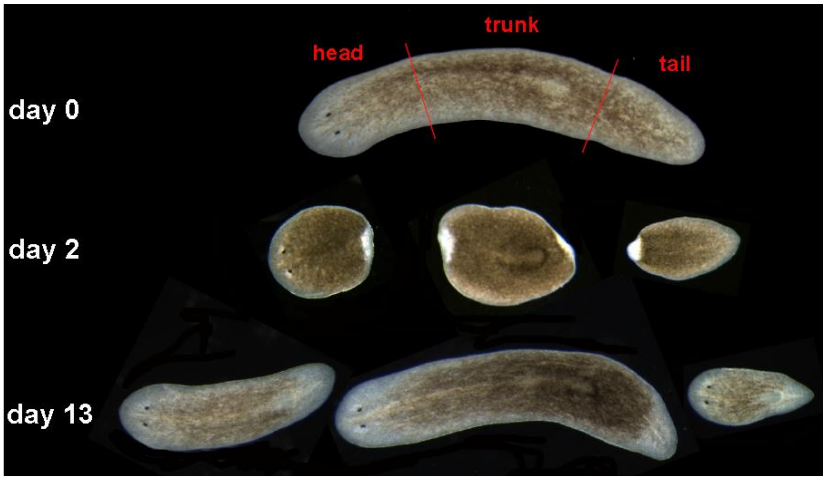

Figure A3.6: Live images of planarians before and after the amputation.

Table A3.5: Input data summary

Feature	Value
Reads length	50
Single-End? Paired-End	Single
Directional	Yes
Di-multiplexed	No
Replicates	Yes
Species	*S. mediterranea*

Original reads were tested for the presence of rRNAs by using the program riboPicker after the standard quality control performed at Genomics Unit by using FastQC tool. Then, reads were mapped to the reference transcriptome using bowtie2 adapting the parameters for mapping to the transcriptome as indicated by the authors of the method we used for processing the mapping data: http://bio.math.berkeley.edu/eXpress/faq.html. Finally, aligned reads were evaluated

and assigned to each transcript by Express (Figure A3.7 represents an overview of the protocol used for the whole analysis is shown).

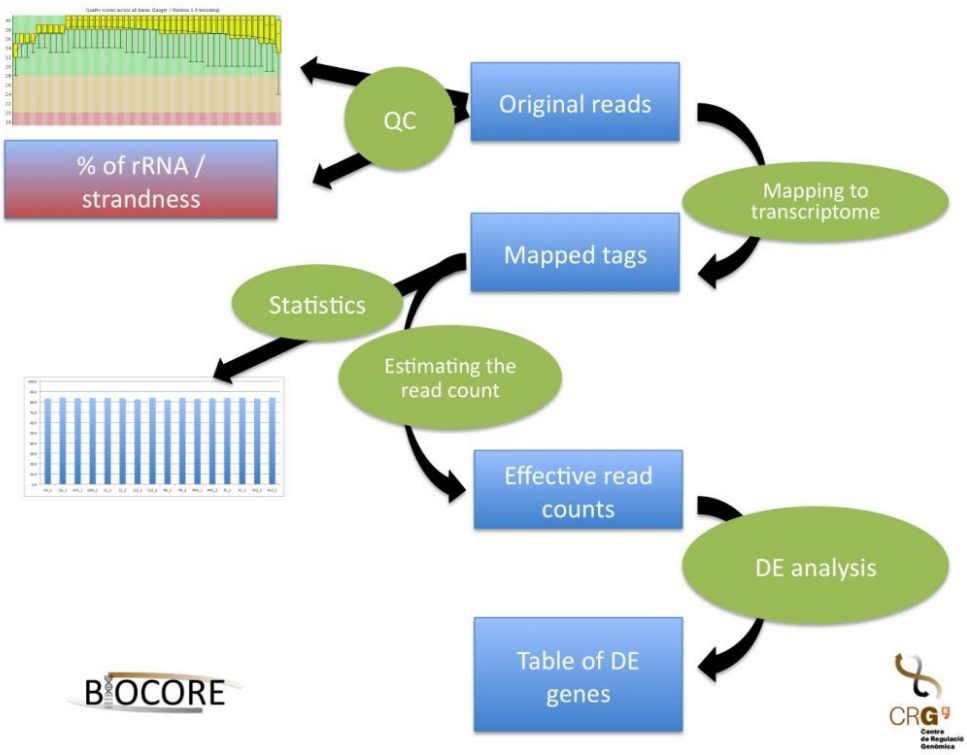

Figure A3.7: Flow charts explaining how small ncRNA reads were aligned to a reference genome.

References

1. Adell, T., Saló, E., Van Loon, J. J. W. A. & Auletta, G. Planarians Sense Simulated Microgravity and Hypergravity. Biomed Res. Int. 2014, (2014).
2. Adell, T., Cebrià, F. & Saló, E. Gradients in planarian regeneration and homeostasis. Cold Spring Harb. Perspect. Biol. **2**, 1–13 (2010).
3. Salo, E. et al. Planarian regeneration: achievements and future directions after 20 years of research. Int. J. Dev. Biol. **53**, 1317–1327 (2009).
4. Reddien, P. W. & Alvarado, A. S. Fundamentals of Planarian Regeneration. Annu. Rev. Cell Dev. Biol. **20**, 725–757 (2004).
5. Saló, E. The power of regeneration and the stem-cell kingdom: Freshwater planarians (Platyhelminthes). BioEssays **28**, 546–559 (2006).
6. Ruggero, D. & Pandolfi, P. P. Does the ribosome translate cancer? Nat. Rev. Cancer **3**, 179–192 (2003).
7. van Sluis, M. & McStay, B. Ribosome biogenesis: Achilles heel of cancer? Genes Cancer **5**, 152–3 (2014).
8. Beane, N. O. and W. Regeneration : The Origin of Cancer or a Possible Cure ? Semin. Cell Dev. Biol. **20**, 557–564 (2009).
9. Hanahan, D. & Weinberg, R. A. Hallmarks of cancer: The next generation. Cell **144**, 646–674 (2011).
10. Yu, F. X., Zhao, B. & Guan, K. L. Hippo Pathway in Organ Size Control, Tissue Homeostasis, and Cancer. Cell **163**, 811–828 (2015).
11. Irvine, K. D. & Harvey, K. F. Control of Organ Growth by Patterning and Hippo Signaling in Drosophila. Cold Hpring harb Perspect Biol **7**, 1–16 (2015).
12. S Plouffe, A. W. H. and K.-L. G. Disease implications of the Hippo/YAP pathway Steven. trends Mol. Med. **21**, 212–222 (2015).
13. N de Sousa, G Rodriguez-Estevez, E. S. & T. A. Hippo signaling controls cell plasticity in planarians. Prep. (2017).

Annex 4

Transcriptional impact of short vibration and/or hypergravity in planarian regeneration

Nídia de Sousa[1], Marcello Caporicci[2], Jeroen Vandersteen[2], Jack van Loon[2,3], Emili Saló[1], Teresa Adell[1,*] and Gennaro Auletta[5,6,*]

[1]Department of Genetics, Microbiology and Statistics. Institute of Biomedicine, University of Barcelona (IBUB), Barcelona, Spain.

[2] European Space Agency (ESA). European Space Research and Technology Centre (ESTEC), Noordwijk, The Netherlands.

[3]DESC (Dutch Experiment Support Center), Dept. Oral and Maxillofacial Surgery / Oral Pathology, VU University Medical Center & Academic Centre for Dentistry Amsterdam (ACTA), Gustav Mahlerlaan 3004, 1081 LA Amsterdam, The Netherlands.

[4] Pontifical Gregorian University, Piazza della Pilotta 4, 00187 Roma, Italy

[5]University of Cassino, Via Zamosch, 43, 03043 Cassino (FR), Italy

[*] corresponding authors: tadellc@ub.edu, gennaro.auletta@gmail.com

Introduction

There is currently an intense research interest in space science, since space travels open broad and new perspectives to earth inhabitants, in terms of territorial expansion, medical research or just innovative tourism. In this scenario, more research is required on the mechanisms of the effect of space flights on the function of cells and organisms. Fluctuations in gravity, vibration, temperature and radiation are the main parameters to take into account in space flights[1]. While many examples on simulated and real microgravity are found in the literature demonstrating its profound effect on biological systems[2], few reports deal with hypergravity and vibration effects, which levels are severely increased in any space flights, especially during the launch.

To learn on the effect of hypergravity and vibration in living beings, we studied the impact of both parameters in planarians, flatworms, with a unique ability to regenerate any missing part of their body, even the head, after amputation[3,4]. Planarians show a centralized nervous system, with an anterior brain to which two eyes are connected, a digestive system that connects to an evaginable pharynx, and an excretory system[4]. The amazing regenerative ability of planarians is due the presence of a population of adult stem cells – called neoblasts – that are totipotent, and thus able to give rise to any planarian cell type[3,4]. Planarians plasticity is also showed during their normal homeostasis, since they continuously grow and degrow depending of the environmental conditions and food availability[5]. The presence of these unique adult stem cells and its plasticity converts planarians in a unique model to study the impact of hypergravity and vibration in adult cells in the context of a "whole animal", in contrast to the partial view inherent to "in vitro" cell cultures.

In the present study planarians were subjected to hypergravity (4g) in a Large Diameter Centrifuge (LDC) and/or to vibration during 6-8,5 minutes, simulating the conditions of a standard launch. The transcriptional levels of genes related with stem cell activity and the early regenerative response were quantified through qPCR. The

results show that, despite planarians regenerate apparently as good as controls, a high increase of both type of genes is observed immediately after the treatment. Four days after, the transcriptional levels of those genes are still above the controls. Our results highlight the deep impact that short exposures to hypergravity and vibration have in organisms, and thus the implications that space flights could have in human health.

Results

Planarians under short vibration and/or 4g hypergravity are able to regenerate the missing head

In order to check whether vibration and hypergravity conditions, similar to the ones suffered by humans during a rocket launch, affected planarian regeneration, 1 day regenerating planarian trunks (the head was amputated the day before), were loaded into the LDC in which a vibration system was adapted (FigureA4.1 and A4.2) (see materials and methods). To check the effect of hypergravity and vibration individually and combined, four animal groups were included (see material and methods and Table A4.2). The visual observation of the animals immediately after the treatment and 4 days after showed no difference between the different planarian groups (Figure A4.3). Thus, planarians under vibration and/or 4g hypergravity are able to regenerate an apparent proper head.

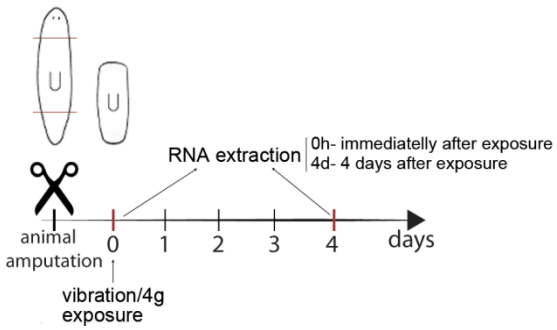

Figure A4.1: Experimental design. Animals were amputated the day before the experiment. At day 0, animals were loaded on flasks and exposed to vibration and/ hypergravity. Immediately after the exposure (0h) and 4 days after the exposure (4d) RNA was extracted the animals.

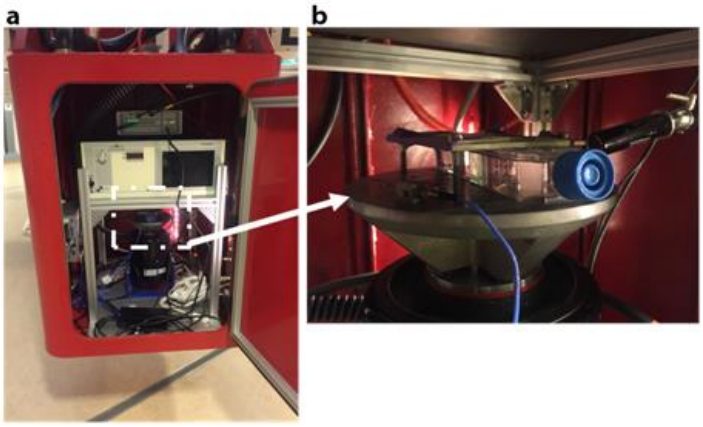

Figure A4.2: Vibration system.
(a) Inside the LDC the vibration system was installed. **(b)** Image of the vibration system with the flasks containing the animals.

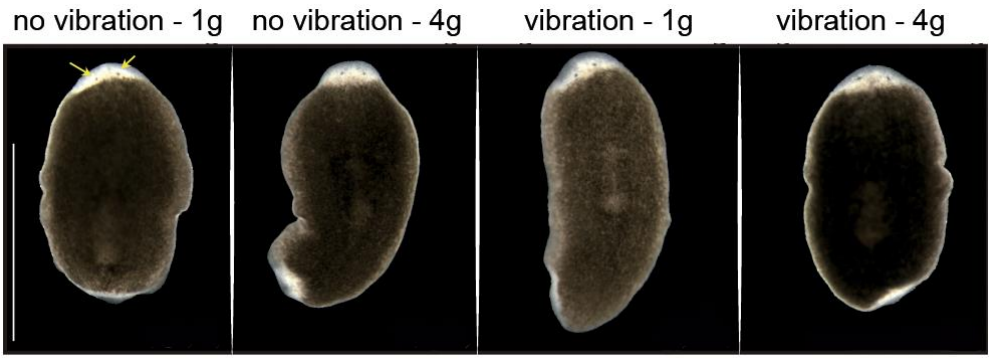

Figure A4.3: In vivo phenotype of the animals 4 days after the exposure.
No differences are observed between the animals from the four different conditions. Note the presence of the differentiating eyes in the anterior blastema. n≥15. Scale bar = 1mm.

Planarians under short vibration and/or 4g hypergravity show a high increase in the transcriptional levels of genes essential for stem cell maintenance and regeneration.

In planarians the onset of regeneration relies on the transcriptional activation of early response genes, which are known to be quickly activated after any kind of wound[6,7].

Those genes are mainly expressed in neoblasts and they are essential for their proper proliferation and differentiation[6,7]. We performed a qPCR analysis of the animals corresponding to the four conditions studied in order to check the transcriptional levels of some early response genes. We analyzed the expression of *runt-1*, which is expressed 3-6 h after wounding and is required for specifying different cell types during regeneration; *egr-1*, which is expressed 1 h after wounding, and JNK pathway-related genes (*fos-1*, *JNK* and *klf*), which coordinated the apoptotic and the mitotic response required for proper regeneration[6–8]. Our results show that immediately after the exposure planarians that were subjected to 4g hypergravity show a general increase in the transcriptional levels of the early genes (Figure A4.4). Planarians which were only subjected to vibration showed a slight increase also in the levels of those genes. Interestingly, the simultaneous exposure of planarians to 4g hypergravity and vibration produced a synergic effect on the increase of the transcription of the early genes. Four days after the exposure the levels of the early genes remained significantly increased in the animals subjected to 4g hypergravity and 4g hypergravity with vibration. Interestingly, the group of animals subjected only to vibration showed as well a significant increase on the transcription of the early genes (Figure A4.4).

Since the expression of the early response genes controls stem cell proliferation and differentiation, we checked whether the different treatments produced changes in the transcriptional levels of *piwi*, which is a stem cell marker[9], and *yorkie* (*yki)*, which expression is directly related with stemness[10,11]. The results show that there is an increase in the transcriptional levels of both genes in the three experimental groups (4g, vibration, and 4g/vibration) with respect to the controls. Importantly, the levels of those transcripts are higher at 4d than at 0h, suggesting that despite the short exposure of the animals to the experimental conditions, the impact at a cellular level lasts at least for several days.

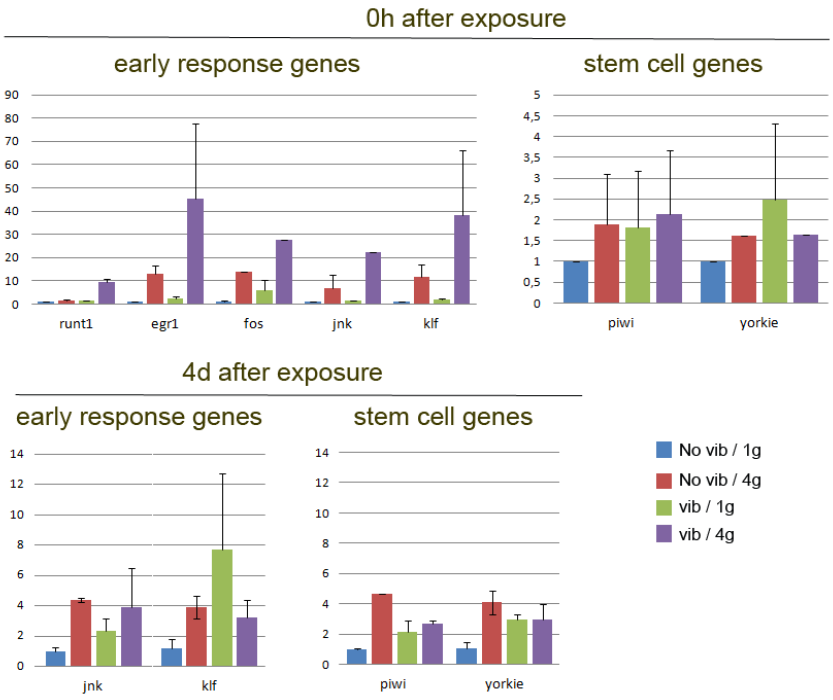

Figure A4.4: Transcriptional levels of early genes and stem cell markers

Discussion

Although planarians regenerate an apparent proper head, our results indicate that hypergravity and vibration trigger important transcriptional changes at a cellular level. The increase of the early genes at 0h could indicate that in fact the early regeneration genes respond to any 'stressing' stimulus that sense the cells. However, the most important result is the finding that the levels of those genes remain elevated 4d after the exposure, indicating that a short exposure can elicit a long-lasting cellular response. The sustained activation of the early response genes, which main function is to control apoptosis, stem cell proliferation and differentiation can have an impact

in the cell renewal of the organisms affected. A prove of that is that we found also increased levels of *piwi*, a marker of stem cells, and *yki*, a marker of stemness, at 0h and at 4 d. It must be noted that *yki* is the nuclear effector of the Hippo pathway, a cell-cell communication pathway that is found systematically involved in human cancer[12,13].

Previous studies of our group showed that exposure to planarians to hypergravity (4g and 8g) during two weeks produced mild defects in the regenerative response and a decrease of mitotic cells[14]. Here we found that short exposure to hypergravity produces an increase in the expression of regenerative and stem cell genes, which could produce an increase in the mitotic index rather than a decrease. Although, it would be necessary to check the mitotic index in our present experimental approach, an explanation could be that hypergravity does not solely affect the number of cycling cells but the progression of the cell cycle. Furthermore, this result also suggests that the time of exposure to a specific condition, as hypergravity, could elicit different responses.

Finally, our results indicate that the simultaneous exposure to hypergravity and vibration triggers a much higher transcriptional response than any of them alone, suggesting that both conditions act in a synergistic manner. Taking into account that humans in space flights are not only subjected to hypergravity and vibration but also to changes in temperature and to radiation, it could be anticipated that the synergy between all those inputs could have a serious impact on human health and should be further studied.

Materials and methods

Planarian culture

Asexual planarians from a clonal strain of *S. mediterranea* BCN-10 maintained at 20ºC in artificial water as described[15] were used in the experiments. Animals were fed with veal liver and starved for at least 1 week before starting the experiment.

Simulation of rocket launch

Simulations were performed in ESTEC (ESA). Planarians were loaded in the Large Diameter Centrifuge (LDC) to simulate hypergravity (4g) in which a vibration system was bolted to the floor plate of a gondola. The vibration system was obtained from Jeroen Vandersteen from the ESTEC (ESA) lab Eg019. The components include a shaker (2075E), an amplifier (2050E09), a front-end (Syscon Vibco – Siemens), a cooling system (Asynchronous Motors Cl. 71\2), and a laptop with which to control the shaker with the programs installed on it (sine control and random control). Planarians were amputated (head and tail) one day before the beginning of the experiment (Figure1). Twenty trunk fragments were loaded into 25 mL flasks at day 1 of regeneration. To hold flasks on the shaker, an aluminum plate wrapped in a thin rubber sheet was used (Figure A4.2). The rubber sheet, made from a glove, decreased the ability of the flasks to slide along the metal plate. To test the planarians abilities to survive a launch, they were subjected to vibrations and gravity at the same time. The parameters used to simulate launch vibration can be found in Table A4.1.

Table A4.1: Vibration profiles for the shaker and resulting quantities.

	Maximum acceleration (g)	Maximum velocity (m/s)	Maximum displacement (mm)	Maximum force (N)	Frequency (Hz)	Slope (dB/Oct)	Amplitude (g^2/Hz)
High Vibration	48	0.378	1.42	213	20	3	0.021
					150		0.13
					600	-6	0.13
					2000		0.014

Four groups of animals were analyzed (Table A4.2): planarians at 1g without vibration (control), planarians at 4g without vibration, planarians at 1g with vibration, and planarians at 4g with vibration.

TableA4.2: The different groups analyzed in the experiment.

No vibration -1g	Control
No vibration - 4 g	Hypergravity
vibration -1g	Vibration
vibration - 4 g	Hypergravity and vibration

RNA extraction

To perform the transcriptomic analysis through quantitative real-time PCR (qPCR), total RNA was extracted from the four groups immediately after the experiment (0h after experiment) and four days after the experiment (4 days after experiment) (Figure A4.2). Three replicates were analyzed per condition, and 5 animals were included in each replicate. RNA was extracted with Trizol® (Invitrogen) following the

manufacturer's instructions. RNA was quantified with a Nanodrop ND-1000 spectrophotometer (Thermo Scientific) and cDNA was done using SuperScript™ III Reverse Transcriptase (Thermo Scientific) following the manufacturer's instructions.

Quantitative real-time PCR

Quantitative real-time PCR was performed as previously described[16], and data was normalized based on the expression of EF2 as internal control. All the experiments were performed using two biological replicates. The following sets of specific primers were used:

Gene	5'-3'	
piwi	ATCCTATGGCACCGAATGAG	CCCTTATGCACCTTTCCAAC
runt1	TCCTATCGGAGACGGACA	GCTTCACCGTTGACGAGT
egr1	GTTAGCGTGCCATTTTTGT	AGCTGCATTGATAAGGCTTC
fos	GAACGACGCCAATTTCAG	CGCTTCGAGTTGTTTGAGT
jnk	TCAACGAATCTCGGTCG	AGTGAGCTCTCTTTCATCAACC
yorkie	ATTTGTGTCGACTCCATCC	CCATTAAGACATGTCGACAAG
klf	AGATCCGATGAGCTGTCTCG	AATGATCGCTCCGATTGAAC

References

1. Sonnenfeld, G. Space flight, microgravity, stress, and immune responses. *14 Exerc.* **23,** 1945–53 (1999).
2. Crawford-Young, S. J. Effects of microgravity on cell cytoskeleton and embryogenesis. *Int. J. Dev. Biol.* **50,** 183–191 (2006).
3. Reddien, P. W. & Alvarado, A. S. Fundamentals of Planarian Regeneration. *Annu. Rev. Cell Dev. Biol.* **20,** 725–757 (2004).
4. Saló, E. The power of regeneration and the stem-cell kingdom: Freshwater planarians (Platyhelminthes). *BioEssays* **28,** 546–559 (2006).
5. Baguñá, J. & Romero, R. Quantitative analysis of cell types during growth, degrowth and regeneration in the planarians Dugesia mediterranea and Dugesia tigrina. *Hydrobiologia* **84,** 181–194 (1981).
6. Wenemoser, D., Lapan, S. W., Wilkinson, A. W., Bell, G. W. & Reddien, P. W. A molecular wound response program associated with regeneration initiation in planarians. *Genes Dev.* **26,** 988–1002 (2012).
7. Sandmann, T., Vogg, M. C., Owlarn, S., Boutros, M. & Bartscherer, K. The head-regeneration transcriptome of the planarian Schmidtea mediterranea. *Genome Biol.* **12,** 1–19 (2011).
8. Almuedo-Castillo, M. *et al.* JNK Controls the Onset of Mitosis in Planarian Stem Cells and Triggers Apoptotic Cell Death Required for Regeneration and Remodeling. *PLoS Genet.* **10,** 1–15 (2014).
9. Reddien, P. W. SMEDWI-2 Is a PIWI-Like Protein That Regulates Planarian Stem Cells. *Science (80-.).* **310,** 1327–1330 (2005).
10. Ramos, A. & Camargo, F. D. The Hippo signaling pathway and stem cell biology. *Trends Cell Biol.* **22,** 339–346 (2012).
11. Ramalho-Santos, M., Yoon, S., Matsuzaki, Y., Mulligan, R. C. & Melton, D. a. Transcriptional Profiling of Embryonic and Adult Stem Cells. *October* **302,** 37102–37102 (2003).
12. R. Johnson, G. H. The two faces of Hippo: targeting the Hippo pathway for regenerative medicine and cancer treatment. *Nat Rev Drug Discov* **144,** 724–732 (2014).
13. Yu, F. X., Zhao, B. & Guan, K. L. Hippo Pathway in Organ Size Control, Tissue Homeostasis, and Cancer. *Cell* **163,** 811–828 (2015).
14. Adell, T., Saló, E., Van Loon, J. J. W. A. & Auletta, G. Planarians Sense Simulated Microgravity and Hypergravity. *Biomed Res. Int.* **2014,** (2014).
15. Cebrià, F. & Newmark, P. a. Planarian homologs of netrin and netrin receptor are required for proper regeneration of the central nervous system and the maintenance of nervous system architecture. *Development* **132,** 3691–3703 (2005).
16. Solana, J. *et al.* Defining the molecular profile of planarian pluripotent stem cells using a combinatorial RNAseq, RNA interference and irradiation approach. *Genome Biol.* **13,** 1–23 (2012).